WEATHERING OF PYRITE-BEARING GREENSCHIST FROM THE ELY GREENSTONE: TWELVE YEAR LABORATORY AND FIELD EXPERIMENTS

April 2014

Minnesota Department of Natural Resources
Division of Lands and Minerals
500 Lafayette Road, Box 45
Saint Paul, MN 55155-4045

WEATHERING OF PYRITE-BEARING GREENSCHIST FROM THE ELY GREENSTONE: TWELVE YEAR LABORATORY AND FIELD EXPERIMENTS

April 2014

Zach Wenz
Kim Lapakko
David Antonson

Minnesota Department of Natural Resources
Division of Lands and Minerals
Reclamation Section
500 Lafayette Road
Saint Paul, MN 55155

TABLE OF CONTENTS

TABLES 38

EXECUTIVE SUMMARY

Results from this study benefit the state of Minnesota in two fundamental ways. First, this study has provided a large geochemical data set that can be compared to data collected by mining companies and their consultants as required by Minnesota Rule 6132.100. Second, data from this study has provided a quantitative measure of rock reactivity which can be used to aid state agencies regulatory decisions on projects that require excavation of rock similar in composition to the rock tested.

This study began in 2000 and is ongoing at the time of this report. The study includes both laboratory and field experiments of well characterized (particle size distribution, rock composition, modal mineralogy, mineral composition, and petrology) sulfide-bearing greenschist from the Ely Greenstone rock formation. For the laboratory experiment, standardized humidity cell tests were conducted on 18 samples (one kilogram each); four of the samples were duplicates. The field experiments included four rock piles (~65 tonnes each) and six rock filled tanks (~1.6 tonnes each). Four of the tanks were mixed with different amounts of dolostone to evaluate the effect of alkaline addition on rock leachate acidity. The rock samples were rinsed with deionized water in the laboratory and natural precipitation in the field. The leachate produced from rinsing was analyzed for composition and volume. From the leachate composition and volume sulfate and metal release rates were calculated.

Petrographic analysis indicated the rock used in this study was primarily composed of the minerals quartz, chlorite and muscovite. Compositional analysis of the laboratory samples indicated total sulfur (S_T) concentrations ranging from 0.04 to 1.22 wt% and CO_2 concentrations less than or equal to 0.05 wt% except for two samples with CO_2 concentrations of 1.76 and 6.85 wt%. Field rock piles 1, 2, 3, and 4 had respective S_T concentrations of 0.02, 0.22, 0.37, and 0.63 wt% and respective CO_2 concentrations of 0.16, 0.26, 0.08 and 0.47 wt%. The field tanks were filled with the same rock that was used to construct rock pile 4.

In general, leachate pH decreased (acidity increased) with increasing rock sulfur concentration. Humidity cell samples with a S_T concentration greater than or equal to 0.1 wt% and a CO_2 concentration less than or equal to 0.05 wt% produced a leachate pH less than 6. Only the 0.63 wt% S_T rock pile generated a leachate pH less than 6. Leachate from the 0.02, 0.22, and 0.37 wt% S_T rock piles generally had a pH greater than 7. Leachate from tanks with no dolostone added had a similar small leachate pH as that of the 0.63 wt% S_T rock pile. Leachate from the four tanks with dolostone added (both with dolostone amounts that should neutralize all the acid generated) consistently had a pH greater than 7. Collectively, these experiments have indicated Ely Greenstone greenschist with a S_T concentration greater than or equal to 0.1 wt% and CO_2 concentration less than 0.05 wt% has the potential to generate a fluid with a pH less than 6.

For both the field and laboratory experiments, sulfate release rates increased with increasing rock sulfur concentration. The ratio of field to laboratory sulfate release rates ranged from 0.05 to 0.20 with a preferred value of 0.14. The smaller field sulfate release rate was likely due to a smaller total reactive surface area of the field rock per unit mass, in particular the surface area of the sulfide minerals.

Data from the laboratory experiments was used to assign a level of environmental risk for carbonate mineral deficient, sulfide-bearing, Ely Greenstone greenschist if crushed and allowed to react with the natural environment. The categorization was based on the level of treatment that would be required to neutralize rock leachate acidity. Greenschist with wt% S_T concentrations between 0-0.5, 0.10-0.16, and 0.2-1.22 were assigned with environmental risk levels of low, moderate, and high, respectively.

1. EXPERIMENT HISTORY

This study was designed to determine the reactivity of sulfide-bearing rock from a portion of the Archean Ely Greenstone rock formation located in northern Minnesota. The Ely Greenstone has been identified as a potential ore bearing host rock and thus at some time could be mined leading to production of waste rock. This study includes both laboratory and field scale rock weathering experiments to collect information on rock leachate composition.

In the year 2000, the Minnesota Department of Natural Resources (MN DNR) began operating and monitoring 18 humidity cell tests, four rock pile weathering tests, and six rock filled tank weathering tests, some tanks had dolostone added. As of 2012, only 12 of the laboratory humidity cells are operational while all the field scale piles and tanks are still under test. Various aspects of these experiments have been previously reported on in a series of individual papers and reports (Lapakko et al., 2001, 2002, 2003, 2004a, 2006 and 2012; Lapakko and Antonson 2001, and 2002). This report is a comprehensive volume which includes an additional 418 weeks of data for trend analysis as well as additional interpretation of the chemical and physical processes responsible for generating the leachate compositions.

2. INTRODUCTION

Mine wastes (e.g. tailing, waste rock, and mine pits) are components of mines which remain long after mining operations have ceased. When mine wastes are exposed to the atmosphere they react with oxygen and water. The degree to which the materials react depends on the chemical and physical properties of the mine wastes and atmospheric conditions. Some mine wastes can be relatively unreactive and/or produce benign reaction products and therefore will not negatively impact the environment. Alternatively, mining wastes can be very reactive and negatively impact the environment. A common negative impact is degradation of water quality in watersheds containing mine wastes. Degradation of water quality can occur immediately after mining or long after mining has ceased. Acidic drainage from mining areas has impacted thousands of miles of streams in the United States (U.S. Bureau of Mines, 1985).

Remediation of these environmental impacts can cost tens to hundreds of millions of dollars. Therefore, prior to mining it is critical to understand how mine wastes will react once exposed to the atmosphere. This understanding can be established by solid phase characterization and weathering tests of potential mine wastes. The data collected from these types of tests is essential for developing mitigation plans to ensure compliance with water quality standards. Solid phase rock analyses typically include: acid base accounting (ABA), particle size distribution, modal mineralogy, and elemental composition of the whole rock and individual minerals. The degree to which sulfide and carbonate minerals are exposed may also be estimated to approximate the mineral surface areas available for reaction. Rock weathering tests are commonly performed in a laboratory using humidity cell tests, such as the standardized ASTM D5744-13i procedure, and may also be conducted as non-standardized larger scale rock weathering tests in a field setting.

Humidity cells are small cylindrical columns filled with rock < 6.35 mm in diameter. The rock is rinsed weekly with deionized water. The rinse water drains through the humidity cell, reacting with the rock and dissolving some reaction products that have accumulated on the rock particle surfaces. The water that has drained through the humidity cell is called a leachate. The leachate is collected and measured for volume and chemical composition. The composition and volume of the leachate is used to determine the rate of solute release from the rock. Solute release rates are one of many parameters used to predict how rock weathering may or may not impact the environment. Early determination of rock leachate composition allows more effective and economical mitigation techniques to be developed and employed prior to and during the mining process.

For a particular rock type, the degree of reactivity with the atmosphere will vary with small changes in the abundance of carbonate and sulfide minerals. Therefore, for this study a series of different carbonate and sulfur concentration greenschists from the Ely Greenstone were collected to establish long term rock leachate composition trends to aid in future regulatory decisions regarding mining and mitigation.

The Ely Greenstone belongs to the Wawa Subprovince of the Superior Province of the Canadian Shield (Card and Ciesielski, 1986). In Canada greenstone belts in the Wabigoon and Wawa Subprovinces are host to numerous gold and base metal deposits. In Minnesota, there are no active mines in the Wabigoon or Wawa Subprovinces greenstone belts despite containing similar rock types, structures, and sharing a geologic history similar to that of the Canadian equivalents. Why no ore deposits have been discovered in Minnesota may largely be due to the greater thickness of glacial deposits, in comparison to Canada, which pose a challenge to mineral exploration techniques. Despite no active mining, greenstone belts in Minnesota have been explored for precious and base metal deposits and various types of mineralization have been located (Peterson and Patelke, 2003). Continued exploration driven by increasing metal prices may lead to future deposit discovery and mine plan development.

The Ely Greenstone greenschist samples for this study were collected during excavation of an underground cavern near Soudan, MN. These samples included rock recovered from blasting and drilling. The blast rock was used to construct four field scale rock piles and fill six tanks (plastic barrels). The drill core was crushed and used in eighteen humidity cell tests. This report includes the solid phase characterization and leachate composition from the laboratory and field tests. For the laboratory experiment, 622 weeks of laboratory humidity cell data for 12 samples (January 24, 2000 through December 27, 2011) and 154 weeks for six samples (terminated on January 8, 2003) are presented. For the field experiments, data collected from 2000 to 2011 are presented.

2.1 Acid Generation and Neutralization

The major environmental concerns regarding mine waste are generation of acidic leachate and associated increased metal concentrations. In addition, some waste rock types can generate neutral leachate with increased metal concentrations. Reaction of iron sulfide minerals such as pyrite (FeS_2) with oxygen and water results in acid generation as shown by reaction 1. The rate at which this reaction proceeds is dependent on the sulfide surface area, availability of the oxidant (either O_2 or Fe^{3+}), microbial activity, and fluid pH. For a fluid pH between about 5 and 10, O_2 is the most important oxidant whereas for fluid pH values less than 5, Fe^{3+} becomes more soluble and becomes the most important oxidant. Williamson and Rimstidt (1994) developed abiotic pyrite oxidation rate laws based on experimental data for oxidation by O_2 (eq. 1) and Fe^{3+} (eq. 2) in the presence of oxygen.

$$FeS_{2(s)} + \frac{15}{4}O_{2(aq)} + \frac{7}{2}H_2O_{(l)} = Fe(OH)_{3(s)} + 2SO^{2-}_{4(aq)} + 4H^{+}_{(aq)} \quad \text{(rxn. 1)}$$

$$\frac{dFeS_2}{dt} = 10^{-8.19(\pm 0.10)} \times m_{DO}^{0.5(\pm 0.04)} \times m_{H+}^{(-0.11\pm 0.01)} \quad \text{(eq. 1)}$$

$$\frac{dFeS_2}{dt} = 10^{-6.07(\pm 0.57)} \times m_{Fe^{3+}}^{0.93(\pm 0.07)} \times m_{Fe^{2+}}^{(-0.40\pm 0.06)} \quad \text{(eq. 2)}$$

Figure 2.1 shows the pyrite oxidation rate and fluid pH relationship based on equations 1 and 2. The calculations assumed an aqueous O_2 concentration in equilibrium with the atmosphere and iron concentrations based on ferrihydrite ($Fe(OH)_3$) saturation. For pyrite oxidation by O_2 the oxidation rate gradually increases with increasing pH whereas for pyrite oxidation by Fe^{3+} the oxidation rate rapidly increases with decreasing pH. For these modeled conditions, Fe^{3+} becomes the most important oxidant at a pH of about 4.7.

In a mine waste, acid generated as a result of sulfide oxidation can be rapidly neutralized by the dissolution of carbonate and silicate minerals. The greenschist in this study contains variable amounts of carbonate minerals including calcite ($CaCO_3$), dolomite ($CaMg(CO_3)_2$) and siderite ($FeCO_3$). Reactions 2 and 3 demonstrate the acid neutralizing capability of calcite and dolomite under acidic conditions whereas reactions 4, 5, and 6 combine to result in no net neutralization for siderite dissolution due to precipitation of iron hydroxide (rxn.7). For siderite with a Ca and/or Mg component ($(Fe, Ca, Mg)CO_3$) the Ca and Mg components could neutralize acid whereas the Fe component could not.

$$CaCO_{3(s)} + 2H^+_{(aq)} = H_2CO_{3(aq)} + Ca^{2+}_{(aq)} \qquad \text{(rxn. 2)}$$

$$CaMg(CO_3)_{2(s)} + 4H^+_{(aq)} = 2H_2CO_{3(aq)} + Ca^{2+}_{(aq)} + Mg^{2+}_{(aq)} \qquad \text{(rxn. 3)}$$

$$FeCO_{3(s)} + H^+_{(aq)} = Fe^{2+}_{(aq)} + HCO^-_{3(aq)} \qquad \text{(rxn. 4)}$$

$$Fe^{2+}_{(aq)} + \frac{1}{2}O_{2(aq)} + H^+_{(aq)} = Fe^{3+}_{(aq)} + \frac{1}{2}H_2O_{(l)} \qquad \text{(rxn. 5)}$$

$$Fe^{3+}_{(aq)} + 3H_2O_{(l)} = Fe(OH)_{3(s)} + 3H^+_{(aq)} \qquad \text{(rxn. 6)}$$

$$FeCO_{3(s)} + \frac{1}{4}O_{2(aq)} + \frac{5}{2}H_2O_{(l)} = Fe(OH)_{3(s)} + H_2CO_{3(aq)} \qquad \text{(rxn. 7)}$$

The samples from this study predominantly contain the silicate minerals chlorite ($Mg_5Al_2Si_3O_{10}(OH)_8$), muscovite ($KAl_3Si_3O_{10})(OH)_2$), albite ($NaAlSi_3O_8$), and quartz (SiO_2). Reaction 8 is a possible dissolution reaction for a pure Mg-chlorite demonstrating the acid neutralization. However, most chlorites contain significant Fe substituted for Mg. Thus inferring from reactions 6 and 8, for each Mg replaced by Fe, 2 less moles of acid (H^+) could be neutralized.

$$Mg_5Al_2Si_3O_{10}(OH)_{8(s)} + 10H^+_{(aq)} = 2Al(OH)_{3(s)} + 3SiO_{2(aq)} + 5Mg^{2+}_{(aq)} + 6H_2O_{(l)} \qquad \text{(rxn. 8)}$$

The minerals muscovite and albite have a much smaller acid neutralizing capability per mole demonstrated by reactions 9 and 10, respectively. Quartz dissolution does not yield significant acid neutralization.

$$KAl_3Si_3O_{10}(OH)_2 + H^+ + 3H_2O_{(l)} = K^+ + 3Al(OH)_{3(s)} + 3SiO_{2(aq)} \qquad \text{(rxn. 9)}$$

$$NaAlSi_3O_8 + H^+_{(aq)} + H_2O_{(l)} = 3SiO_{2(aq)} + Al(OH)_3 + Na^+_{(aq)} \qquad \text{(rxn.10)}$$

The effectiveness of acid neutralization is fundamentally dependant on the reaction rate of the neutralizing mineral. Figure 2.2 shows the dissolution rate of some minerals present in the Ely Greenstone greenschist samples as a function of pH (from Palandri and Kharaka, 2004). At pH 6 the approximate rates of calcite and chlorite dissolution are about 5×10^{-7} and 8×10^{-15} $mol\cdot m^{-2}\cdot s^{-1}$, respectively. In comparison, pyrite dissolution at pH 6 is about 5×10^{-10} $mol\cdot m^{-2}\cdot s^{-1}$ (see fig. 2.1). Thus, for a pyritic mine waste, calcite would require about 1/1000 the surface area of pyrite to produce a circumneutral leachate whereas chlorite would need about 60,000 times the surface area of pyrite to produce a circumneutral leachate.

2.2 Hydrology of Waste Rock Piles

The only hydrologic parameter considered in this study was the yield coefficient. The yield coefficient was calculated as the ratio between the volume of water leaching from the field rock and the volume of precipitation falling onto the field rock. Yield coefficients are specific to climate, vegetative cover, material type and particle size. Two uncovered waste rock test piles in northeastern Minnesota had average yield coefficients over 15 years of 0.51 and 0.54 (Lapakko et al., 2004b). More recently Smith and Beckie (2003) reported a yield coefficient of 0.55 for a test rock pile in northern Saskatchewan.

2.3 Alkaline Addition to Waste Rock

The development of acidic leachate from a mine waste can be negated by adding an alkaline material, such as dolostone, during disposal. Dolostone is predominantly comprised of the mineral dolomite which upon dissolution can neutralize acid increasing fluid pH (see rxn. 2). Increasing fluid pH through carbonate dissolution yields three secondary effects. First, a fluid pH above about 5 is a chemical environment unfavorable for *Acidithiobacillus ferrooxidans*, a bacterium which catalyzes sulfide oxidation. The exclusion of these bacteria limits the rate of sulfide oxidation, and therefore, the rate of acid production. Second, increasing pH enhances the oxidation of ferrous iron and the subsequent precipitation of ferric oxyhydroxides. If the pH is locally greater on the iron sulfide mineral surfaces, precipitates may form on the mineral surface inhibiting chemical transport to and from the iron sulfide mineral surface. This surface coating would in effect slow the sulfide oxidation rate and decrease acid production. Third, as pH increases the equilibrium concentrations of metals decrease due to increased metal precipitation (as hydroxides, oxides, and/or carbonates) and adsorption effectively decreasing the metal concentration of a fluid.

For mitigation design, neutralizing acidic leachate can be achieved by adding an appropriate amount of alkaline material to the waste rock. Determining the amount of alkaline material required to neutralize acid can be achieved by calculating the acid production potential (AP) of the waste rock (eq. 3) and the required amount of neutralization potential (NP; eq. 4) to produce an NP to AP (NP/AP) ratio of 1. In theory, a waste rock pile with a NP/AP ratio of 1 should produce a neutral leachate. However, all the calculated AP and NP may not be available in equal proportions due to mineral precipitation on reactive surfaces and the relative degree of exposure for acid generating and acid neutralizing minerals. Thus, alkaline addition beyond a NP/AP ratio of 1 is preferred to ensure complete neutralization. For waste rock with a small carbonate concentration, silicate minerals can provide sufficient neutralization if the sulfide concentration is small enough.

$$AP\ (g\ CaCO_3 eq \cdot kg_{rock}^{-1})\ =\ wt\%\ S \times \frac{100.0869\ gCaCO_3}{32.065\ gS} \times \frac{10\ g \cdot kg^{-1}}{wt\%} = \ wt\%\ S \times 31.21 \qquad \text{(eq.3)}$$

$$NP(g\ CaCO_3 eq \cdot kg_{rock}^{-1}) =\ wt\%\ CO_2 \times \frac{100.0869\ gCaCO_3}{44.0095\ gCO_2} \times \frac{10\ g \cdot kg^{-1}}{wt\%} = wt\%\ CO_2 \times 22.74 \qquad \text{(eq. 4)}$$

Numerous studies have been conducted on the application of alkaline materials to neutralize acid released from reactive mine wastes. Fine grained mine wastes, such as tailings, are easily well mixed with alkaline solids due to a relatively fine particle size. In addition, flow through fine grained material tends to be more uniform than heterogeneously sized waste rock. These two factors may be more conducive to neutralization of acid generated by sulfide-bearing mine wastes. Studies have been conducted to examine the effectiveness of adding limestone (Lapakko et al., 1997) and rotary kiln fines (Lapakko et al., 2000) to fine grained ($0.053 < d < 0.149$ mm) acidic leachate producing Duluth Complex rock. In these studies, addition of limestone increased leachate pH and alkalinity and decreased the rate of sulfide oxidation during the 397 week period of record. Leachate remained circumneutral even after complete depletion of limestone because neutralization from incongruent dissolution of the silicate minerals was sufficient to neutralize the acid produced at a decreased rate of sulfide oxidation. Addition of rotary kiln fines also increased leachate pH and alkalinity and decreased the rate of sulfide oxidation. However, once these alkaline solids were depleted, leachate became acidic and sulfate concentrations increased, presumably due to the small amount of alkaline solids in comparison to the relatively greater sulfide concentration (i.e., a low NP/AP ratio).

Factors other than NP/AP may determine if mine waste leachate is maintained in the neutral range. With waste rock, the blending and layering of acid neutralizing solids are reported to be of minimal mitigative success, due to insufficient homogeneity of mixtures and preferential flow through acid generating layers (Mehling et al., 1997). Analyses by Kempton et al. (1997) and Morin and Hutt (2000) indicate that preferential flow has a dominant influence on the effectiveness of waste rock blending with alkaline material. The latter publication indicated that waste rock leachate acidity is dependent on the flow path length between acid neutralizing rock and acid generating rock. This study showed that waste rock with a bulk NP/AP ratio of up to 300 could produce acidic leachate if an appropriate neutralizing rock flow path length was not attained.

Day (1994) concluded that limestone ($d < 0.6$ mm) mixed with acid generating rock (2.1 wt% sulfur) should provide a neutralization potential at least double the AP of the rock to ensure a neutral leachate pH. However, MEND (1994) indicated that 60 percent of the limestone was finer than 0.6 mm, and that 81.9 percent of the rock was finer than 3.35 mm, suggesting the relative size of the particles may be important in these calculations. Day (1994) further noted that iron precipitate coatings did not reduce the availability of the limestone during a 5 year column study.

In column experiments lasting a total of 24 weeks, O'Hagan (1986) found that a well blended 5 wt% $CaCO_3$ addition was required to neutralize leachate from shale with a 1 wt% sulfur and 0.7 wt% pyritic sulfur concentration. The limestone and shale used in this experiment had a particle size range of 2.0 to 5.6 mm. Rose and Daub (1994) conducted a 15 week column experiment, and concluded that the 2-5 mm limestone particles mixed with a 7.0 wt% sulfur, pyritic shale (diameter < 1 cm and NP/AP = 1) were ineffective because they did not impart adequate alkalinity to the pore water. This ineffectiveness was attributed to large limestone particle size and precipitated iron hydroxide surface coatings.

Donovan and Ziemkiewicz (1994) added limestone layers to 400 ton piles of sandstone and shale coal overburden roughly 1-8 inches in diameter, to produce limestone concentrations of 0.46, 1.07, and 1.26 wt% ($0.56 < NP/AP < 2.38$). The authors concluded that these and other layered alkaline additions did not consistently affect leachate quality during the year after construction "due to their inhomogeneous distribution, to heterogeneity in NP or MPA (Maximum Potential Acidity) within the piles, to hydroxide armoring of the amendment layers, or to time lag in reaching the outflow." The site was resampled 11 years later and leachate from the two larger limestone additions was circumneutral (Ziemkiewicz and Meek, 1994).

In summary, the main difficulties for ensuring an effective alkaline addition treatment are achieving a homogenous mixture of alkaline material and waste rock and limiting the development of preferential flow paths within waste rock stockpile.

Most mining operations have either constructed layers of acid producing rock with acid neutralizing material, or tried to blend materials by dumping alternate loads of acid neutralizing material with acid producing material. For the alternating layer approach, acid is generated within the acid producing layer and can flow preferentially through this layer resulting in limited neutralization. Similar problems can occur for alternating dumping between waste rock and alkaline material. An effective acid neutralization treatment technique could be achieved by adding an adequate amount of neutralizing material to each haul truck carrying waste rock. This could be accomplished by a truck driving under a limestone dispensing hopper where the limestone would be added directly to the top of the load. The limestone would begin to mix with the waste rock as the truck drives to the waste dump and then would be further mixed as the material is dumped. This approach has been used at the Gold Quarry Mine in Nevada were lime (CaO) is added to sulfidic gold ore to maintain neutral conditions in the leach pad (Bolin et al., 2000).

Another consideration for addition of alkaline materials is the relative particle size between the waste rock and neutralizing material. Despite waste rock piles having the appearance of a substantial component of large sized material, waste rock stockpiles typically contain a considerable amount of small sized particle sizes. For example, the rock excavated for the AMAX exploration shaft near Babbitt, MN, was comprised of 38 wt% of less than 25.4 mm (1 inch) and 3 wt% of silt to clay size material (Lapakko et al., 2004b). Specific surface area increased from 0.6 $m^2 \cdot g^{-1}$ for the coarse material to 2.6 to 4.7 $m^2 \cdot g^{-1}$ for the silt and clay sized material. Sulfur concentration increased from 0.67 wt% for coarse material to 1.65 to 1.94 wt% for the silt and clay sized material. As a result, most of the reactive sulfide surface area of the pile was contained in the fine grained material and was likely the source from which the majority of the acid was generated in the stockpiled rock. Therefore, in this case, not only an appropriate amount of neutralizing material need be added, but an appropriate grain size to ensure a large enough specific surface area of the neutralizing material to neutralize acid generated by the greater sulfide concentration and specific surface area of the small particle sized waste rock.

3. METHODS

3.1 Sampling Process

The University of Minnesota initiated a project to expand its underground physics laboratory at the Soudan Mine near Soudan, MN. This expansion resulted in excavation of approximately 17,000 m^3 (~22,000 y^3) of rock. Prior to excavation, a 5 cm drill hole was bored through the center of the cavern to characterize the rock. The rock was then blasted using an explosive consisting of 75% ANFO, a commercially prepared combination of ammonium nitrate and fuel oil, and 25% Mine Rite, an ammonium nitrate based water gel. As the rock was removed the walls of the cavern were sealed with shotcrete, a mixture of Portland cement containing 11% silica fume and < 13.4 mm aggregate. The blasted rock was removed in four lifts from which all of the samples for the field experiments were collected.

3.1.1 Laboratory Samples

The 5 cm drill core was analyzed for sulfur, carbon, major oxides, and trace metals for length intervals of about 5 ft (Appendix 1). Based on the sulfur analyses, 12 samples of different sulfur concentration were selected for laboratory testing. These samples were crushed to a < 0.64 cm diameter by Lerch Brothers Inc. (Hibbing, MN) and subsequently sent to Actlabs for sulfur concentration analysis. Based on the sulfur concentration of these samples an additional six samples were selected from the drill core samples to provide a sample set representative of the entire range of measured sulfur concentrations. The final 18 samples were analyzed again for sulfur concentration at Lerch Brothers Inc. (Hibbing, MN). Based on these sulfur analyses 18 samples (including four duplicates) were selected for humidity cell tests and a sample split was sent to Actlabs for additional compositional analysis.

The 18 selected samples were submitted to Lerch Brothers Inc. for crushing. The samples were crushed to

< 0.64 cm with a stage crusher to limit generation of fines. The crushing process entailed screening the drill core sample to < 0.64 cm and three crushing steps (large jaw crusher set at 1.92 cm, small jaw crusher set at 0.95 cm, roll crusher set at 0.64 cm). After each of the first two crushing steps, the < 0.64 cm fraction was collected and the larger material was passed to the next crushing phase. Five 250 g samples and one 300 g sample were split from each bulk sample. The five 250 gram samples were stored in sealed plastic bags until filling the cells. The 300 g samples were pulverized to a pulp for subsequent analysis.

3.1.2 Rock Pile Samples

During removal of the top lift rock at the Soudan Mine drill cuttings samples were collected. The drill cuttings were analyzed for sulfur concentration. Based on the sulfur analyses, areas within the bottom three lifts were selected as target zones for obtaining a range of sulfur concentrations for the field experiments. After a targeted area was blasted, approximately 50 yd^3 of rock was removed from the mine in approximately 1.5 yd^3 muck boxes. Rock designated for field weathering tests was hauled by truck to the MN DNR research site in Hibbing, MN.

Three types of samples were selected for characterization of the rock piles. First, as each muck box was emptied a random sample was taken and placed in a one gallon plastic container. Each time a targeted area was removed from the shaft, 25 samples were collected and analyzed at Lerch Brothers Inc. to determine if sulfur concentration was relatively homogenous and would produce a test plot of the desired sulfur concentration. If the results were suitable the rock was loaded into 10 yd^3 dump trucks and hauled to the research site. The 25 samples were retained and later analyzed for total sulfur, sulfate, evolved carbon dioxide, and whole rock composition. Thirteen of the samples were analyzed for trace metal concentrations by Actlabs. A second sample was collected to determine particle size distribution and the composition of individual particle size fractions.

The rock containment bins were loaded by placing the rock onto a conveyer, which piled the rock in the center of the bin (fig. 3.1). The rock was then leveled using a backhoe, forming a truncated pyramid (fig. 3.2). Based on the dimensions of the truncated pyramid it was determined that the piles contained approximately 39 m^3 of rock. As the rock was loaded onto the conveyer, a random sample (approximately 1 y^3) was set aside for analyses of particle size distribution.

A third set of 20 samples was collected to further assess compositional variability, including modes of sulfide mineral occurrence, of rock piles 2, 3, and 4. Samples were not collected from test pile 1 since analyses of muck box samples indicated sulfur concentrations were relatively uniform. Furthermore, visual inspection of the rock confirmed pyrite occurrence homogeneity. All the samples were collected as the bins were being loaded. For rock piles 2 and 3, four samples were taken from the top of the pile after each 10 y^3 was added and leveled off, and one from each side of the pile. For rock pile 4, two samples were collected while the first three feet of rock was being placed in the bin, eight random samples when the first three feet of rock had been leveled off, six random samples after an additional foot of rock had been added, and four samples when the pile was completed. This third set of samples has not been analyzed.

3.1.3 Dolostone Addition Samples

The same rock that was used to construct rock pile 4 (0.67 wt% S_T) was selected for use in the dolostone addition experiment. The greenschist was screened to pass a 1.5 inch screen at Casper Construction Inc. in Grand Rapids, MN (fig. 3.3). Three skid loader bucket loads of rock were placed in each tank. For tanks with dolostone added, each of three bucket loads had one third of the total dolostone placed on the top of the load (fig. 3.4). The rock mixture was manually scooped from the bucket and placed in the tank (fig. 3.5). A total of 55 lbs of dolostone was added to tanks 2 and 5 and 165 lbs of dolostone was added to tanks 3 and 4. This technique provided a very well mixed sample composite. A rock sample was collected from each bucket load (prior to dolostone addition) for a total of 18 samples from the six tanks.

3.2 Experiment Design

The humidity cells were constructed of acrylic plastic cylindrical columns with an interior diameter of 10.2 cm and height of 19 cm. A 0.64 cm high acrylic sleeve was glued into the bottom of the cell to support a 0.16 cm thick PVC plate, which was perforated with 0.32 cm holes spaced 0.48 cm on center. The plate was covered with a polypropylene filter (National Filter Media Corporation, Polymax B, Style 226-075-2) which supported the solids. The bottom was sealed with an acrylic plate with a 0.85 cm outlet port in the center. The top of the cell has a removable cover with a single 0.85 cm vent hole (fig. 3.6). Prior to filling with rock, the cells were rinsed with a 10 wt% HNO_3 solution and then rinsed three times with distilled water. The individual cells were weighed and the weight was recorded for each cell.

For the field rock piles, four 20 × 20 ft bins were constructed to contain the rock for the experiment using two stacked 8 in × 8 in × 20 ft pressure treated timbers (fig. 3.7). The timbers were placed on a compacted sand pad overlain with a 36 mil Reinforced Polypropylene (RPP) liner covered with 2 to 4 inches of sand followed by a second 36 mil RPP liner, sloped to one end of the bin, which was covered with six inches of sand (fig. 3.8). A 1.5 in slotted PVC pipe, covered with a geotextile sleeve, was installed between the two liners as a leak detection system. A 1.5 in slotted PVC pipe with a geotextile sleeve was also placed on the top liner to collect percolating water. This collection pipe spans the entire length of the bin and exits in the center of the bin to a collection sump.

The collection sump, as well as flow instrumentation, is housed in a 60 gal polyethylene plastic tank (fig. 3.9). The leachate flows into a 7 gal polyethylene plastic sump equipped with two Madison Co. polypropylene hinged liquid level sensors (fig. 3.10). When the flow reaches the upper sensor, a MARCH model LC-SCP-MD pump is triggered initiating pumping until the water level reaches the lower level sensor. The water is pumped through a JLC International Inc. IR-Opflow flow meter and flow is recorded on a Precision Digital model 94788 flow totalizer. A portion of each pump cycle is collected in a 2 L sample bottle for analyses and the remainder of the flow is pumped to a treatment plant.

Before the rock was loaded into the bins, temperature and oxygen concentration measuring instruments were placed on the top of the sand layer (fig. 3.11). Rock was hand placed over the instruments to prevent any damage while the bins were filled. Test piles 2, 3, and 4 had the same instrumentation installed approximately 3 feet from the base. The temperature probe was placed in a 2 in PVC pipe 10 ft long and the oxygen sampling instrument was contained in a 0.1875 in (interior diameter) plastic Tygon tubing with a 0.25 in (interior diameter) slotted PVC pipe attached to each end of the pipe. The slotted pipe was covered with a geotextile fabric to prevent plugging from fine rock particles. On one end of the pipe the sampling port was placed at 10 ft and the other at 5 ft.

The dolostone addition experiment materials are contained in six polyethylene plastic tanks (d = 48 in, h = 42 in). The tanks are housed in a 20 × 20 ft lined bin that serves as a double containment system (fig. 3.12). The tanks were fitted with a two inch slotted PVC outlet pipe on the bottom, which drained into a 22 gal polyethylene sample collection sump (fig. 3.13). The bottom of the outlet pipe was installed approximately two inches above the bottom of the tank which created a zone of saturation, to ensure waste rock did not enter the saturated zone. Three inches of silica sand was placed in the bottom of each tank. The tanks were then filled to a height of approximately 31 in with either rock (control tanks) or rock mixed with dolostone, yielding a bed volume of 0.917 m^3 (32.4 ft^2). Bulk density of the rock was determined as 1.73 $g{\cdot}cm^{-3}$ (108.2 $lbs{\cdot}ft^{-3}$), yielding a sample mass of 1,590 kg (3,506 lbs). The dolostone had a bulk density of 1.39 g·cm^{-3} (86.6 lbs·ft^{-3}). The tanks were filled with crushed rock on October 24, 2000.

The NP/AP ratio of the tanks were determined by calculating AP from the 0.67 wt% S_T of rock pile 4 and the sum of the rock and dolostone NP. Rock pile 4 AP was 15.3. The average Sobek NP for rock pile 4 was 6.3 and the dolostone NP was calculated assuming the LOI (41.6 wt%) equalled the dolostone CO_2 concentration resulting in $CaCO_3$ additions of 23.7 (52.25 lbs) and 71.1 kg (156.75 lbs) corresponding to NP(CO_2) values of 14.9 and 44.7 (calculated using eq. 5). This leads to NP/AP ratios of 0.41, 1.4 and 3.3 for tanks 1 and 6 (control tanks), tanks 2 and 5, and tanks 3 and 4, respectively.

$$Tank\ NP\ (g\ CaCO_3\ eq \cdot kg_{rock}^{-1}) = \frac{CaCO_3\ g}{1590.3\ kg\ rock} + 6.3g\ CaCO_3\ eq \cdot kg_{rock}^{-1} \qquad \text{(eq. 5)}$$

3.3 Experiment Procedures

3.3.1 Laboratory Experiment Procedure

On January 24, 2000 the laboratory experiment was initiated following the MN DNR humidity cell method (Lapakko and White, 2000), a modification of ASTM D5744-96 (ASTM, 2000). The 18 humidity cells were rinsed once a day for three days to remove oxidation products accumulated on the solids from the time they were crushed until the beginning of the experiment. A rubber cap was placed on the humidity cell outlet port and 500 mL of distilled water was slowly poured into each cell with a graduated cylinder. The cells were allowed to sit for ten minutes after the last one was filled and then they were uncapped and allowed to drain. Following the initial 3 day rinse schedule, the cells have been rinsed weekly with 500 mL of distilled water using a separatory funnel to slowly drip the rinse water instead of a direct pouring with a graduated cylinder. Cells were allowed to drain for approximately 24 hours prior to sample collection and analysis. Water samples were analyzed at the MN DNR Hibbing lab for specific conductance, pH, alkalinity, acidity, and Eh. Specific conductance was measured using a Myron L conductivity meter, and pH was measured with an Orion SA720 meter equipped with a Ross combination pH electrode (8165). Alkalinity (for pH > 6.3) and acidity were determined using standard titration techniques to pH endpoints of 4.5 and 8.3, respectively (APHA et al., 1992). Eh readings were collected generally two to four times annually using a Beckman model 11 meter with an Orion electrode (9678BN).

An alternative procedure for Eh measurements designed to reduce the exposure of the humidity cell leachate to air began week 65 (April 24, 2001). For this procedure a flow cell was constructed by gluing a four inch piece of acrylic plastic pipe (1 inch I.D.) to a three in^2 piece of 0.25 in acrylic, which served as the base of the cell. One hole was drilled into the pipe roughly 0.25 in above the base piece (inlet), and a second hole (outlet) was drilled 1.5 in from the base on the opposite side of the pipe. Hose fittings were glued into each of the holes and Tygon tubing was attached to each of the fittings. A hole was drilled into a rubber stopper, placed into the opening at the top of the flow cell, through which the Eh probe accessed the cell. The inlet tubing was connected to the fitting on the bottom of the humidity cell after the stopper was removed. The effluent flow varied among humidity cells, and the control valve on the outlet was used to control the flow and minimize air bubbles in the inlet line and the flow cell. After the cell filled and the air was removed from the cell, Eh was allowed to stabilize before the readings were recorded. The flow cell was then drained, rinsed with deionized water, and connected to the next humidity cell. Due to time constraints, Eh measurements were not collected on weeks leachate samples were collected for metal and sulfate analysis.

Leachate mass was measured and subsequently analyzed for pH and specific conductance at the MN DNR laboratory in Hibbing, MN. From the remaining leachate, samples were filtered (0.45 um filter) and treated with 0.2 mL of Baker Instra-Analyzed nitric acid per 50 mL sample. The treated samples were then submitted for chemical analysis to the Minnesota Department of Agriculture (MDA) in Saint Paul, MN. The volume weighted concentration for the initial three rinses was calculated to represent the leachate composition for week zero. Laboratory leachate samples were generally analyzed by the MDA every week for the first four weeks, every two weeks through week 20, every four weeks through week 108, and every eight weeks thereafter. An additional 100 mL sample was filtered and frozen for phosphate analyses on weeks 56 and 60.

On week 154 (January 8, 2003) samples 11 (0.26 wt% S_T) and 12 (0.39 wt% S_T) were discontinued, as were duplicate samples 5 (0.1 wt% S_T), 9 (0.16 wt% S_T), 15 (0.59 wt% S_T), and 17 (1.22 wt% S_T). The remaining 12 humidity cells had a period of record of 622 weeks as of December 27, 2011.

3.3.2 Field Rock Piles Experiment Procedure

Water volume input to the rock piles consisted entirely of natural precipitation. Annual precipitation was determined using a US Standard rain gauge at the MN DNR Hibbing field research site (Appendix 2). Flow volume from the rock piles was recorded, on average, biweekly after initial flow was observed. Flow volume was measured using an IR-Opflow flow meter and recorded using a Precision Digital flow totalizer (model 94788). Initial instrumental electrical malfunctions precluded flow measurements from July 21 to November 9, 2000 for which flow measurements were estimated in earlier reports (see Section 3.6.2 Yield Coefficients). Composite rock pile leachate samples were generally collected biweekly after consistent flow was established. Samples of the initial flow waters were collected from the sumps receiving leachate from rock piles 1 and 4. A portion of the leachate samples were analyzed for specific conductance, pH, alkalinity and/or acidity at the MN DNR Hibbing lab. Specific conductance was measured using a Myron L conductivity meter, and pH with an Orion SA720 meter, equipped with a Ross combination pH electrode (model 8165). Alkalinity (for pH ≥ 6.3) and acidity were determined using standard titration techniques to pH endpoints of 4.5 and 8.3, respectively (APHA et al., 1992). The remaining leachate was filtered (0.45 um filter) prior to submittal to MDA for sulfate and metal analysis. Samples for chemical analysis were treated with 0.2 mL of Baker Instra-Analyzed nitric acid per 50 mL. An additional 500 mL sample was treated with 1.0 mL of Baker Analyzed sulfuric acid for nutrient analyses.

3.3.3 Field Tanks Dolostone Addition Experiment Procedure

The sampling schedule was designed to collect samples on a biweekly basis and after select large rainfall events. Water input to the tanks consisted entirely of precipitation. The collection sump was calibrated in five liter increments and total flow was measured with a ruler. One inch of precipitation is about the equivalent to 30 liters of input water. A 250 mL sample was collected for pH, specific conductance, alkalinity (for pH ≤ 6.3) or acidity, metals, and sulfate analysis. These samples were analyzed for pH and specific conductance directly in the bottle. A 20 mL sample was then taken for analysis of alkalinity or acidity. The remaining sample was filtered for metals and sulfate analysis. Samples for metal analysis were treated with 0.2 mL of Baker Instra-Analyzed nitric acid per 50 mL. Samples were periodically collected for nutrient analysis (500 mL). Nutrient samples were treated with 2 mL of Baker Analyzed sulfuric acid per 500 mL sample.

3.4 Laboratory Conditions

Between rinses the laboratory samples were retained in the cells to oxidize. The cells were stored in a temperature and humidity controlled room. Temperature was maintained by a thermostatically controlled heater (Lakewood 750) and humidity was maintained by a Holmes HM 3500 humidifier and Sears Kenmore dehumidifier, both controlled by Honeywell humidistats. Temperature and relative humidity were measured three to four times weekly with a Taylor wet-bulb, dry-bulb hygrometer, and average weekly values were determined. Average weekly temperature ranged from 20.3 ^{o}C to 27.9 ^{o}C and averaged 23.8 ^{o}C, with a standard deviation of 1.4 ^{o}C. Average weekly relative humidity ranged from 42.0% to 75.0% and averaged 58.3%, with a standard deviation of 4.0%.

Rinse water was purified by a Culligan purification system. Rinse water pH and specific conductivity were measured weekly. Rinse water pH ranged from 5.0 to 7.7 with an average value of 6.2 and standard deviation of 0.3. The rinse water specific conductivity ranged from 0.20 to 7.00 (µS/cm) with an average value of 0.49 and standard deviation of 0.46.

3.5 Analytical Techniques

3.5.1 Solid Phase Analysis of Laboratory Samples

Particle size distribution of the laboratory samples were determined by Lerch Brothers Inc. using method ASTM E 276-93. The rock samples were analyzed for total sulfur (S_T), sulfate (sulfide was determined by difference), and evolved carbon dioxide by Actlabs in Tucson, AZ using ASTM E-1915-97. A 10 wt% hydrochloric acid solution was used to dissolve the carbonate minerals, and the amount of carbonate present was calculated as the difference between total carbon in the initial sample and that in the residue.

The remaining solid phase constituents were determined by Actlabs. Whole rock constituents were determined using a lithium tetraborate fusion modified from ASTM E886-94 and analysis by inductively coupled plasma-atomic emission spectroscopy (ICP-AES) using a Thermo Jarrell-Ash ENVIRO II ICP. Concentrations of Ag, Cd, Cu, Ni, Pb, Zn, and Bi were determined using a total digestion modified from Crock et al. (1983), with analysis by ICP-AES. Other trace elements were determined using instrumental neutron activation analysis (Hoffman, 1992). In addition to analyses of the bulk samples, 11 individual size fractions from each sample were analyzed for S_T, sulfide, sulfate, evolved carbon dioxide, and major oxides.

Modal mineralogy of the 14 bulk samples were determined using sample chemistry, optical microscopy, and previous x-ray diffraction (XRD) data collected from drill core samples (see Lapakko et al. (2004) for details).

Major oxide compositions of muscovite, chlorite, and siderite (for the 0.5 and 0.72 wt% S_T samples) were determined by energy dispersive spectrometry using a Zeiss DSM 960A scanning electron microscope at Macalester College, St. Paul, MN. The operating beam conditions were 20 kV and 50 nA with a working distance of 25 mm and a magnification of 1000. Three to five analyses of each mineral were conducted from at least two different rock chips from a single thin section. Polished thin sections were made by Spectrum Petrography from approximately 0.25 in rock chips of 14 fourteen greenstone samples.
Water and CO_2 concentrations were estimated to equal mass totals of 100%. In house biotite, chlorite, and dolomite mineral standards were analyzed before and after each analytical session to correct for instrumental drift.

Neutralization potential (NP) measurements were conducted by two separate methods, both of which are modifications of methods described by Skousen et al. (1997). The first method was similar to that of Sobek et al. (1978), with the exception that instead of conducting a “fizz” test, a 20 mL volume of 0.1N HCl was added to a 2 g sample of ground rock in a 250 mL Erlenmeyer flask. This is the smallest acid addition allowed by the Sobek et al. (1978) method and was selected based on the known small carbonate concentration of the greenstone rock.

During the digestion phase of the NP determination, the mixture of acid and rock was placed in a hot water bath at 90 to 95 °C until the reaction ended (determined by cessation of bubble production). Distilled water was added to the flask to attain a total volume of 125 mL. The mixture was boiled for one minute, and then allowed to cool to room temperature. The cooled mixture was titrated to pH 7.0 and 8.3 with 0.1N NaOH solution to determine the amount of acid (as $g\ CaCO_3eq \cdot kg_{rock}^{-1}$) neutralized by the rock. The second method used the same digestion procedure described above. However, after the sample cooled, it was filtered through a 0.45 µm filter, poured into a 250 mL Erlenmeyer flask, and 5 mL of 30 wt% hydrogen peroxide was added. The flask was covered with a watch glass and boiled gently for five minutes. After the sample cooled it was titrated as described previously.

3.5.2 Solid Phase Analysis of Field Samples

Particle size distribution of a one m^3 sample was determined at the MN DNR Hibbing laboratory. The greater than 30.48 cm and 15.24 to 30.48 cm fractions were removed from the sample and manually measured for length and mass. The remaining sample was sieved through screens to separate the 6.35 to 15.24, 1.905 to 6.35, and less than 6.35 cm size fractions. One third of the less than 6.35 cm fraction was split using the four corners method (Scott, 1942). One of these quarter splits was used to determine the particle size distribution of the less than 6.35 cm rock using a Gilson Ro-Tap equipped with Tyler standard sieves.

Chemical analyses were performed by Lerch Brothers Inc. and Actlabs. Lerch Brothers Inc. performed the initial sulfur analyses of 25 muck boxes using a LECO combustion furnace following ASTM E395-95A. The mean of these S_T values were used to identify bulk sulfur concentrations to build four rock piles of different sulfur concentration. Subsequent chemical analyses were performed by Actlabs. The analyses included: (1) S_T, sulfate (sulfide by difference), and evolved CO_2 following ASTM E-1915-97, (2) major oxide analysis by lithium tetraborate fusion (modified from ASTM E886-94) followed by inductively coupled plasma-atomic emission spectroscopy (ICP-AES) using a Thermo Jarrell-Ash ENVIRO II ICP, and (3) elemental analysis of Ag, Cd, Cu, Ni, Pb, Zn, and Bi by total digestion, modified from Crock et al. (1983), followed by ICP-AES analysis. Additional elemental concentrations were determined using neutron activation analysis (Hoffman, 1992).

Mineralogic analyses were conducted by McSwiggen & Associates (St. Anthony, MN). Analyses included determination of mineral modal abundance, mineral composition by electron microprobe analysis, and estimation of the degree of sulfide and carbonate mineral surface area exposure. Polished grain mounts were prepared from the 2.0 to 6.35 mm particle size fraction from which a series of microprobe spot analyses were taken. The random location for spot analysis combined with the fine grained texture of the rock resulted in some composite mineral analyses. The extreme composite analyses were excluded and only the analyses believed to closely represent individual mineral compositions are reported.

The three samples collected from each dolostone addition tank were combined. Both combined rock samples and dolostone samples were submitted to Actlabs for the same type of analyses as the rock pile samples. The dolostone was obtained from the Shiely Division of Camas Inc. (Eagan, MN). Particle size distribution of the Ely Greenstone and dolostone samples was determined by Lerch Brothers.

3.5.3 Aqueous Phase Analysis

All aqueous elemental analyses were performed at MDA following their standard analytical procedures. Generally, the concentration of Ca, Mg, Na and K were determined by atomic adsorption with a Varian SPECTRAA, samples were analyzed by ICP-MS on a Hewlett Packard HP4500 (model G1820A) when smaller detection limits were required. The concentrations of Al, Co, Cu, Fe, Mn, Ni, Si, and Zn were routinely analyzed by ICP-MS on a Hewlett Packard HP4500 (model G1820A). Sulfate concentrations were determined using a Lachat QuickChem 8000 or a Dionex ion chromatograph when SO_4 concentrations were < 5 mg/L. Nitrogen ($NO_3 + NO_2$) concentration was analyzed using the Automated Cadmium Reduction Method (Wastewater Method 4500-NO_3F) with a Technicon AA11. Ammonia concentration was measured using the Ammonia-Selective Electrode Method (Wastewater Method 4500 NH_3F) with an Accumet 950 pH/ion meter. Total phosphorous concentration was determined using the Ascorbic Acid Method (Wastewater Method 4500-P E) with a Perkin Elmer 552 Spectrophotometer. Total Kjeldahl Nitrogen was measured using the Semi-Automated Colorometric Method (EPA 351.2) with a Bran & Luebbe Traacs 800.

3.5.4 Temperature and Oxygen Concentrations of Rock Piles

Temperature was measured with a Cole-Parmer model 8402-00 meter. Oxygen concentrations were measured with a GC Industries probe (model GC-502) and a YSI probe (model 57). The oxygen sampling apparatus (fig. 3.10) includes a sampling chamber connected to a sampling port. The sampling port is connected to a vacuum pump to evacuate the air prior to inserting the probe into the chamber to collect an oxygen concentration. The oxygen port outside of the chamber was evacuated for 5 minutes prior to inserting the probe into the chamber. Temperature was measured at the same time as oxygen.

3.6 Data Calculations

Sulfur analyses of the laboratory samples performed by the Lerch Brothers were not in agreement with the initial Actlabs analyses (table 3.1). Sample heterogeneity most likely contributed to the variability in sulfur concentrations. In contrast there was close agreement between analyses performed by Lerch Brothers and the subsequent Actlabs analyses. The second set of Actlabs analyses are used for calculations in this report as was the case with previous reports.

3.6.1 Solute Release Rates

Although the laboratory samples were rinsed weekly, the leachate collected was not always analyzed for all solute concentrations. For the unanalyzed leachate, solute concentrations were interpolated as the average of the bounding measured values (excluding anomalous values). Laboratory solute release rates were calculated for each sample week using equation 6. In the text, release rates are presented in units with the rock subscript following kg removed ($mmol \cdot kg^{-1} \cdot wk^{-1}$). Field solute release rates were calculated both on an annual basis and for each sampling period. Annual solute release rates were calculated as the sum of solute mass (as mmol) from samples collected over the entire year. This mass was attributed to one year of leaching, despite the fact that no leachate occurred over the winter period. This annual calculation assumes reaction products accumulating over the winter are included in the early leachate collection samples. Solute release rates for individual sampling periods varied in time length from about two to six weeks. Generally there were seven to nine sampling events per year. Similar to annual release rates, the individual release rates were calculated as the sum of the solute mass (as mmol) collected for each sample period.

$$solute\ release\ rate(mmol \cdot kg_{rock}^{-1} \cdot wk^{-1}) = m_i \times V_{leach} \div M_{rock} \qquad \text{(eq. 6)}$$

m_i= molal concentration of solute i
V_{leach}= volume of leachate in liters
M_{rock}= mass of rock sample in kilograms

3.6.2 Yield Coefficients

Yield coefficients (eq. 7) were calculated to express the amount of flow as a fraction of the precipitation falling on the pile.

$$Y_{b,t} = V_{b,t} \div ((P_t \div 12) \times A_b \times 28.2) \qquad \text{(eq. 7)}$$

$Y_{b,t}$ = yield coefficient for pile b for flow period t, dimensionless
$V_{b,t}$ = liters of flow from pile b during flow period t
P_t = inches precipitation during flow period t (division by 12 converts to feet);
A_b= horizontal cross sectional area of pile b in ft^2
28.2 = factor to convert ft^3 to liters

When rock pile flow was not measured (e.g. due to failure of equipment), flow was estimated as the product of the yield coefficient for the pile and the volume of precipitation onto the pile. This calculation was performed for the year 2000 in previous reports. The specifics of this calculation are presented in Appendix 2 of Lapakko et al. (2002).

3.6.3 Field Rock Pile Mass

Because solute release rates are calculated as mass dependant it is necessary to know the total mass of rock for the field rock piles and tanks. A bulk density of 1.73 $g \cdot cm^{-3}$ was estimated for the tanks without dolostone addition by measuring the mass of a five gallon bucket of the Ely Greenstone. This calculation assumes the pore volume is the same between the tanks and bucket. Because rock in the bucket and tanks was the same size material, assuming a similar porosity for rock in the tank and bucket is reasonable. However, because the field rock piles are significantly larger and comprised of a different rock particle size distribution, using the calculated bulk density from the bucket measurement is not appropriate. Therefore, a separate density determination was required for the rock piles. To calculate a rock pile mass, the density of the greenschist was measured from 10 representative samples (table 3.2). The samples were individual solid rock fragments ranging in mass from 328 to 839 g. Sample volume was measured by displacement of water and ranged from 110-300 mL. The average calculated density was 2.79 $g \cdot cm^{-3}$ with a standard deviation of 0.16 (0.2-10 % difference). The individual measurements were corroborated by measuring the combined volume of samples 1 thru 5 resulting in a density of 2.86 $g \cdot cm^{-3}$ which is only 2.6 % different from the average density of the ten samples. A rock density of 2.79 $g \cdot cm^{-3}$ was used in the mass calculations. The dimensions of the rock piles were measured and a total volume of 38.9 m^3 was determined. Using the measured bulk density (for the tanks) with the actual rock density provides a porosity estimate of about 40%. This porosity estimate was extended by ±10 % to provide a reasonable range of porosity to estimate the total mass of the rock piles (table 3.3). This corresponds to calculated total rock masses for the smallest, middle, and greatest porosity estimates of 76, 65, and 54 tonnes, respectively. Calculations requiring rock pile mass used the 65 tonne estimated value.

4. RESULTS

4.1 Introduction

The primary objectives of this study were to 1) determine the relationship between leachate pH and rock sulfur concentration for the Ely Greenstone greenschist, and 2) calculate empirical scale factors for SO_4 release rates using the laboratory and field experiment data. Ultimately, the results from this study could be used to predict leachate pH and SO_4 release rates from future Ely Greenstone greenschist mine wastes.

4.2 Laboratory Samples Solid Phase Analyses

Rock from the humidity cell sample splits were analyzed for particle size distribution, bulk and individual particle size fraction compositions, neutralization potential, and modal mineral abundances.

4.2.1 Particle Size Distribution

Sample splits of duplicate humidity cells were not analyzed for particle size distribution. Instead the duplicates were assumed to have the same particle size distribution as that of their respective counterpart. Therefore, a total 14 samples were analyzed for particle size distribution. The 14 samples were crushed and sieved into 11 different particle size fractions from 6.35 mm to < 0.074 mm (table 4.1). The particle size fraction mass distributions for all samples were very similar, indicating relatively similar crushing behavior among the samples. Excluding the two largest and smallest particle size fractions, the mass fraction of an individual size fraction tended to increase with increasing particle size. About 60% of the sample mass was comprised of two size categories encompassing the 0.841-4.76 mm sized material. The largest size fraction (4.76-6.35) contained the third largest mass percent for all samples (except sample 7 (0.16 wt %S_T)) and ranged from 8-14.7 wt%. Eight of the samples contained particles greater than 6.35 mm accounting for ≤ 0.6 wt% of the total sample mass.

4.2.2 Bulk Composition

Humidity cell samples were numbered one through 18 with S_T concentrations increasing with increasing sample number, ranging from 0.04 to 1.22 wt% (table 4.2). The SO_4 concentration of the samples was less than the detection limit (0.05 wt%) for all but three samples. Sample 13 had a SO_4 concentration of 0.1 wt% and samples 12 and 18 had SO_4 concentrations of 0.05 wt%. The evolved CO_2 concentration of the samples exceeded 0.05 wt% for samples 13 and 16 with respective values of 1.76 and 6.85 wt%. The major whole rock oxides, in decreasing concentration, were SiO_2 (49.4-84.8 wt%), Al_2O_3 (7.4-21.3 wt%), FeO (3.5-14.8 wt%), MgO (1.1-6.4 wt%), K_2O (0.6-4.5 wt%), Fe_2O_3 (0.2-2.2 wt%), TiO_2 (0.1-1.1 wt%), Na_2O (0.1-1.0 wt%), MnO (0.03-0.94 wt%), CaO (0.03-0.68 wt%), and P_2O_5 (0.02-0.49 wt%) (table 4.3).

Trace metal concentrations were generally small (table 4.4). The maximum reported concentrations for elements Ag, As, Be, Bi, Cd, Cs, Dy, Er, Eu, Ge, Hf, Ho, In, Lu, Mo, Nb, Pb, Pr, Sb, Sm, Sn, Ta, Tb, Th, Ti, Tm, U, W, and Yb were less than 20 parts per million (ppm). Metals present at greater concentrations were Sc (38 ppm), La (50.4 ppm), Nd (54 ppm) Y (76 ppm), Sr (94 ppm), Cu (99 ppm), Co (103 ppm), Rb (108 ppm), Ce (112 ppm), Zn (194 ppm), V (240 ppm), Ni (318 ppm), Cr (366 ppm), Zr (368 ppm), and Ba (622 ppm).

The small base and precious metal (such as Ag, As, Cu, Ni, Pb, Sb, Sn, W, and Zn) concentrations of the samples indicate that these rocks are not associated to any type of ore mineralization. Therefore, these samples would likely not provide trace metal release values representative of waste rock from an ore deposit.

4.2.3 Particle Size Fraction Compositions

Of the 14 samples analyzed for particle size distribution, 11 size fractions were analyzed for sulfur, carbon, and major oxides (table 4.5). The concentration of SiO_2 generally increased with increasing particle size. For the greater SiO_2 concentration samples (samples 10-18) the concentration of Al_2O_3 and K_2O generally decreased with increasing particle size. The negative correlation between particle size and Al and K concentrations is likely due to the small size and hardness of muscovite being preferentially concentrated in the finer size fractions during sample crushing. The increase in SiO_2 concentration in the coarser fraction is presumably the result of the larger mineral grain size and greater hardness of the mineral quartz. No consistent concentration trends were observed for the other major oxides, sulfur concentration, or CO_2 concentration. Individual particle size fraction CO_2 concentration measurements variably agreed with the bulk sample values. The main discrepancies were for samples 3, 7, 8, and 9 which had bulk wt% CO_2 values less than 0.05, whereas individual size fractions commonly had above detection limit values between 0.07 and 0.48 wt% CO_2.

4.2.4 Mineralogy and Petrology

The Ely Greenstone laboratory samples predominantly contained quartz, chlorite, muscovite, and pyrite (table 4.6). Texturally, the samples are fine to medium grained and exhibit schistosity. Thus, these samples represent quartz-chlorite-muscovite schists of the petrologically diverse Ely Greenstone. For simplicity, the samples are referred to as greenschists owing to the green color and foliated texture of the rock as well as having the appropriate mineral assemblage for a greenschist facies grade pelitic protolith. In general, as quartz abundance increased pyrite abundance increased and the abundances of chlorite and muscovite decreased. The chlorite and muscovite are generally fine grained with rare large muscovite porphyroblasts. Pyrite grain size diameters ranged from < 10 to 600 μm. Two samples contained a significant proportion of carbonate.

Scanning electron microscopy energy dispersive spectrometry (SEM EDS) was used to determine the mineral composition of chlorite, muscovite, and siderite. The individual mineral analyses are provided in Appendix 3. The average mineral formula for chlorite, muscovite, and siderite were $(Fe_{2.75}Mg_{1.7}Al_{1.45}Na_{0.07}K_{0.01}Mn_{0.01})(Si_{2.67}Al_{1.33}O_{10})(OH)_8$, $(K_{0.78}Na_{0.15}Mg_{0.08})(Al_{1.82}Fe_{0.13}Ti_{0.01})(Si_{3.14}Al_{0.86}O_{10})(OH)_2$, and $Fe_{0.85}Mg_{0.09}Mn_{0.09}Na_{0.02}C_{0.97}O_3$, respectively. The carbonate mineral formula is the average from two different samples from which the carbonate was compositionally zoned. The measured siderite growth zones varied compositionally with a MgO concentration varying between 0.1 and 10.7 wt% and a CaO concentration varying between 0 to 1.0 wt%.

4.2.5 Digestion-Titration Neutralization Potentials

Neutralization potentials were determined using two different digestion-titration methods at two different pH titration endpoints (described in section 3.5.1), yielding four values for each sample. Replicate analyses were conducted on samples duplicated in humidity cell tests, the two samples with large carbonate concentrations, and a few select samples. All solid phase digestion-titration NP determinations are presented in table 4.7. The digestion-titration NP values determined by the hydrogen peroxide addition method were generally greater than those determined by the Sobek et al. (1978) method at both back titration endpoints for all samples with ≤ 0.05 wt% CO_2. For the two samples with greater CO_2 concentration (samples 13 and 16), NP values decreased in the order Sobek (pH 7.0) >> Sobek (pH 8.3) > peroxide (pH 7.0) > peroxide (pH 8.3).

For the greater CO_2 concentration samples (samples 13 and 16), the major reason for NP variability among the methods was the difference of the digestion-titration methods to correct for the neutralization contribution from the iron fraction of the carbonate. To account for the iron carbonate fraction it is necessary for the ferrous iron released from carbonate minerals (or other minerals) to oxidize to ferric iron and precipitate as ferric hydroxide. When a pH 8.3 endpoint was used for the back titration (rather than the standard pH 7.0 endpoint), the average NP for the Sobek NP values decreased by about 10 to 20 whereas for the Peroxide NP values the decrease was only about one. The difference in Sobek NP values at different pH titration endpoints suggested that more iron (and possibly manganese) was released to solution during the digestion and was precipitated during the back titration using the pH 8.3 endpoint. This is expected because the oxidation of ferrous to ferric iron is second order with respect to OH^- concentration (Sung and Morgan, 1980; Eary and Schramke, 1990). Consequently, oxidation rates at pH

8.3 would be more than 100 times those at pH 7.0 and would enhance the precipitation of ferric hydroxide, thereby including the acidity occurring as ferrous iron in solution. The addition of hydrogen peroxide also accelerates ferrous iron oxidation and, consequently, the peroxide method yielded smaller values for the greater CO_2 concentration samples than the increased pH endpoint did alone.

4.3 Humidity Cell Experiments

4.3.1 Water Retention

The mass of each humidity cell was measured before and after rinsing. The mass of the humidity cell minus cylinder and sample mass was assumed to be the retained water. Water retention data is listed in Appendix 4. For all samples the amount of water retained before rinsing declined over time (fig. 4.1). A similar trend was observed for water retention after rinsing. There are likely two contributing factors that may account for this decreasing trend. First, the samples with large mica and chlorite mineral abundances may have lost some sample mass during the initial weeks of the experiment. That is, the extremely fine grained micas and clays may have been flushed through or around the filter and into the leachate collection bottle. Second, some of the finer sized particles may have gradually moved towards the bottom of the humidity cell resulting in a greater porosity for the overlying rock. The greater porosity of the top layer of rock would tend to drain more freely during the rinse cycle and be more susceptible to evaporation. Sample 13 (0.5 wt% S_T and 1.76 wt% CO_2) exhibited the smallest water retention and greatest decline in water retention overtime (fig. 4.1). Sample 13 did not have an increased leachate volume suggesting the greater water loss was due to a greater degree of evaporation than the other samples.

4.3.2 Leachate Composition and Reproducibility

For all samples, leachate SO_4 concentrations and pH generally decreased with time except for the two large carbonate concentration samples. The four duplicate samples (number 4 (0.10 wt% S_T), 8 (0.16 wt% S_T), 14 (0.59 wt% S_T), and 18 (1.22 wt% S_T)) were in excellent agreement for most solute parameters. Figures 4.2 to 4.5 show pH and SO_4 concentration for the long term and duplicate humidity cells illustrating near identical values for these parameters for 154 weeks.

Of the 12 samples with a period of record of 622 weeks, four distinct groups can be defined based on similarities of leachate pH time series trends (fig. 4.6). This group classification forms the basis for presenting humidity cell test results in the following sections. Complete leachate compositions are listed in Appendix 5.

4.3.2.1 Group 1

Group 1 includes samples 1, 2, and 3 with corresponding wt% S_T concentrations of 0.04, 0.04, and 0.05, respectively. These samples are characterized by a gradually decreasing pH from an initial value of about 8 to between 6 to 6.5 through 622 weeks (fig. 4.7). Leachate SO_4 concentrations decreased steadily from about 4 mg/L to about 0.5 mg/L by about week 300 (fig. 4.8). After week 300, SO_4 concentrations were near or less than the detection limit (0.5 mg/L) through week 622. Group 1 leachate Ca and Mg concentrations gradually decreased from about 0.7 to 0.1 mg/L over 622 weeks with the exception that samples 2 and 3 generally had leachate Mg concentrations less than the detection limit (0.1 mg/L) after about 500 weeks (figs. 4.9 and 4.10). Compared to Ca and Mg concentrations, leachate K and Na concentrations declined relatively rapidly through about week 200 and 300, respectively, after which the values were less than the detection limit (0.1 mg/L) (fig. 4.11). Sample 1 leachate commonly had the greatest K concentration of all the samples from week 14 to 276. The large leachate K concentrations are unexpected because the solid phase bulk sample K concentration was substantially less than many of the other samples (table 4.3). Sample 1 leachate also had much greater Mg concentrations than samples 2 and 3, which is consistent with the greater Mg concentration of this sample (table 4.3). Group 1 samples had leachate Mg/Ca molar ratios between about 0.5 and 2 (fig. 4.12).

4.3.2.2 Group 2

Group 2 includes samples 4, 6, 7, and 8 with respective wt% S_T concentrations of 0.10, 0.12, 0.16, and 0.16. Leachate pH from these samples gradually declined from initial values of about 7.5 to a pH between 4.8 and 5.4 (fig. 4.13). Although all group 2 samples exhibited a gradual leachate pH decrease the exact trend of pH decrease was different. Leachate pH for samples 4, 6, 7, and 8 was generally less than 6 by weeks 144, 192, 144, and 104, respectively. Leachate SO_4 concentrations decreased rapidly from 10 to 4 mg/L from week 1 to 10. After week 10 leachate SO_4 concentrations decreased steadily from about 4 to between 1.2 to 0.7 mg/L through week 622 (fig. 4.14). Generally, leachate Ca concentrations decreased from about 1 to 0.1 mg/L whereas leachate Mg concentrations decreased from about 0.6 to 0.1 mg/L (figs. 4.15 and 4.16). Leachate from samples 7 and 8 was regularly less than the Ca detection limit after week 491 and 406, respectively, and leachate from samples 4, 6 and 8 was regularly less than the Mg detection limit after week 204, 515 and 481, respectively. Leachate K and Na concentrations declined quickly through about week 200 and 300, respectively, after which the leachate concentrations were less than the detection limit (0.1 mg/L; fig. 4.11). Samples 6, 7, and 8 had leachate Mg/Ca molar ratios of about 1 through week 515, 350, and 350, respectively, whereas sample 4 leachate had a Mg/Ca ratio of about 1 through week 100 (fig. 4.12). Sample 7 had the greatest leachate Mg/Ca ratio of about 3 from week 389 to 508 (fig. 4.12).

4.3.2.3 Group 3

Group 3 includes samples 10, 14, and 18 with respective wt% S_T values of 0.20, 0.59, and 1.22. The leachate pH of these samples sharply decreased to a pH of about 5 by week 30 and reached minimum pH values in the range of 3.1 to 3.9 by week 108 (fig. 4.17). Leachate pH for samples 10, 14 and 18 has gradually increased since about weeks 200, 100 and 200, respectively. The pH of leachate from sample 14 has increased the most by about a value of 0.7 whereas samples 10 and 18 have increased by about 0.4 and 0.2 pH units, respectively. Leachate compositions for group 3 samples exhibit the greatest variability among the sample groups. The variability is likely resultant from the significantly different sulfur concentrations of the samples. Leachate SO_4 concentrations generally decreased over time from about 10 to 80 mg/L to about 4 to 40 by week 622 (fig. 4.18). Leachate Ca concentrations decreased from about 1 to 10 mg/L to < 0.1 to 0.4 mg/L through week 622 (fig. 4.19). Leachate Mg concentrations were less variable decreasing from about 1 to 8 mg/L to about 0.2 to 1.5 through week 622 (fig. 4.20). Similar to groups 1 and 2, group 3 leachate K and Na concentrations decreased rapidly through the first 200 weeks (fig. 4.11). Group 3 samples had initial leachate Mg/Ca molar ratios of about 1 which rapidly increased to > 2 by week 100 after which the Ca/Mg ratios were generally between 3 and 6 through about week 380 (fig. 4.12). Leachate Mg/Ca ratios were not calculated for sample 10 after about week 350 due to less than detection limit Ca concentrations. Sample 14 and 18 leachate Mg/Ca ratios gradually increased after week 380 up to values of about 8.

4.3.2.4 Group 4

Group 4 includes samples 13 and 16 with respective wt% S_T concentrations of 0.5 and 0.72 and respective wt% CO_2 concentrations of 1.76 and 6.85. Leachate from group 4 samples initially exhibited a pH decrease for about 15 weeks followed by a more gradual pH increase to a maximum value followed by a gradual pH decrease (fig. 4.21). Sample 13 exhibited a much greater initial pH decrease and a later smaller pH maximum in comparison to sample 16. Sample 13 leachate SO_4 concentrations gradually decreased from about 50 to 3 mg/L over 622 weeks whereas sample 16 leachate SO_4 concentrations initially decreased through about week 100 then gradually increased up to about 25 mg/L by week 350 after which SO_4 concentration decreased to about 6.5 mg/L at week 622 (fig. 4.22). Sample 13 leachate Ca concentrations rapidly decreased from about 7 mg/L to about 0.3 mg/L by week 125 after which Ca concentrations have decreased to less than the detection limit (0.1 mg/L; fig. 4.23). Sample 16 leachate Ca concentrations decreased from about 7 to 1 mg/L over the first 50 weeks, then increased to about 2 by week 100 through 200 after which the concentration steadily decreased to about 0.2 mg/L through week 622 (fig. 4.23). Leachate magnesium concentrations reached a maximum value of about 5 and 20 near week 100 for samples 13 and 16 and then decreased to 0.6 and 1.6 by week 622, respectively (fig. 4.24). Group 4 samples leachate Mg/Ca ratio increased sharply from about 1 to 14 through week 100. After week 100 leachate Mg/Ca ratios have remained relatively consistent at about 14 (fig. 4.12).

4.3.3 Solute Release Rates

Solute release rates were calculated weekly and are presented graphically by group for SO_4, Ca, Mg, K and Na in figures 4.25, 4.26, 4.27, 4.28, and 4.29, respectively. Annual average SO_4, Ca, Mg, K and Na release rates are listed in table 4.8. Sulfate release rates for groups 1 and 2 decreased rapidly over the first 10 weeks, then remained relatively constant through about week 100, and then decreased steadily. Sulfate release rates for group 3 samples decreased for about the first 15 weeks and then increased, coinciding with decreasing pH, up to about week 100 after which the rates gradually decreased. For group 4 (samples 13 and 16), the SO_4 release rates decreased for about the first 100 weeks. After week 100, the SO_4 release rate from sample 13 (0.5 wt% S_T and 1.76 wt% CO_2) continued to decrease and SO_4 release from sample 16 (0.72 wt% S_T and 6.85 wt% CO_2) gradually increased through about week 300 and then steadily decreased.

In general, SO_4 release rates increased with increasing sample sulfur concentration. The few exceptions are samples 13 and 16 (0.5 and 0.72 wt% S_T, respectively) which had larger carbonate mineral concentrations. Sulfate release rates for sample 16 were consistently less than those for sample 14 (0.59 wt% S_T), presumably resultant from the large difference in leachate pH, a controlling factor for sulfide oxidation. Likewise sample 13 leachate SO_4 release rate was less than that of sample 10 (0.2 wt% S_T) after about week 400 despite having more than double the sulfur concentration. Among all samples, Ca and Mg release rates decreased at a much slower rate than that of K and Na.

4.3.4 Sulfide Depletion

For kinetic tests, oxidation of sulfides will decrease the sulfide mass and surface area available for reaction which, in turn, reduces the rate of SO_4 release. Accumulation of reaction products on the sulfide mineral surface will also reduce the rate of sulfide oxidation by limiting the transport of reactants (e.g. oxygen) to the mineral surface and products (e.g. SO_4) from the mineral surface. In addition, some of the sulfide minerals in a crushed rock sample will be completely enclosed in a rock particle and unavailable for reaction. For a humidity cell test, the smallest sized sulfides are generally the greatest contributors for acid generation and SO_4 release. This is due to mineral reactions being surface area dependent and the greater specific surface area afforded by small particles. For example, long term kinetic testing of Duluth Complex norite has shown near total depletion of sulfides after about 500 weeks for particles less than 0.149 mm whereas particles from 0.149 to 19 mm exhibited only 10 to 70% sulfur depletion through 943 weeks (Wenz et al., 2013). For the Ely Greenstone laboratory samples, generally less than 10 wt% of the sample was less than 0.149 mm in diameter (see table 4.1). Thus, a small percentage of the overall sulfide concentration is contained in the small (< 0.149 mm) particle size fraction which has the greatest reactivity per unit mass. Therefore, the early rapid SO_4 release rate decrease (within about 20 weeks for group 1 and 2) is likely due to oxidation of the smallest sized wholly exposed sulfides and partly exposed sulfides contained in larger rock particles. The later gradual decrease in SO_4 release rate (after about week 100 for group 1 and 2 samples) is likely due to accumulation of reactant products on the remaining sulfide mineral surfaces, and a decrease in available fresh sulfide surface areas due to progression of the oxidation reaction.

Sulfide depletion time series plots illustrate the amount of sulfide leached as SO_4 and the rate of depletion over time. These plots can also be used to predict long term sulfide oxidation rates by extension of the depletion trends. However, prediction of future sulfide oxidation rates must also consider the leachate pH trend. If pH decreases to the point where ferric iron is the dominant iron species, sulfide oxidation rates can increase substantially leading to much greater sulfide oxidation rates. However, depending on the relative rates of acid production and acid neutralization, pH may not sufficiently decrease for ferric iron to become the dominant oxidant.

Groups 1 and 2 (sample numbers 1-4 and 6-8) had wt% S_T depletions between 12 and 15 (fig. 4.30). Group 4 samples (samples 13 and 16) both had wt% S_T depletions of 24. Group 3 samples exhibited the greatest variation in wt% S_T depletion, ranging from about 38 for samples 10 and 18 to about 54 for sample 14. The greater depletion for sample 14 was likely due to the initial large SO_4 release rate for this sample, which was up to twice that of sample 18 during the first 63 weeks of the experiment and again from weeks 105 to 115.

4.3.5 Calculated AP, NP, and ENP Values

The AP(S_T) of the samples was determined using eq. 3, which assumes all sulfur occurs as a pure iron sulfide. For the laboratory samples this is a reasonable assumption, because no sulfate minerals and no sulfides other than pyrite were identified. The neutralization potential of the samples was calculated as NP(CO_2) using eq. 4 and NP($MgCO_3$) using eq. 8. Equation 8 was derived from the average siderite mineral formula determined by SEM EDS and only includes neutralization from the Mg component of the siderite. Neutralization was also calculated as an empirical neutralization potential (ENP(pH 6); Price, 2009; White et al. 1999; and Lapakko, 1994). The ENP(pH 6) was calculated by summation of the total Ca and Mg mass released when leachate pH was ≥ 6. Total acid neutralization (∑(Ca+Mg)) was also calculated as summation of the total Ca and Mg mass released from each humidity cell over the 622 week period of record. Neutralization potential was also determined by digestion-titration methods described in section 4.2.5. All AP, ENP, and NP determinations are presented in table 4.9.

$$NP(MgCO_3)\ (g\ CaCO_3\ eq\cdot kg^{-1}_{rock}) = 0.09\ \times wt\%\ CO_2 \times\ 22.74 \qquad \text{(eq.8)}$$

By calculation, NP(CO_2) values must be greater than the NP($MgCO_3$) values and may overestimate the actual NP because a substantial amount of the carbonate polyatomic ion (CO_3^{-2}) was bonded with iron, and does not contribute to acid neutralization under oxidizing conditions (see rxns. 4 thru 7). However, siderite was only identified in the two large CO_2 concentration samples (13 and 16) and it is possible that all the samples contained other types of carbonates such as calcite or dolomite at less than the detection limit. Calcite and dolomite were identified in samples from the field rock piles, indicating that Ca- and Mg-carbonates are variably present in the Ely Greenstone greenschist samples collected for these experiments.

For the two large CO_2 concentration samples, the NP($MgCO_3$) values were in reasonable agreement with the peroxide NP(pH 8.3) values. For samples with NP($MgCO_3$) ≤ 0.1, the peroxide NP(pH 8.3) values were in the typical range of 1 to 6 (table 4.9) indicating silicate mineral contributions to the digestion-titration NP values or any carbonates present in the sample had a combined Ca and Mg fraction greater than the 0.09 Mg atomic fraction of eq. 8.

Because the ENP(pH 6) values quantify the observed acid neutralization from the humidity cell experiments, they represent the best measure of the available neutralizing capacity of the rock. Other NP values are measurements of the total NP afforded by near complete digestion of the sample or calculations from solid phase analysis (e.g., NP(CO2) and NP($MgCO_3$)). Therefore, the ENP(pH 6) values provide an experimental standard to which other NP values can be evaluated. For group 1 and 2 samples, the ENP(pH 6) values were greater than the maximum NP($MgCO_3$) values indicating that these samples had a greater Ca and Mg carbonate component than that of eq. 8. For groups 1 and 2, it is unlikely that silicate minerals (e.g., albite and chlorite) contributed substantially to neutralization. This is evident from the greenschist samples containing an abundance of chlorite (a Mg-rich, Ca-poor mineral) and lack of an abundant Ca-rich mineral generating a ENP(pH 6) Mg/Ca ratio between 0.7 and 1.1 (table 4.9). That is, for group 1 and 2 samples the small leachate Mg/Ca ratio cannot be explained by incongruent dissolution of the silicate mineral assemblage, but could be explained by the presence of less than detection limit Ca- and Mg-bearing carbonates. For group 3 samples, the ENP(pH 6) values were less than the maximum NP($MgCO_3$) values indicating that either all of the NP($MgCO_3$) was not available for neutralization or the carbonate had a smaller Mg concentration than that in eq. 8. Samples 14 and 18 NP($MgCO_3$) values may reflect the ENP(pH 6) values if the actual less than detection limit wt% CO_2 values were about 0.0004 and 0.0018, respectively. For group 4 samples, the ENP(pH 6) values were less than the NP($MgCO_3$) values (table 4.9) indicating that 1) the fraction of Mg in the carbonate that was available to maintain a pH of 6 was less than the average value used in eq. 8, and/or 2) not all the carbonate was available for reaction, and/or 3) there was neutralization provided by Ca that was unaccounted for in eq. 8 (leachate pH from sample 16 has not yet decreased to less than 6, but is steadily declining and very near a pH of 6 strongly suggesting little neutralization is available to maintain a pH above 6 despite only about 50% of the NP($MgCO_3$) being consumed).

The ENP(pH 6) values were less than the peroxide NP(pH 8.3) values except for sample 16 (table 4.9). The greater peroxide NP(pH 8.3) values suggest neutralization contribution from non-carbonate minerals during digestion of the samples and/or some carbonate in the humidity cell experiments was unavailable to provide neutralization. For sample 16, because the ENP(pH 6) is greater than the peroxide NP(pH 8.3) value the humidity cell sample may have had a greater amount of carbonate and/or the carbonate mineral may have a greater amount of Ca and Mg.

The peroxide NP(pH 8.3)/$AP_{(ST)}$ values were less than one for samples 6, 7, 8, and all group 3 and 4 samples indicating development of an acidic leachate is likely. The peroxide NP(pH 8.3)/$AP_{(ST)}$ values were greater than one for sample 4 and all group 1 samples indicating development of acidic leachate is unlikely. The peroxide NP(pH 8.3)/$AP_{(ST)}$ values were good indicators of leachate pH for all samples except sample 4 and 16. Sample 4 leachate pH decreased to less than 6 on week 140 (fig. 4.13, table 4.9) and sample 16 leachate pH has yet to decrease to less than 6. However, for sample 16 the current leachate pH trend is decreasing (fig. 4.21) and it is likely pH will decrease to less than 6 in the near future. Therefore, it appears only sample 4 was incorrectly identified by the peroxide NP(pH 8.3)/AP(ST) values. This outcome stresses the importance of long term humidity cell testing for samples with compositions that do not provide a clear indication of whether or not generation of acidic leachate is likely.

The ENP(pH 6) values for group 1 samples were the same as the $\sum$(Ca+Mg) values. For group 2 and 3 samples, the ENP(pH 6) values were less than the $\sum$(Ca+Mg) values indicating silicate mineral acid neutralization and/or kinetically limited carbonate mineral dissolution later in the experiment. The ENP Mg/Ca ratios for the group 2 and 3 samples (except for sample 14 which never had a leachate pH $\geq$ 6) were all either close to or less than 1 indicating that neutralization while leachate pH was $\geq$ 6 was most likely from carbonates with a combined Mg/Ca ratio of about one. After leachate pH decreased to < 6, group 3 samples leachate Mg/Ca ratios were greater than one suggesting some acid neutralization was from silicate minerals, namely chlorite (fig. 4.12). In contrast, group 2 samples maintained small leachate Mg/Ca ratios long after leachate pH had decreased to < 6, indicating kinetically limited carbonate dissolution and some minor neutralization from dissolving silicate minerals long after pH decreased to < 6 (up to about week 380; fig. 4.12). The ENP(pH 6) Mg/Ca ratios were about 11 for group 4 samples consistent with the Mg-rich siderite identified in these samples (table 4.9).

For group 1 samples, the ∑(Ca+Mg) values exceeded the calculated carbonate present with magnesium (as NP($MgCO_3$)), possibly indicating the reported siderite composition may have underestimated the Ca and Mg concentration. This could be due to the zoned nature of the siderite and compositional analyses determined from spot analyses not identifying all types of carbonate present and/or not fully characterizing the separate carbonate growth zones. Alternatively, the ENP(pH 6) Mg/Ca ratios suggest there may have been an entirely different type of carbonate(s) in the group 1 to 3 samples, such as calcite and dolomite.

To assess whether or not carbonate dissolution could be responsible for all the Ca and Mg release, the ∑(Ca+Mg) values were used to calculate hypothetical NP($(Ca,Mg)CO_3$) values by increasing the atomic fraction of the Ca and Mg component of the carbonate beyond the 0.09 atomic fraction determined for the average of siderite analyses and used in eq. 8 (table 4.10). This calculation demonstrated that group 1 and 2 samples total Ca and Mg mass release can be explained by dissolution of a Ca- and Mg-bearing carbonate if the combined atomic fraction of Ca and Mg was 0.37 and the CO_2 concentration of the samples were at the detection limit of 0.05 wt%. A combined carbonate Ca and Mg atomic fraction of 0.37 is 0.05 greater than the maximum Mg and Ca concentration determined by SEM EDS (Appendix 3) and is 0.63 less than that of calcite or dolomite. Thus for group 1 and 2 samples, if there were other carbonates present, such as calcite or dolomite, a smaller siderite Ca and Mg atomic fraction (i.e., less than 0.37) would be required to account for all of the Ca and Mg mass released.

4.3.6 Leachate Concentration of Some Metals

Group 3 samples tended to have the greatest trace metal (Co, Cu, Ni, Zn) leachate concentrations. The greater leachate trace element compositions were likely resultant from greater metal solubility for the smaller leachate pH of these samples. However, leachate from group 2 samples 7 and 8 (both 0.16 wt% S_T) exhibited some of the greatest Co and Ni concentrations, especially after about week 200 (figs. 4.31, and 4.32, respectively). For samples 7 and 8, Co and Ni concentrations increased by up to a factor of five while pH decreased from roughly 5.6 to 5.2 from week 200 to 400. Although pH subsequently decreased comparatively slowly, cobalt and nickel concentrations did not increase further. Leachate Cu concentrations from samples 7 and 8 increased by over one order of magnitude between weeks 200 and 596 (fig. 4.33). Sample 4 (0.10 wt% S_T, from group 2) showed a similar but smaller magnitude increase for Cu, Co and Ni concentrations as that of samples 7 and 8.

Leachate concentrations of Al, Fe, and Si gradually decreased over time and were generally greater for the smaller pH leachates (Appendix 5). Leachate Mn concentration trends were variable among the three groups (fig. 4.34). Group 1 leachate Mn concentrations generally increased over the first 200 weeks and then stabilized. Group 2 leachate Mn concentrations generally increased over the first 100 weeks and subsequently decreased. Group 3 leachate Mn concentrations were initially much greater than those of groups 1 and 2 but decreased over the first 200 weeks into a similar concentration range. Initially, group 4 leachate Mn concentrations sharply increased up to about week 25 after which the concentrations decreased through about week 200 and have since remained relatively constant.

4.4 Field Rock Piles Solid Phase Analyses

Rock from the four field rock piles was analyzed for particle size distribution, major oxide concentration of the bulk rock and particle size fractions, modal mineralogy, and mineral compositions. Sulfur concentration (and CO_2 concentration for rock pile 4) was analyzed from a representative sample from each of the 25 muck boxes during construction to provide an average sulfur concentration for each of the rock piles. More complete analyses of the muck box samples, including sulfur, carbon, CO_2, major oxide components, and trace elements, were performed later by Actlabs. The later sulfur analyses were in excellent agreement with those determined from the initial measurements. The composition of individual particle size fractions was also analyzed. The 25 individual muck box sample compositions from each rock pile and individual mineral composition analyses are in Appendices 6 and 7, respectively.

4.4.1 Particle Size Distribution

For all four field rock piles, less than 5 wt% of the sample was finer than 0.5 mm (table 4.11). Rock piles 1 and 2 contained a similar particle size distribution with greater than 40 wt% consisting of > 64 mm sized particles. In contrast, rock piles 3 and 4 contained a greater percentage of the finer 2.0-6.35 and 6.35-19 mm sized material and about one half of the > 64 mm sized particles as that of rock piles 1 and 2.

4.4.2 Bulk Composition

The average compositions of the rock piles were generally similar indicating broadly similar mineralogy (table 4.12). Similar to the laboratory samples, with increasing rock sulfur concentration, SiO_2 increased and Al_2O_3 decreased, indicating greater sulfur concentration rocks had greater amounts of quartz and smaller amounts of chlorite and muscovite. Bulk rock pile compositions were also calculated from the composition of different particle size fractions weighted by the percent mass in each fraction. Because the rock particles larger than 152 mm were not analyzed, the composition of these larger particles was assumed to be the same as the largest size fraction (64-152 mm) analyzed.

The weighted averages of the particle size fraction compositions were variably in agreement with the average of the muck boxes. The largest discrepancies between the two bulk compositions were the sulfur concentration for rock piles 1 and 2 and the CO_2 concentration of piles 3 and 4 (table 4.12). For rock pile 1 the particle size fraction weighted sulfur concentration was twice that of the muck box average and for rock pile 2 the particle size fraction weighted S_T concentration was 0.36 wt% greater than that of the average value (0.22 wt% S_T) of the muck boxes. For CO_2 concentration, the particle size fraction weighted concentration for rock pile 3 was about twice that of the muck box average and for rock pile 4 the particle size fraction weighted concentration was about four times less than the average from the muck boxes. The discrepancies between muck box average and particle size fraction weighted concentrations is likely due to natural heterogeneity of the samples. The muck box average values are likely more representative because they are the average of 25 separate samples, whereas the particle size fraction weighted averages are from a single sample.

4.4.3 Particle Size Fraction Compositions

All rock pile samples exhibited an increasing CaO, CO_2, and Na_2O concentration with decreasing particle size (table 4.13). The increasing Ca and CO_2 concentration suggest enrichment of Ca-bearing carbonate in the fine particle size fraction. As particle size in piles 2, 3, and 4 increased, SiO_2 concentration generally increased and K_2O decreased. The increasing SiO_2 likely indicates increased quartz abundance in the larger particles and the decreased K_2O concentration may indicate decreased muscovite abundance in the larger fractions. There was no consistent variation of sulfur concentration with particle size. However, samples from rock piles 2 and 4 exhibited a positive correlation between increasing particle size and sulfur concentration illustrating a positive mineral abundance correlation between quartz and pyrite, as was the case with the laboratory samples. The sample from rock pile 1 exhibited a positive correlation between increasing particle size and Al_2O_3 and TiO_2 concentrations whereas samples from rock piles 2, 3, and 4 exhibited the opposite trend.

4.4.4 Mineralogy and Petrology

Mineral compositions and modalities were determined for each field rock pile from the 2.0-6.35 mm size fraction. Random microprobe analyses of each mineral were used in conjunction with the bulk major oxide rock composition to estimate mineral modality for each size fraction. The samples were predominantly comprised of medium grained quartz and fine grained muscovite and chlorite in different proportions among the rock piles. Thus, like the laboratory samples the field rock type is a greenschist. Average mineral compositions are presented in table 4.14 and modal mineralogy in table 4.15. Unlike the laboratory samples, the field rock piles contained trace amounts of calcite and dolomite. Additional minerals identified include: albite, apatite, barite, chalcopyrite, ilmenite, K-feldspar, magnetite, pyrite, REE-phosphates, rutile, spinel, and zircon.

4.5 Field Rock Pile Weathering Experiments

The rock piles are exposed to the atmosphere therefore water and rock reactions and the rinsing of reaction products are dependent on natural weather conditions. As weather controlled tests, the field experiments more closely simulate leachate composition that would be expected from waste rock piles. Due to the high latitude location of the experiment there are a number of months when precipitation is in the form of snow and accumulates on the rock piles. Thus, during the winter months, there was little to no leachate from the rock piles and reaction products would have likely accumulated on the mineral surfaces. These accumulated reaction products may have inhibited sulfide oxidation during the winter. Complete rock pile leachate data are in Appendix 8.

4.5.1 Leachate Flow Rate

Leachate flow rates were calculated based on the sampling frequency which varied from weeks to months. Flow rates were not determined for the annual initial sample because the date leachate was initially collected was not recorded. Flow rates were variable as they are dependent upon the frequency and amount of precipitation. Flow rates generally ranged between 10 to 200 L/day (fig. 4.35). The greatest flow rates typically occurred during the spring and summer months when the largest amounts of precipitation occurred. Variability of flow rates for different collection periods were likely due to differences among the rock pile physical characteristics (porosity and permeability) and internal channelization enabling greater flow rates and limiting storage and evaporation. For the sample collection period (which excludes winter months), annual (2001 to 2011) average flow rates were generally between 40 and 100 L/day with generally less than 20 L/day difference among rock piles.

4.5.2 Leachate Composition

Leachate pH from rock piles 1, 2, and 3 was consistently ≥ 7 except for a single value of 6.8 for rock pile 3 (fig. 4.36). Rock pile 4 leachate pH was above 7 through 2005. For the next four years (2005 to 2008) the first leachate sample collected for each year had a pH < 7 whereas the subsequent leachate samples had a pH > 6. The first leachate pH measurement in 2010 was 4.7 and pH has been between 4 to 5 for all subsequent measurements as of 2011.

Leachate alkalinity was generally greatest for rock piles 1 and 2 ranging between about 50 to 80 mg/L (as $CaCO_3$ eq) for the first 9 years of the experiment (thru 2008) and then slightly decreasing to a range of about 30 to 70 for the next three years (fig. 4.37). Leachate alkalinity from rock pile 3 was generally less than that from rock piles 1 and 2 ranging from about 10 to 60 mg/L after the second year of the experiment (starting year 2002). Leachate from rock pile 4 generally exhibited the smallest alkalinity values ranging from about 10 to 40 mg/L after the third year of the experiment. Over the period of record leachate alkalinity from rock piles 3 and 4 generally decreased with time. In contrast, the alkalinity of leachate from rock piles 1 and 2 appears to have only begun decreasing over the last four and two years, respectively. Because leachate alkalinity from rock pile 4 consistently decreased overtime and became acidic after 10 years of experiment length, the decreasing leachate alkalinity from rock pile 3 suggests a progression towards leachate becoming acidic. This acidic progression is further indicated by the initial annual small pH values (fig. 4.36).

Rock pile leachate SO_4 concentrations generally increased with increasing rock sulfur concentration (fig 4.38). However, rock pile 1 leachate SO_4 concentration decreased with time going from about 100 to 10 mg/L. Leachate SO_4 concentrations from rock pile 4 were relatively constant until pH decreased (around year 2007) at which point the leachate SO_4 concentration approximately doubled. Leachate from rock piles 2 and 3 exhibited no clear SO_4 concentration trends with time.

In general, temporal variations in leachate Ca and Mg concentrations from individual piles were similar to that of SO_4. As with the laboratory samples, leachate concentrations of K and Na rapidly decreased for about the first three years after which the decrease in concentration was gradual.

4.5.3 Solute Release Rates

Annual field release rates were calculated for the entire year although leachate was typically only collected from April to November. Therefore, the first leachate volume collected likely included some of the reaction products that had accumulated over the winter period. Table 4.16 lists the average annual solute release rates, minimum pH , and total annual leachate volume for each rock pile.

Annual SO_4 release rates and rates for individual sampling periods increased with increasing rock sulfur concentration (table 4.16 and fig. 4.32). Annual SO_4 release rates ranged from about 5×10^{-4} to 2×10^{-2} $\mathrm{mmol\cdot kg^{-1}\cdot wk^{-1}}$. For individual sampling periods, SO_4 release rates ranged from about 4×10^{-4} to 6×10^{-2} $\mathrm{mmol\cdot kg^{-1}\cdot wk^{-1}}$ and varied by up to about a factor of ten within a given year (fig. 4.39). For rock piles 1, 2, and 3, variability of the individual sampling rates was greater than the variation of annual rates. Sulfate release rates from rock pile 4 were on average slightly greater after 2006, despite leachate pH not being consistently small throughout an entire year until 2010. This rate increase may be due to localized areas of increased acidity increasing the rate of sulfide oxidation.

Individual sampling period Ca release rates ranged from about 1×10^{-3} to 5×10^{-2} $\mathrm{mmol\cdot kg^{-1}\cdot wk^{-1}}$ and increased with increasing rock sulfur concentration (fig. 4.40). After an initial decrease, Ca release rates were relatively stable from 2002 to 2011. Individual sampling period Mg release rates from rock piles 1, 2, and 3 ranged from about 2×10^{-4} to 4×10^{-3} $\mathrm{mmol\cdot kg^{-1}\cdot wk^{-1}}$, with the first two years of data collection having slightly greater values (fig. 4.41). For rock pile 4, the temporal variation in Mg release rates paralleled that for SO_4 rates, increasing after 2006 to values between about 5×10^{-3} to 2×10^{-2} $\mathrm{mmol\cdot kg^{-1}\cdot wk^{-1}}$. For all rock piles, leachate Mg/Ca molar ratios slightly decreased from 2000 to 2005 (fig. 4.42). Subsequently, leachate Mg/Ca ratios from rock pile 4 increased by about a factor of eight through 2011 and leachate Mg/Ca ratios from rock piles 1 and 3 approximately doubled. The increase in leachate Mg/Ca ratio for rock pile 4 is likely due to dissolution of chlorite at smaller pH values. Rock piles 1 to 3 had leachate Mg/Ca ratios of about 0.1 to 0.2, which is significantly less than that of group 1 and 2 laboratory Mg/Ca ratios (which had values of about 1) possibly indicating a different mineral assemblage responsible for neutralizing the acid generated in the rock piles.

The K and Na release rates decreased rapidly during the first two full years of measurement and then gradually decreased through 2011 (figs. 4.43 and 4.44). Over the experiment time frame K and Na release rates generally ranged from about 2×10^{-4} to 5×10^{-3} $\mathrm{mmol\cdot kg^{-1}\cdot wk^{-1}}$ and 2×10^{-4} to 2×10^{-2} $\mathrm{mmol\cdot kg^{-1}\cdot wk^{-1}}$, respectively. Leachate from rock pile 1 had the largest Na release rates. Because rock pile 1 had the greatest albite mineral abundance, incongruent dissolution of albite was likely responsible for the greater Na release rates.

4.5.4 NP and ENP

Digestion-titration NP values were determined from the 25 muck box samples collected from rock pile 4 (Appendix 9). The average NP(pH 8.3) of these 25 measurements was 6.3 which is roughly half the NP(CO_2) value calculated for this rock pile (table 4.17). This indicates that the carbonate phase(s) in the field rock pile likely contained some impure Ca- and Mg-carbonate although only calcite and dolomite were identified. The ENP(pH 6) for rock pile 4 was 0.86 significantly less than that of either of the NP measurements further indicating the occurrence of an impure Ca- and Mg-carbonate and that the digestion-titration NP values likely included a substantial amount of neutralization from silicate minerals and ferrous iron from carbonate dissolution (table 4.17). The substantially smaller ENP(pH 6), as compared to the NP(pH 8.3) and NP(CO_2) values, could also indicate that a significant proportion of the carbonate in the rock pile may not have been available for reaction. That is, the carbonate could be encased in larger rock particles whereas the pyrite may be preferentially exposed along rock surfaces that parted along the natural foliation of the greenschist. The NP/AP ratios for rock piles 2, 3, and 4 were less than one indicating high potential for generating an acidic fluid despite only leachate from rock pile 4 being acidic. For rock piles 2 and 3, the combination of a slower rate of acid generation (inferred from the relatively smaller SO_4 release rates as compared to rock pile 4) and presence of Ca and Mg carbonates are likely slowing the progression towards acidic leachate development. It is possible that with time leachate from rock piles 2 and 3 will become acidic.

4.5.5 Temperature and O_2 Measurements

The internal rock pile temperature and O_2 concentration was measured intermittently from 2000 to 2009 (Appendix 10). Rock pile average internal temperatures were between 9 and 12 °C. Internal rock pile temperatures fluctuated seasonally with the greatest temperature of 23.9 °C being measured in early August and the coldest temperature of −2.1 °C measured in early May. No temperature measurements were recorded for the months of January and February, when temperatures could have been at the smallest values. Oxygen concentrations within the rock piles averaged between 18 to 20 vol%, except for the lower sample ports of rock piles 3 and 4 which had average O_2 concentrations of about 15 vol%. Although the average oxygen concentrations were less than atmospheric values the concentrations are substantially greater than zero indicating the system was not oxygen deficient.

4.6 Field Tanks Dolostone Addition Experiments

The dolostone and rock from the six field tanks were analyzed for particle size distribution, sulfur and CO_2 concentration, major oxides and trace elements. All six tanks in the dolostone addition experiment used the same rock as that in rock pile 4 (0.67 wt% S_T) crushed to less than 50.8 mm (2 in). Tanks 1 and 6 were control tanks with no dolostone added, whereas tanks 2 thru 5 had dolostone added. Including the NP from the greenschist, tanks 1 and 6 had NP/AP ratios of 0.41, tanks 2 and 5 had NP/AP ratios of 1.4 and tanks 3 and 4 had NP/AP ratios of 3.3. Complete tank leachate data is in Appendix 11.

4.6.1 Particle Size Distribution

Particle size distributions among the tank rock were generally similar with average particle size diameters ranging from 22 to 28 mm (table 4.18). The crushed dolostone used for treatment was all less than 4.76 mm in diameter with an average diameter of 2 mm.

4.6.2 Bulk Compositions

The composition of the greenschist placed in the tanks was generally similar to that of the rock pile 4 except for S_T wt% which was consistently less than that of rock pile 4 (table 4.19). The average wt% S_T of the six tanks was 0.49 which is 0.14 wt% S_T less than the average of rock pile 4. The major oxide composition of the dolostone had a CO_2 concentration of 41.6 wt% and a molar Mg/Ca ratio of 0.95 demonstrating the rock is predominantly composed of dolomite with minor amounts of quartz (9.68 wt% SiO_2).

4.6.3 Leachate Composition

Leachate pH for the control tanks (tanks 1 and 6) was greater than or equal to 7 for the first full three years of the experiment (fig. 4.45). In 2004 pH decreased from about 7 to 5 and by 2006 pH was consistently less than 5. For tanks with dolostone added leachate pH was consistently greater than 7 from 2000 to 2011.

Consistent with pH data, leachate alkalinity from the control tanks rapidly decreased over the first five years after which leachate from these tanks was acidic (fig. 4.46). Leachate alkalinity from tanks 3 and 4 was generally between 40 and 80 mg/L (as $CaCO_3$ eq) whereas leachate from tanks 2 and 5 was generally between 20 and 60 mg/L, reflecting the smaller amount of dolostone added to tanks 2 and 5.

4.6.4 Solute Release Rates

Annual SO_4 release rates were generally within the range of 5.0×10^{-3} to 2.5×10^{-2} $mmol\cdot kg^{-1}\cdot wk^{-1}$ and did not vary significantly among the six tanks despite the substantially smaller pH for the control tanks later in the experiment (table 4.20). Annual Ca release rates were initially similar to the SO_4 release rates (between about 1.0×10^{-2} to 1.4×10^{-2} $mmol\cdot kg^{-1}\cdot wk^{-1}$), but subsequently decreased to relatively stable values by 2005 (between about 1×10^{-3} to 5×10^{-3} $mmol\cdot kg^{-1}\cdot wk^{-1}$). In contrast, Mg release rates were smaller (between about 2×10^{-4} to 1.7×10^{-3} $mmol\cdot kg^{-1}\cdot wk^{-1}$) and relatively consistent throughout the experiment (table 4.19). The individual sampling period SO_4 release rates for all tanks gradually decreased over time and ranged from about 4×10^{-3} to 1×10^{-1} $mmol\cdot kg^{-1}\cdot wk^{-1}$ (fig. 4.47). Leachate Mg/Ca molar ratios increased from 2001 to 2009 and appear to have stabilized from 2010 to 2011 (fig. 4.48). After 2007 the leachate Mg/Ca ratio for the control tanks increased at a slower rate than that of the dolostone addition tanks.

5. DISCUSSION

5.1 Sulfate Release Rate and Rock Sulfur Concentration Relationship

For the laboratory and field experiments SO_4 release rates increased with increasing rock sulfur concentration. This relationship was expected because rocks with a greater sulfur concentration generally have a larger pyrite surface area available for reaction. The relationship between sulfur concentration and SO_4 release rates was quantified by linear regression. The approach inherently assumes a linear correlation and also included the assumption that a zero wt% S_T rock will have a SO_4 release rate of zero.

For the laboratory experiments the average annual release rate from years 2001 to 2003 (weeks 49-205) were used to quantify the sulfur concentration and SO_4 release rate relationship. This interval was selected because it covers a relatively stable period of SO_4 release before sulfide depletion became a dominant control of the release rates. Because of the disparity in leachate pH among the sample groups, two separate regressions were performed (fig. 5.1). First, groups 1, 2 and 4 were combined to mathematically describe the SO_4 release rate and rock sulfur concentration correlation for relatively small rock sulfur concentrations and/or leachate with a pH generally greater than 5.5. Second, group 3 samples were combined to mathematically describe the SO_4 release rate and sulfur concentration correlation for a leachate pH of about 3.5. Linear regression of the group 1, 2 and 4 average SO_4 release rates resulted in equation 9 with an r^2 value of 0.92 and regression of the group 3 values produced equation 10 with an r^2 value of 0.63.

$$Groups\ 1, 2, and\ 4\text{:}\ SO_4\ release\ rate\ (mmol \cdot kg_{rock}^{-1} \cdot wk^{-1}) = 0.14 \times S_T\ wt\% \qquad \text{eq. 9}$$

$$Group\ 3\text{:}\ SO_4\ release\ rate\ (mmol \cdot kg_{rock}^{-1} \cdot wk^{-1}) = 0.27 \times S_T\ wt\% \qquad \text{eq. 10}$$

For the field rock piles, the annual SO_4 release rate from 2001 to 2011 for rock piles 1 to 3 and 2001 to 2006 for rock pile 4 were used to mathematically describe the positive correlation between rock sulfur concentration and SO_4 release rate (fig. 5.2). The shorter interval for rock pile 4 was selected to exclude the interval over which leachate pH was smaller than that of the other rock piles. For these time periods, leachate pH from all the rock piles ranged between about 7 to 7.5. Regression of this data set resulted in equation 11 with an r^2 value of 0.99.

$$Group\ 3\text{:}\ SO_4\ release\ rate\ (mmol \cdot kg_{rock}^{-1} \cdot wk^{-1}) = 0.02 \times S_T\ wt\% \qquad \text{eq. 11}$$

5.2 Sulfate Release Rate and Leachate pH Relationship

Two distinct SO_4 release rate and pH trends are represented by the laboratory experiment data (fig. 5.3). For groups 1 and 2, SO_4 release rates increased with increasing pH over the range of about 4.5 to 8. In contrast, SO_4 release rates from group 3 samples increased as pH decreased from 4.5 to 3. The greater SO_4 release rate for group 2 samples over group 1 samples for the same pH is likely due to the greater sulfide surface area afforded by the greater sulfur concentration for group 2 samples. These two trends can be explained by the pyrite oxidation rate dependence on the type of oxidant and fluid pH characterized by Williamson and Rimstidt (1994).

For pyrite oxidation by oxygen there is a small inverse relationship to H^+ and for pyrite oxidation by ferric iron the oxidation rate depends on the ratio of ferric to ferrous iron (see eqs. 1 and 2). If the total aqueous iron concentration is assumed to be saturated with respect to ferrihydrite, the activity of ferric and ferrous iron can be determined by geochemical modeling and the resultant values used to calculate pyrite oxidation rates by ferric iron from equation 2. Inherent to this calculation is the assumption that the various iron species are in equilibrium with ferrihydrite which may not be representative if the reaction of ferrous to ferric iron is slow. Singer and Stumm (1970) identified the oxidation of ferrous iron as the rate limiting step in pyrite oxidation. So pyrite oxidation rates calculated from ferrihydrite equilibrium would represent maximum values since a kinetically slow ferrous to ferric reaction would result in smaller ferric iron activity. However, if bacteria were present to catalyze the ferrous to ferric iron reaction the calculated pyrite oxidation rates would not necessarily represent maximum rates.

The sulfide oxidation rates calculated by the equations of Williamson and Rimstidt (1994), assuming modeled ferrihydrite equilibrium, exhibit the two same trends as the SO_4 release rate trends from the humidity cell data suggesting that the two different trends are the result of oxidation by O_2 and ferric iron under different fluid pH (compare fig. 2.1 with fig. 5.3). The transition between the two lab experiment trends lies near a pH of 4.5 which is approximately the maximum pH value that is commonly reported for increased stability of ferric iron. Despite the similarities in sulfide oxidation or SO_4 release rate and fluid pH trends between the calculated and laboratory data, additional factors are likely partly responsible for decreasing SO_4 release rate trends. Of particular importance is the decrease in sulfide surface area and neutralization capacity overtime (see section 4.3.4 for a more detailed discussion). Explicitly, as the availability of reactive sulfide surface area decreases the SO_4 release rate decreases and as the sample neutralization capacity decreases leachate pH decreases. These two processes may explain the observed late SO_4 release rate and pH decrease after about week 100 for the group 1 and 2 samples (fig 5.3). The opposite trend (i.e., SO_4 release rate increasing with decreasing pH) was observed for the group 3 samples over the first 100 weeks (compare figs. 4.21 and 4.22). For this trend, the reactions occurring in the group 3 humidity cell samples were apparently consistent with the ferric iron oxidation trend of Williamson and Rimstidt (1994).

Because pH is still declining for samples 6, 7, 13, and 16 (fig. 4.8) it is possible that the dominant oxidant could switch to ferric iron resulting in a substantial increase of the rate of sulfide oxidation and resultant acid generation. An important difference between the humidity cell experiments and the experiments used to derive the rate equations of Williamson and Rimstidt (1994) is that the humidity cell experiments included depletion of the available sulfide surface area and may have included bacterially mediated sulfide oxidation. Presumably, the depletion of sulfide in the humidity cell samples would result in smaller sulfide oxidation rates, especially as the experiment progresses, than the rate predicted by Williamson and Rimstidt (1994).

5.3 Relationship Between Leachate pH and Mineralogy

Laboratory sample leachate pH generally decreased with increasing sulfur concentration (except for the two large CO_2 concentration samples). The initial decrease in leachate pH was much greater for group 3 samples despite only a 0.04 wt% S_T increase between samples 8 and 10. Because the increase in rock sulfur concentration was small in comparison to the change in leachate pH some other factor most likely contributed to the very different leachate pH values between group 2 and 3 samples (fig. 4.6).

A possible factor for the large difference in leachate pH may have been the much smaller chlorite abundance of group 3 samples. Decreasing the modal proportion of chlorite relative to pyrite will decrease the net neutralizing capacity of a rock because leachate acidity is determined by the difference between the rate of acid production and the rate of acid neutralization. The pH dependence on mineral abundances can be numerically expressed by dividing the wt% S_T by the modal percent of chlorite. This normalization calculation shows that samples with a wt% $S_T \geq 0.2$ (all group 3 samples) have greater than twice the amount of chlorite-normalized wt% S_T (table 4.6). Thus, in addition to increasing sulfur concentration the associated decrease in chlorite abundance may have been an important factor for the faster onset to a minimum leachate pH for group 3 over group 2 samples (see fig. 4.6). In particular, the substantial difference in pH time series trend and minimum pH for the relatively similar sulfur concentration samples 8 (0.16 wt% S_T) and 10 (0.2 wt% S_T). The influence of the overall mineral concentration on leachate pH highlights the importance of fully characterizing rock samples for humidity cell tests to accurately interpret the experiment results.

5.4 Implications of Ca, K, Mg, Na, and SO_4 Release Rate Trends to Mineral Reactions

Two major temporal trends are apparent for the SO_4, Ca, Mg, Na, and K solute release rates from the laboratory samples. One trend is an overall gradual release rate decrease for SO_4, Ca, and Mg and the other trend is a rapid release rate decrease for K and Na (fig. 5.4). These two trends suggest two distinct types of water and rock reactions have occurred during the laboratory experiment.

The gradual Ca, Mg, and SO_4 release rate decrease indicates a sustained set of water and rock reactions that have continued for over 12 years. For SO_4, the gradual decrease over time is likely due to reduced availability of reactive pyrite surface area for oxidation. Decreasing pyrite oxidation, in effect, decreases the release of Ca and Mg from the acid neutralizing minerals. For a fluid pH less than about 5, chlorite is likely contributing more towards buffering pH and releasing Mg into solution. Dissolution of chlorite is apparent from the greater Mg/Ca ratios and smaller leachate pH of group 3 samples (fig. 4.12).

The release of Ca and Mg from group 1 and 2 samples can be explained by dissolution of small amounts of carbonate minerals. The greenschist rock samples (table 4.3) had Mg/Ca molar ratios between 6 and 105 with an average of about 40. Additionally, SEM EDS analyses indicated very small Ca concentrations in all the major mineral phases identified. Despite the small Ca concentrations of the whole rock and minerals, leachate Mg/Ca ratios were about one for groups 1 and 2, one to ten for group 3 and about ten for group 4. The greater than one Mg/Ca ratios for groups 3 and 4 are likely resultant from incongruent dissolution of chlorite and Mg-siderite, respectively. The substantially smaller leachate Mg/Ca ratio for groups 1 and 2 imply a greater Ca release relative to that of Mg. However, for group 1 and 2 samples no Ca-bearing mineral was identified that could explain the small leachate Mg/Ca ratio from the Mg-rich greenschist samples.

The discrepancy between leachate Mg/Ca ratios and whole rock composition Mg/Ca ratios can be explained by a couple reaction scenarios. These scenarios include: 1) the mineral releasing Ca had a solubility or surface area about 40 times greater than that of the mineral(s) responsible for releasing Mg, 2) Ca and some Mg are released into solution from the same mineral which has a Mg/Ca molar ratio of about one, or 3) a combination of a little Ca and Mg release from silicates and Ca and Mg release from some other mineral in a proportion resulting in the average Mg/Ca ratio of one. Because Ca-bearing silicate mineral phases in the greenschist samples (such as, albite, apatite, and chlorite) have either small abundances or small Ca concentrations and dissolution rates orders of magnitude less than carbonates, it is most likely the majority of Ca released was from a carbonate mineral. Some SEM EDS siderite analyses had appreciable Ca concentrations (Appendix 3) and, although no calcite or dolomite was observed in the laboratory samples, calcite and dolomite were identified in the field rock piles. Furthermore, the total Ca and Mg released from group 1 and 2 samples could be explained by dissolution of less than detection limit quantities of carbonate (see section 4.3.5).

However, despite the bulk rock and leachate compositions suggesting the presence of less than detection limit Ca- and Mg-carbonate(s), the leachate pH of group 1 and 2 samples is less than that expected for Ca- and Mg-carbonate equilibria. That is, a Ca- and Mg-carbonate mineral typically would buffer a fluid to a pH around 8 whereas the leachate pH of group 1 and 2 samples was commonly less than 8. Thus, if a Ca- and Mg-bearing carbonate was responsible for Ca and Mg release from the rock the reaction must not have been in equilibrium and was instead kinetically inhibited. The inhibition could be due to: 1) limited mineral surface exposure in the rock matrix, 2) reaction product coatings on the carbonate mineral surfaces, 3) limited transport of acidic reaction products from the pyrite surfaces to the carbonate surfaces, or 4) a combination of the former three reaction inhibitions in varying proportions. For a kinetically inhibited carbonate dissolution scenario, the Ca- and Mg-bearing carbonate would neutralize acid to the capacity allowed by the limited experimental reaction time and available carbonate surface area. These reaction limitations could then result in a leachate pH less than that expected for a carbonate buffered fluid. An important factor for the apparent kinetically limited carbonate dissolution is related to the experimental protocol of allowing only 10 minutes for the rinse water to fill the cell prior to draining. If there were a longer hold time for the rinse water in the cell, carbonate mineral dissolution equilibria may be attained. Therefore, for group 1 and 2 samples the leachate pH of less than eight and small leachate Mg/Ca ratio is best explained by kinetically inhibited dissolution of Ca- and Mg-bearing carbonates.

For the second concentration trend, Na and K release rates for all samples decreased by about three and two orders of magnitude, respectively, during the first 200 weeks of the experiment (fig. 5.4). This decrease is much more rapid than the decrease observed for Ca, Mg, and SO_4 over the first 200 weeks of the experiment indicating a much different type of reaction. The greater K and Na release rate decrease can be explained by mineral surface ion exchange of K and Na and incongruent dissolution of the finest sized muscovite and albite mineral grains.

Surface ion exchange and incongruent dissolution of the finest sized mineral grains is indicated by the relationship between leachate pH and K and Na concentration. For all the laboratory samples, as leachate pH decreased the release of K and Na also decreased. This is opposite of the well-established fundamental relationship of silicate mineral dissolution rates increasing with decreasing pH under acidic conditions (fig. 2.2). Thus, despite the large muscovite abundance of the samples, the K concentration decrease appears to be more likely related to rapid mineral surface ion exchange and/or early incongruent dissolution of extremely fine grained muscovite grains instead of sustained incongruent dissolution of muscovite. Similarly, the rapid decrease in Na concentration is likely due to surface ion exchange and/or incongruent dissolution of extremely fine grained albite.

In summary, the gradual release rate decrease for SO_4, Ca, and Mg likely represents pyrite oxidation and incongruent dissolution of silicate minerals and magnesian siderite (and Ca- and Mg-carbonate dissolution for groups 1 and 2), whereas the rapid release rate decrease for K and Na is likely due to early cation surface exchange and/or incongruent dissolution of extremely fine grained mineral particles.

5.5 Scaling SO_4 Release Rates from the Laboratory to the Field

Extrapolating laboratory determined release rates to the field requires scaling to account for the differences in the chemical and physical conditions between the laboratory and field settings. Some important differences between laboratory and field conditions include the particle size distribution, temperature, frequency of rinsing events, and extent of water contact. When both laboratory kinetic tests and larger field scale weathering tests are conducted on the same rock an empirical solute release rate scale factor can be calculated by dividing the field rate by the laboratory rate (eq. 12). In this case, the calculated scale factor represents the value a laboratory determined release rate would be multiplied by to predict the field release rate.

$$Scale\ Factor = field\ release\ rate/laboratory\ release\ rate \qquad \text{eq.12}$$

The similarity in rock type between the field and laboratory components of this study provide the opportunity to calculate empirical scale factors. Two different methods were used to calculate empirical scale factors for the Ely Greenstone greenschist. For the first method, average SO_4 release rates for the field rock piles and select individual laboratory samples were used to calculate a scale factor for different rock sulfur concentrations. For the second method, the slope of the linear regression lines derived from the SO_4 release rate dependence on wt% S_T for the field and laboratory experiments (presented in section 5.1) were used to calculate a scale factor. This scale factor is referred to as a comprehensive scale factor because it includes a range of different rock sulfur concentrations. Scale factors for Ca and Mg release rates were not calculated due to large differences in CO_2 concentration and carbonate mineralogy between laboratory and field rock compositions.

For the first method, the scale factor calculations used average SO_4 release rates of an individual laboratory sample with a similar sulfur concentration as that of the field rock piles and tanks (table 5.1). Scale factors were calculated by dividing the average annual field SO_4 release rate by the average laboratory rate from table 5.1. The individual rock pile/laboratory scale factor for rock piles 2 to 4 were relatively consistent ranging from 0.05 to 0.08, whereas the scale factor calculated for rock pile 1 was 0.2 (table 5.2). For the second method, the comprehensive scale factor was calculated as the ratio of the slopes of equations 11 and 9, a value of 0.14.

The individual rock pile/laboratory scale factors for rock piles 2, 3 and 4 were substantially less than that of rock pile 1 and the comprehensive scale factor. For the individual rock pile/laboratory scale factors, the difference in scale factor was likely related to the rock sulfur contents and leachate pH ranges the field and laboratory SO_4 release rates were calculated from. The rock pile/laboratory scale factors for rock piles 2, 3, and 4, were calculated from a leachate pH that was substantially smaller than the field leachate pH (especially for rock pile 2 and 3; table 5.1). Because SO_4 release increases with decreasing pH (for fluid pH less than about 5), using a laboratory SO_4 release rate calculated from a small leachate pH and a field SO_4 release rate from a larger leachate pH would result in an erroneously small scale factor. Application of this erroneous scale factor would result in over predicting field scale SO_4 release rates. Therefore, an important consideration when developing scale factors is accounting for the range in pH from which the solute release rate is calculated to that expected in the field. The greater similarity in leachate pH for determining the comprehensive scale factor and individual scale factor for rock pile 1 provide a basis for considering these the most accurate rock pile/laboratory scale factors for the Ely Greenstone greenschist.

Scale factors for the rock pile/tank and tank/laboratory were opposite of the scale relationship determined from the rock pile/laboratory values (table 5.2). That is, scaling from the tank to field would require increasing the SO_4 release rate of the rock pile. The irregularity of the tank scale factors may be due to the SO_4 release rates for the tanks not increasing when pH decreased to less than about 5 as was observed for the field rock piles and laboratory humidity cells. The tank experiments also had numerous flow related problems and a combined measured average S_T concentration of 0.49 wt% as compared to the 0.63 wt% of rock pile 4. A combination of an irregular sulfur concentration and SO_4 release rate relationship, flow problems, and measured wt% S_T concentrations substantially less than that of rock pile 4 likely contributed to the abnormal tank scale factors.

Importantly, the scale factors presented are only applicable to scaling for rock piles similar in composition and size to the rock piles in this study. For significantly larger rock piles it is likely that scale factors would be smaller due to the increased differences between the laboratory and field settings. For the comprehensive scale factor, because the calculation only included data for fluid pH above about 5.5, this scale factor is not directly applicable for smaller pH fluids. However, because this comprehensive scale factor incorporates rates over a range of sulfur concentrations it is likely on average more accurate than those calculated from individual laboratory experiments.

5.6 Implications for Waste Rock Management

Laboratory samples indicate that small CO_2 concentration greenschists with a wt% $S_T \leq 0.05$ will generally not produce a leachate with a pH less than about six. In addition, because natural rainfall (and the rinse water used in this experiment) has a pH of 5.6 the samples with ≤ 0.05 wt% S_T were net neutralizing. Samples with wt% S_T values between 0.1 and 0.16 produced a leachate pH minimum between about 4.75 and 5.5 and samples with wt% S_T values between 0.2 and 1.22 produced a leachate pH minimum between about 3 and 4.5. Combined, these three sulfur concentration ranges provide thresholds for which the greenschist can be categorized to assign a level of environmental risk for extraction of greenschist and subsequent disposal. Based on the laboratory experimental results three levels of environmental risk were assigned as low, moderate and high (table 5.3). Greenschist with a high environmental risk will require the greatest amount of management such as encapsulation, subaqueous disposal, alkaline addition treatment, effluent treatment, leachate monitoring, etc. These environmental risk guidelines are only representative for the specific greenschist rock type tested in this study. For other rock types, these sulfur concentration ranges may generate a fluid with a significantly different pH. For the large CO_2 concentration samples, magnesian siderite appears to be an ineffective acid neutralizing mineral. The ineffective buffering ability is apparent from the initial pH decline for the group 4 samples (fig. 4.21). It is not clear why pH decreased for these samples despite having an apparent neutralization potential that should have neutralized acid initially. This result demonstrates characterization of the carbonate mineral type(s) is critical for accurate assessment of the acid generating potential of a rock.

For the field rock piles, leachate pH was less than 6 for only rock pile 4 (0.63 wt% S_T). However, assuming a pure Ca and/or Mg carbonate and all the sulfur exists as sulfide, the $NP(CO_2)/AP(S_T)$ ratios are less than one for rock piles 2, 3, and 4 (table 4.17) indicating that leachate from rock piles 2 and 3 will eventually become acidic. Explicitly, after the available carbonate has dissolved and the rate of silicate dissolution is not sufficiently fast to neutralize the acid generated by sulfide oxidation leachate from rock piles 2 and 3 will progress towards an acidic pH. Alternatively, if the surfaces of the sulfides are sufficiently covered to inhibit sulfide oxidation rate to the point that the remaining carbonate and/or silicates could neutralize acid generated the resultant leachate would not become acidic. Continuation of the rock pile experiments will provide useful information on the time required for the onset of acidic conditions for carbonate- and sulfide-bearing greenschist in a field setting.

6. ACKNOWLEDGEMENTS

Funding for this report was provided by state and industry contributions to the Iron Ore Cooperative Research and Cooperative Environmental Research (CER) programs. Previous funding was provided by the US BLM Utah State office, the US BLM Applications of Science program, and the Minnesota CER program, and the Minnesota Minerals Coordinating Committee. Patrick Geiselman, Anne Jagunich, and John Folman conducted the experiments, with supervision by David Antonson. Erin Phillips, Bryn Milne, and Jennifer Engstrom analyzed the samples by XRD and SEM-EDS analysis under the guidance of Karl Wirth and Jeff Thole at Macalester College.

REFERENCES

APHA (American Public Health Association), American Water Works Association, Water Environment Federation. 1992. Standard Methods for the Examination of Water and Wastewater, 18th edition. American Public Health Association, Washington, D.C.

Blowes, D.W., Ptacek, C.J., 1994. Acid-neutralization mechanisms in inactive mine tailings. In The Environmental Geochemistry of Sulfide Mine-Wastes. Eds. D.W. Blowes and J.L. Jambor, Mineralogical Association of Canada Short Course Handbook, v. 22, p. 271-292.

Bolin, C.L., Seal, T., Jung, S.J. 2000. Open pit ore control for cyanide heap leaching. Presented at the Society of Mining, Metallurgy and Exploration Inc. Annual Meeting & Exhibit, Salt Lake City, February 28 to March 1, 2000, Open Pit Mining Session II.

Card, K.D., and Ciesielski, A. 1986. DNAG subdivisions of the Superior Province of the Canadian Shield: Geoscience Canada, v. 13, no. 1, p. 5-13.

Day, S.J. 1994. Evaluation of acid generating rock and acid consuming rock mixing to prevent acid rock drainage. In Proceedings of the International Land Reclamation and Mine Drainage Conference and Third International Conference on the Abatement of Acidic Drainage, Pittsburgh, PA, April 2529, 1994. V2. United States Department of the Interior, Bureau of Mines Special Publication SP 06A-94. p. 77-86.

Donovan, J.J., and Ziemkiewicz, P.F. 1994. Early weathering behavior of pyritic coal spoil piles interstratified with chemical amendments. In Proceedings of the International Land Reclamation and Mine Drainage Conference and Third International Conference on the Abatement of Acidic Drainage, Pittsburgh, PA, April 25-29, 1994. VI. United States Department of the Interior, Bureau of Mines Special Publication SP 06A-94. p. 119-128.

Eger, P., Lapakko, K.A. 1985. Heavy metals study: Progress report on the field leaching and reclamation program: 1977-1983. Minnesota Department of Natural Resources. 53p.

Eary, E.L., Schramke, J.A. 1990 Rates of inorganic oxidation reactions involving dissolved oxygen. In Chemical Modeling of Aqueous Systems II, Melchior, D.C. and Basset, R.L. eds. ACS Symposium series 416, American Chemical Society, Washington, D.C. p. 379-396.

Hoffman, E.L. 1992. Instrumental neutron activation in geoanalysis. Journal of Geochemical Exploration, v. 44. p. 297-319.

Janzen, M.P., Nicholson, R.V., Scharer, J.M. 1997. The role of enhanced particle surface area, crystal structure and trace metal content on pyrrhotite oxidation rates in tailings. In Proceeding of the Fourth International Conference on Acid Rock Drainage. Vol. 1. Vancouver, British Columbia, May 31 - June 6, 1997.

Janzen, M.P., Nicholson, R.V., Scharer, J.M. 2000. Pyrrhotite reaction kinetics: reaction rates for oxidation by oxygen, ferric iron, and for nonoxidative dissolution. Geochimica et Cosmochimica Acta, v. 64, p. 511-1522.

Kempton, J.H., Swanson, D., Bennett, M., MacDonald, R., Locke, W., Gillespie, c., Lechner, M., Maley, P. 1997. Application of probabilistic acid/base accounting to minimize waste-rock handling in semi-arid climates. In Proceedings of the Fourth International Conference on Acid Rock Drainage, Vancouver, B.C. Canada, May 31 to June 6, V. 2, p. 871-888.

Lapakko, K.A. 1994. Comparison of Duluth Complex rock dissolution in the laboratory and field. In Proc. Third International Conference on the Abatement of Acidic Drainage, April 25-29, 1994, Pittsburgh, PA. Vol 1. p. 419-428.

Lapakko, K.A., Antonson, D.A, Wagner, J.R 1997. Mixing of limestone with finely-crushed acid producing rock. In Proceedings of the Fourth International Conference on Acid Rock Drainage, Vancouver, B.C., Canada. May 31-June 6, 1997. v.3. p. 1345-1360.

Lapakko, KA, Antonson, D.A, Wagner, J.R. 2000. Mixing of rotary kiln fines with finely-crushed acid-producing rock. In Proceedings of the Fifth International Conference on Acid Rock Drainage, Denver, CO. SME, Littleton, CO. p. 901-910.

Lapakko, K.A., Antonson, D.A. 2001. Laboratory drainage pH and sulfate release rates from Archean Greenstone rock. In Securing the Future, International Conference on Mining and the Environment. June 25-July 1, Skellefteå, Sweden. p. 384-393.

Lapakko, K.A., Antonson, D.A. 2002. Drainage pH, acid production, and acid neutralization for Archean greenstone rock. Preprint 02-73 In Proc. 2002 SME Annual Meeting, February 25-27, Phoenix, AZ (CD-ROM). Soc. For Mining, Metallurgy, and Exploration, Inc. Littleton, CO.

Lapakko, K.A., Antonson, D.A. 2006. Pyrite oxidation rates from humidity cell testing of greenstone rock. In Proc. 2006, 7th ICARD, March 26-30, 2006, St. Louis MO. Published by ASMR, 3134 Montavesta Rd., Lexington, KY 40502. p. 1007-1025.

Lapakko, K.A., Antonson, D.A., Johnson, A. 2001. Archean greenstone laboratory and field dissolution experiments. Controlling mine drainage problems - New approaches for waste rock stockpiles. Final Report to Minerals Coordinating Committee. 30 June 2001. Minnesota Department of Natural Resources. 79 p. plus appendices.

Lapakko, K.A., Antonson, D.A., Johnson, A. 2002. Controlling mine drainage problems - New approaches for waste rock stockpiles. First year progress report to the Minnesota Minerals Coordinating Committee, 30 June 2002. Minnesota Department of Natural Resources. 67 p. plus appendices.

Lapakko, K.A., Antonson, D.A., Folman, J.T., Johnson, A. 2003. Controlling mine drainage problems - New approaches for waste rock stockpiles. Final report to the Minnesota Minerals Coordinating Committee, 30 June 2003. Minnesota Department of Natural Resources. 77 p. plus appendices.

Lapakko, K.A., Antonson, D.A., Folman, J., Engstrom, J.N. 2004a. Archean greenstone laboratory dissolution experiment. Final Report on Contract JSP012018 to the U.S. Bureau of Land Management, Salt Lake City Office. 93 p. plus appendices.

Lapakko, K.A., Antonson, D.A., and Engstrom, J.N. 2004b. Analytical screening of abandoned waste rock piles. Report on Contract No. DACW45-02-P-0212 to US Army Corps of Engineers by the Minnesota Department of Natural Resources. 91 p. plus appendices.

Lapakko, K.A., Antonson, D.A. 2012. Sericite and chlorite dissolution rates from humidity cell testing of greenstone rock. 9th ICARD, May 20-26, 2012, Ottawa, Canada. 13 p.

Lapakko, K.A., Olson, M.C., Antonson, D.A. 2013. Dissolution of Duluth Complex rock from the Babbitt and Dunka Road prospects: Eight-year laboratory experiment. Minnesota Department of Natural Resources. 106 p. plus appendices.

Lapakko, K.A., White, W.W. III. 2000. Modification of the ASTM D5744-96 kinetic test. In Proc. from the Fifth International Conference on Acid Rock Drainage. SME, Littleton, CO. p. 631-639.

Mehling, P.E., Day, S.J, Sexsmith, K.S. 1997. Blending and layering waste rock to delay, mitigate or prevent acid generation: A case study review. In Proceedings of the Fourth International Conference on Acid Rock Drainage, May 31 - June 6, 1997, Vancouver, British Columbia, Canada. p.951-969.

MEND. 1994. Long Term Acid Generation Studies: Cinola Project, Queen Charlotte Islands, British Columbia. Norecol, Dames and Moore. MEND Report 1.19.1.

Morin, K.A., Hutt, N.M. 2000. Discrete-zone blending of net-acid-neutralizing and net-acid-generating rock: Avoiding the argument over appropriate ratios. In Proceedings of the Fifth International Conference on Acid Rock Drainage, Denver, CO. SME, Littleton, CO. V. 2. p.797803.

O'Hagan, M. 1986. Admixing limestone with rocks having low, medium and high sulfur content to mitigate acid mine drainage. M.S. Thesis. Univ. South Carolina. 103 p.

Palandri, J.L., Kharaka, Y.K. 2004. A compilation of rate parameters of water-mineral interaction kinetics for application to geochemical modeling. U.S. Geological Survey Open File Report 2004-1068. U.S. Geological Survey in cooperation with the National Energy Technology Laboratory - United States Department of Energy. 70 p.

Peterson, D.M., and Patelke, R.L. 2003. National underground science and engineering laboratory (NUSEL): Geological site investigation for the Soudan mine, northeastern Minnesota. Natural Resources Research Institute, Technical Report NRRI/TR-2003/29. 87 p., 3 pl.

Price, W.A., 2009. Prediction manual of drainage chemistry from sulphidic geologic materials. MEND Report 1.20.1.
http://wman-info.org/resources/technicalreports/MENDPredictionManual-Jan05.pdf/file_view

Rose, A.W., Daub, G.A., 1994. Simulated weathering of pyritic shale with added limestone and lime. In Proceedings of the International Land Reclamation and Mine Drainage Conference and Third International Conference on the Abatement of Acidic Drainage, Pittsburgh, PA, April 25-29, 1994. V.2. U.S. Dept. Interior, Bureau of Mines Special Publication SP06A-94. p. 334-340.

Scott, W.W. 1942. Scott's standard methods of chemical analysis. D. Van Norstrand Co. Inc., New York, NY.

Singer, P.C., Stumm, W. 1970. Acid mine drainage: The rate determining step. Science, 167. p. 1121-1123.

Skousen, J., Renton, J, Brown, H., Evans, B., Leavitt, B., Brady, K., Cohen, L., Ziemkiewicz, P. 1997. Neutralization potential of overburden samples containing siderite. J. Env. Qual., 26 (3). P. 673-681.

Sobek, A.A., Schuller, W.A., Freeman, J.R., Smith, R.M. 1978. Field and laboratory methods applicable to overburden and minesoils. EPA 600/2-78-054. 203 p.

Sung, W., Morgan, J.J. 1980. Kinetics and product of ferrous iron oxygenation in aqueous systems. Environ. Sci. Technol. 14. p. 561-568.

U.S. Bureau of Mines. 1985. Control of acid mine drainage. Proceedings of a Technology Transfer Seminar, U.S. Department of the Interior, BuMines IC 9027.

White, W.W. III, Lapakko, K.A., Cox, R.L. 1999. Static-test methods most commonly used to predict acid-mine drainage: Practical guidelines for use and interpretation. In Reviews in Economic Geology, Volume 7. The Environmental Geochemistry of Mineral Deposits, Part A: Processes, techniques, techniques, and health issues. G.S. Plumlee, M.J. Logsdon (eds.). Society of Economic Geologists. p. 325-338.

Williamson, M.A., Rimstidt, J.D. 1994. The kinetics and electrochemical rate-determining step of aqueous pyrite oxidation. Geochimica et Cosmochimica Acta, 58. p. 5443-5454.

Ziemkiewicz, P.F., Meek Jr., F. A. 1994. Long term behavior of acid forming rock: Results of II-year field studies. In Proc. Of the In1'l Land Reclamation and Mine Drainage Conference and Third In1'l Conference on the Abatement of Acidic Drainage, Pittsburgh, PA, April 25-29, 1994. V.2. U.S. Dept. Interior, Bureau of Mines Special Publication SP 06A-94. p. 49-56.

TABLES

Table 3.1 Comparison of wt% S_T values determined by different labs.

Sample #	S_T wt%[1]	S_T wt%[2]	S_T wt%[3]	DNR Drill Core Sample #
1	--	0.04	0.02	3260000102
2	--	0.05	0.06	3260000106
3	--	0.05	0.09	3260000103
4,5	1.05	0.1	0.12	3260000058
6	--	0.12	0.12	3260000105
7	--	0.16	0.15	3260000100
8,9	0.22	0.16	0.18	3260000057
10	0.19	0.2	0.23	3260000066
11	0.3	0.26	0.28	3260000068
12	0.24	0.39	0.39	3260000063
13	0.51	0.5	0.59	3260000060
14,15	0.64	0.59	0.65	3260000067
16	0.81	0.72	0.78	3260000064
17,18	1.43	1.22	1.36	3260000062
Samples crushed but not used in the experiment				
na	0.1	--	0.21	3260000065
na	--	--	0.4	3260000101
na	0.24	--	0.58	3260000059
na	0.42	--	0.61	3260000061

[1] Initial Actlabs analysis of drill core samples
[2] Actlabs analysis of selected laboratory samples
[3] Verification analysis by Lerch Brothers Inc.

Table 3.2 Rock density measurements.

n	rock mass (g)	rock volume (cm^3)	density (g/cm^3)
1	620	210	2.95
2	524	180	2.91
3	611	225	2.72
4	537	195	2.75
5	629	215	2.93
6	328	110	2.98
7	626	225	2.78
8	533	205	2.60
9	501	200	2.51
10	839	300	2.80
		average=	2.79
		std dev=	0.16

Table 3.3 Field rock pile mass calculations.

volume (y^3)	volume (m^3)	volume (cm^3)	porosity	density (g/cm^3)	mass (g)	mass (kg)	mass (tonnes)
51	38.9	38900000	0.3	2.79	75971700	75971.7	76
51	38.9	38900000	0.4	2.79	65118600	65118.6	65
51	38.9	38900000	0.5	2.79	54265500	54265.5	54

Table 4.1 Laboratory bulk sample particle size distribution.

		Laboratory Sample Number													
Sample	**Size (mm)**	**1**	**2**	**3**	**4,5**	**6**	**7**	**8, 9**	**10**	**11**	**12**	**13**	**14, 15**	**16**	**17, 18**
1	> 6.35	0	0	0.3	0.4	0	0	0	0.4	0.6	0.4	0.5	0.2	0.1	0
1	4.76-6.35	8.4	10.9	9.0	14.3	9.4	8.0	13.5	12.4	11.0	12.9	10.4	11.3	14.7	10.8
1	2.0-4.76	41.5	38.0	38.7	37.0	38.3	38.7	36.8	37.2	34.1	38.1	37.8	37.3	47.4	43.8
1	0.841-2.0	21.8	21.7	22.6	18.6	22.4	22.8	18.7	20.0	19.6	19.4	19.1	19.7	15.1	17.3
1	0.545-0.841	6.9	8.5	7.2	6.9	8.5	9.0	6.7	6.9	7.6	6.7	7.0	7.1	5.3	6.2
1	0.5-0.545	4.0	3.8	4.2	4.5	4.0	4.0	4.2	4.4	4.9	4.2	4.4	4.6	3.2	4.0
1	0.3-0.5	3.5	3.5	3.7	4.0	3.7	3.8	3.9	3.7	4.8	3.6	4.0	4.0	2.9	3.6
1	0.21-0.3	2.9	2.8	2.9	3.2	2.9	3.0	3.3	2.9	3.4	3.2	3.2	3.3	2.1	3.6
1	0.149-0.21	2.2	2.1	2.2	2.5	2.2	2.3	2.4	2.1	2.8	1.7	2.4	2.4	1.6	1.5
1	0.105-0.149	1.9	1.7	1.8	2.1	1.8	2.0	2.1	1.6	2.2	1.6	1.9	2.0	1.3	1.7
1	0.074-0.105	1.4	1.2	1.2	1.6	1.2	1.3	1.5	1.2	1.7	1.2	1.4	1.4	1.0	1.2
1	< 0.074	5.5	5.8	6.2	4.9	5.6	5.1	6.9	7.2	7.3	7.0	7.9	6.7	5.3	6.3

Values represent mass % of each size fraction for each sample.

Table 4.2 Laboratory bulk sample sulfur and CO_2 concentrations.

Sample	S_T wt%	SO_4 wt%	CO_2 wt%
1	0.04	<0.05	<0.05
2	0.05	<0.05	<0.05
3	0.05	<0.05	<0.05
4,5	0.1	<0.05	<0.05
6	0.12	<0.05	<0.05
7	0.16	<0.05	<0.05
8,9	0.16	<0.05	<0.05
10	0.2	<0.05	0.05
11	0.26	<0.05	<0.05
12	0.39	0.05	<0.05
13	0.5	0.1	1.76
14,15	0.59	<0.05	<0.05
16	0.72	<0.05	6.85
17,18	1.22	0.05	<0.05

Analyses performed by Actlabs

Table 4.3 Laboratory bulk sample major oxide concentrations.

Sample	S_T	CO_2	Al_2O_3	CaO	Fe_2O_3	FeO	K_2O	MgO	MnO	Na_2O	P_2O_5	SiO_2	TiO_2	LOI	Total
1	0.04	<0.05	19.79	0.29	0.69	13.7	1.24	6.36	0.10	0.15	0.2	49.58	1.14	5.7	98.93
2	0.05	<0.05	21.25	0.23	0.78	12.35	4.48	2.44	0.07	0.13	0.16	51.85	0.91	3.93	98.57
3	0.05	<0.05	21.21	0.44	1.62	11.67	3.44	4.86	0.08	0.18	0.34	49.41	1.12	4.83	99.20
4,5	0.1	<0.05	12.5	0.68	0.32	8.24	1.38	2.89	0.07	0.2	0.49	69.83	0.74	3.09	100.43
6	0.12	<0.05	18.57	0.06	2.23	14.81	3.01	3.28	0.09	0.08	0.06	51.99	0.80	4.56	99.54
7	0.16	<0.05	15.27	0.04	0.63	9.9	1.37	1.86	0.09	0.75	0.02	65.78	0.88	3.51	100.10
8,9	0.16	<0.05	16.16	0.03	1.17	14.49	2.03	2.27	0.11	0.27	0.02	61.45	0.92	4.08	103.00
10	0.2	0.05	8.13	0.04	0.27	3.84	1.34	1.97	0.03	0.12	0.03	82.48	0.10	1.68	100.03
11	0.26	<0.05	10.65	0.12	0.15	4.08	0.81	1.42	0.03	0.97	0.09	79.46	0.35	2.09	100.22
12	0.39	<0.05	11.82	0.13	0.88	7	1.74	2.45	0.04	0.14	0.12	72.68	0.61	2.75	100.36
13	0.5	1.76	11.53	0.03	1.09	6.91	2.31	1.68	0.21	0.17	0.03	73.01	0.18	3.34	100.49
14,15	0.59	<0.05	7.35	0.05	0.31	3.47	0.55	1.11	0.03	0.64	0.04	84.79	0.18	1.78	100.30
16	0.72	6.85	8.52	0.07	1.85	14.77	1.58	1.56	0.94	0.07	0.02	61.82	0.34	7.36	98.90
17,18	1.22	<0.05	13.15	0.15	1.59	9.37	1.39	4.51	0.04	0.13	0.12	64.1	0.70	3.85	99.11

Values are in wt%.

Table 4.4 Laboratory bulk sample trace metal concentrations.

Sample	S_T wt%	Ag	As	Ba	Be	Bi	Co	Cr	Cs	Cu	Hf	Mo	Ni	Pb	Rb	Sb	Sn	Sr	Ta	V	W	Y	Zn	Zr
1	0.04	<0.5	<5	110	<1	<0.4	54	294	2	25	2	<2	179	<5	37	0.7	<1	30	0.3	233	<1	12	87	80
2	0.05	<0.5	<5	590	<1	<0.4	67	366	4.2	97	2.6	<2	243	<5	108	1.2	<1	16	0.4	203	<1	14	40	102
3	0.05	<0.5	<5	378	<1	<0.4	59	342	4.2	70	2.2	<2	204	<5	98	<0.5	<1	23	0.4	240	<1	17	98	88
4,5	0.1	<0.5	6	313	<1	<0.4	43	362	1.7	88	1.9	3	169	<5	45	1	<1	29	0.3	145	<1	7	47	77
6	0.12	<0.5	<5	622	<1	<0.4	51	295	3.7	43	2.3	<2	261	<5	80	<0.5	<1	15	0.4	182	<1	13	170	95
7	0.16	<0.5	17	112	<1	<0.4	103	268	1.7	82	1.6	<2	318	<5	34	0.7	<1	88	0.3	194	<1	14	114	62
8,9	0.16	<0.5	<5	154	<1	<0.4	66	271	2.3	71	1.6	<2	252	<5	50	<0.5	<1	35	0.3	200	<1	9	117	62
10	0.2	<0.5	<5	150	1	<0.4	3	76	1.3	34	5.5	<2	21	<5	49	<0.5	2	17	1.3	<5	<1	35	93	192
11	0.26	<0.5	<5	94	<1	<0.4	15	148	1	33	5.4	<2	65	<5	28	<0.5	2	94	1	61	<1	29	71	185
12	0.39	<0.5	<5	190	1	<0.4	21	51	1.8	59	6.2	<2	49	<5	66	<0.5	2	26	1.2	102	<1	69	113	204
13	0.5	<0.5	<5	298	2	<0.4	8	43	2.7	29	10.6	<2	20	7	82	<0.5	4	19	1.9	15	<1	76	194	368
14,15	0.59	<0.5	<5	69	<1	<0.4	9	149	0.7	40	4.9	<2	40	<5	19	<0.5	1	63	1	27	<1	19	69	164
16	0.72	<0.5	6	181	<1	<0.4	37	209	2.6	99	1.6	<2	111	<5	44	<0.5	1	9	0.3	78	<1	13	84	61
17,18	1.22	6.1	5	192	<1	<0.4	29	54	1.4	73	3.4	<2	36	<5	52	0.9	1	20	0.6	191	<1	24	99	125

Sample	S_T wt%	Ce	La	Lu	Nd	Sc	Tb	Th	U	Yb	Ga	Ge	Nb	In	Pr	Sm	Gd	Dy	Ho	Er	Tm	Ti	Eu
1	0.04	20.1	8.8	0.19	10.8	38	0.4	0.8	0.1	1.3	17	1	4	<0.2	2.46	2.5	2.3	2.3	0.4	1.3	0.2	0.1	0.97
2	0.05	29.1	12.5	0.19	13.9	33	0.4	1.2	0.3	1.4	19	1	5	<0.2	3.42	2.7	2.5	2.4	0.5	1.5	0.21	0.2	0.87
3	0.05	26.3	11.2	0.24	14.3	38	0.5	0.9	0.2	1.6	19	1	5	<0.2	3.23	3.1	3.1	3.2	0.6	1.8	0.25	0.4	1.14
4,5	0.1	15.2	6.6	0.15	8.3	21	0.3	0.9	0.2	0.9	13	1	4	<0.2	1.88	1.9	1.8	1.3	0.2	0.8	0.12	0.1	0.69
6	0.12	26.5	11.5	0.17	13.3	29	0.3	1.1	0.3	1.3	17	2	5	<0.2	3.14	2.5	2.1	2.2	0.4	1.3	0.2	0.2	0.8
7	0.16	14.4	6.1	0.18	8.9	29	0.4	0.6	0.2	1.3	14	<1	3	<0.2	1.84	2.2	2.1	2.2	0.5	1.4	0.2	0.1	0.76
8,9	0.16	10.3	4.1	0.1	5.9	30	0.3	0.6	0.1	0.7	16	<1	4	<0.2	1.3	1.5	1.8	1.8	0.3	0.9	0.12	0.2	0.74
10	0.2	80.4	36.9	0.63	38.1	3	1.3	7.1	1.6	4.2	14	<1	8	<0.2	9.4	8.1	7.8	7.8	1.5	4.4	0.64	0.2	1.08
11	0.26	61.8	28.1	0.47	28.4	12	0.9	5.2	1.1	3.4	14	<1	9	<0.2	7.11	6	5.7	5.3	1	3.2	0.52	0.2	1.09
12	0.39	74.4	35.5	0.99	35.6	17	1.6	5.5	1.2	7	17	<1	12	<0.2	8.66	7.9	8.5	9.9	2.2	7	1.09	0.2	1.58
13	0.5	112	50.4	1.2	54.1	5	2.1	8.7	1.9	8.5	21	2	20	<0.2	13.2	12.2	12.2	12.9	2.6	8.1	1.26	0.4	2.28
14,15	0.59	53.2	23.2	0.36	25	5	0.8	4.8	1.1	2.5	11	<1	9	<0.2	6.26	5.3	4.9	4.5	0.8	2.5	0.37	0.1	0.78
16	0.72	20.1	9	0.18	9.1	13	0.3	1.2	0.2	1.2	10	1	3	<0.2	2.19	1.9	2	2	0.4	1.3	0.19	0.2	0.67
17,18	1.22	30.3	13.2	0.37	15.9	26	0.7	2.3	0.6	2.5	16	1	7	<0.2	3.68	3.8	4	4.1	0.8	2.4	0.37	0.1	0.9

Values in ppm.

Table 4.5 Laboratory samples particle size fraction major oxide concentrations (1 of 7).

Sample	Size (mm)	S_T	CO_2	Al_2O_3	CaO	Fe_2O_3	FeO	K_2O	MgO	MnO	Na_2O	P_2O_5	SiO_2	TiO_2	LOI	Total
1	< 0.074	0.06	<0.05	19.83	0.3	16.91		1.49	6.4	0.11	0.28	0.2	47.68	1.20	5.98	100.38
1	0.074-0.105	0.05	<0.05	19.29	0.28	16.91		1.34	6.34	0.11	0.23	0.21	48.51	1.18	5.68	100.06
1	0.105-0.149	0.04	<0.05	19.21	0.29	16.92		1.29	6.42	0.10	0.25	0.21	48.45	1.14	5.91	100.17
1	0.149-0.21	0.04	<0.05	19.11	0.28	16.8		1.28	6.39	0.10	0.26	0.21	48.33	1.13	5.85	99.75
1	0.21-0.3	0.03	0.11	19.34	0.29	16.8		1.29	6.44	0.10	0.27	0.21	48.43	1.13	5.91	100.19
1	0.3-0.5	0.02	<0.05	19.27	0.28	16.68		1.3	6.37	0.10	0.24	0.21	48.6	1.12	5.88	100.05
1	0.5-0.545	0.02	<0.05	19.27	0.28	15.72		1.27	6.32	0.10	0.23	0.19	48.43	1.12	5.85	98.78
1	0.545-0.841	0.02	<0.05	19.3	0.29	16.6		1.3	6.36	0.10	0.26	0.23	48.74	1.12	5.95	100.26
1	0.84-2.0	0.02	<0.05	19.39	0.29	16.5		1.34	6.34	0.10	0.25	0.21	48.93	1.13	5.81	100.28
1	2.0-4.76	0.01	<0.05	19.15	0.28	16.3		1.33	6.29	0.10	0.26	0.21	48.84	1.13	5.9	99.77
1	4.76-6.35	0.02	<0.05	19.22	0.28	16.03		1.35	6.15	0.09	0.27	0.21	48.74	1.12	6.06	99.51
1	bulk	0.04	<0.05	19.79	0.29	0.69	13.7	1.24	6.36	0.10	0.15	0.2	49.58	1.14	5.7	98.934
2	< 0.074	0.07	<0.05	21.67	0.24	15.32		4.62	2.53	0.07	0.27	0.17	49.41	1.04	4.5	99.83
2	0.074-0.105	0.11	<0.05	20.89	0.23	15.75		4.26	2.54	0.07	0.26	0.17	50.61	1.09	4.39	100.25
2	0.105-0.149	0.09	0.07	21.12	0.23	15.56		4.4	2.6	0.07	0.23	0.17	50.34	1.00	4.72	100.44
2	0.149-0.21	0.08	<0.05	21.01	0.23	15.31		4.4	2.53	0.07	0.23	0.17	49.78	0.97	4.67	99.37
2	0.21-0.3	0.06	0.07	21.17	0.23	15.31		4.46	2.48	0.07	0.26	0.18	50.13	0.95	4.6	99.83
2	0.3-0.5	0.05	<0.05	21.07	0.23	15.34		4.51	2.48	0.06	0.23	0.17	50.25	0.93	4.65	99.93
2	0.5-0.545	0.07	<0.05	20.89	0.23	15.46		4.43	2.49	0.07	0.25	0.18	50.67	0.92	4.59	100.16
2	0.545-0.841	0.07	<0.05	20.75	0.23	15.57		4.38	2.49	0.07	0.23	0.17	50.76	0.90	4.63	100.17
2	0.84-2.0	0.07	<0.05	20.13	0.23	15.58		4.05	2.47	0.07	0.23	0.18	50.79	0.87	4.37	98.97
2	2.0-4.76	0.06	<0.05	20.67	0.23	15.61		4.19	2.47	0.07	0.22	0.18	51.57	0.90	4.53	100.63
2	4.76-6.35	0.04	<0.05	20.16	0.25	15.38		4.28	2.43	0.07	0.17	0.18	51.92	0.88	4.5	100.2
2	bulk	0.05	<0.05	21.25	0.23	0.78	12.35	4.48	2.44	0.07	0.13	0.16	51.85	0.91	3.93	98.573

Concentration values in wt%.

Table 4.5 Laboratory samples particle size fraction major oxide concentrations (2 of 7).

Sample	Size (mm)	S_T	CO_2	Al_2O_3	CaO	Fe_2O_3	FeO	K_2O	MgO	MnO	Na_2O	P_2O_5	SiO_2	TiO_2	LOI	Total
3	< 0.074	0.05	0.07	21.83	0.46	14.96		3.7	4.91	0.09	0.26	0.32	47.07	1.24	5.34	100.18
3	0.074-0.105	0.07	<0.05	21	0.43	15.21		3.3	5.05	0.09	0.26	0.34	48.43	1.21	5.11	100.43
3	0.105-0.149	0.05	<0.05	21.01	0.41	14.92		3.48	4.86	0.09	0.24	0.29	48.5	1.16	5.47	100.41
3	0.149-0.21	0.06	0.11	20.86	0.4	14.61		3.58	4.71	0.08	0.26	0.29	48.22	1.13	5.49	99.64
3	0.21-0.3	0.05	0.07	20.9	0.42	14.55		3.54	4.76	0.09	0.23	0.3	48.86	1.13	5.34	100.11
3	0.3-0.5	0.05	<0.05	20.84	0.42	14.44		3.53	4.73	0.08	0.24	0.31	48.75	1.12	5.22	99.68
3	0.5-0.545	0.04	<0.05	20.91	0.43	14.42		3.5	4.72	0.08	0.22	0.31	49.23	1.12	5.32	100.27
3	0.545-0.841	0.05	0.07	20.79	0.43	14.46		3.46	4.7	0.08	0.22	0.31	49.38	1.12	5.53	100.49
3	0.84-2.0	0.03	<0.05	20.82	0.45	14.48		3.32	4.84	0.08	0.23	0.32	49.18	1.11	5.22	100.05
3	2.0-4.76	0.03	0.07	20.59	0.46	14.37		3.4	4.73	0.08	0.24	0.33	48.34	1.09	5.2	98.84
3	4.76-6.35	0.07	0.18	20.55	0.46	14.8		3.33	4.91	0.20	0.26	0.33	48.66	1.09	5.76	100.32
3	bulk	0.05	<0.05	21.21	0.44	1.62	11.67	3.44	4.86	0.08	0.18	0.34	49.41	1.12	4.83	99.201
4,5	< 0.074	0.12	<0.05	15.42	0.95	11.31		2.16	3.51	0.10	0.36	0.61	61	0.94	3.68	100.04
4,5	0.074-0.105	0.11	<0.05	12.31	0.64	9.72		1.56	2.98	0.09	0.3	0.41	67.88	0.81	2.96	99.67
4,5	0.105-0.149	0.1	<0.05	12.27	0.57	9.63		1.62	2.9	0.08	0.31	0.37	66.76	0.78	3.26	98.53
4,5	0.149-0.21	0.08	<0.05	12.24	0.55	9.4		1.61	2.86	0.08	0.3	0.37	68.05	0.77	3.12	99.34
4,5	0.21-0.3	0.08	<0.05	11.88	0.56	9.25		1.57	2.74	0.07	0.26	0.36	69	0.75	3.07	99.52
4,5	0.3-0.5	0.07	<0.05	11.64	0.56	9.07		1.58	2.69	0.08	0.25	0.37	70.3	0.73	2.97	100.25
4,5	0.5-0.545	0.07	<0.05	11.63	0.56	9.11		1.54	2.69	0.07	0.26	0.38	69.94	0.73	3.03	99.94
4,5	0.545-0.841	0.07	<0.05	11.4	0.58	8.94		1.46	2.67	0.07	0.24	0.4	70.3	0.72	2.94	99.71
4,5	0.84-2.0	0.08	0.07	11.78	0.58	9.3		1.55	2.81	0.07	0.27	0.41	69.82	0.71	2.97	100.25
4,5	2.0-4.76	0.05	<0.05	13.18	0.63	10.63		1.63	3.27	0.08	0.27	0.51	64.44	0.85	3.5	98.97
4,5	4.76-6.35	0.06	<0.05	12.5	0.88	10.43		1.6	2.97	0.08	0.26	0.64	66.08	0.83	3.25	99.5
4,5	bulk	0.1	<0.05	12.5	0.68	0.32	8.24	1.38	2.89	0.07	0.2	0.49	69.83	0.74	3.09	100.43

Concentration values in wt%.

Table 4.5 Laboratory samples particle size fraction major oxide concentrations (3 of 7).

Sample	Size (mm)	S_T	CO_2	Al_2O_3	CaO	Fe_2O_3	FeO	K_2O	MgO	MnO	Na_2O	P_2O_5	SiO_2	TiO_2	LOI	Total
6	< 0.074	0.13	<0.05	19.24	0.08	19.22		3.22	3.42	0.10	0.17	0.05	49.15	0.94	4.61	100.19
6	0.074-0.105	0.15	<0.05	18.76	0.06	19.33		3.1	3.41	0.10	0.18	0.05	49.49	1.10	4.51	100.11
6	0.105-0.149	0.1	<0.05	18.71	0.07	18.98		3.07	3.33	0.09	0.17	0.05	49.77	0.96	4.94	100.13
6	0.149-0.21	0.11	<0.05	18.78	0.07	19.02		3.12	3.38	0.09	0.19	0.05	49.77	0.90	4.76	100.12
6	0.21-0.3	0.11	<0.05	18.7	0.06	18.89		3.08	3.35	0.09	0.19	0.05	49.84	0.86	4.88	100.01
6	0.3-0.5	0.09	<0.05	18.45	0.06	18.7		3.01	3.4	0.09	0.17	0.05	48.96	0.83	4.9	98.62
6	0.5-0.545	0.09	<0.05	18.28	0.06	18.58		2.92	3.36	0.09	0.15	0.05	49.49	0.81	4.98	98.77
6	0.545-0.841	0.1	<0.05	18.14	0.06	18.62		2.98	3.36	0.09	0.16	0.05	49.96	0.80	4.7	98.93
6	0.84-2.0	0.13	<0.05	17.85	0.1	18.52		2.79	3.3	0.09	0.06	0.05	51.99	0.78	4.61	100.13
6	2.0-4.76	0.08	<0.05	18.43	0.06	18.4		3.02	3.29	0.09	0.07	0.05	51.25	0.81	4.71	100.18
6	4.76-6.35	0.12	<0.05	17.68	0.05	17.8		2.88	3.15	0.08	0.07	0.04	52.87	0.78	4.53	99.93
6	bulk	0.12	<0.05	18.57	0.06	2.23	14.81	3.01	3.28	0.09	0.08	0.06	51.99	0.80	4.56	99.537
7	< 0.074	0.15	0.48	16.09	0.11	14.62		1.67	2.15	0.14	0.78	0.02	59.97	1.05	3.82	100.42
7	0.074-0.105	0.13	0.18	16.43	0.06	12.59		1.77	1.88	0.11	0.85	0.02	61.71	1.13	3.6	100.14
7	0.105-0.149	0.12	<0.05	16.88	0.05	12.63		1.94	2	0.10	0.82	0.02	60.3	1.08	4.24	100.07
7	0.149-0.21	0.11	<0.05	16.64	0.04	12.16		1.87	1.98	0.09	0.85	0.02	61.08	1.03	4.4	100.15
7	0.21-0.3	0.1	<0.05	16.41	0.04	11.74		1.78	1.91	0.09	0.86	0.02	62.51	1.02	4.06	100.43
7	0.3-0.5	0.11	<0.05	16.01	0.03	11.52		1.71	1.88	0.08	0.84	0.02	63.06	0.97	4.03	100.16
7	0.5-0.545	0.13	<0.05	15.56	0.03	11.45		1.63	1.87	0.08	0.83	0.02	63.9	0.94	3.89	100.2
7	0.545-0.841	0.16	0.07	15.25	0.03	11.34		1.6	1.86	0.08	0.82	0.02	64.28	0.90	3.68	99.87
7	0.84-2.0	0.14	<0.05	14.61	0.03	11.24		1.44	1.85	0.08	0.74	0.02	65.65	0.85	3.37	99.86
7	2.0-4.76	0.15	<0.05	14.91	0.02	11.37		1.5	1.85	0.08	0.72	0.02	65.18	0.87	3.51	100.03
7	4.76-6.35	0.04	0.07	15.37	0.02	11.09		1.57	1.84	0.07	0.78	0.02	65.01	0.90	3.57	100.24
7	bulk	0.16	<0.05	15.27	0.04	0.63	9.9	1.37	1.86	0.09	0.75	0.02	65.78	0.88	3.51	100.1

Concentration values in wt%.

Table 4.5 Laboratory samples particle size fraction major oxide concentrations (4 of 7).

Sample	Size (mm)	S_T	CO_2	Al_2O_3	CaO	Fe_2O_3	FeO	K_2O	MgO	MnO	Na_2O	P_2O_5	SiO_2	TiO_2	LOI	Total
8,9	< 0.074	0.12	<0.05	17.95	0.06	14.67		2.61	2.47	0.12	0.32	0.07	56.96	1.11	3.94	100.27
8,9	0.074-0.105	0.11	<0.05	17.1	0.06	13		2.69	2.18	0.10	0.27	0.02	60.1	1.10	3.64	100.27
8,9	0.105-0.149	0.11	0.07	17.08	0.05	12.98		2.57	2.17	0.10	0.31	0.02	59.51	1.05	4.2	100.05
8,9	0.149-0.21	0.11	0.15	17.09	0.04	13.05		2.67	2.18	0.10	0.3	0.03	59.9	1.03	4.07	100.45
8,9	0.21-0.3	0.11	0.15	16.62	0.04	13.19		2.63	2.18	0.11	0.25	0.02	60.31	0.99	4.11	100.44
8,9	0.3-0.5	0.11	0.11	16.3	0.03	13.09		2.54	2.17	0.10	0.26	0.02	60.22	0.96	4.06	99.74
8,9	0.5-0.545	0.13	<0.05	16.14	0.03	13.22		2.4	2.18	0.10	0.27	0.01	60.5	0.94	4.11	99.91
8,9	0.545-0.841	0.12	0.15	15.81	0.03	13.09		2.4	2.16	0.10	0.26	0.01	59.84	0.92	3.99	98.59
8,9	0.84-2.0	0.11	<0.05	15.62	0.02	13.52		2.27	2.23	0.10	0.21	0.02	61.63	0.91	3.81	100.33
8,9	2.0-4.76	0.12	<0.05	15.46	0.02	14.08		2.16	2.3	0.11	0.18	0.02	60.61	0.90	3.95	99.75
8,9	4.76-6.35	0.14	<0.05	15.53	0.02	14.96		2.02	2.44	0.11	0.18	0.02	59.51	0.90	4.22	99.89
8,9	bulk	0.16	<0.05	16.16	0.03	1.17	14.49	2.03	2.27	0.11	0.27	0.02	61.45	0.92	4.08	103
10	< 0.074	0.39	<0.05	11.2	0.07	5		2.4	2.03	0.04	0.18	0.03	76.39	0.19	2.73	100.25
10	0.074-0.105	0.43	<0.05	10.63	0.09	5.11		2.27	1.97	0.05	0.17	0.04	76.99	0.19	2.63	100.14
10	0.105-0.149	0.27	<0.05	10.52	0.07	4.98		2.19	1.97	0.05	0.12	0.04	77.69	0.18	2.46	100.26
10	0.149-0.21	0.17	<0.05	10.15	0.04	4.61		2.2	1.95	0.04	0.11	0.03	78.37	0.16	2.38	100.04
10	0.21-0.3	0.17	<0.05	9.74	0.03	4.82		1.98	1.98	0.05	0.13	0.04	79.1	0.15	2.41	100.42
10	0.3-0.5	0.18	<0.05	9.27	0.02	4.47		1.94	1.97	0.03	0.15	0.02	79.82	0.14	2.43	100.27
10	0.5-0.545	0.18	<0.05	8.75	0.03	4.6		1.72	1.97	0.03	0.16	0.02	80.69	0.12	2.25	100.36
10	0.545-0.841	0.17	<0.05	8.29	0.02	4.44		1.53	1.99	0.03	0.2	0.03	81.55	0.12	2.21	100.39
10	0.84-2.0	0.17	<0.05	7.56	0.01	4.53		1.34	1.96	0.03	0.1	0.02	82.47	0.10	2.05	100.18
10	2.0-4.76	0.13	<0.05	7.12	0.01	4.47		1.21	2.01	0.03	0.08	0.02	83.33	0.09	1.98	100.35
10	4.76-6.35	0.19	<0.05	6.55	0.03	4.54		1.05	1.94	0.03	0.05	0.02	84.01	0.09	1.88	100.18
10	bulk	0.2	0.05	8.13	0.04	0.27	3.84	1.34	1.97	0.03	0.12	0.03	82.48	0.10	1.68	100.03

Concentration values in wt%.

Table 4.5 Laboratory samples particle size fraction major oxide concentrations (5 of 7).

Sample	Size (mm)	S_T	CO_2	Al_2O_3	CaO	Fe_2O_3	FeO	K_2O	MgO	MnO	Na_2O	P_2O_5	SiO_2	TiO_2	LOI	Total
11	< 0.074	0.32	<0.05	13.64	0.17	5.3		1.21	1.59	0.04	1.32	0.1	73.62	0.48	2.95	100.43
11	0.074-0.105	0.28	<0.05	14.93	0.18	5.02		1.41	1.53	0.05	1.57	0.1	71.74	0.58	2.96	100.05
11	0.105-0.149	0.24	<0.05	14.2	0.17	5.07		1.29	1.52	0.04	1.42	0.1	72.84	0.53	2.87	100.06
11	0.149-0.21	0.23	<0.05	13.84	0.16	4.88		1.27	1.5	0.04	1.38	0.1	73.53	0.51	2.97	100.18
11	0.21-0.3	0.21	<0.05	13.08	0.15	4.9		1.2	1.47	0.04	1.27	0.1	74.99	0.47	2.69	100.36
11	0.3-0.5	0.19	0.07	12.52	0.14	4.78		1.1	1.47	0.04	1.21	0.09	75.72	0.45	3.01	100.51
11	0.5-0.545	0.2	<0.05	11.84	0.13	4.67		1.06	1.46	0.03	1.15	0.09	77.05	0.41	2.52	100.42
11	0.545-0.841	0.22	<0.05	11.07	0.12	4.44		0.98	1.42	0.03	1.05	0.08	76.83	0.38	2.43	98.82
11	0.84-2.0	0.24	<0.05	10.23	0.11	4.56		0.88	1.44	0.03	0.91	0.07	79.45	0.34	2.19	100.21
11	2.0-4.76	0.16	<0.05	9.49	0.1	4.28		0.74	1.38	0.03	0.81	0.07	80.96	0.33	2.1	100.28
11	4.76-6.35	0.35	<0.05	7.42	0.09	4.7		0.59	1.37	0.03	0.61	0.06	83.32	0.25	1.95	100.37
11	bulk	0.26	<0.05	10.65	0.12	0.15	4.08	0.81	1.42	0.03	0.97	0.09	79.46	0.35	2.09	100.22
12	< 0.074	0.47	<0.05	14.1	0.17	9.08		2.58	2.61	0.06	0.21	0.1	66.91	0.71	3.54	100.05
12	0.074-0.105	0.51	<0.05	13.82	0.18	9.45		2.42	2.61	0.06	0.22	0.13	67.24	0.90	3.42	100.46
12	0.105-0.149	0.51	<0.05	13.43	0.17	9.17		2.36	2.53	0.06	0.19	0.13	67.99	0.81	3.43	100.27
12	0.149-0.21	0.41	<0.05	13.34	0.17	8.93		2.34	2.49	0.05	0.2	0.12	68.41	0.76	3.4	100.2
12	0.21-0.3	0.36	<0.05	13.34	0.15	8.85		2.37	2.47	0.04	0.16	0.12	68.8	0.73	3.33	100.36
12	0.3-0.5	0.33	<0.05	12.73	0.14	8.55		2.27	2.43	0.04	0.14	0.12	69.87	0.67	3.31	100.26
12	0.5-0.545	0.32	<0.05	12.54	0.14	8.57		2.17	2.44	0.04	0.17	0.11	70.48	0.65	3.19	100.49
12	0.545-0.841	0.34	<0.05	12.07	0.13	8.39		2	2.42	0.04	0.16	0.11	71.29	0.62	3.14	100.36
12	0.84-2.0	0.36	<0.05	11.49	0.13	8.45		1.87	2.43	0.04	0.16	0.12	71.93	0.59	3.05	100.25
12	2.0-4.76	0.32	<0.05	11.27	0.13	8.69		1.75	2.5	0.04	0.13	0.11	72.11	0.62	3.02	100.37
12	4.76-6.35	0.47	<0.05	11.35	0.14	9.26		1.7	2.58	0.05	0.12	0.13	71.2	0.69	3.27	100.48
12	bulk	0.39	<0.05	11.82	0.13	0.88	7	1.74	2.45	0.04	0.14	0.12	72.68	0.61	2.75	100.36

Concentration values in wt%.

Table 4.5 Laboratory samples particle size fraction major oxide concentrations (6 of 7).

Sample	Size (mm)	S_T	CO_2	Al_2O_3	CaO	Fe_2O_3	FeO	K_2O	MgO	MnO	Na_2O	P_2O_5	SiO_2	TiO_2	LOI	Total
13	< 0.074	0.65	1.9	14.62	0.06	8.88		3.48	1.64	0.21	0.27	0.04	66.22	0.25	4.53	100.19
13	0.074-0.105	0.65	2.1	13.58	0.05	9.42		3.15	1.72	0.24	0.21	0.04	67.29	0.26	4.4	100.36
13	0.105-0.149	0.53	1.7	13.28	0.05	8.84		3.01	1.73	0.20	0.21	0.03	68.27	0.28	4.26	100.16
13	0.149-0.21	0.53	1.7	12.95	0.04	8.49		2.93	1.66	0.20	0.21	0.04	68.9	0.26	4.39	100.07
13	0.21-0.3	0.5	1.7	12.6	0.03	8.51		2.93	1.66	0.20	0.21	0.08	69.69	0.25	4.12	100.28
13	0.3-0.5	0.48	1.7	12.17	0.03	8.42		2.72	1.66	0.20	0.22	0.03	70.37	0.22	4.12	100.17
13	0.5-0.545	0.49	1.85	11.78	0.03	8.61		2.61	1.68	0.20	0.23	0.03	70.55	0.21	4.03	99.97
13	0.545-0.841	0.47	1.85	11.42	0.03	8.65		2.46	1.68	0.21	0.2	0.03	70.88	0.19	4.22	99.98
13	0.84-2.0	0.43	1.85	10.83	0.03	8.72		2.26	1.71	0.21	0.21	0.03	71.79	0.18	4	99.98
13	2.0-4.76	0.47	1.7	10.66	0.03	8.62		2.28	1.72	0.19	0.12	0.03	72.43	0.18	3.94	100.21
13	4.76-6.35	0.63	1.8	10.29	0.02	9.55		2.04	1.79	0.21	0.13	0.03	72.17	0.20	4	100.42
13	bulk	0.5	1.76	11.53	0.03	1.09	6.91	2.31	1.68	0.21	0.17	0.03	73.01	0.18	3.34	100.49
14,15	< 0.074	0.9	<0.05	10.36	0.1	5.02		0.99	1.28	0.05	0.97	0.04	78.78	0.27	2.57	100.44
14,15	0.074-0.105	0.66	<0.05	11.99	0.11	4.52		1.09	1.22	0.06	1.21	0.05	76.86	0.35	2.45	99.91
14,15	0.105-0.149	0.61	0.07	11.37	0.1	4.73		1.1	1.24	0.05	1.12	0.05	77.46	0.32	2.7	100.24
14,15	0.149-0.21	0.58	<0.05	10.72	0.09	4.67		1	1.21	0.04	1.04	0.05	78.88	0.29	2.49	100.47
14,15	0.21-0.3	0.59	<0.05	9.98	0.08	4.49		0.89	1.18	0.04	0.97	0.05	80.17	0.27	2.38	100.48
14,15	0.3-0.5	0.57	<0.05	9.3	0.07	4.39		0.82	1.16	0.03	0.9	0.05	80.89	0.24	2.25	100.1
14,15	0.5-0.545	0.59	<0.05	8.73	0.06	4.2		0.76	1.14	0.03	0.82	0.04	81.99	0.23	2.21	100.21
14,15	0.545-0.841	0.61	<0.05	8.1	0.06	4.25		0.69	1.14	0.03	0.73	0.04	83.05	0.21	2.04	100.34
14,15	0.84-2.0	0.56	<0.05	6.95	0.05	4.07		0.59	1.12	0.03	0.58	0.03	84.91	0.17	1.9	100.38
14,15	2.0-4.76	0.53	<0.05	6.3	0.04	4.07		0.5	1.12	0.03	0.49	0.03	85.76	0.15	1.8	100.29
14,15	4.76-6.35	0.48	<0.05	5.22	0.03	3.69		0.35	1.04	0.02	0.4	0.03	87.91	0.10	1.57	100.38
14,15	bulk	0.59	<0.05	7.35	0.05	0.31	3.47	0.55	1.11	0.03	0.64	0.04	84.79	0.18	1.78	100.3

Concentration values in wt%.

Table 4.5 Laboratory samples particle size fraction major oxide concentrations (7 of 7).

Sample	Size (mm)	S_T	CO_2	Al_2O_3	CaO	Fe_2O_3	FeO	K_2O	MgO	MnO	Na_2O	P_2O_5	SiO_2	TiO_2	LOI	Total
16	< 0.074	0.78	5.6	11.79	0.11	17.35		2.62	1.68	0.74	0.12	0.01	57.91	0.54	7.18	100.06
16	0.074-0.105	0.95	4	11.32	0.14	15.18		2.4	1.62	0.58	0.15	0.02	62.38	0.64	6.01	100.42
16	0.105-0.149	0.97	4.1	11.91	0.11	16.57		2.49	1.66	0.61	0.13	0.02	59.74	0.59	6.57	100.39
16	0.149-0.21	0.94	4.6	11.63	0.08	17.02		2.47	1.66	0.67	0.13	0.01	59.25	0.54	6.71	100.17
16	0.21-0.3	0.94	5	11.04	0.08	17.09		2.44	1.63	0.72	0.16	0.02	59.49	0.50	7.11	100.26
16	0.3-0.5	0.82	5.4	10.59	0.08	17.2		2.3	1.61	0.75	0.1	0.01	59.97	0.46	7.04	100.11
16	0.5-0.545	0.65	5.7	10.15	0.06	17.44		2.15	1.59	0.79	0.06	0.08	60.3	0.44	7.3	100.36
16	0.545-0.841	0.72	5.8	9.7	0.06	17.43		2.07	1.57	0.83	0.08	0.01	60.7	0.41	7.34	100.21
16	0.84-2.0	0.62	6.35	8.98	0.06	17.7		1.85	1.56	0.89	0.07	0.01	61.4	0.37	7.6	100.47
16	2.0-4.76	0.64	6.65	8.24	0.06	17.61		1.65	1.53	0.91	0.11	0.02	62.12	0.34	7.55	100.13
16	4.76-6.35	0.47	6.55	8.2	0.06	17.84		1.61	1.55	0.94	0.09	0.03	61.64	0.33	7.72	100.01
16	bulk	0.72	6.85	8.52	0.07	1.85	14.77	1.58	1.56	0.94	0.07	0.02	61.82	0.34	7.36	98.901
17,18	< 0.074	1.16	<0.05	16.63	0.19	13.25		2.36	5.11	0.05	0.25	0.12	56	1.03	5.09	100.08
17,18	0.074-0.105	1.02	<0.05	16.24	0.19	13.55		2.09	5.37	0.05	0.2	0.12	56.3	1.04	5.07	100.24
17,18	0.105-0.149	0.79	0.29	16.3	0.18	13.73		2.11	5.26	0.08	0.22	0.12	55.59	0.99	5.46	100.03
17,18	0.149-0.21	0.72	0.4	15.85	0.16	13.52		2.02	5.1	0.10	0.2	0.12	56.82	0.93	5.53	100.35
17,18	0.21-0.3	0.67	<0.05	15.73	0.17	12.75		2.03	5.31	0.05	0.26	0.13	55.63	0.91	5.17	98.13
17,18	0.3-0.5	0.75	<0.05	15.12	0.16	12.69		1.88	5.26	0.05	0.28	0.12	57.43	0.85	5.17	99
17,18	0.5-0.545	0.81	<0.05	14.83	0.16	12.56		1.8	5.1	0.05	0.21	0.12	58	0.82	5.09	98.74
17,18	0.545-0.841	0.89	<0.05	14.54	0.15	12.45		1.77	4.97	0.05	0.15	0.12	59.96	0.79	4.9	99.82
17,18	0.84-2.0	1	<0.05	13.6	0.18	12.15		1.48	4.78	0.04	0.15	0.13	61.81	0.73	4.76	99.8
17,18	2.0-4.76	1.33	<0.05	12.56	0.21	11.79		1.47	4.29	0.04	0.11	0.17	64.68	0.65	4.53	100.5
17,18	4.76-6.35	1.29	<0.05	12.11	0.14	11.41		1.45	4.1	0.04	0.13	0.11	65.9	0.64	4.37	100.41
17,18	bulk	1.22	<0.05	13.15	0.15	1.59	9.37	1.39	4.51	0.04	0.13	0.12	64.1	0.70	3.85	99.105

Concentration values in wt%.

Table 4.6 Laboratory bulk sample modal mineral abundance.

Sample	S_T wt%	S_T wt%[1]	Pyrite	Quartz	Chlorite	Muscovite	Albite	Ilmenite	Apatite	Siderite	Melanterite	Hematite	Total
1	0.04	0.07	0.1	29	55	12	1	2.2	0.5	< 0.1	< 0.1	< 0.1	99.8
2	0.05	0.17	0.1	24	30	42	1	1.7	0.4	< 0.1	< 0.1	< 0.1	99.2
3	0.05	0.13	0.1	24	39	32	2	2.1	0.8	< 0.1	< 0.1	< 0.1	100
4	0.1	0.38	0.2	56	26	13	2	1.4	1.2	< 0.1	< 0.1	< 0.1	99.8
6	0.12	0.29	0.2	28	41	28	1	1.5	0.1	< 0.1	< 0.1	0.2	100
7	0.16	0.52	0.3	48	31	13	6	1.7	0.1	< 0.1	< 0.1	< 0.1	100.1
8	0.16	0.46	0.3	42	35	19	2	1.8	0.1	< 0.1	< 0.1	< 0.1	100.2
10	0.2	1.43	0.4	72	14	12	1	0.2	0.1	< 0.1	< 0.1	< 0.1	99.7
11	0.26	1.86	0.5	68	14	8	8	0.7	0.2	< 0.1	< 0.1	< 0.1	99.4
12	0.39	1.86	0.7	59	21	16	1	1.2	0.3	< 0.1	0.1	< 0.1	99.3
13	0.5	4.17	0.9	59	12	21	1	0.4	0.1	4.6	0.3	0.6	99.9
14	0.59	5.90	1.1	77	10	5	6	0.3	0.1	< 0.1	< 0.1	< 0.1	99.5
16	0.72	6.00	1.4	51	12	14	1	0.6	0.1	17.9	< 0.1	1.6	99.6
18	1.22	3.70	2.2	48	33	13	1	1.3	0.3	< 0.1	0.1	0.7	99.6

[1] S_T wt% values normalized to chlorite modality.

Values in volume percent (vol %) unless otherwise indicated.

All samples contained trace amounts (< 0.1 vol%) of magnetite, tourmaline, and zircon.

Previously determined Ely Greenstone mineral assemblages, assumed mineral compositions and whole rock data was used to estimate the modal mineralogy for all the samples. Melanterite was assumed to be present to account for the measured SO_4 concentration in the rocks.

Table 4.7 Laboratory bulk sample neutralization potential.

Sample #	S_T wt%	CO_2 wt%	Sobek NP(pH 7.0)	Peroxide NP(pH 7.0)	Sobek NP(pH 8.3)	Peroxide NP(pH 8.3)	NP($MgCO_3$)
1	0.04	<0.05	-2.5	2.8	-5	1.2	<0.1
1	0.04	--	**7.2 / 4.0**	**--**	**1.6 / 0.3**	**--**	--
2	0.05	<0.05	4.5	4.8	2.25	4	<0.1
3	0.05	<0.05	4	5.8	2.5	5.2	<0.1
4,5	0.1	<0.05	5	6.8	3	6	<0.1
4,5	0.1	--	6	6.2	3.5	5.2	--
6	0.12	<0.05	0.5	3	-1	2.2	<0.1
7	0.16	<0.05	0.75	4	0	3.2	<0.1
8,9	0.16	<0.05	2.75 / 2.7	3.8	1.0 / 1.7	3	<0.1
8,9	0.16	--	1.5 / 4.6	**--**	2.2 / 3.9	**--**	--
10	0.2	0.05	2.9	4	2.4	3.2	0.10
11	0.26	<0.05	4.9	3.5	4	2.8	<0.1
12	0.39	<0.05	4.6	5.25	3.8	4.8	<0.1
13	0.5	1.76	24.5 / 16.9	4	9.2 / 6.9	3.2	3.6
13	**0.5**	--	**16.3 / 20.3**	**--**	**7.3 / 9.1**	**--**	--
14,15	0.59	<0.05	2.2	1.5	1.2	0.8	<0.1
14,15	**0.59**	--	**--**	**3.2**	**--**	**2.4**	--
14,15	0.59	--	3.2	8.8	2	7.8	--
14,15	**0.59**	--	**--**	**2.4**	**--**	**1.9**	--
16	0.72	6.85	30.6	9.8	10.5	8.8	14
16	**0.72**	--	**32.4**	**7.2**	**12.3 / 10.7**	**5.4**	--
17,18	1.22	<0.05	6.4	5.25	2.7	4.5	<0.1
17,18	1.22	--	6.6	**--**	4.6	**--**	--

Values in g $CaCO_3$ eq·kg^{-1}

Bold values are duplicate analyses values.

-- indicates no analysis

Table 4.8 Humidity cells average annual solute release rates in mmol·kg^{-1}·wk^{-1} (1 of 3).

	Sample 1 (0.04 wt% S_T)					
year	pH$_{min}$	SO$_4$	Ca	Mg	Na	K
2000	6.94	5.83E-03	6.32E-03	7.53E-03	2.59E-02	2.14E-02
2001	6.87	4.60E-03	6.75E-03	9.78E-03	7.51E-04	1.25E-02
2002	6.93	3.67E-03	4.87E-03	7.35E-03	4.84E-04	7.50E-03
2003	6.82	3.15E-03	5.18E-03	6.00E-03	3.90E-04	5.13E-03
2004	6.46	2.20E-03	4.54E-03	5.02E-03	--	--
2005	6.63	2.16E-03	3.41E-03	4.73E-03	--	--
2006	6.48	2.18E-03	3.37E-03	4.36E-03	--	--
2007	6.43	1.26E-03	2.70E-03	4.13E-03	--	--
2008	6.37	1.27E-03	2.18E-03	3.53E-03	--	--
2009	6.21	1.27E-03	2.13E-03	3.04E-03	--	--
2010	6.33	1.46E-03	1.87E-03	2.98E-03	--	--
2011	6.09	1.19E-03	1.47E-03	2.42E-03	--	--

Sample 2 (0.04 wt% S_T)					
pH$_{min}$	SO$_4$	Ca	Mg	Na	K
6.84	9.24E-03	6.85E-03	5.75E-03	6.60E-03	2.33E-02
6.55	6.76E-03	6.70E-03	6.21E-03	5.38E-04	5.75E-03
6.55	4.91E-03	4.56E-03	4.26E-03	4.22E-04	3.85E-03
6.41	3.87E-03	4.84E-03	3.07E-03	3.78E-04	2.12E-03
6.28	3.36E-03	4.01E-03	2.69E-03	--	--
6.24	2.69E-03	3.13E-03	2.73E-03	--	--
6.19	3.10E-03	3.23E-03	2.20E-03	--	--
6.17	2.70E-03	2.34E-03	2.40E-03	--	--
6.00	2.63E-03	2.08E-03	1.90E-03	--	--
5.97	1.49E-03	2.16E-03	1.47E-03	--	--
6.00	2.39E-03	1.85E-03	1.01E-03	--	--
5.87	1.41E-03	1.54E-03	9.45E-04	--	--

	Sample 3 (0.05 wt% S_T)					
year	pH$_{min}$	SO$_4$	Ca	Mg	Na	K
2000	6.86	5.90E-03	6.28E-03	5.43E-03	1.26E-02	2.17E-02
2001	6.64	5.06E-03	5.72E-03	6.03E-03	5.17E-04	5.30E-03
2002	6.54	4.17E-03	4.38E-03	4.15E-03	3.66E-04	2.84E-03
2003	6.41	4.14E-03	4.57E-03	2.89E-03	4.77E-04	2.47E-03
2004	6.25	3.15E-03	3.71E-03	2.80E-03	--	--
2005	6.18	2.19E-03	2.69E-03	2.76E-03	--	--
2006	6.16	2.66E-03	2.81E-03	2.33E-03	--	--
2007	6.12	1.95E-03	1.98E-03	2.72E-03	--	--
2008	6.08	1.82E-03	1.75E-03	2.03E-03	--	--
2009	6.00	1.27E-03	1.90E-03	1.62E-03	--	--
2010	6.00	1.59E-03	1.36E-03	1.00E-03	--	--
2011	5.92	1.19E-03	1.07E-03	9.40E-04	--	--

Sample 4 (0.1 wt% S_T)					
pH$_{min}$	SO$_4$	Ca	Mg	Na	K
6.58	1.49E-02	1.09E-02	1.05E-02	5.04E-03	1.22E-02
6.02	1.19E-02	6.85E-03	7.12E-03	7.94E-04	3.45E-03
5.92	9.45E-03	5.20E-03	3.64E-03	7.28E-04	2.43E-03
5.76	6.85E-03	5.07E-03	1.92E-03	4.70E-04	8.30E-04
5.68	6.22E-03	4.59E-03	1.24E-03	--	--
5.59	5.19E-03	3.78E-03	1.16E-03	--	--
5.56	5.05E-03	3.75E-03	1.13E-03	--	--
5.56	4.30E-03	2.58E-03	1.39E-03	--	--
5.55	4.27E-03	2.39E-03	9.84E-04	--	--
5.38	3.73E-03	2.91E-03	9.85E-04	--	--
5.46	3.78E-03	2.24E-03	9.96E-04	--	--
5.30	3.35E-03	1.64E-03	9.29E-04	--	--

.

Table 4.8 Humidity cells average annual solute release rates in mmol·kg^{-1}·wk^{-1} (2 of 3).

	Sample 6 (0.12 wt% S_T)						Sample 7 (0.16 wt% S_T)					
year	pH_{min}	SO_4	Ca	Mg	Na	K	pH_{min}	SO_4	Ca	Mg	Na	K
2000	6.50	1.81E-02	8.41E-03	1.07E-02	3.78E-03	1.73E-02	6.55	2.08E-02	1.49E-02	9.22E-03	1.65E-02	1.81E-02
2001	6.11	1.14E-02	5.69E-03	8.00E-03	4.25E-04	3.09E-03	6.15	1.95E-02	1.11E-02	9.48E-03	9.27E-04	3.83E-03
2002	6.08	8.13E-03	4.00E-03	4.63E-03	3.15E-04	1.92E-03	5.95	1.66E-02	7.17E-03	7.20E-03	1.10E-03	2.33E-03
2003	5.85	6.91E-03	4.70E-03	3.64E-03	4.39E-04	1.25E-03	5.71	1.36E-02	6.15E-03	5.97E-03	6.81E-04	2.03E-03
2004	5.75	6.76E-03	4.31E-03	3.26E-03	--	--	5.49	1.25E-02	4.84E-03	5.58E-03	--	--
2005	5.59	6.27E-03	3.45E-03	3.42E-03	--	--	5.41	1.13E-02	3.43E-03	5.66E-03	--	--
2006	5.39	6.52E-03	3.47E-03	2.77E-03	--	--	5.18	1.07E-02	2.99E-03	5.19E-03	--	--
2007	5.00	5.78E-03	3.29E-03	2.40E-03	--	--	5.27	9.21E-03	1.94E-03	4.97E-03	--	--
2008	5.39	5.59E-03	2.16E-03	2.29E-03	--	--	5.22	8.39E-03	1.26E-03	4.25E-03	--	--
2009	5.27	4.90E-03	2.29E-03	2.01E-03	--	--	5.11	7.61E-03	1.04E-03	3.96E-03	--	--
2010	5.25	4.97E-03	1.39E-03	1.04E-03	--	--	5.06	7.10E-03	6.11E-04	3.14E-03	--	--
2011	5.05	4.86E-03	9.20E-04	1.14E-03	--	--	4.89	6.37E-03	5.77E-04	2.55E-03	--	--

	Sample 8 (0.16 wt% S_T)						Sample 10 (0.2 wt% S_T)					
year	pH_{min}	SO_4	Ca	Mg	Na	K	pH_{min}	SO_4	Ca	Mg	Na	K
2000	6.23	2.14E-02	9.12E-03	7.25E-03	1.26E-02	2.29E-02	4.32	5.53E-02	1.35E-02	2.37E-02	4.04E-03	1.66E-02
2001	5.87	1.52E-02	7.42E-03	7.18E-03	7.52E-04	4.24E-03	3.90	6.46E-02	3.42E-03	7.09E-03	8.88E-04	3.41E-03
2002	5.66	1.30E-02	5.44E-03	5.29E-03	5.11E-04	2.46E-03	3.89	5.60E-02	2.37E-03	7.45E-03	5.92E-04	2.13E-03
2003	5.44	1.08E-02	4.98E-03	4.28E-03	6.53E-04	1.76E-03	4.07	4.63E-02	2.71E-03	8.58E-03	5.70E-04	1.47E-03
2004	5.31	1.01E-02	4.34E-03	4.62E-03	--	--	4.01	3.95E-02	2.17E-03	7.12E-03	--	--
2005	5.17	9.18E-03	3.00E-03	4.60E-03	--	--	4.06	4.05E-02	1.52E-03	8.02E-03	--	--
2006	5.09	9.01E-03	2.63E-03	3.82E-03	--	--	4.18	3.52E-02	1.52E-03	6.66E-03	--	--
2007	4.96	7.73E-03	2.05E-03	3.62E-03	--	--	4.21	3.10E-02	7.97E-04	6.65E-03	--	--
2008	4.90	7.02E-03	6.07E-04	2.40E-03	--	--	4.25	2.70E-02	6.07E-04	5.40E-03	--	--
2009	4.82	6.24E-03	6.75E-04	1.39E-03	--	--	4.25	2.45E-02	6.09E-04	5.03E-03	--	--
2010	4.81	6.44E-03	6.31E-04	1.01E-03	--	--	4.09	2.30E-02	6.08E-04	4.28E-03	--	--
2011	4.78	5.94E-03	5.77E-04	9.51E-04	--	--	4.23	2.00E-02	5.69E-04	3.55E-03	--	--

Table 4.8 Humidity cells average annual solute release rates in mmol·kg^{-1}·wk^{-1} (3 of 3).

	Sample 13 (0.5 wt% S_T)					
year	pH$_{min}$	SO$_4$	Ca	Mg	Na	K
2000	4.35	2.06E-01	2.74E-02	8.27E-02	5.21E-03	2.56E-02
2001	5.09	1.20E-01	6.46E-03	7.12E-02	6.94E-04	2.33E-03
2002	6.15	8.91E-02	4.53E-03	7.79E-02	3.44E-04	2.10E-03
2003	6.70	6.94E-02	4.91E-03	7.58E-02	3.77E-04	1.51E-03
2004	6.69	5.25E-02	4.21E-03	6.01E-02	--	--
2005	6.60	4.65E-02	3.05E-03	4.92E-02	--	--
2006	6.43	3.93E-02	2.77E-03	3.93E-02	--	--
2007	6.15	2.97E-02	1.86E-03	3.13E-02	--	--
2008	6.01	2.50E-02	1.41E-03	2.43E-02	--	--
2009	5.77	2.00E-02	1.47E-03	1.92E-02	--	--
2010	5.43	1.88E-02	9.74E-04	1.69E-02	--	--
2011	5.48	1.71E-02	5.68E-04	1.33E-02	--	--

	Sample 14 (0.59 wt% S_T)					
year	pH$_{min}$	SO$_4$	Ca	Mg	Na	K
2000	3.21	3.13E-01	3.37E-02	5.14E-02	1.18E-02	1.55E-02
2001	3.11	3.12E-01	1.20E-02	4.56E-02	2.09E-03	1.96E-03
2002	3.06	2.74E-01	7.31E-03	3.80E-02	1.36E-03	1.44E-03
2003	3.39	1.95E-01	5.99E-03	2.63E-02	1.04E-03	1.25E-03
2004	3.39	1.54E-01	4.48E-03	2.01E-02	--	--
2005	3.40	1.39E-01	3.27E-03	1.94E-02	--	--
2006	3.54	1.27E-01	2.99E-03	1.69E-02	--	--
2007	3.62	1.01E-01	2.45E-03	1.48E-02	--	--
2008	3.68	9.01E-02	1.67E-03	1.24E-02	--	--
2009	3.61	8.38E-02	1.69E-03	1.23E-02	--	--
2010	3.69	7.68E-02	1.47E-03	1.12E-02	--	--
2011	3.75	6.81E-02	9.57E-04	9.12E-03	--	--

	Sample 16 (0.72 wt% S_T)					
year	pH$_{min}$	SO$_4$	Ca	Mg	Na	K
2000	6.19	1.29E-01	2.15E-02	9.80E-02	3.24E-03	1.29E-02
2001	7.22	8.74E-02	1.56E-02	2.20E-01	6.18E-04	3.66E-03
2002	7.74	8.83E-02	1.99E-02	3.12E-01	6.44E-04	2.97E-03
2003	7.74	9.87E-02	2.05E-02	3.00E-01	7.42E-04	1.55E-03
2004	7.59	1.08E-01	1.84E-02	2.54E-01	--	--
2005	7.39	1.15E-01	1.47E-02	2.07E-01	--	--
2006	7.20	1.14E-01	1.18E-02	1.62E-01	--	--
2007	7.02	9.71E-02	9.24E-03	1.37E-01	--	--
2008	6.85	7.91E-02	7.14E-03	9.94E-02	--	--
2009	6.35	6.23E-02	5.44E-03	7.32E-02	--	--
2010	6.17	4.74E-02	3.70E-03	5.05E-02	--	--
2011	6.13	3.53E-02	2.35E-03	3.40E-02	--	--

	Sample 18 (1.22 wt% S_T)					
year	pH$_{min}$	SO$_4$	Ca	Mg	Na	K
2000	3.44	2.42E-01	3.18E-02	6.80E-02	4.02E-03	1.58E-02
2001	3.35	3.01E-01	2.46E-02	6.25E-02	1.06E-03	2.22E-03
2002	3.33	2.86E-01	1.89E-02	5.97E-02	6.30E-04	1.64E-03
2003	3.45	2.73E-01	1.64E-02	5.41E-02	7.82E-04	1.38E-03
2004	3.39	2.43E-01	1.40E-02	4.63E-02	--	--
2005	3.39	2.43E-01	1.15E-02	4.79E-02	--	--
2006	3.49	2.44E-01	9.99E-03	4.59E-02	--	--
2007	3.45	2.16E-01	1.01E-02	4.22E-02	--	--
2008	3.51	2.10E-01	6.93E-03	3.45E-02	--	--
2009	3.47	2.06E-01	7.13E-03	3.85E-02	--	--
2010	3.46	1.89E-01	6.89E-03	3.73E-02	--	--
2011	3.44	1.78E-01	5.27E-03	2.94E-02	--	--

Table 4.9 Humidity cells AP, NP, ENP(pH 6), and ∑(Ca+Mg) values.

Sample	Group	Weeks pH ≥ 6	S_T wt%	CO_2 wt%	AP (S_T)	NP (CO_2)	NP ($MgCO_3$)	ENP (pH 6)	∑(Ca+Mg)	ENP Mg/Ca	Peroxide NP(pH 8.3)	Peroxide NP(pH 8.3) /AP(S_T)
1	1	622	0.04	<0.05	1.2	< 1.1	< 0.1	0.36	0.36	1.1	1.2	0.96
2	1	622	0.05	<0.05	1.6	< 1.1	< 0.1	0.27	0.27	0.7	4	2.56
3	1	622	0.05	<0.05	1.6	< 1.1	< 0.1	0.25	0.25	0.8	5.2	3.33
4	2	0-140	0.1	<0.05	3.1	< 1.1	< 0.1	0.14	0.29	0.8	6	1.92
6	2	0-188	0.12	<0.05	3.7	< 1.1	< 0.1	0.16	0.30	1.0	2.2	0.59
7	2	0-154	0.16	<0.05	5.0	< 1.1	< 0.1	0.20	0.41	0.7	3.2	0.64
8	2	0-102	0.16	<0.05	5.0	< 1.1	< 0.1	0.11	0.30	0.7	3	0.60
10	3	0-17	0.2	0.05	6.2	1.1	0.1	0.05	0.40	1.1	3.2	0.51
13	4	0-3, 98-476	0.5	1.76	16	40	3.6	1.28	1.97	10.9	3.2	0.21
14	3	0	0.59	<0.05	18	< 1.1	< 0.1	0.01	1.15	0.4	2.4/1.9	0.12
16	4	622	0.72	6.85	22	156	14	6.67	6.68	10.9	5.4	0.24
18	3	0-2	1.22	<0.05	38	< 1.1	< 0.1	0.04	2.38	1.2	4.5	0.12

The ENP Mg/Ca values were calculated as the molar ratio of the cumulative Ca and Mg mass released when leachate pH was ≥ 6.

Table 4.10 Humidity cell NP values comparison.

Sample	CO_2 (wt %)	Cumulative Ca release (g $CaCO_3 \cdot kg^{-1}_{rock}$)	Cumulative Mg release (g $CaCO_3 \cdot kg^{-1}_{rock}$)	∑(Ca+Mg)	NP ($MgCO_3$)	NP ($(Ca,Mg)CO_3$)	NP ($MgCO_3$) consumed	NP ($(Ca,Mg)CO_3$) consumed
1	< 0.05	1.65E-01	1.90E-01	0.36	< 0.10	0.42	348%	85%
2	< 0.05	1.60E-01	1.08E-01	0.27	< 0.10	0.42	262%	64%
3	< 0.05	1.41E-01	1.08E-01	0.25	< 0.10	0.42	244%	59%
4	< 0.05	1.93E-01	9.92E-02	0.29	< 0.10	0.42	286%	69%
6	< 0.05	1.63E-01	1.40E-01	0.30	< 0.10	0.42	296%	72%
7	< 0.05	2.05E-01	2.09E-01	0.41	< 0.10	0.42	405%	99%
8	< 0.05	1.52E-01	1.44E-01	0.30	< 0.10	0.42	290%	71%
10	0.05	1.12E-01	2.90E-01	0.40	0.10	0.42	393%	95%
13	1.76	2.18E-01	1.75E+00	1.97	3.6	14.8	55%	13%
14	< 0.05	2.84E-01	8.60E-01	1.14	< 0.10	0.42	1119%	272%
16	6.85	5.61E-01	6.11E+00	6.67	14	57.6	48%	12%
18	< 0.05	6.04E-01	1.77E+00	2.37	< 0.10	0.42	2320%	564%

Ca and Mg cumulative release were calculated for the entire 622 weeks of record.
NP($MgCO_3$) calculated using equation 8 $NP(MgCO_3) = 0.09 \times wt\%\ CO_2 \times 22.74$
NP($(Ca,Mg)CO_3$) was calculated as $NP((Ca,Mg)CO_3) = 0.37 \times wt\%\ CO_2 \times 22.74$
NP values in g $CaCO_3 \cdot kg^{-1}_{rock}$

Table 4.11 Field rock piles particle size distribution

Particle Size (mm)	Rock Pile 1	Rock Pile 2	Rock Pile 3	Rock Pile 4
>305	12.2	8.7	3	7.9
152-305	10.6	8.9	6.2	6.1
64-152	21.4	23.3	12.5	11.1
19-64	33	32.7	30.9	32.7
6.35-19	11.4	10.5	22.1	19.3
2.0-6.35	5.2	6.2	12.1	11.7
0.5-2.0	3.8	6.2	8.4	6.9
0.149-0.5	1.5	2.3	3.1	2.4
0.074-0.149	0.3	0.4	0.7	0.7
<0.074	0.5	0.8	1	1.2

Values are in percent total mass.

Table 4.12 Field rock piles average sulfur, carbonate, and major oxide composition.

Muck Box Average														
Rock Pile	S_T	SO_4	CO_2	SiO_2	Al_2O_3	Fe_2O_3	MnO	MgO	CaO	Na_2O	K_2O	TiO_2	P_2O_5	LOI	Total
1	0.02	0.02	0.16	52.05	19.74	11.27	0.13	6.35	0.72	0.40	2.54	0.87	0.40	5.80	100.28
2	0.22	0.03	0.26	60.76	14.96	10.09	0.09	5.26	0.77	0.28	1.83	0.67	0.41	4.78	99.89
3	0.37	0.03	0.08	67.92	13.09	8.66	0.07	3.25	0.38	0.39	1.70	0.54	0.26	3.53	99.78
4	0.63	0.03	0.47	65.99	12.85	10.48	0.09	3.38	0.23	0.20	1.90	0.51	0.13	4.02	99.78
Mass Weighted Particle Size Average															
Rock Pile	S_T	SO_4	CO_2	SiO_2	Al_2O_3	Fe_2O_3	MnO	MgO	CaO	Na_2O	K_2O	TiO_2	P_2O_5	LOI	Total
1	0.04	0.05	0.12	51.47	20.00	11.61	0.13	6.46	0.56	0.53	2.19	0.86	0.30	6.12	100.23
2	0.58	0.05	0.23	68.56	12.25	9.25	0.08	3.09	0.50	0.21	1.79	0.42	0.18	3.71	100.06
3	0.35	0.05	0.14	66.29	12.27	9.72	0.07	4.47	0.63	0.26	1.27	0.54	0.37	4.03	99.92
4	0.60	0.08	0.11	73.24	12.36	8.28	0.04	2.93	0.20	0.23	2.00	0.43	0.09	3.46	103.27

The Muck box averages represent the average value from 25 samples. The mass weighted particle size average values were determined by weighting each value by the mass fraction determined from the particle size distribution analysis using data from table 4.11 and 4.13. Values in wt%.

Table 4.13 Field rock piles particle size fraction compositions (1 of 2).

Particle Size (mm)	S_T	S^{2-} [1]	SO_4 as S	CO_2	SiO_2	Al_2O_3	Fe_2O_3	MnO	MgO	CaO	Na_2O	K_2O	TiO_2	P_2O_5	LOI	TOTAL[2]
	Rock Pile 1 (0.02 wt% S_T)															
64-152	0.04	0.02	0.05	<0.05	50.43	21.22	11.59	0.11	6.61	0.42	0.67	1.85	0.94	0.29	6.45	100.59
19-64	0.04	0.02	0.05	<0.05	52.18	19.34	11.66	0.13	6.74	0.43	0.34	2.42	0.78	0.28	5.96	100.27
6.35-19	0.06	0.06	<0.05	<0.05	51.41	19.08	12.2	0.18	6.09	0.9	0.46	2.53	0.88	0.35	5.63	99.72
2.0-6.35	0.04	0.04	<0.05	0.37	53.89	18.33	11.38	0.12	5.67	1	0.53	2.55	0.83	0.36	5.79	100.44
0.5-2.0	0.05	0.05	<0.05	0.81	54.41	18.33	10.83	0.12	5.44	1.06	0.62	2.52	0.76	0.38	5.73	100.2
0.149-0.5	0.05	0.05	<0.05	1	54.17	17.66	10.31	0.11	5.1	1.25	0.82	2.5	0.75	0.33	6.04	99.04
0.074-0.149	0.07	0.07	<0.05	1.03	53.34	17.88	10.6	0.11	5.21	1.61	0.95	2.41	0.80	0.33	6.38	99.63
<0.074	0.08	0.06	0.05	1.5	50.68	18.64	11.15	0.12	5.49	1.83	0.84	2.56	0.68	0.33	7.33	99.65
	Rock Pile 2 (0.20 wt% S_T)															
64-152	0.8	0.8	<0.05	<0.05	75.83	8.18	9.48	0.08	2.6	0.1	0.09	0.76	0.13	0.06	2.89	100.2
19-64	0.41	0.41	<0.05	0.07	66.39	14.99	8.31	0.08	2.38	0.33	0.2	2.89	0.59	0.21	3.51	99.88
6.35-19	0.73	0.73	<0.05	<0.05	60.94	14.56	11.01	0.10	5.32	0.64	0.3	1.61	0.62	0.3	4.98	100.37
2.0-6.35	0.27	0.27	<0.05	0.81	61.05	14.68	9.61	0.09	4.39	1.65	0.49	2.15	0.66	0.33	5.05	100.14
0.5-2.0	0.25	0.25	<0.05	0.92	60.06	15.55	9.16	0.08	4.27	1.52	0.42	2.28	0.66	0.33	5.04	99.37
0.149-0.5	0.26	0.26	<0.05	1.72	57.3	16.74	9.42	0.08	4.3	2.12	0.56	2.5	0.74	0.29	6.07	100.12
0.074-0.149	0.28	0.28	<0.05	2.13	52.49	17.78	10.23	0.09	4.83	3.16	0.6	2.61	0.84	0.33	7.15	100.09
<0.074	0.25	0.23	0.05	2.9	50.39	18.29	10.15	0.09	4.67	3.85	0.57	2.78	0.78	0.33	8.25	100.14

[1] S^{2-} concentration determined by difference.

[2] Total includes SiO_2 through LOI.

Table 4.13 Field rock piles particle size fraction compositions (2 of 2).

Particle Size (mm)	S_T	S^{2-} [1]	SO_4 as S	CO_2	SiO_2	Al_2O_3	Fe_2O_3	MnO	MgO	CaO	Na_2O	K_2O	TiO_2	P_2O_5	LOI	TOTAL[2]
	Rock Pile 3 (0.39 wt% S_T)															
64-152	0.25	0.25	<0.05	<0.05	47.89	14.9	17.03	0.10	9.74	1.31	0.03	0.18	0.86	0.95	6.41	99.39
19-64	0.5	0.5	<0.05	<0.05	78.51	8.12	6.51	0.05	2.61	0.14	0.13	1.04	0.27	0.1	2.56	100.05
6.35-19	0.28	0.28	<0.05	<0.05	68.71	12.55	8.42	0.06	3.29	0.52	0.34	1.64	0.56	0.32	3.5	99.92
2.0-6.35	0.29	0.29	<0.05	0.37	67.56	13.47	8.12	0.06	3.24	0.77	0.44	1.85	0.53	0.26	3.94	100.24
0.5-2.0	0.33	0.33	<0.05	0.33	64.82	15.22	8.41	0.06	3.2	0.61	0.59	2.26	0.59	0.26	4.11	100.13
0.149-0.5	0.31	0.26	0.15	0.4	60.77	17.37	8.74	0.07	3.36	0.79	0.8	2.59	0.70	0.25	5	100.45
0.074-0.149	0.6	0.6	<0.05	1.1	56.8	17.52	11.49	0.10	3.45	0.93	0.55	3.12	0.77	0.12	5.66	100.49
<0.074	0.55	0.52	0.1	1.1	54.76	18.48	11.46	0.10	3.48	1.05	0.49	3.37	0.72	0.12	6.14	100.17
	Rock Pile 4 (0.67 wt% S_T)															
64-152	0.9	0.9	<0.05	<0.05	75.36	11.59	5.99	0.02	1.65	0.06	0.2	2.54	0.22	0.04	2.78	100.45
19-64	0.25	0.25	<0.05	<0.05	73.04	10.62	7.57	0.05	3.27	0.18	0.18	1.25	0.48	0.13	3.04	99.81
6.35-19	0.75	0.7	0.15	<0.05	68.43	12.28	9.38	0.04	3.33	0.16	0.22	1.82	0.46	0.08	3.64	99.85
2.0-6.35	0.63	0.58	0.15	0.29	66.98	12.9	10.14	0.07	3.18	0.32	0.25	2.01	0.49	0.09	4	100.41
0.5-2.0	0.46	0.46	<0.05	0.22	64.55	14.28	9.97	0.07	3.28	0.29	0.29	2.33	0.52	0.09	4.05	99.71
0.149-0.5	0.43	0.43	<0.05	0.48	60.06	16.54	10.51	0.07	3.43	0.54	0.46	2.9	0.65	0.1	4.82	100.08
0.074-0.149	0.34	0.29	0.15	0.66	57.49	18.31	9.26	0.08	3.64	1.14	0.89	2.8	0.78	0.27	5.78	100.43
<0.074	0.32	0.32	<0.05	0.66	57.32	18.26	9.17	0.08	3.47	1.23	0.84	2.94	0.75	0.26	5.93	100.24

[1] Sulfide sulfur concentration determined by difference.

[2] Total includes SiO_2 through LOI.

Table 4.14 Field rock piles average mineral composition.

Rock Pile	Mineral	SiO_2	Al_2O_3	TiO_2	FeO	MgO	MnO	K_2O	Na_2O	CaO	Cr_2O_3	NiO	P_2O_5	SO_4	CuO	ZnO	H_2O	Total
1	Albite	65.45	21.11	0.05	0.55	0.19	0.05	1.25	10.14	0.37	0.00	0.04	0.12	0.01	0.01	0.08	0.65	100.08
1	Chlorite	32.04	19.71	0.17	18.67	16.29	0.24	0.29	0.13	0.25	0.09	0.11	0.17	0.06	0.25	0.06	11.47	100.00
2	Chlorite	28.81	23.49	0.10	19.55	14.50	0.22	0.22	0.04	0.03	0.13	0.08	0.02	0.03	0.08	0.11	12.57	100.00
3	Chlorite	30.70	23.17	0.08	25.99	8.11	0.18	0.57	0.35	0.06	0.13	0.09	0.09	0.03	0.32	0.31	9.84	100.00
4	Chlorite	27.12	24.11	0.16	22.67	12.60	0.14	0.82	0.05	0.07	0.08	0.02	0.04	0.05	0.17	0.16	11.74	100.00
1	Muscovite	48.04	31.07	0.04	3.75	2.22	0.03	9.54	0.25	0.13	0.11	0.03	0.10	0.05	0.15	0.00	4.50	100.00
2	Muscovite	46.43	33.85	0.16	2.32	1.21	0.05	10.01	0.48	0.02	0.05	0.05	0.01	0.02	0.20	0.09	5.03	100.00
3	Muscovite	46.61	34.11	0.11	3.00	1.24	0.03	9.75	0.54	0.04	0.08	0.03	0.05	0.04	0.18	0.14	4.06	100.00
4	Muscovite	45.98	35.39	0.23	2.30	0.96	0.03	9.32	0.99	0.02	0.01	0.04	0.04	0.08	0.14	0.10	4.36	100.00
2	K-spar	64.18	17.38	0.06	2.47	0.07	0.03	14.28	1.02	0.02	0.02	0.00	0.04	0.00	0.11	0.00	0.51	100.20
4	Magnetite	0.05	0.24	0.03	89.04	0.06	0.12	0.00	0.07	0.01	0.04	0.02	0.01	0.03	0.32	0.01	9.96	100.00

Values in wt%.

Table 4.15 Field rock piles modal mineral abundance of different rock particle sizes.

Particle Size Range (mm)	Quartz	Muscovite	Magnetite	Chlorite	Calcite	Albite	Rutile	Pyrite
	Pile 1							
152.4 - 63.5	13.80	33.07	1.81	39.79	0.41	12.22	0.94	0.07
63.5 - 19.05	20.46	33.19	2.09	38.94	0.45	5.04	0.78	0.07
19.05 - 6.35	19.78	34.19	3.41	34.80	0.97	6.20	0.88	0.10
6.35 - 2.0	23.35	33.47	3.20	32.09	1.40	6.38	0.83	0.07
2.0 - 0.5	23.56	33.51	2.90	30.78	1.87	7.47	0.76	0.08
0.5 - 0.149	23.86	31.91	2.90	28.59	2.21	8.89	0.75	0.08
0.149 - 0.074	22.18	31.00	3.02	29.43	2.63	10.45	0.80	0.12
< 0.074	18.71	33.16	3.15	30.98	3.28	9.35	0.68	0.13
	Pile 2							
152.4 - 63.5	64.81	10.34	4.33	18.16	0.11	1.51	0.13	1.34
63.5 - 19.05	46.17	32.75	3.68	15.17	0.43	0.98	0.59	0.69
19.05 - 6.35	41.54	16.95	1.99	35.69	0.71	1.91	0.62	1.22
6.35 - 2.0	40.83	21.59	2.50	28.65	2.52	2.97	0.66	0.45
2.0 - 0.5	38.74	24.42	2.11	28.15	2.48	2.86	0.66	0.42
0.5 - 0.149	33.87	26.91	2.26	28.32	3.83	4.25	0.74	0.43
0.149 - 0.074	27.69	27.57	2.27	31.77	5.34	4.34	0.84	0.47
< 0.074	24.95	29.89	2.40	30.69	6.77	4.15	0.78	0.42
	Pile 3							
152.4 - 63.5	--	--	--	--	--	--	--	--
63.5 - 19.05	68.25	8.96	0.00	21.51	0.15	--	0.27	0.93
19.05 - 6.35	52.75	17.31	0.12	27.90	0.57	--	0.56	0.52
6.35 - 2.0	50.35	20.22	0.00	27.52	1.17	--	0.53	0.54
2.0 - 0.5	45.26	25.52	0.00	27.15	0.96	--	0.59	0.62
0.5 - 0.149	38.39	30.51	0.00	28.86	1.22	--	0.70	0.58
0.149 - 0.074	34.01	32.21	2.38	27.49	1.98	--	0.77	1.12
< 0.074	30.67	34.93	2.29	27.60	2.11	--	0.72	1.03
	Pile 4							
152.4 - 63.5	60.53	25.26	1.21	11.35	0.07	--	0.22	1.68
63.5 - 19.05	59.90	11.72	0.00	27.39	0.20	--	0.48	0.47
19.05 - 6.35	53.08	16.81	0.89	26.91	0.18	--	0.46	1.40
6.35 - 2.0	50.81	19.41	2.07	25.58	0.60	--	0.49	1.18
2.0 - 0.5	46.61	22.91	1.87	26.16	0.51	--	0.52	0.86
0.5 - 0.149	39.19	28.90	2.13	26.78	0.84	--	0.65	0.80
0.149 - 0.074	34.51	31.53	0.10	29.96	1.83	--	0.78	0.64
< 0.074	34.35	32.58	0.47	28.22	1.93	--	0.75	0.60

Values in vol% unless otherwise indicated.

Table 4.16 Field rock pile annual average solute release rates, total annual flow volume, and minimum pH.

	Rock Pile 1 (0.02 wt% S_T)						
year	pH_{min}	Flow	SO_4	Ca	Mg	Na	K
2000	7.4	7029	1.58E-03	1.62E-02	3.89E-03	2.35E-02	1.47E-03
2001	7.5	19389	1.50E-03	4.70E-03	1.02E-03	1.51E-02	1.24E-03
2002	7.6	14782	8.98E-04	2.07E-03	3.79E-04	5.59E-03	7.79E-04
2003	7.9	14350	7.73E-04	1.84E-03	3.16E-04	4.38E-03	7.16E-04
2004	7.8	17755	8.34E-04	2.16E-03	3.33E-04	4.46E-03	6.44E-04
2005	7.5	13844	7.81E-04	1.75E-03	2.75E-04	3.21E-03	5.30E-04
2006	7.7	13764	7.93E-04	1.67E-03	2.84E-04	2.58E-03	4.64E-04
2007	7.9	16638	8.54E-04	1.98E-03	3.27E-04	3.15E-03	6.05E-04
2008	7.6	14619	5.66E-04	1.57E-03	2.89E-04	2.27E-03	4.83E-04
2009	7.4	10255	5.16E-04	9.56E-04	2.02E-04	1.54E-03	3.23E-04
2010	7.1	17594	5.66E-04	1.58E-03	3.67E-04	2.16E-03	6.06E-04
2011	7.5	17834	5.35E-04	1.71E-03	3.39E-04	2.09E-03	6.03E-04

	Rock Pile 2 (0.20 wt% S_T)						
year	pH_{min}	Flow	SO_4	Ca	Mg	Na	K
2000	7.5	3808	2.42E-03	1.15E-02	2.64E-03	6.03E-03	4.93E-04
2001	7.4	19196	5.64E-03	2.44E-02	4.43E-03	1.50E-02	2.04E-03
2002	7.5	14476	3.38E-03	6.06E-03	8.49E-04	3.05E-03	9.23E-04
2003	7.4	13383	3.33E-03	4.86E-03	6.76E-04	1.65E-03	7.83E-04
2004	7.4	17719	4.04E-03	6.49E-03	7.93E-04	1.41E-03	8.63E-04
2005	7.3	13100	3.11E-03	4.45E-03	5.37E-04	6.99E-04	5.62E-04
2006	7.4	13678	3.84E-03	5.13E-03	6.42E-04	7.06E-04	5.88E-04
2007	7.6	18118	4.98E-03	6.82E-03	8.05E-04	8.98E-04	7.41E-04
2008	7.4	14484	2.84E-03	4.25E-03	5.42E-04	4.92E-04	4.75E-04
2009	7.5	8984	2.57E-03	3.67E-03	4.11E-04	2.96E-04	3.31E-04
2010	7.2	15221	4.38E-03	5.70E-03	6.30E-04	4.34E-04	5.60E-04
2011	7.2	15120	2.77E-03	4.56E-03	5.16E-04	3.06E-04	4.60E-04

	Rock Pile 3 (0.39 wt% S_T)						
year	pH_{min}	Flow	SO_4	Ca	Mg	Na	K
2000	7.4	2951	1.43E-03	8.96E-03	2.53E-03	7.30E-03	6.16E-04
2001	7.3	16612	3.79E-03	1.33E-02	2.65E-03	1.11E-02	1.80E-03
2002	7.5	13042	5.37E-03	6.17E-03	9.77E-04	1.90E-03	9.07E-04
2003	7.5	13337	6.41E-03	6.71E-03	9.98E-04	1.13E-03	8.24E-04
2004	7.3	16916	6.22E-03	7.85E-03	9.67E-04	8.17E-04	8.20E-04
2005	7.4	11447	3.99E-03	4.32E-03	5.31E-04	3.40E-04	4.68E-04
2006	7.4	13830	6.90E-03	6.89E-03	9.86E-04	3.60E-04	5.44E-04
2007	7.5	19917	9.05E-03	9.09E-03	1.45E-03	6.74E-04	7.60E-04
2008	7.1	13947	4.65E-03	4.98E-03	9.01E-04	2.83E-04	4.76E-04
2009	7.0	9308	4.35E-03	4.13E-03	7.43E-04	1.89E-04	3.21E-04
2010	7.2	14421	6.04E-03	5.64E-03	1.15E-03	2.52E-04	4.87E-04
2011	6.8	16343	6.13E-03	5.79E-03	1.26E-03	2.17E-04	4.90E-04

	Rock Pile 4 (0.67 wt% S_T)						
year	pH_{min}	Flow	SO_4	Ca	Mg	Na	K
2000	7.3	6885	5.60E-03	2.05E-02	4.43E-03	1.24E-02	1.31E-03
2001	7.6	18625	9.20E-03	1.36E-02	1.82E-03	6.92E-03	1.62E-03
2002	7.4	16262	1.09E-02	1.11E-02	1.25E-03	1.55E-03	1.14E-03
2003	7.4	16543	1.31E-02	1.26E-02	1.37E-03	9.36E-04	1.12E-03
2004	7.4	19380	1.15E-02	1.33E-02	1.31E-03	6.39E-04	1.00E-03
2005	7.0	12707	8.84E-03	8.61E-03	1.06E-03	2.99E-04	5.65E-04
2006	6.8	12542	1.21E-02	1.24E-02	2.34E-03	3.82E-04	5.86E-04
2007	5.6	17819	2.38E-02	1.76E-02	5.92E-03	6.32E-04	9.06E-04
2008	5.0	14861	1.51E-02	1.08E-02	4.25E-03	3.29E-04	6.03E-04
2009	4.5	9408	1.29E-02	8.58E-03	3.90E-03	2.12E-04	4.56E-04
2010	4.3	16563	2.20E-02	1.10E-02	7.23E-03	3.77E-04	7.46E-04
2011	4.0	16824	1.85E-02	8.03E-03	5.70E-03	2.82E-04	5.72E-04

Solute release rates values are in $mmol \cdot kg^{-1} \cdot wk^{-1}$ units.
Flow values are in liters.
Values for year 2000 only include part of the year

Table 4.17 Field rock piles AP, NP, and ENP values.

Rock Pile	wt% S_T	wt% CO_2	NP(CO_2)	NP(pH 8.3)	AP(S_T)	NP(CO_2)/AP(S_T)	NP(pH 8.3)/AP(S_T)	ENP(pH 6)
1	0.02	0.16	3.6	2.2 est.	0.5	7.3	4.3	> 0.45
2	0.22	0.26	5.8	3.5 est.	6.9	0.8	0.5	> 0.63
3	0.37	0.08	1.9	1.1 est.	11.7	0.2	0.1	> 0.6
4	0.63	0.47	10.6	6.3	19.8	0.5	0.3	0.86

NP and ENP values in g $CaCO_3 \cdot kg^{-1}{}_{rock}$
ENP(pH 6) values include neutralization from Ca, Mg, K, and Na

Table 4.18 Particle size distribution for tank rock and dolostone.

Particle Size (mm)	Tank 1	Tank 2	Tank 3	Tank 4	Tank 5	Tank 6	Dolostone
38.1-50.8	2.9	2.7	8.7	9.9	11.1	4.7	0
25.4-38.1	28.9	19.9	11.1	17.5	11.4	12.9	0
12.7-25.4	24.9	36.9	27	20.2	15.8	27.6	0
6.35-12.7	11.8	13.3	15.7	16.2	17.9	12.8	0
4.76-6.35	4.4	4.3	5.1	5.1	6	4.2	0
2.0-4.76	10.4	8.7	12.8	12.4	14.7	12.5	12.1
0.84-2.0	4.1	3.4	5.2	5.1	6.2	5.8	30.8
0.545-0.84	1.8	1.5	2.4	2.2	2.8	2.5	15.3
0.42-0.545	1.3	1.1	1.8	1.5	2	1.7	11.6
0.297-0.42	1.7	1.5	3.3	2	2.5	2	11.7
0.21-0.297	1.6	1.2	1.8	1.6	2	1.7	9.5
0.149-0.21	0.8	0.9	0.4	1.1	1.3	1.2	4.5
0.074-0.149	2	1.8	2.2	2.1	2.6	2.2	3.1
< 0.074	3.4	2.8	2.5	3.1	3.7	8.2	1.4

Values in wt% unless otherwise indicated.

Table 4.19 Field tank rock and dolostone compositions.

Parameter	Tank 1	Tank 2	Tank 3	Tank 4	Tank 5	Tank 6	Rock Pile 4	Limestone
S_T	0.56	0.4	0.5	0.46	0.55	0.48	0.63	0.01
S^{-2}	0.54	0.34	0.48	0.44	0.53	0.46	--	0
SO_4^{-2} as S	0.016	0.06	0.02	0.016	0.02	0.02	0.03	0.016
CO_2	0.4	0.37	0.22	0.44	0.44	0.48	0.47	41.563
Al_2O_3	13.86	13.09	12.53	13.12	13.28	13	12.85	0.47
CaO	0.41	0.37	0.26	0.46	0.32	0.43	0.23	27.63
Fe_2O_3	10.65	8.83	8.61	9.38	10.3	9.31	10.48	0.87
K_2O	1.86	2.03	1.95	1.91	1.85	2.09	1.90	0.29
MgO	3.59	2.96	2.91	3.26	3.41	2.89	3.38	18.82
MnO	0.068	0.065	0.053	0.089	0.065	0.059	0.09	0.081
Na_2O	0.36	0.38	0.3	0.39	0.34	0.38	0.20	<0.01
P_2O_5	0.15	0.12	0.1	0.12	0.13	0.21	0.13	0.03
SiO_2	64.7	68.4	69.3	65.96	65.38	67.32	65.99	9.68
TiO_2	0.587	0.458	0.452	0.522	0.519	0.514	0.51	0.026
LOI	4.19	3.73	3.62	3.89	4.02	3.72	4.02	41.95
TOTAL	100.42	100.44	100.08	99.11	99.6	99.92	99.78	99.78

S^{-2} was determined by difference between S_T and SO_4.
Total does not include S or CO_2 values.

Table 4.20 Field tanks annual average solute release rates, annual total flow volume, and minimum pH.

	Tank 1 (NP/AP 0.41)					Tank 2 (NP/AP 1.4)					Tank 3 (NP/AP 3.3)				
year	pH$_{min}$	Flow	SO$_4$	Ca	Mg	pH$_{min}$	Flow	SO$_4$	Ca	Mg	pH$_{min}$	Flow	SO$_4$	Ca	Mg
2001	7.2	625	2.12E-02	1.39E-02	1.36E-03	7.5	559	1.50E-02	9.52E-03	1.03E-03	7.5	601	2.00E-02	1.25E-02	1.50E-03
2002	7.1	479	2.01E-02	8.11E-03	8.56E-04	7.4	483	1.31E-02	6.00E-03	7.87E-04	7.4	465	1.48E-02	6.62E-03	9.11E-04
2003	7.0	433	2.46E-02	8.14E-03	1.14E-03	7.5	501	1.25E-02	5.29E-03	8.24E-04	7.8	480	1.22E-02	5.39E-03	8.56E-04
2004	5.2	413	2.31E-02	7.57E-03	1.19E-03	7.6	413	1.06E-02	4.33E-03	7.41E-04	7.7	597	1.37E-02	5.90E-03	1.08E-03
2005	4.7	219	1.24E-02	3.20E-03	8.94E-04	7.6	388	1.15E-02	3.94E-03	9.13E-04	7.7	371	1.00E-02	3.51E-03	8.46E-04
2006	4.3	391	1.81E-02	4.30E-03	1.36E-03	7.5	255	9.84E-03	3.33E-03	7.82E-04	7.6	398	1.44E-02	5.36E-03	1.37E-03
2007	4.2	589	2.44E-02	5.96E-03	1.70E-03	7.5	481	1.45E-02	4.71E-03	1.39E-03	7.7	387	1.13E-02	3.77E-03	1.14E-03
2008	4.3	370	9.66E-03	2.42E-03	6.26E-04	7.1	319	7.38E-03	2.40E-03	7.67E-04	7.6	456	9.20E-03	3.21E-03	9.70E-04
2009	4.0	379	1.60E-02	4.22E-03	1.08E-03	7.4	241	8.35E-03	2.46E-03	8.17E-04	7.8	259	1.03E-02	3.48E-03	1.15E-03
2010	4.1	661	1.74E-02	4.36E-03	1.20E-03	7.2	275	6.86E-03	2.00E-03	7.34E-04	7.4	664	1.37E-02	4.80E-03	1.67E-03
2011	4.1	537	1.24E-02	3.40E-03	7.85E-04	7.5	142	6.83E-03	2.42E-03	4.80E-04	7.8	554	1.02E-02	3.99E-03	1.32E-03

	Tank 4 (NP/AP 3.3)					Tank 5 (NP/AP 1.4)					Tank 6 (NP/AP 0.41)				
year	pH$_{min}$	Flow	SO$_4$	Ca	Mg	pH$_{min}$	Flow	SO$_4$	Ca	Mg	pH$_{min}$	Flow	SO$_4$	Ca	Mg
2001	7.5	569	1.65E-02	1.03E-02	1.23E-03	7.6	553	1.91E-02	1.08E-02	1.09E-03	7.3	557	1.77E-02	1.03E-02	1.07E-03
2002	7.5	471	1.41E-02	6.13E-03	8.46E-04	7.5	471	1.75E-02	7.58E-03	8.28E-04	7.0	505	2.22E-02	8.82E-03	9.75E-04
2003	7.3	329	9.82E-03	4.06E-03	6.39E-04	7.8	482	1.51E-02	6.39E-03	8.42E-04	7.2	280	1.61E-02	5.29E-03	7.22E-04
2004	6.2	289	5.85E-03	2.46E-03	4.48E-04	7.6	533	1.56E-02	6.21E-03	9.85E-04	4.8	371	2.26E-02	6.76E-03	1.44E-03
2005	7.9	322	7.65E-03	2.79E-03	6.67E-04	7.8	433	1.42E-02	5.13E-03	1.06E-03	4.4	388	2.09E-02	4.88E-03	1.34E-03
2006	7.5	274	6.31E-03	2.30E-03	5.93E-04	7.3	407	1.49E-02	5.48E-03	1.18E-03	4.3	404	2.25E-02	5.78E-03	1.60E-03
2007	7.7	434	1.19E-02	4.26E-03	1.19E-03	7.7	350	1.27E-02	3.95E-03	1.12E-03	4.2	509	2.06E-02	5.58E-03	1.32E-03
2008	7.5	164	3.17E-03	1.19E-03	3.56E-04	7.5	99	2.41E-03	7.69E-04	2.25E-04	4.2	279	6.80E-03	1.94E-03	5.25E-04
2009	7.6	373	1.53E-02	4.94E-03	1.64E-03	7.6	141	5.03E-03	1.50E-03	5.05E-04	4.2	361	1.33E-02	3.60E-03	9.20E-04
2010	7.5	642	1.36E-02	4.09E-03	1.39E-03	7.4	256	8.34E-03	2.52E-03	8.69E-04	4.1	644	1.56E-02	3.93E-03	1.10E-03
2011	7.8	550	1.28E-02	4.59E-03	1.51E-03	7.9	107	2.99E-03	1.03E-03	3.43E-04	4.1	530	1.21E-02	3.24E-03	8.54E-04

Solute release rates values are in mmol·kg^{-1}·wk^{-1} units.
Flow values are in liters.

Table 5.1 List of samples and time intervals used to calculate scale factors.

Sample	wt% S_T	pH range	time interval	average SO_4 release rate ($mmol \cdot kg^{-1} \cdot wk^{-1}$)
Humidity Cell 1	0.04	7-7.5	weeks 50-200	3.83E-03
Humidity Cell 10	0.2	4	weeks 50-200	5.60E-02
Humidity Cell 12	0.39	4	weeks 50-154	1.10E-01
Humidity Cell 14	0.59	3-3.5	weeks 50-200	2.62E-01
Tank 1	0.67	4-5	years 2005-2011	1.57E-02
Tank 6	0.67	4-5	years 2005-2011	1.60E-02
Rock Pile 1	0.02	7-9	years 2001-2011	7.83E-04
Rock Pile 2	0.2	7-9	years 2001-2011	3.72E-03
Rock Pile 3	0.39	7-8	years 2001-2011	5.72E-03
Rock Pile 4	0.67	4-5	years 2010-2011	2.03E-02

Table 5.2 Laboratory to field SO_4 release rate scale factors.

From	To	To	Scale Factor (Lab to Rock Pile)	Scale Factor (Lab to Tank)	Scale Factor (Tank to Rock Pile)
Sample 1 (0.04 wt% S)	Rock Pile 1 (0.02 wt% S)		0.20		
Sample 10 (0.2 wt% S)	Rock Pile 2 (0.2 wt% S)		0.07		
Sample 12 (0.39 wt% S)	Rock Pile 3 (0.39 wt% S)		0.05		
Sample 14 (0.59 wt% S)	Tank 1 (0.67 wt% S)	Rock Pile 4 (0.67 wt% S)	0.08	0.06	0.8
Sample 14 (0.59 wt% S)	Tank 6 (0.67 wt% S)	Rock Pile 4 (0.67 wt% S)	0.08	0.06	0.8

Table 5.3 Environmental risk chart.

Greenschist wt% S_T range	leachate pH range	environmental risk
0-0.05	> 6.0	low
0.10-0.16	4.75-5.5	moderate
0.2-1.22	3.0-4.5	high

FIGURES

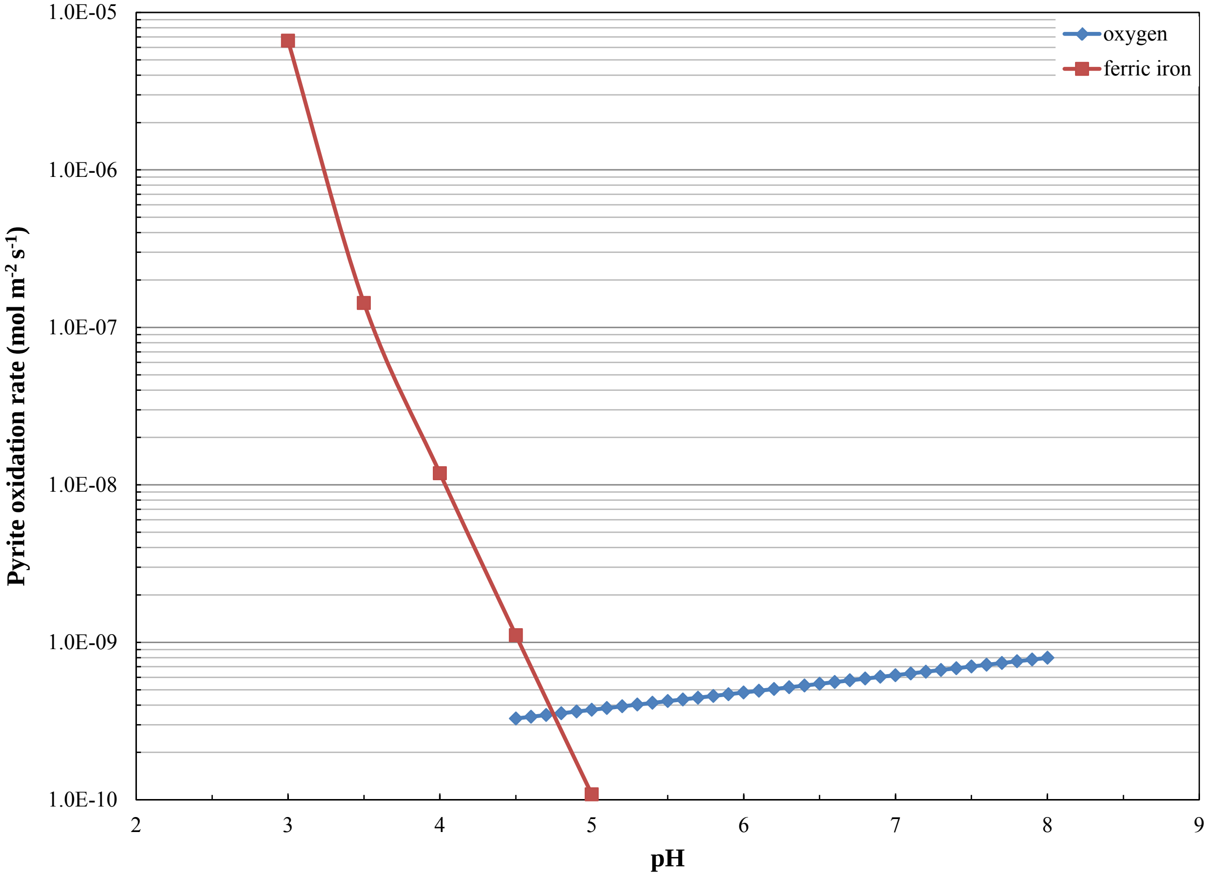

Figure 2.1 Pyrite oxidation rates as a function of pH and oxidant type.

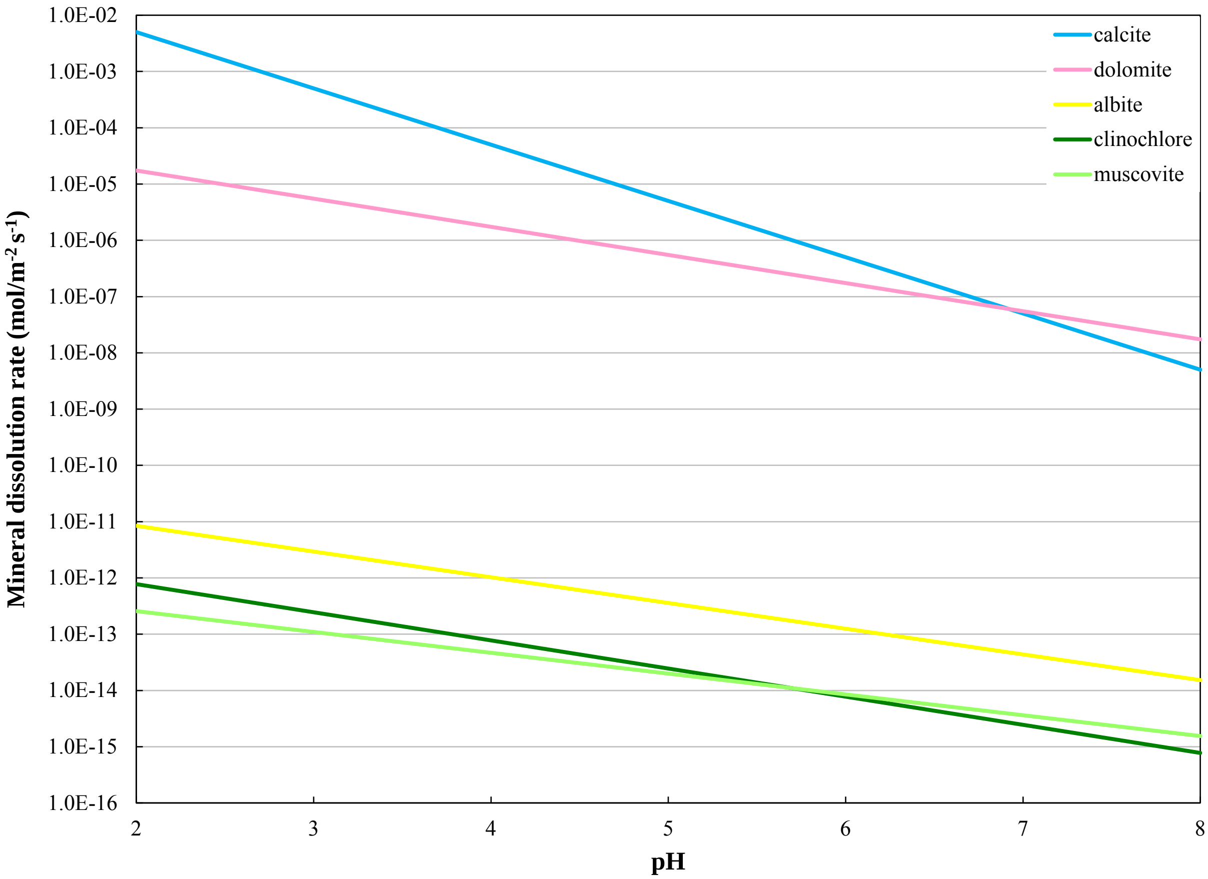

Figure 2.2 Dissolution rates for some carbonate and silicate minerals (calculated from Palandri and Kharaka, 2004).

Figure 3.1 Picture of field rock pile construction.

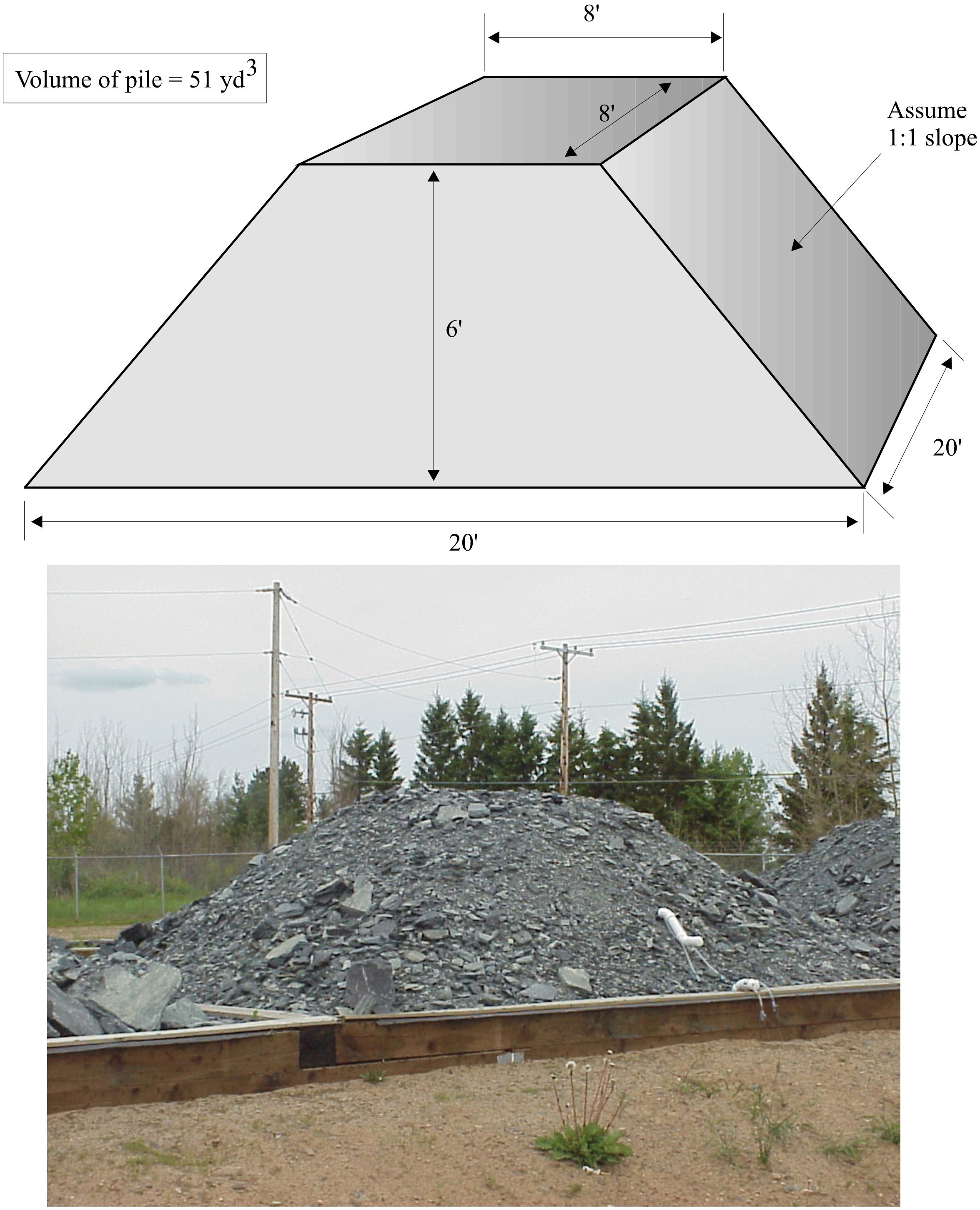

Figure 3.2 Picture of rock piles with inset dimension drawing.

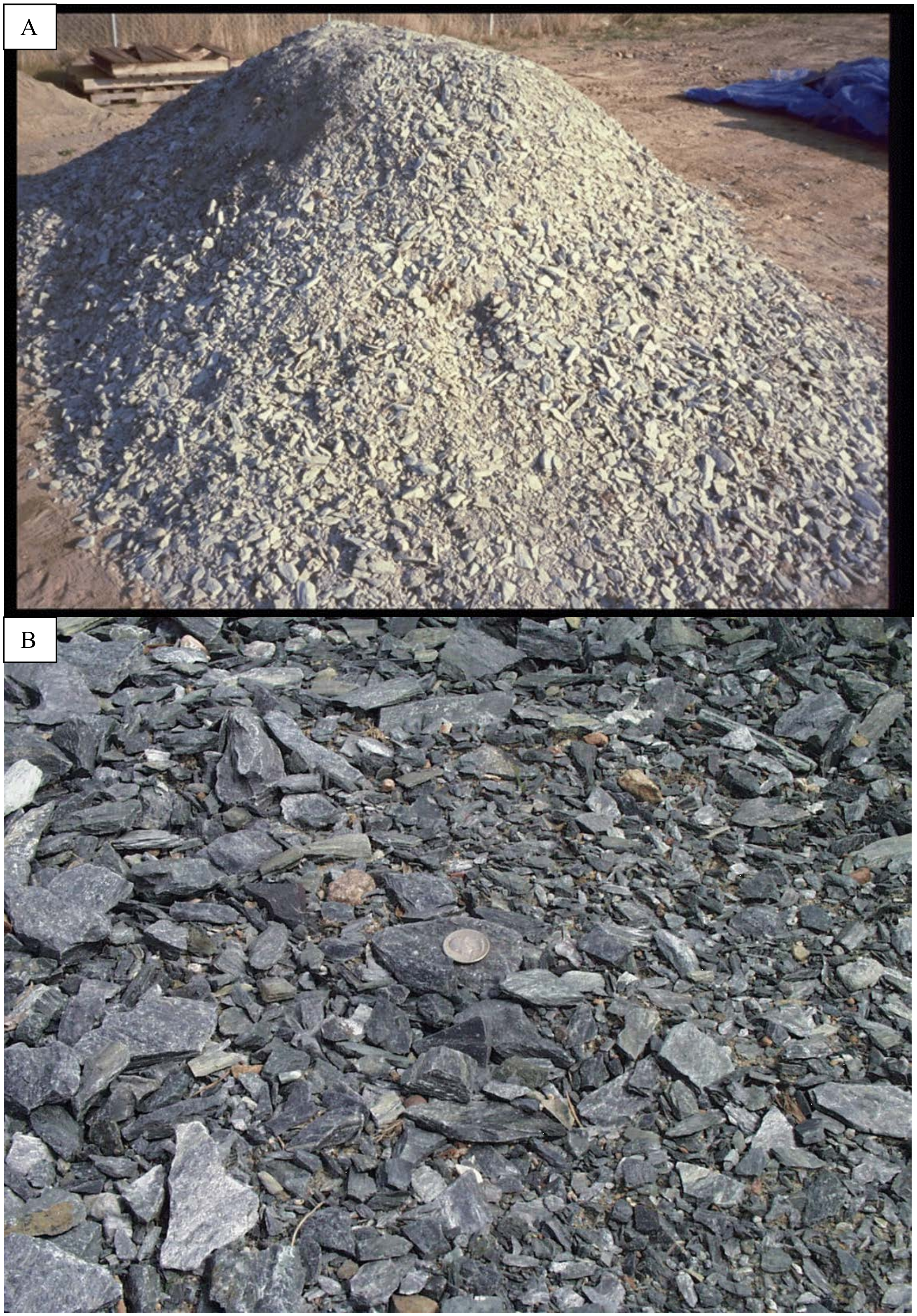

Figure 3.3 Field tank rock and dolostone images. In part A, less than 1.5 inch crushed rock used for the Ely Greenstone dolostone addition tank experiments. In part B, rock in tank (2011) with coin for scale.

Figure 3.4 Images of dolostone addition to tank rock. Addition of dolostone to skid loader bucket (part A) and after mixing (part B). The dolostone product was purchased from Aggregate Resources' Larson Mine on Grey Cloud Island and is called a manufactured sand.

Figure 3.5 Image of placing greenschist and dolostone mixture into tanks. Greenschist and dolostone mixture was scooped from skid loader bucket and placed in the tanks.

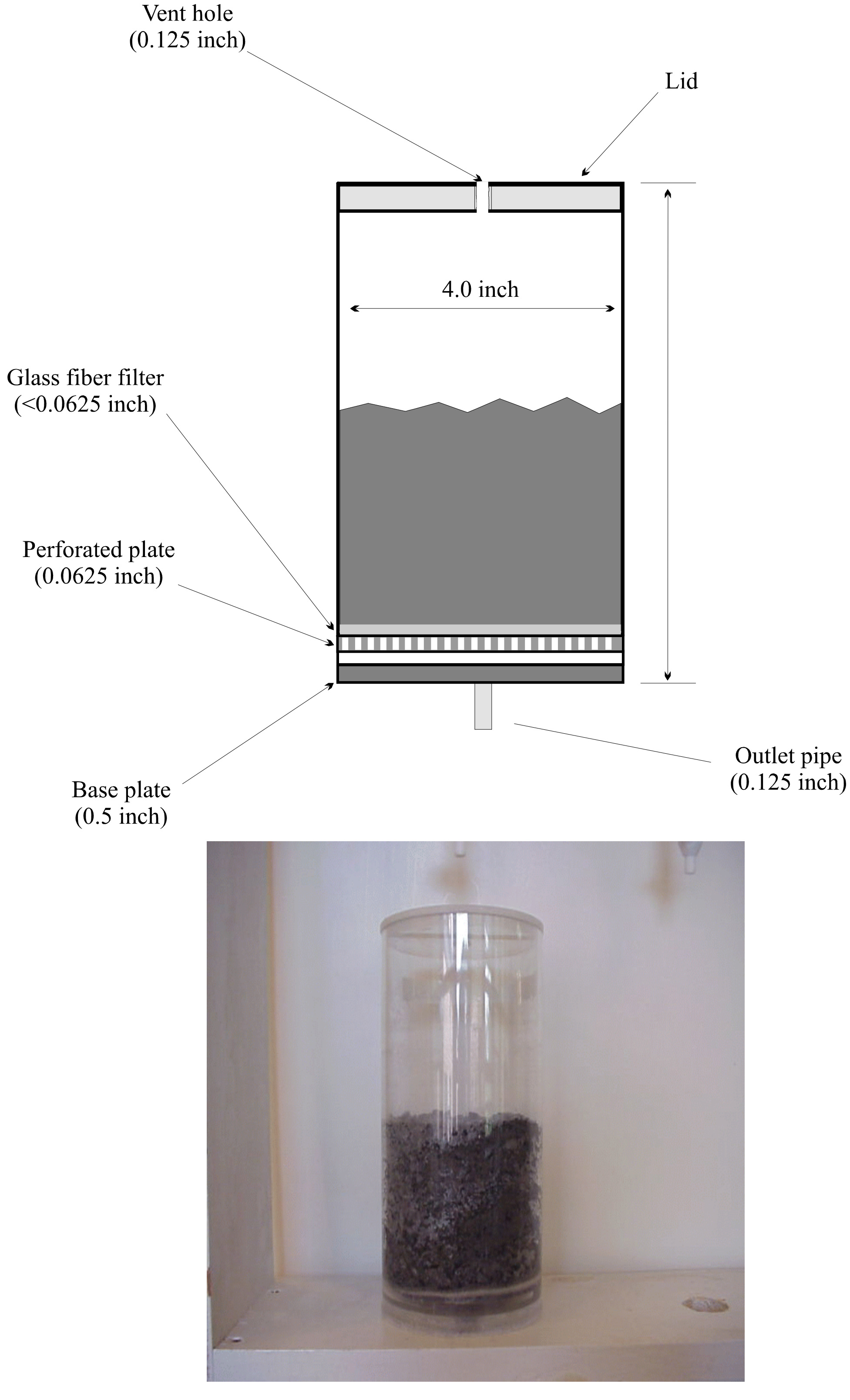

Figure 3.6 Humidity cell picture with dimension diagram.

Figure 3.7 Image of rock pile bin construction.

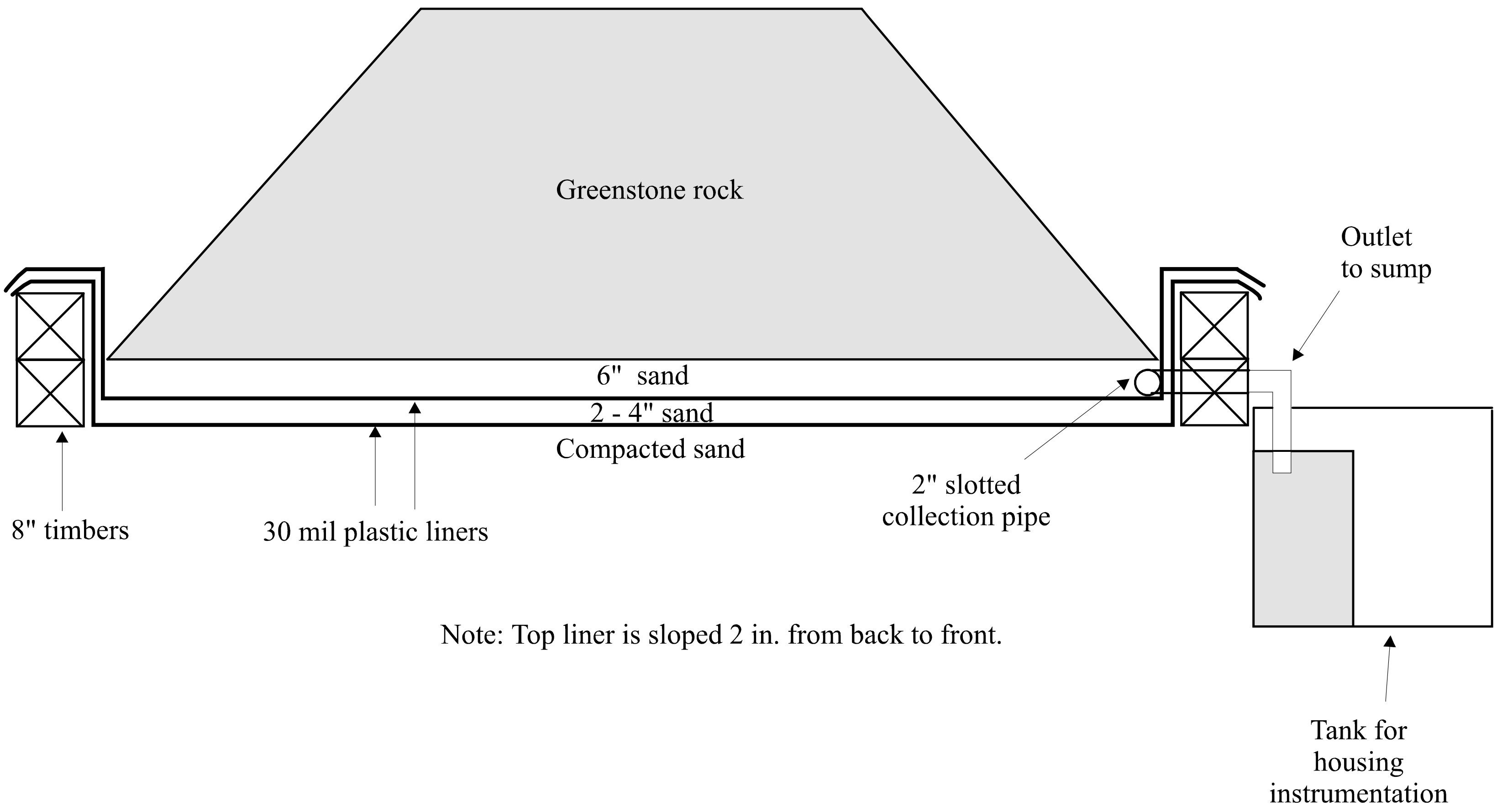

Figure 3.8 Diagram of leachate collection system.

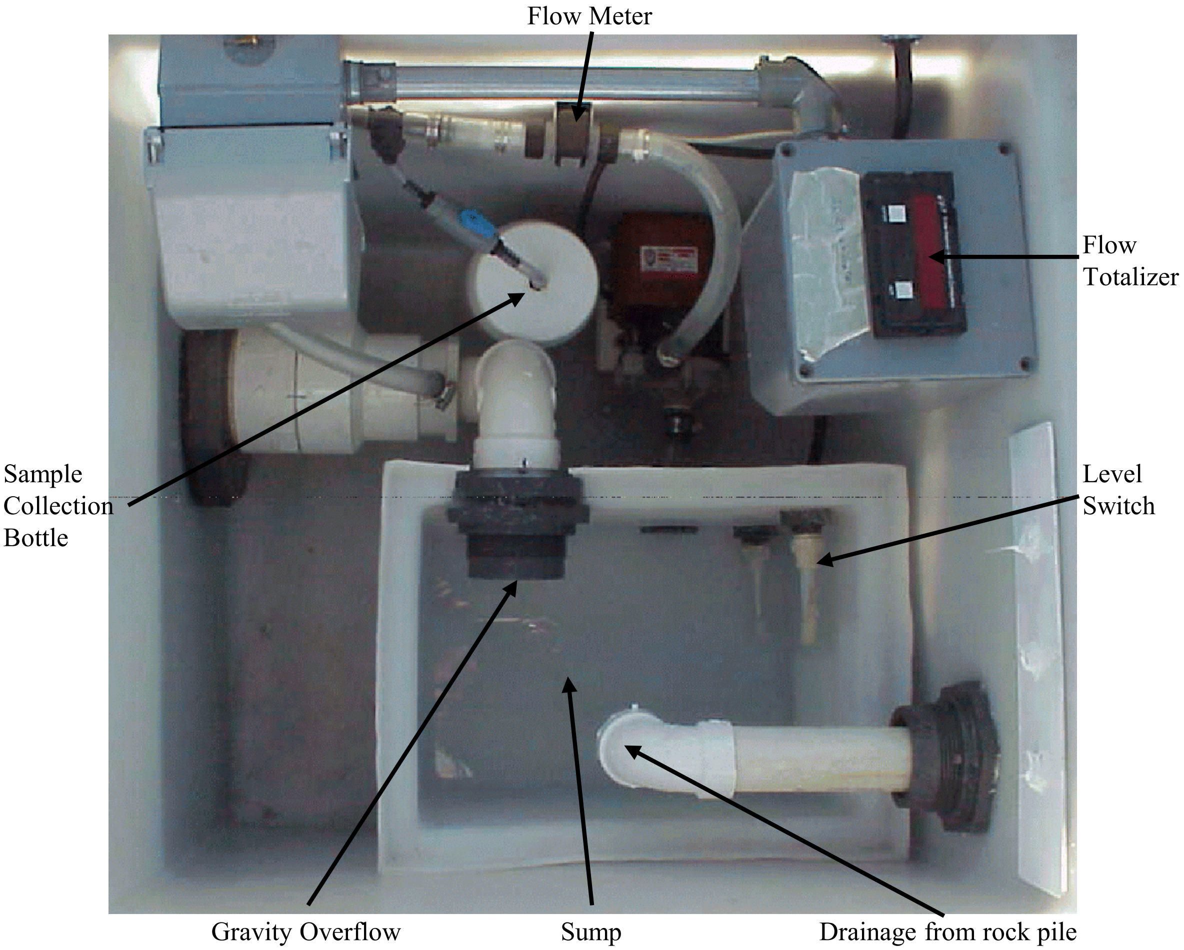

Figure 3.9 Picture of leachate collection sump.

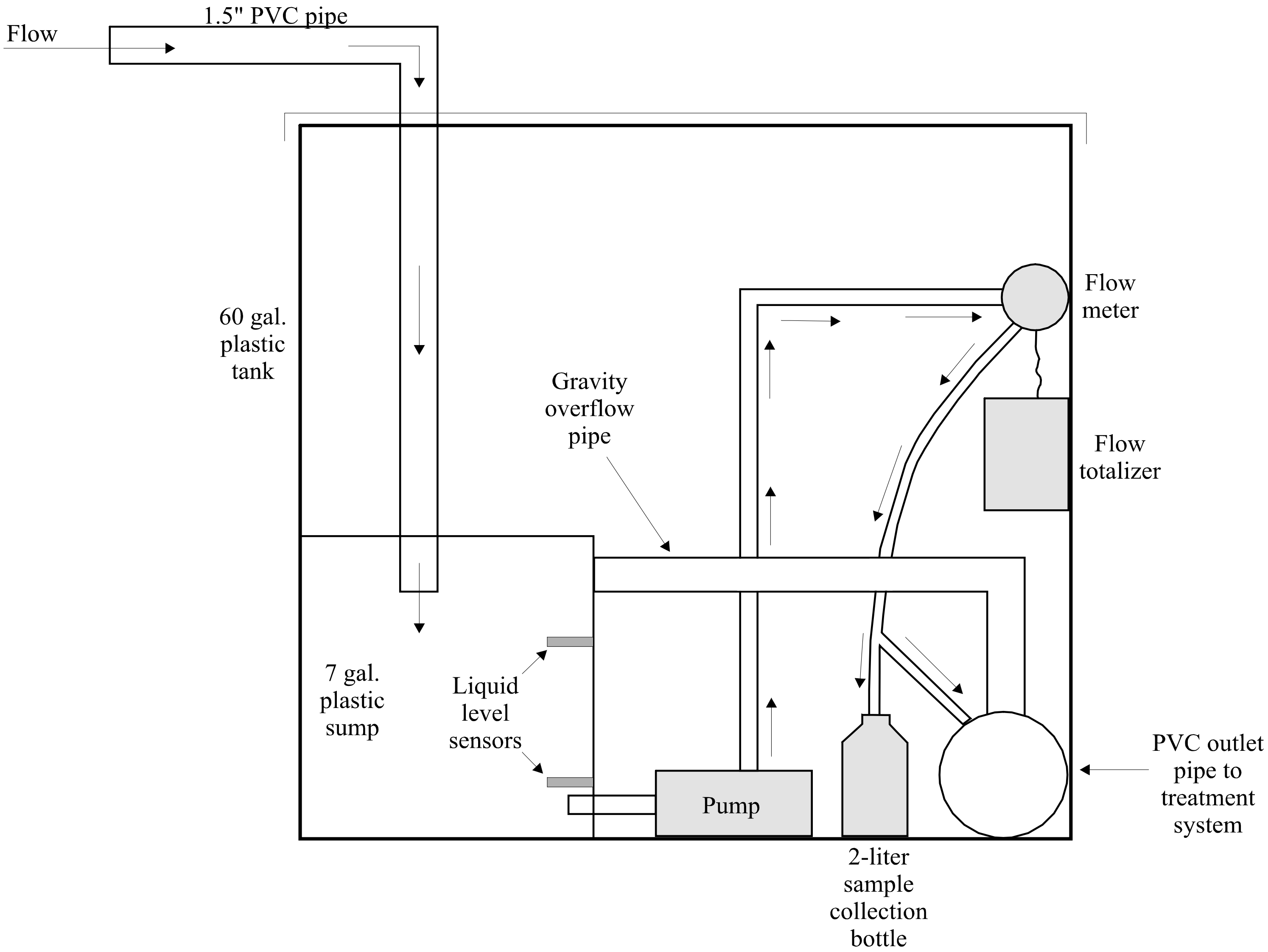

Figure 3.10 Diagram of flow measurement instrumentation.

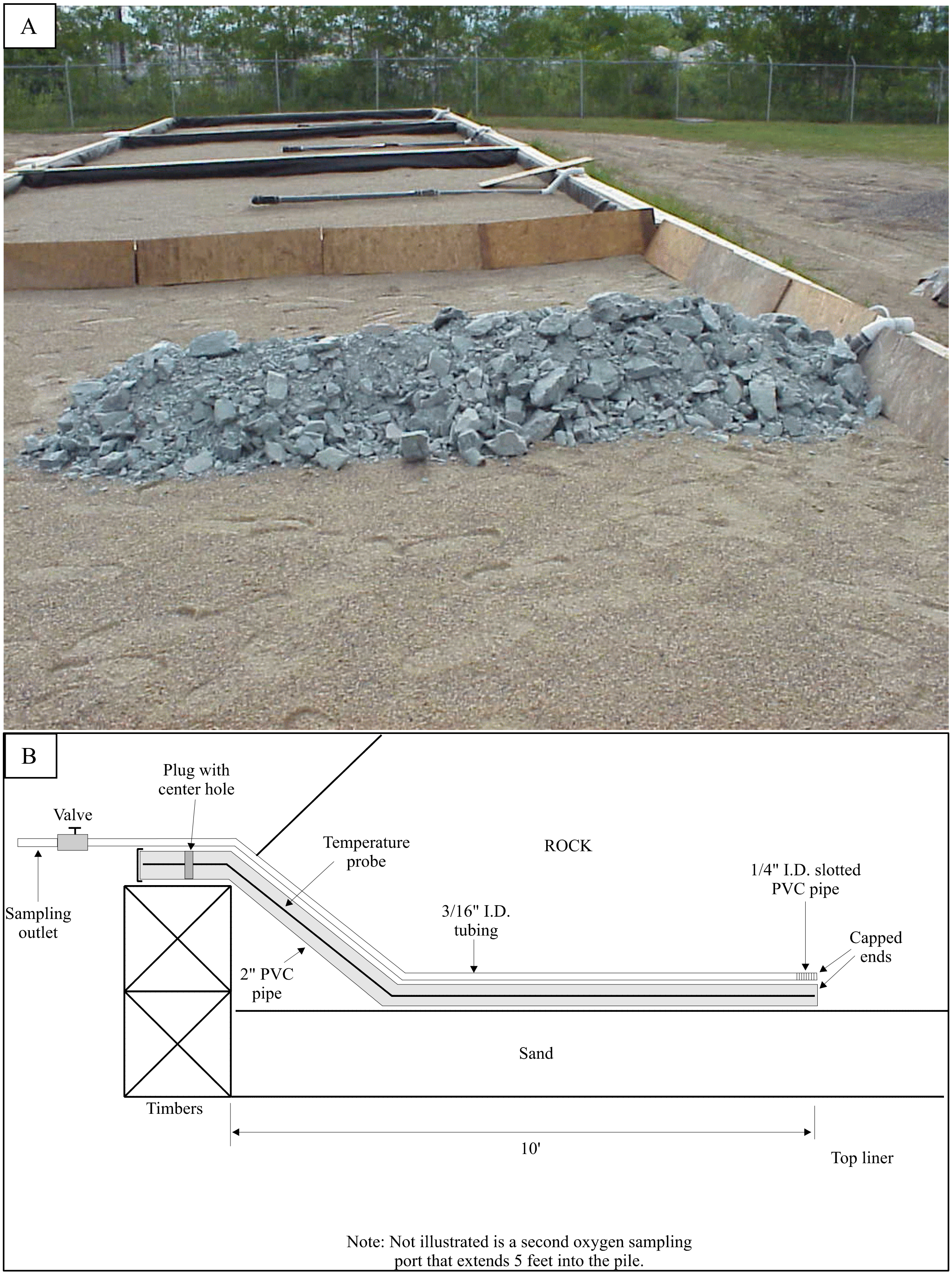

Note: Not illustrated is a second oxygen sampling port that extends 5 feet into the pile.

Figure 3.11 Image and diagram of temperature and oxygen measurement instrumentation. Part A, image of temperature and oxygen set up and part B diagram of temperature and oxygen instrumentation dimension.

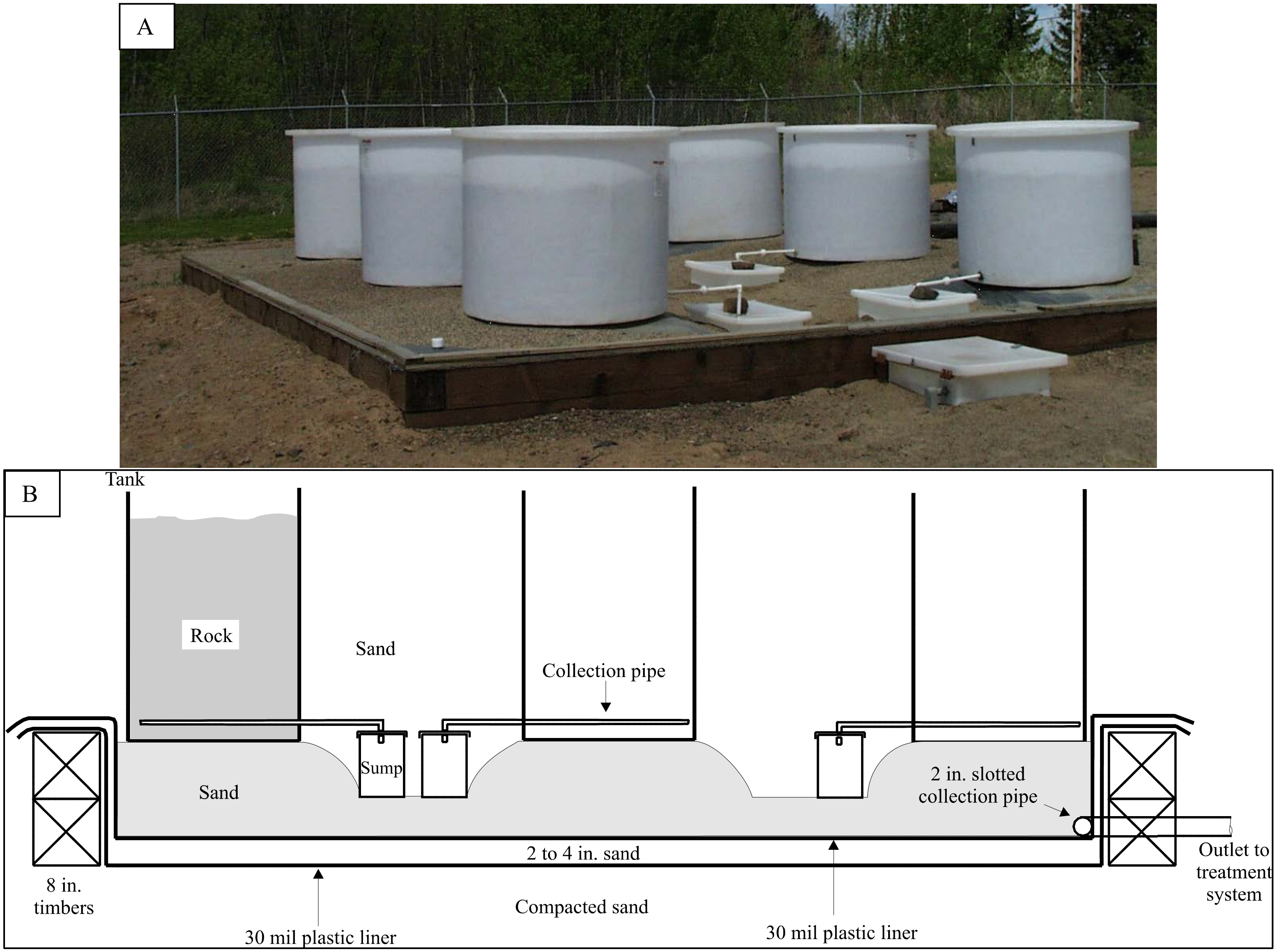

Figure 3.12 Image and diagram of field tanks. Part A, image of field tank experiment and part B diagram of field tanks with double containment system.

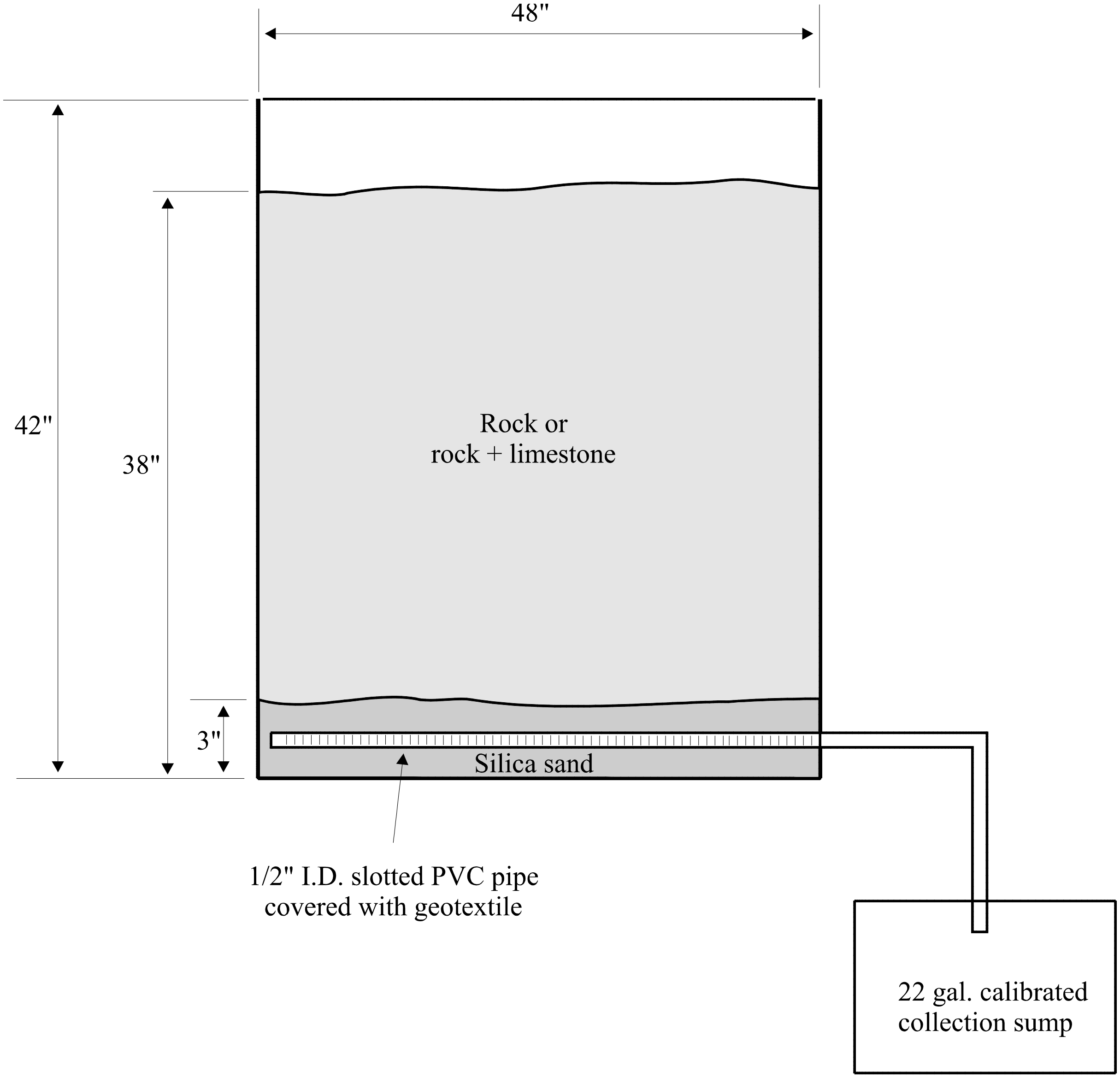

Figure 3.13 Diagram of tank design with dimensions.

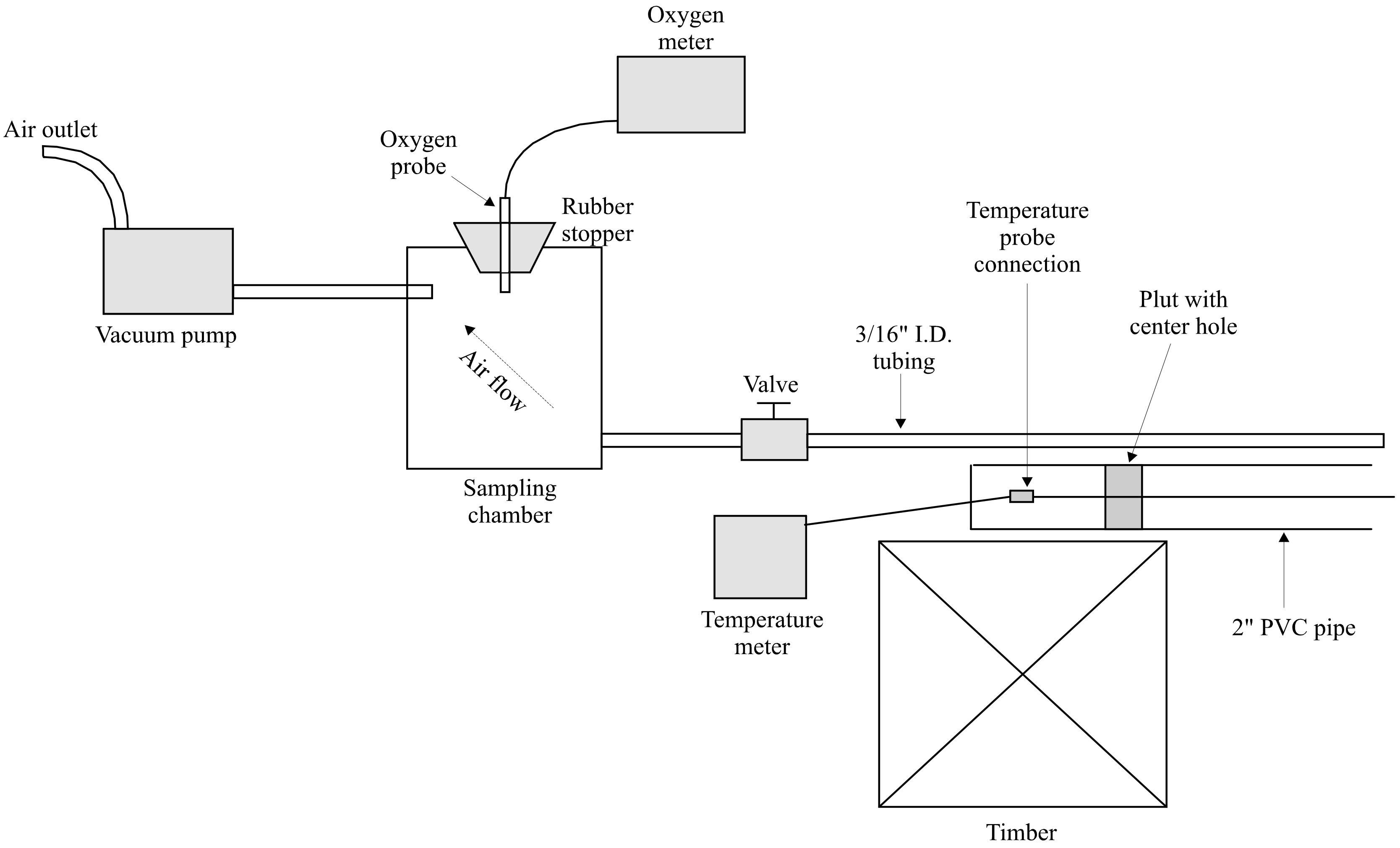

Figure 3.14 Diagram of temperature and oxygen sampling design.

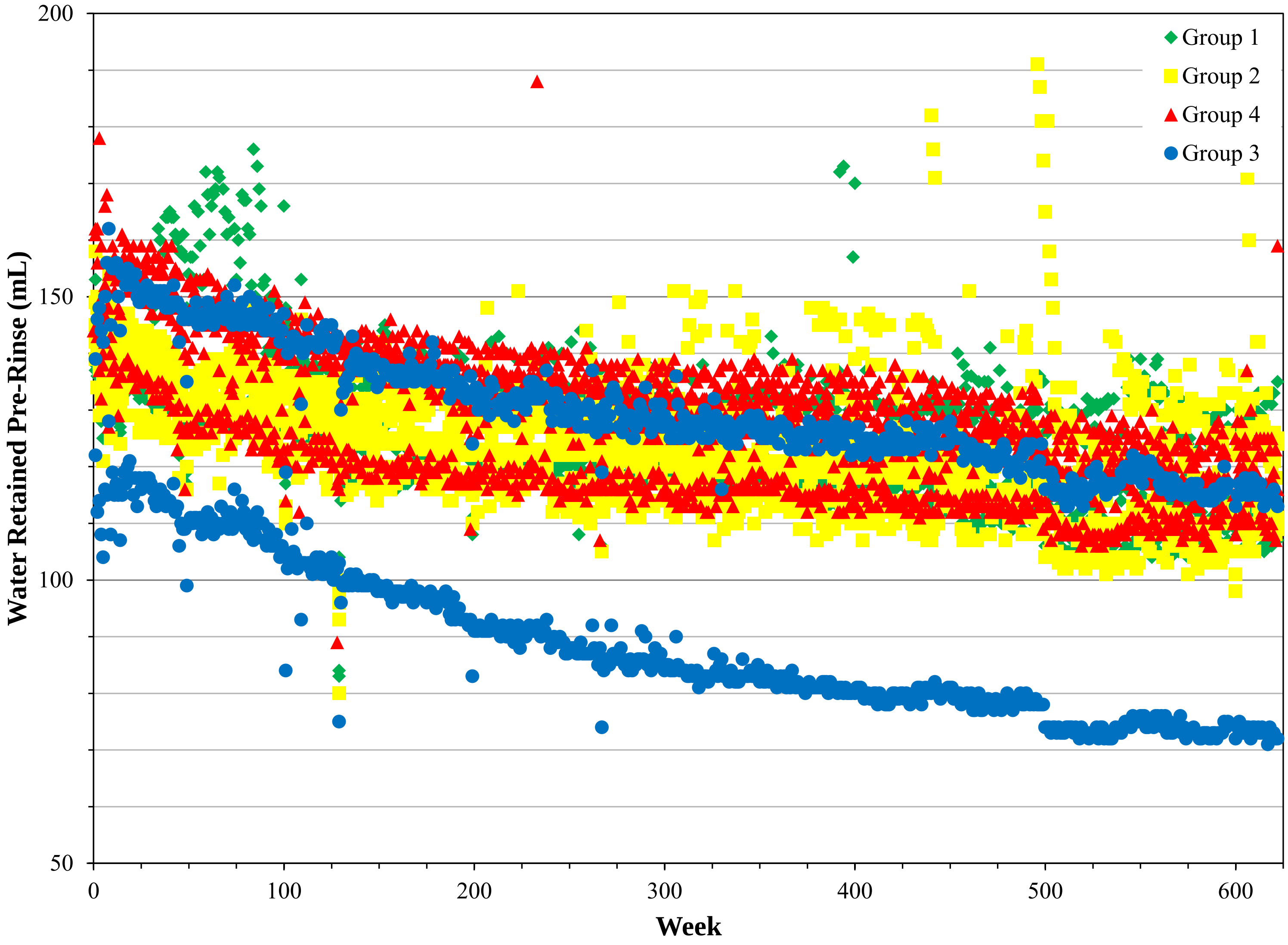

Figure 4.1 Water retention of humidity cells prior to weekly rinsing. The volumes represent the amount of water that remained from the previous weekly rinse.

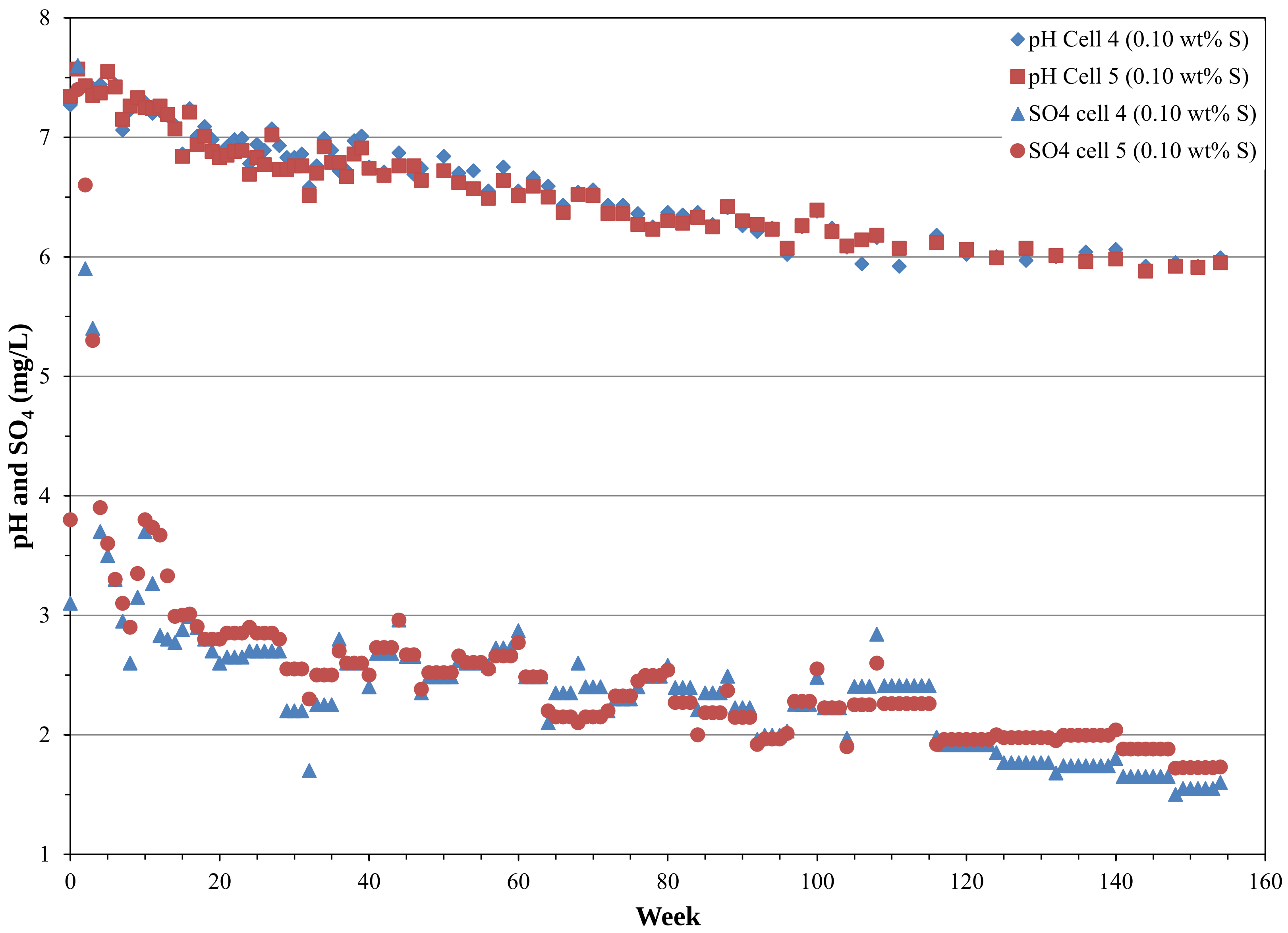

Figure 4.2 Comparison plot of leachate pH and SO_4 concentrations for humidity cells 4 and 5 (duplicate).

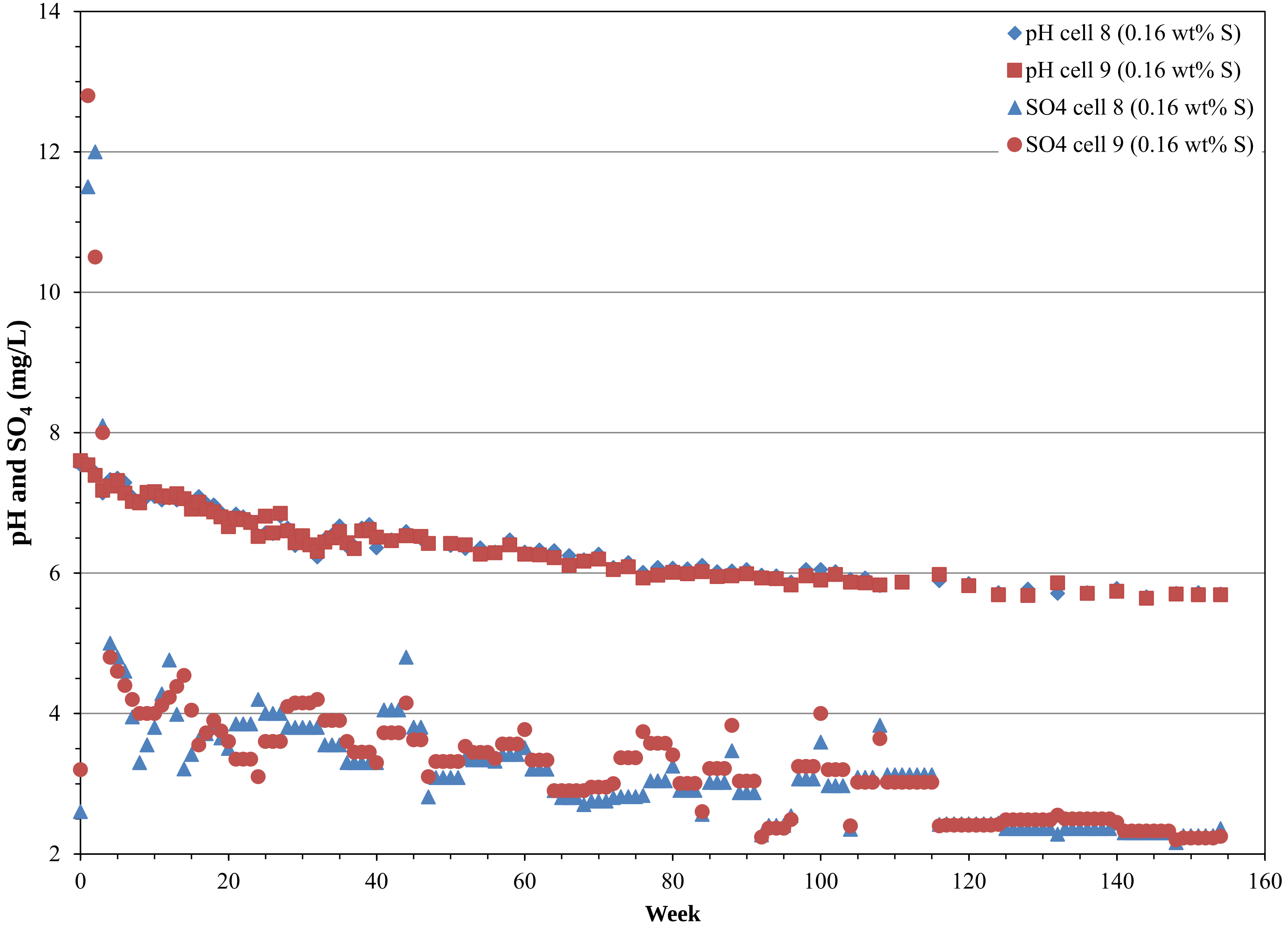

Figure 4.3 Comparison plot of leachate pH and SO_4 concentrations for humidity cells 8 and 9 (duplicate).

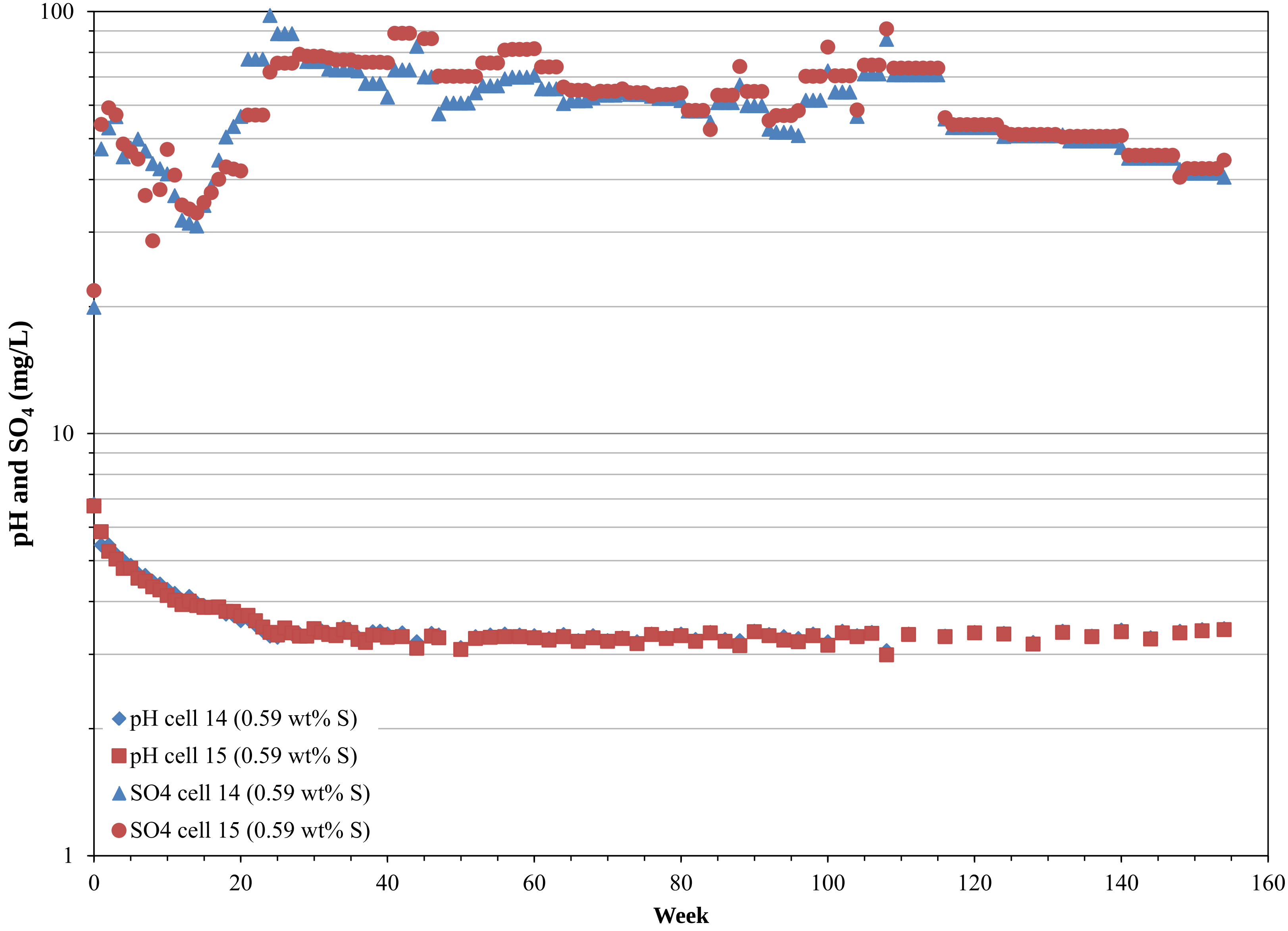

Figure 4.4 Comparison plot of leachate pH and SO_4 concentrations for humidity cells 14 and 15 (duplicate).

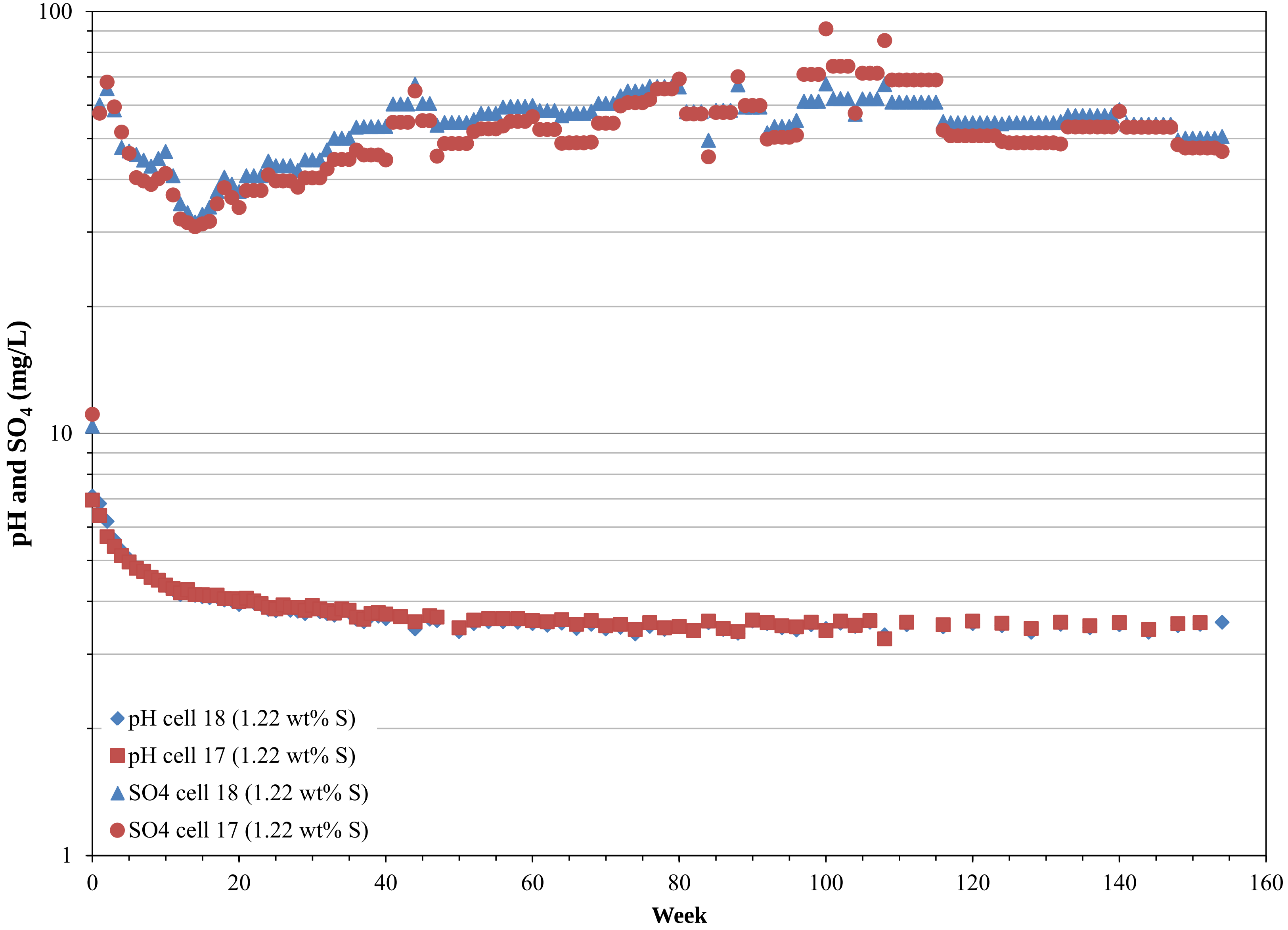

Figure 4.5 Comparison plot of leachate pH and SO_4 concentrations for humidity cells 18 and 17 (duplicate).

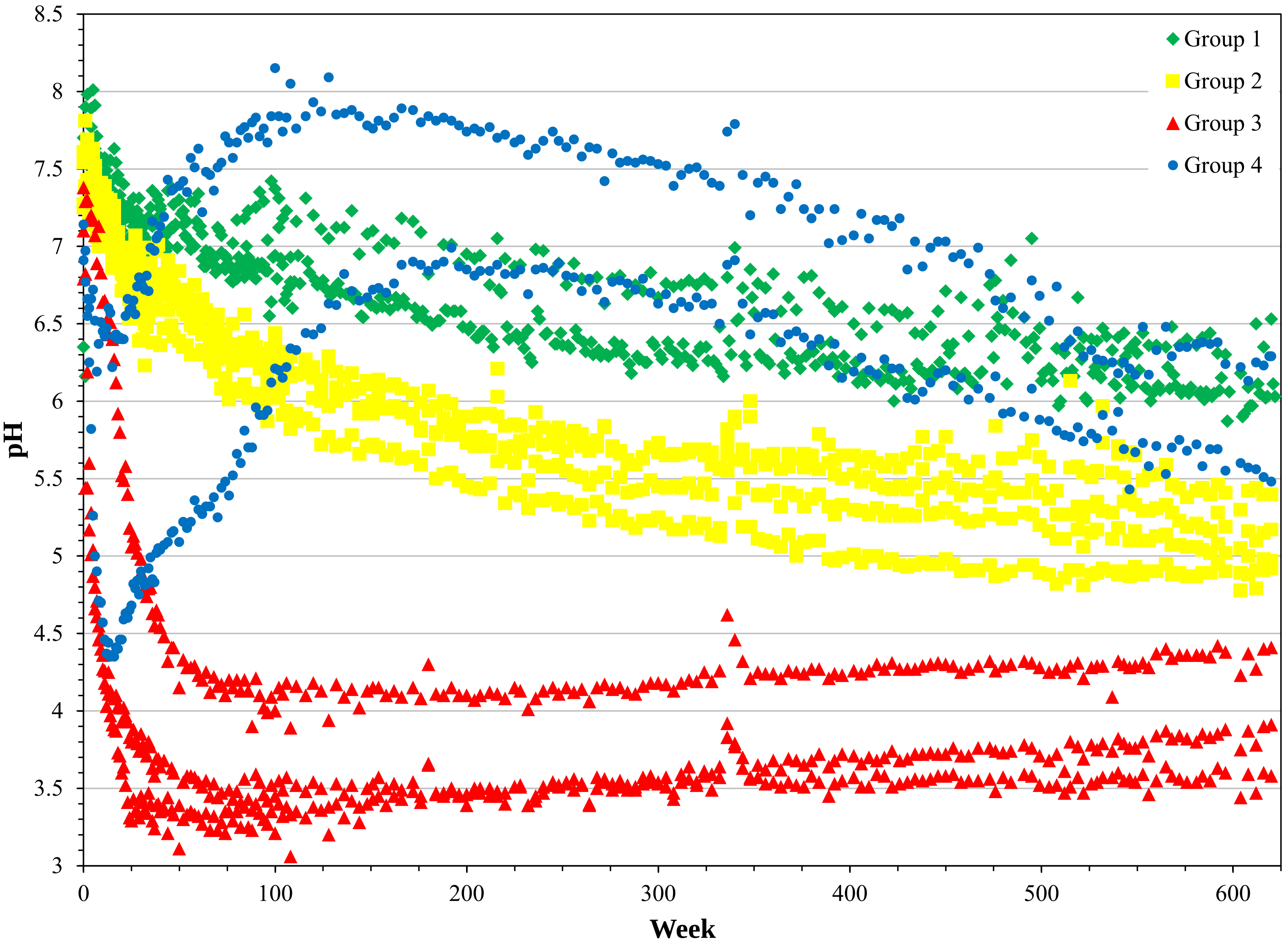

Figure 4.6 All groups leachate pH time series plot.

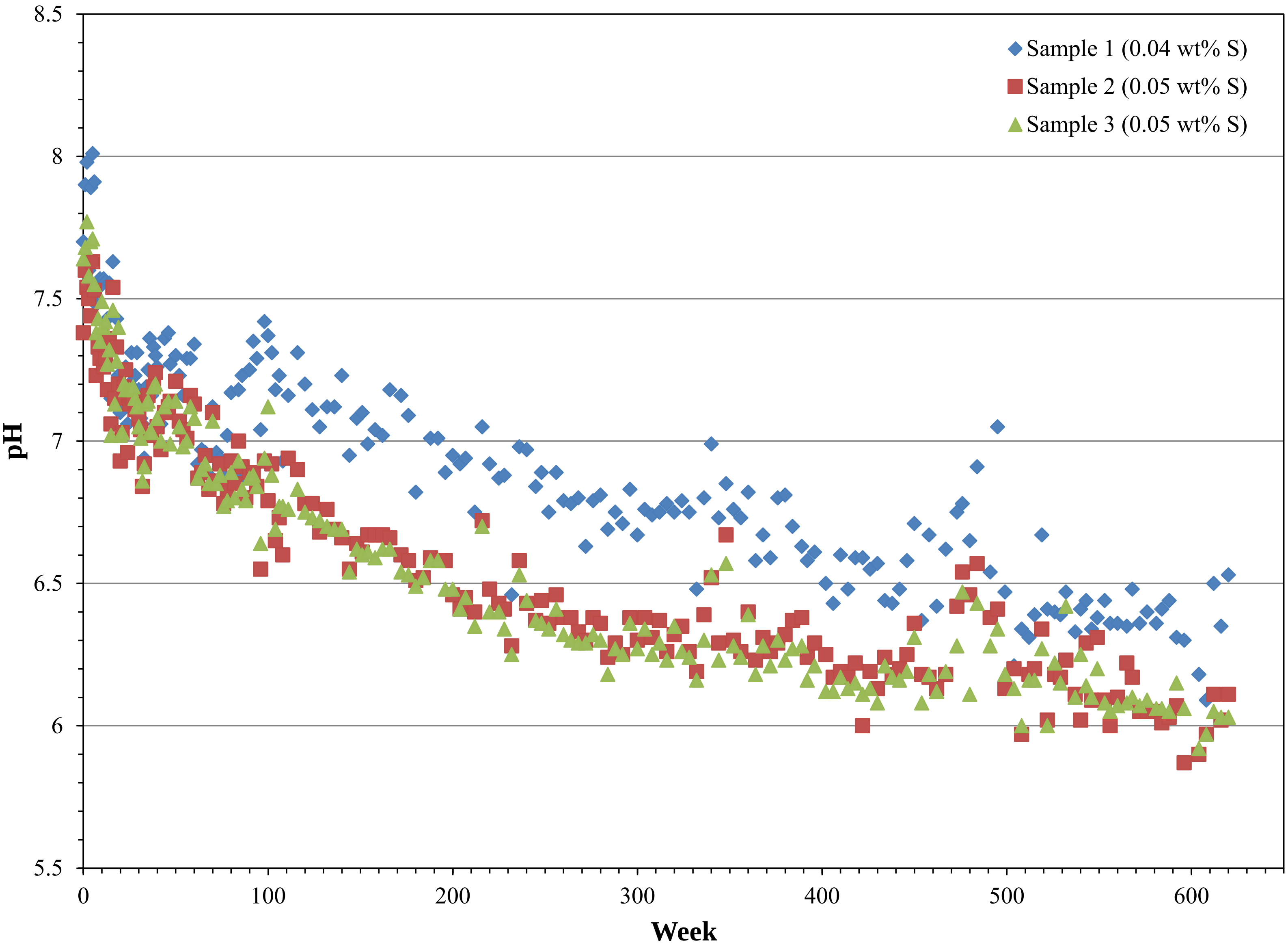

Figure 4.7 Group 1 leachate pH time series plot.

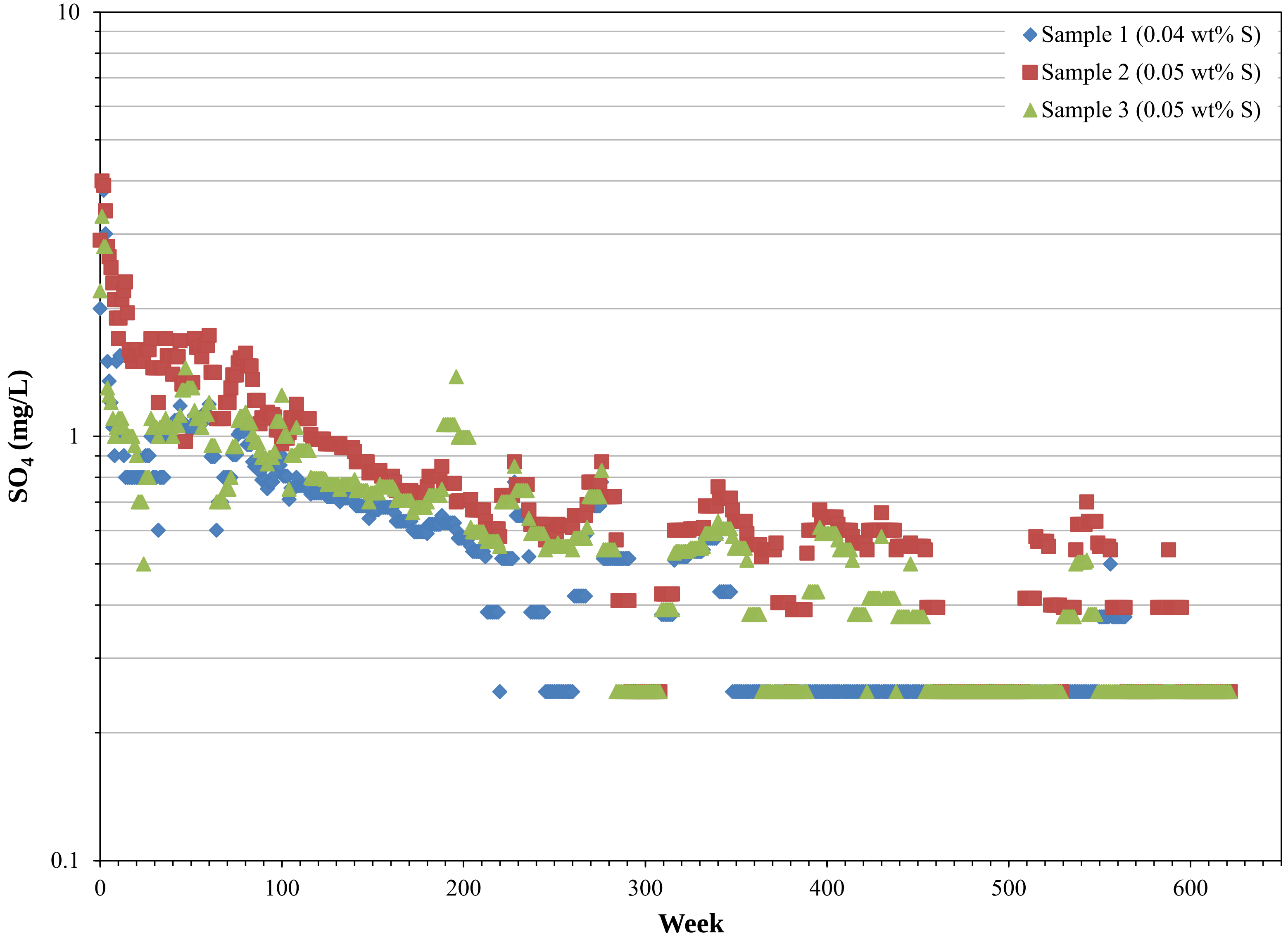

Figure 4.8 Group 1 leachate SO_4 concentration time series plot. Less than detection limit values (0.5 mg/L) plotted as one half the detection limit (0.25 mg/L).

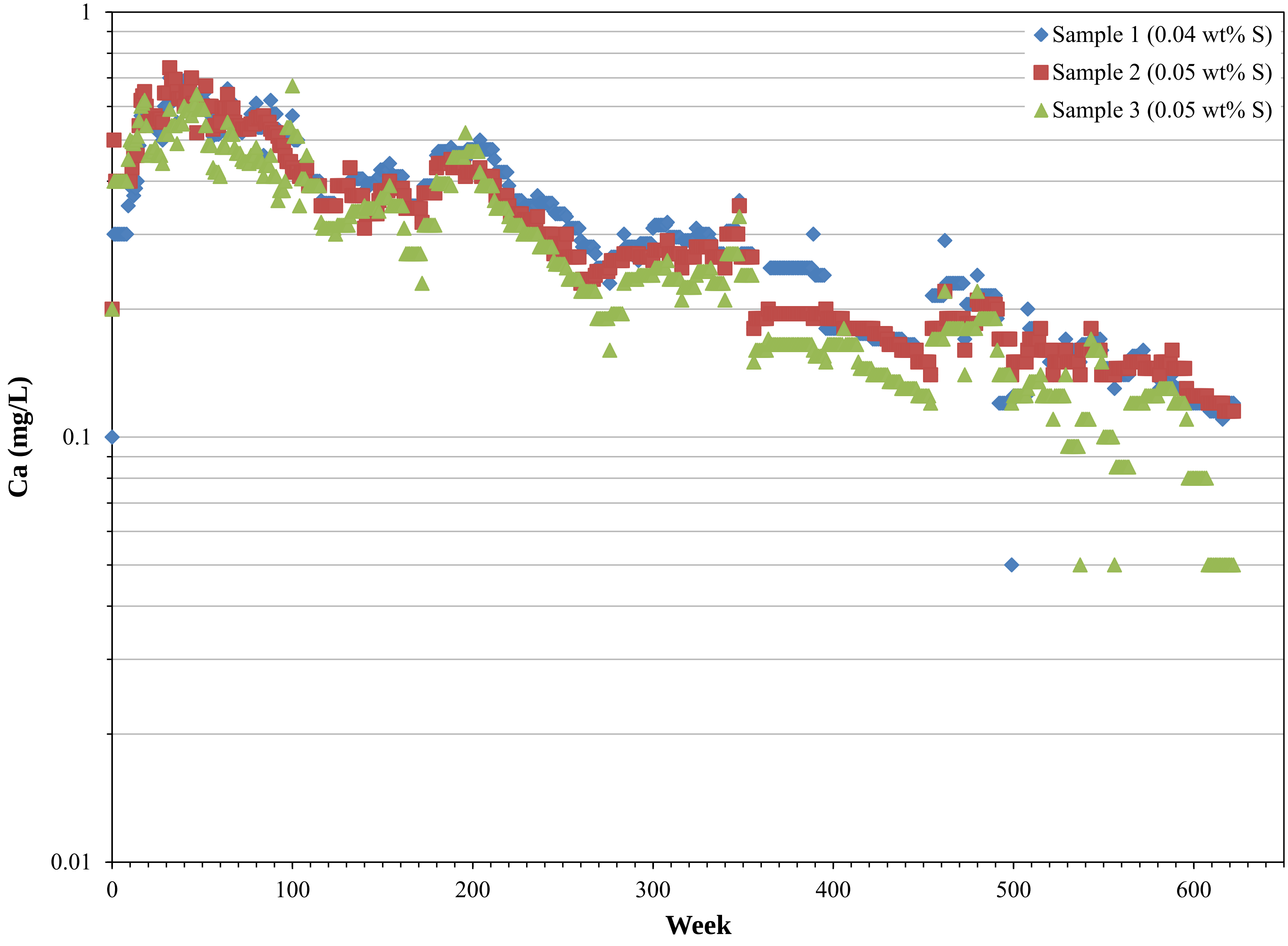

Figure 4.9 Group 1 leachate Ca concentration time series plot. Less than detection limit values (0.1 mg/L) plotted as one half the detection limit (0.05 mg/L).

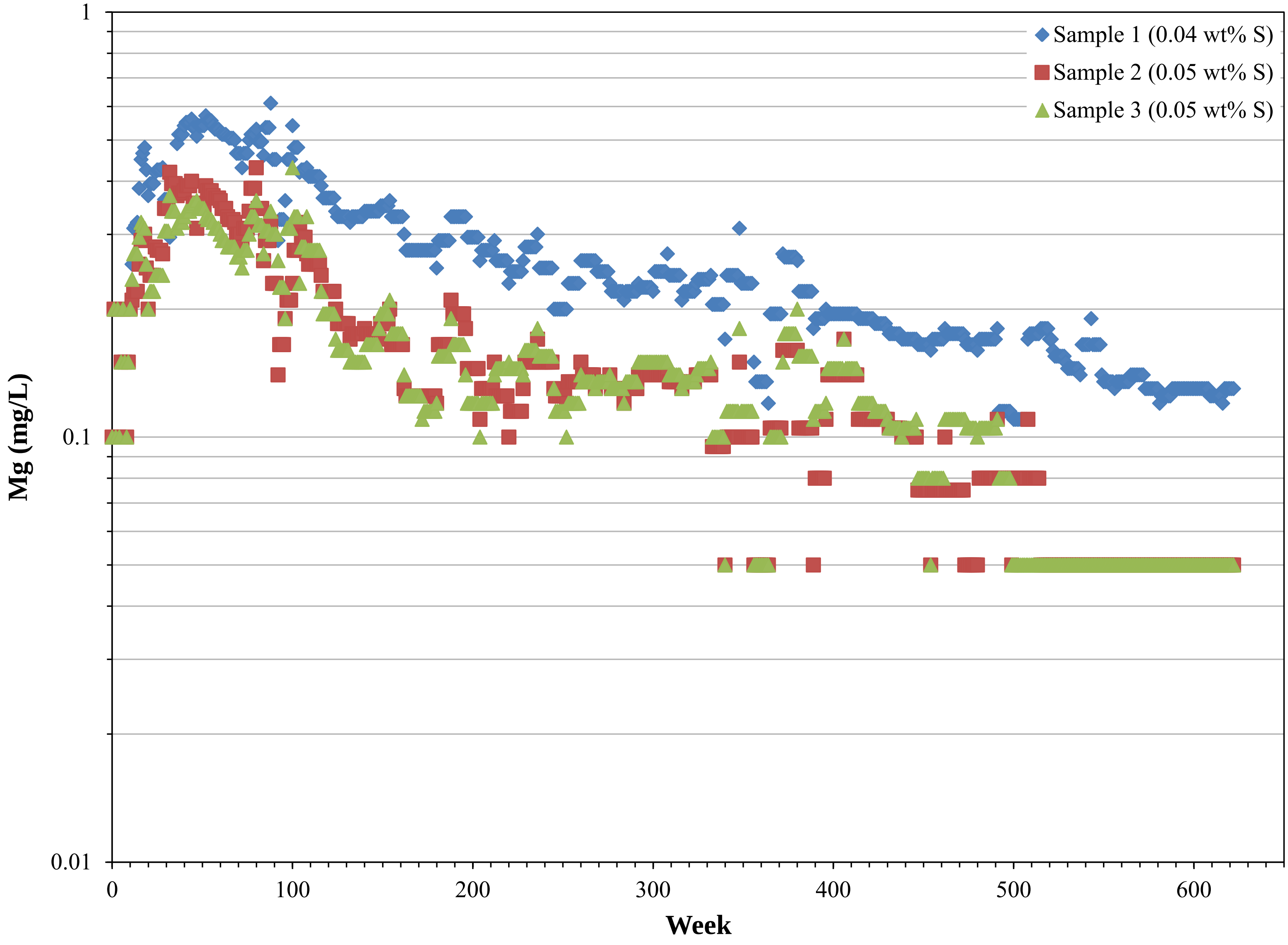

Figure 4.10 Group 1 leachate Mg concentration time series plot. Less than detection limit values (0.1 mg/L) plotted as one half the detection limit (0.05 mg/L).

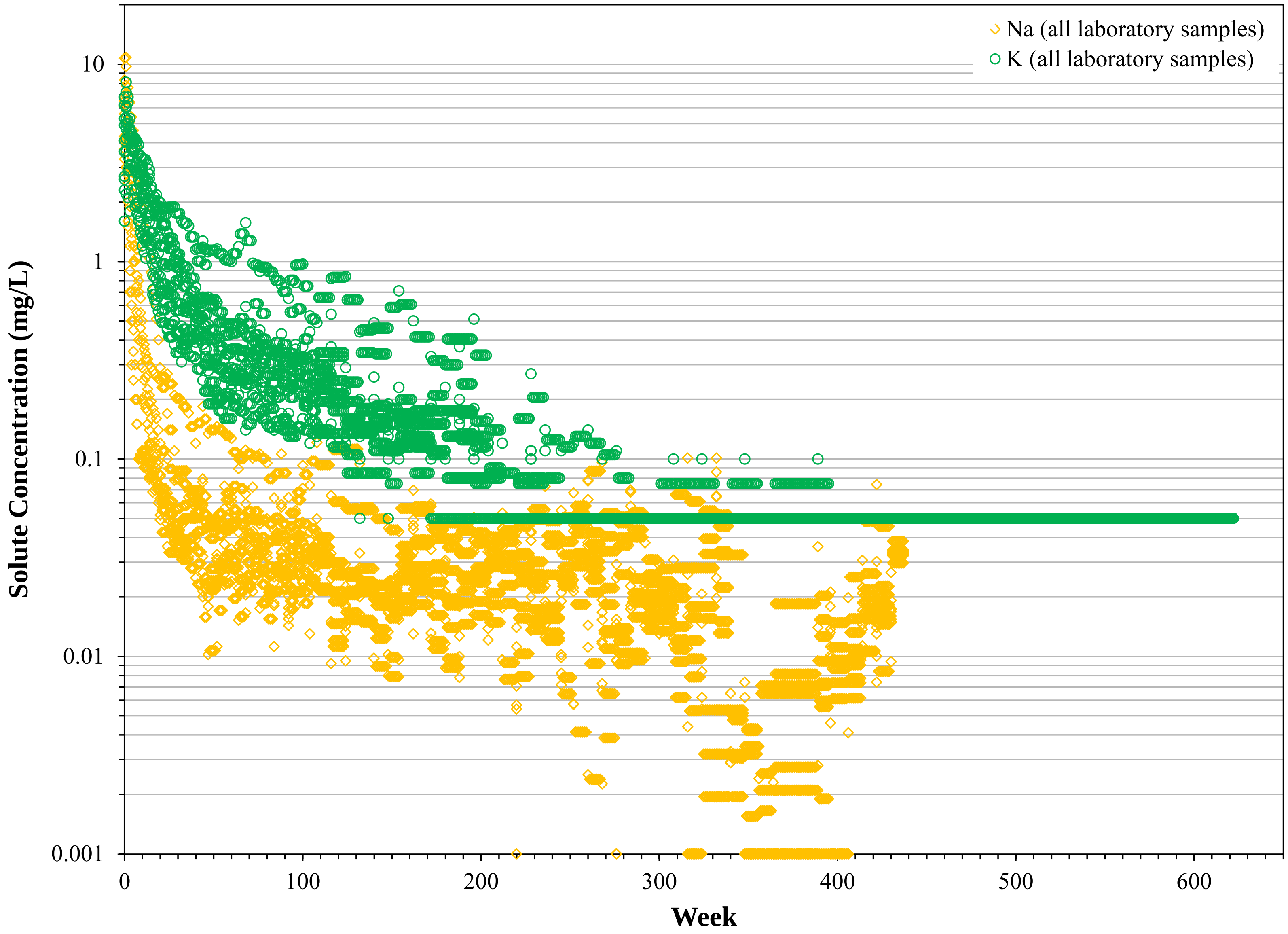

Figure 4.11 All groups leachate K and Na concentrations time series plot.

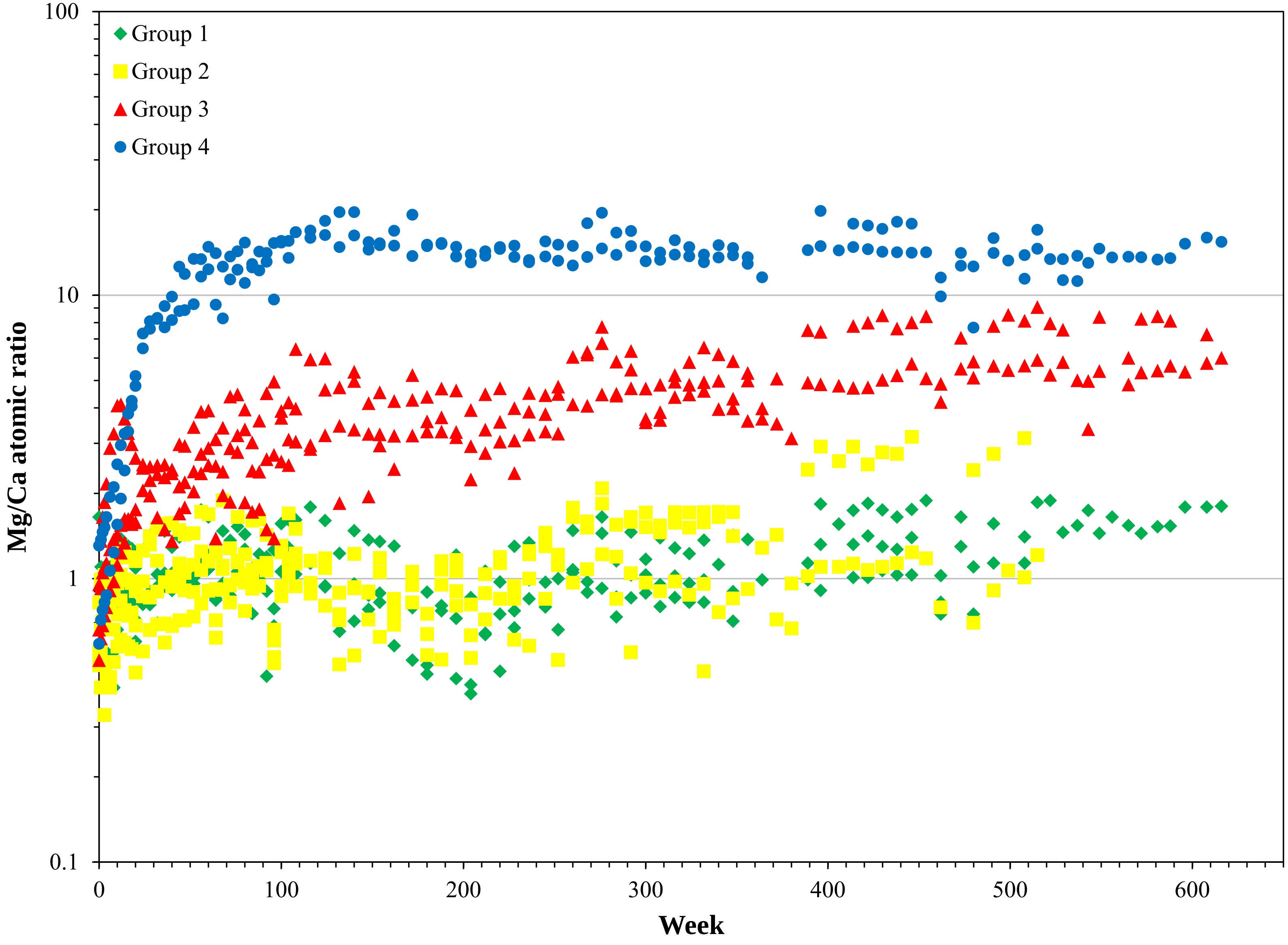

Figure 4.12 All groups leachate Mg/Ca molar ratio time series plot. Plot does not include interpolated or detection limit values.

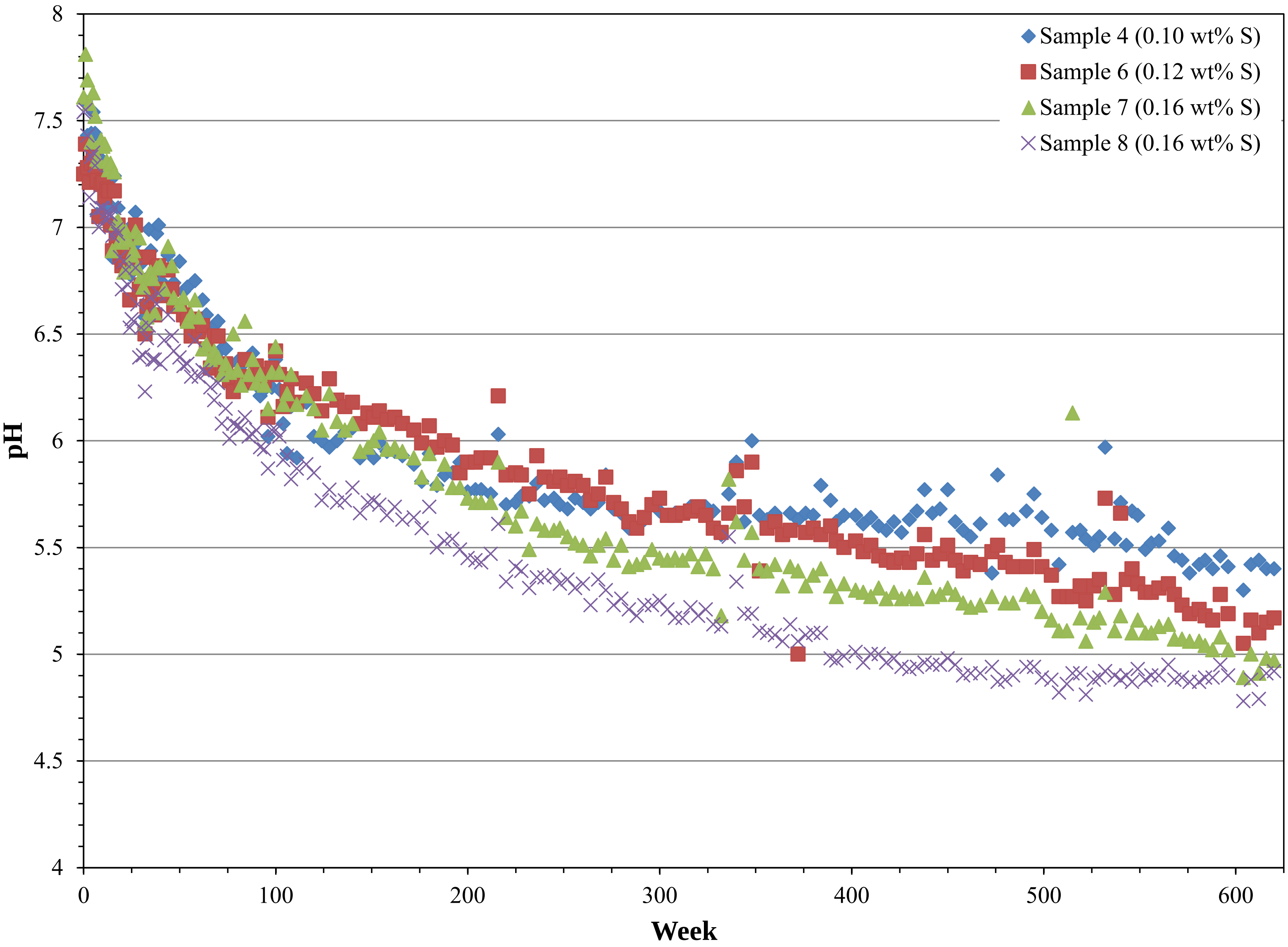

Figure 4.13 Group 2 leachate pH time series plot.

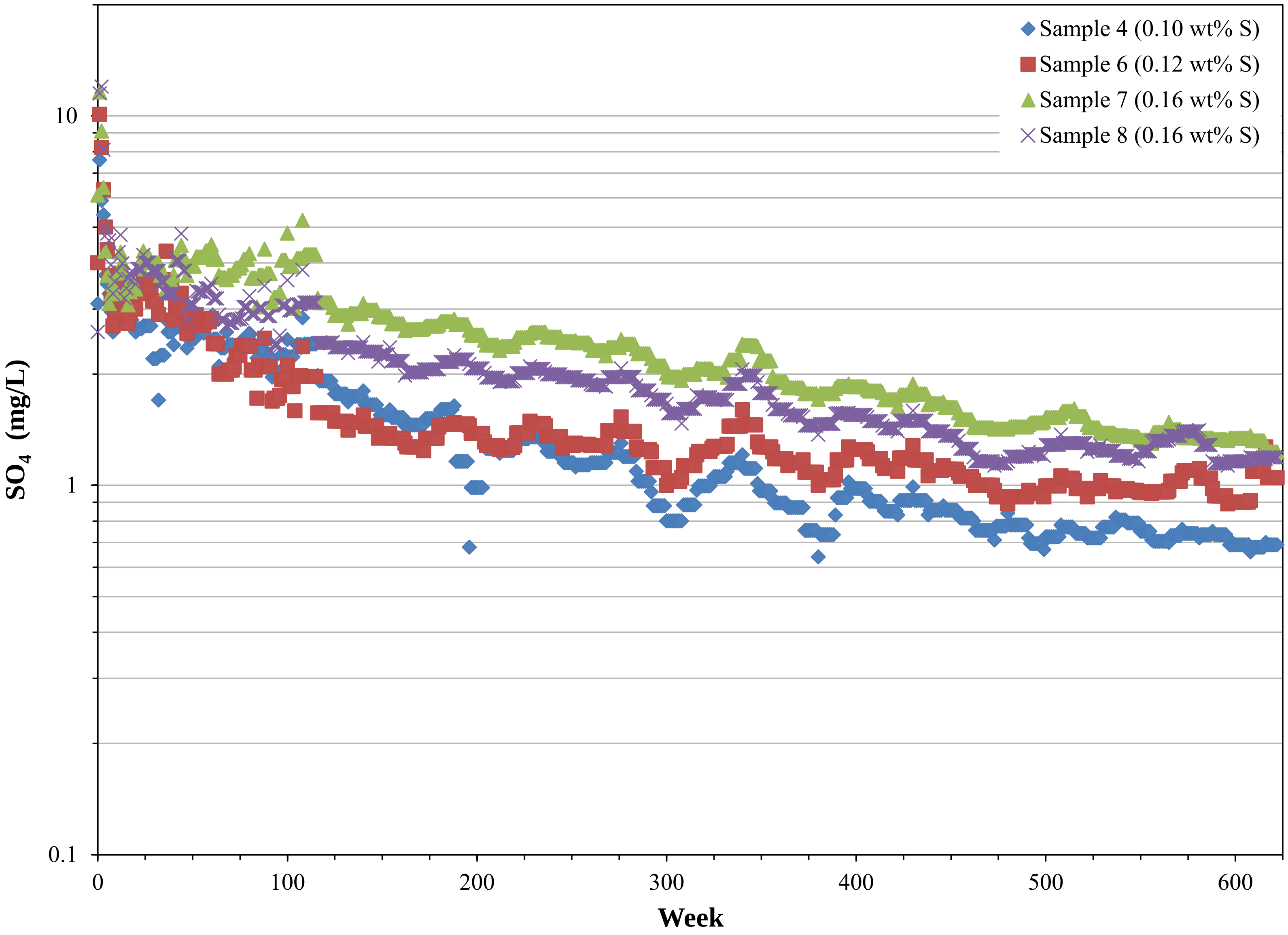

Figure 4.14 Group 2 leachate SO_4 concentration time series plot.

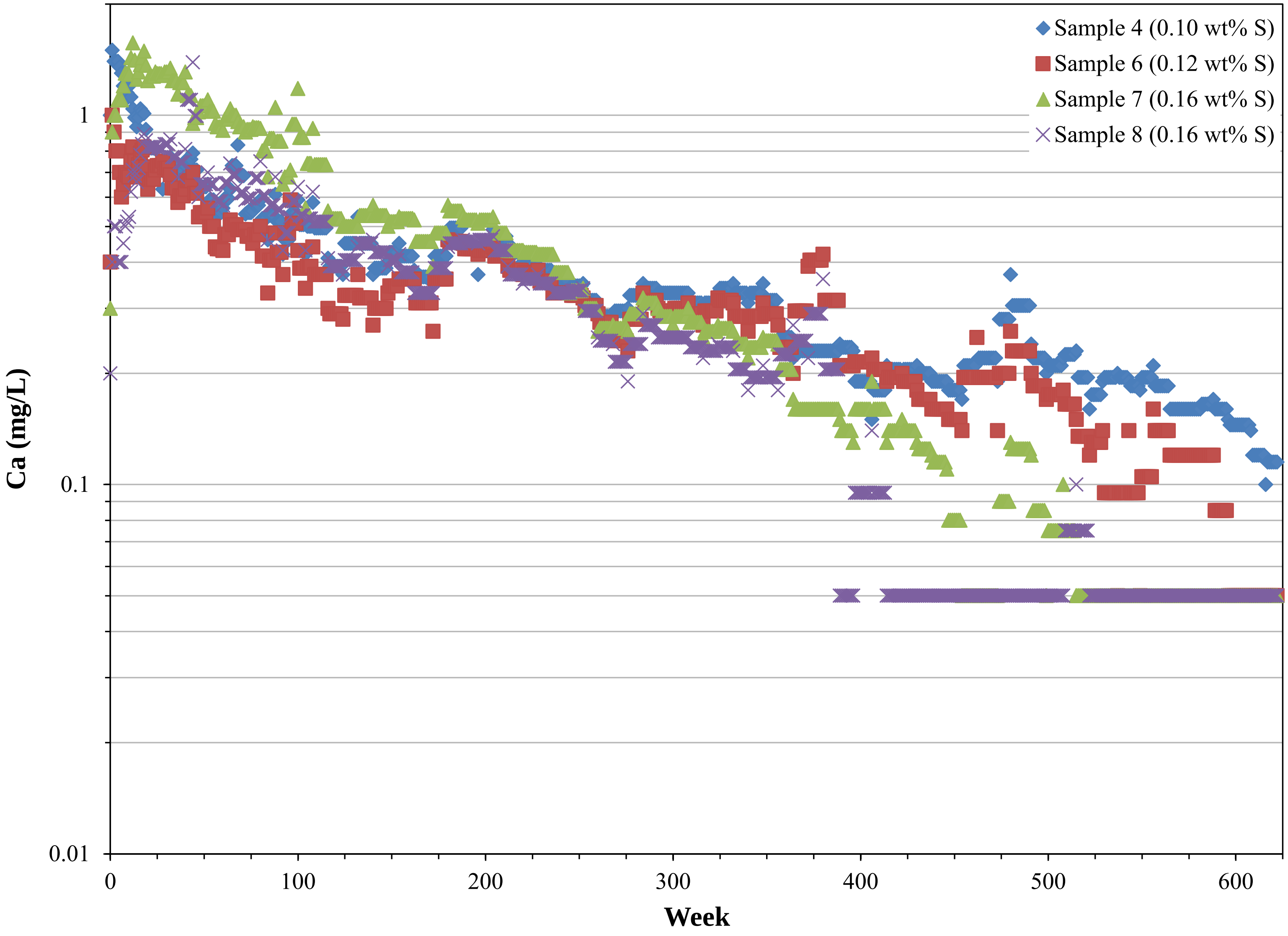

Figure 4.15 Group 2 leachate Ca concentration time series plot. Less than detection limit values (0.1 mg/L) plotted as one half the detection limit (0.05 mg/L).

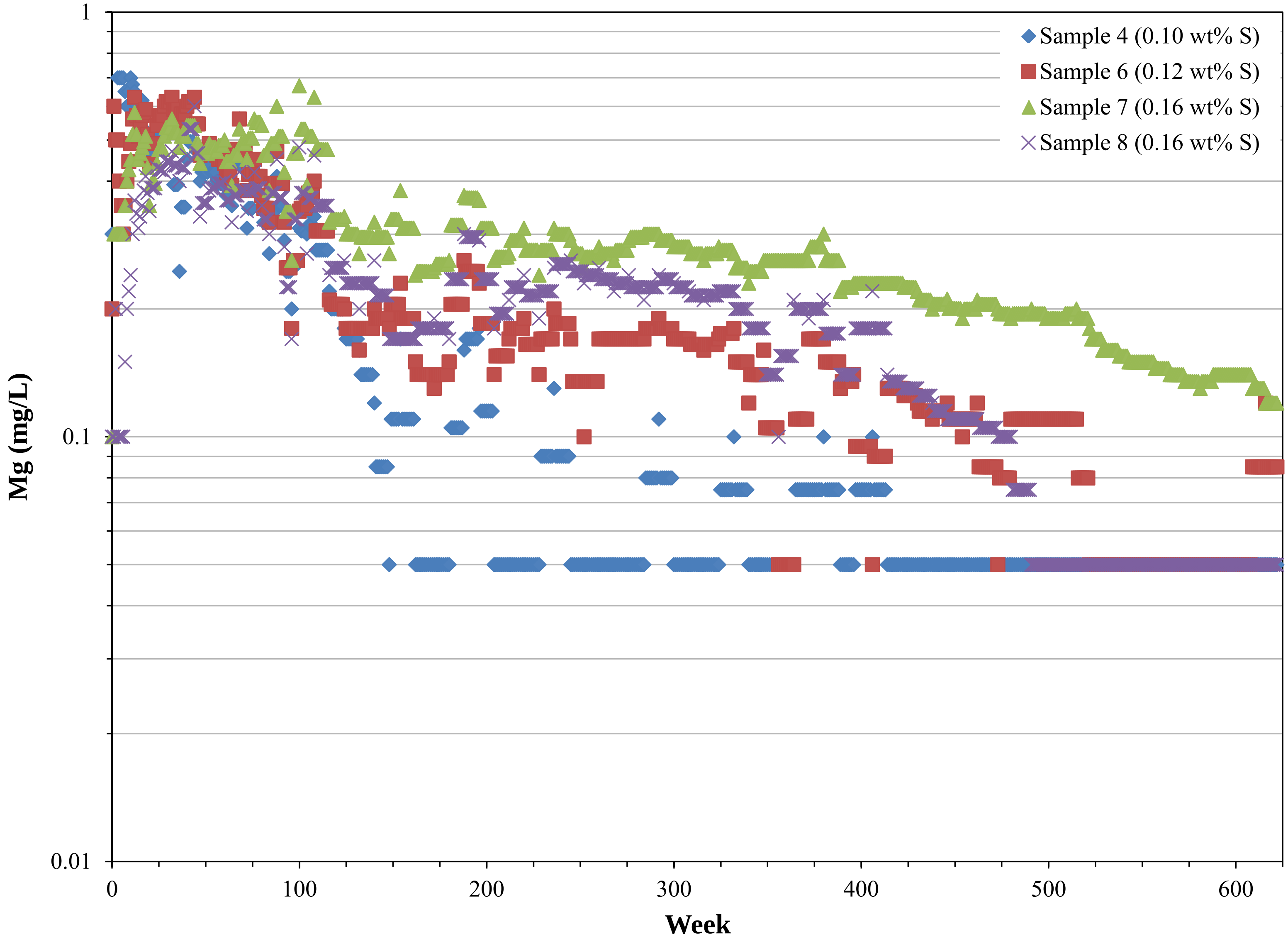

Figure 4.16 Group 2 leachate Mg concentration time series plot. Less than detection limit values (0.1 mg/L) plotted as one half the detection limit (0.05 mg/L).

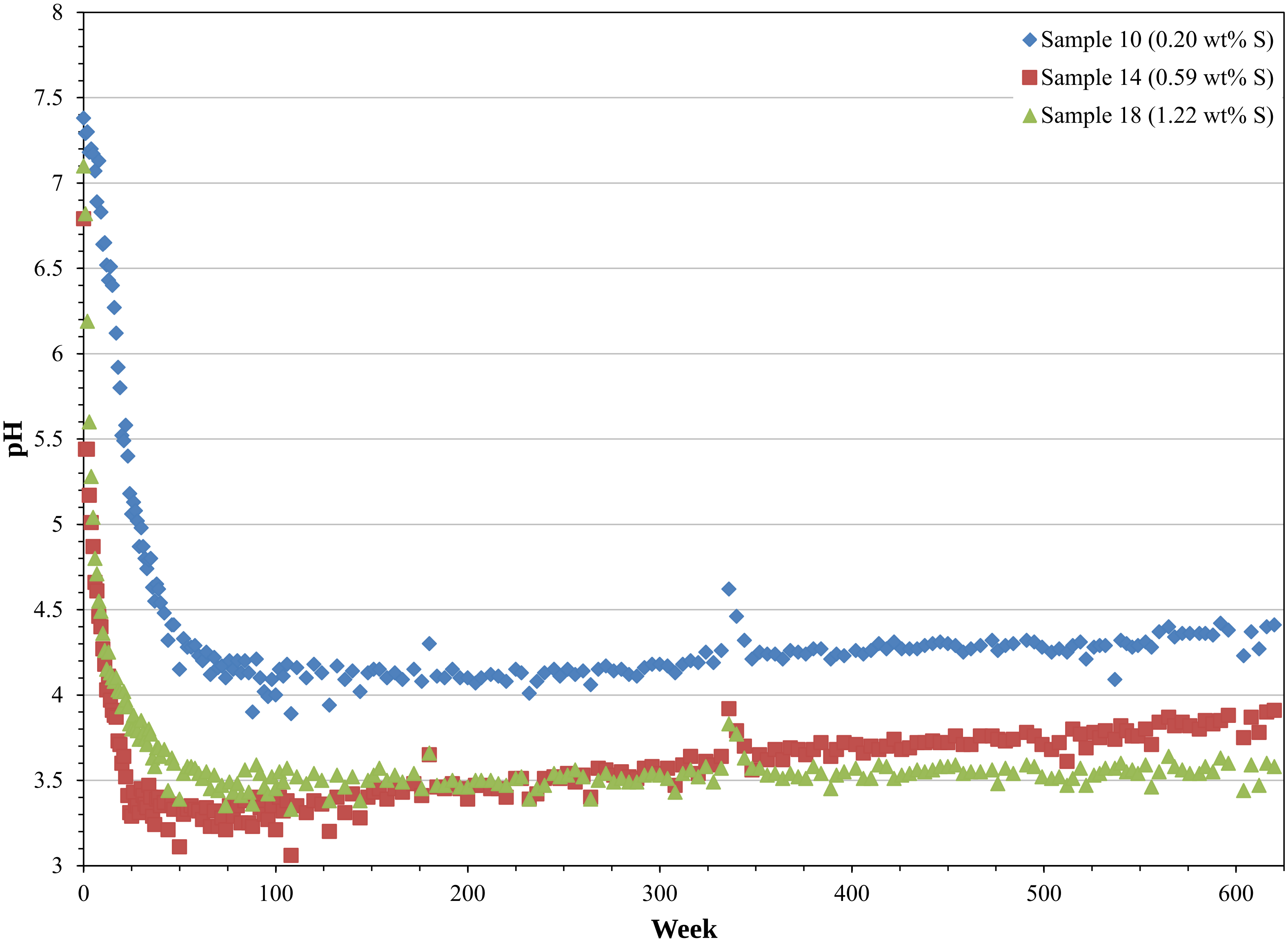

Figure 4.17 Group 3 leachate pH time series plot.

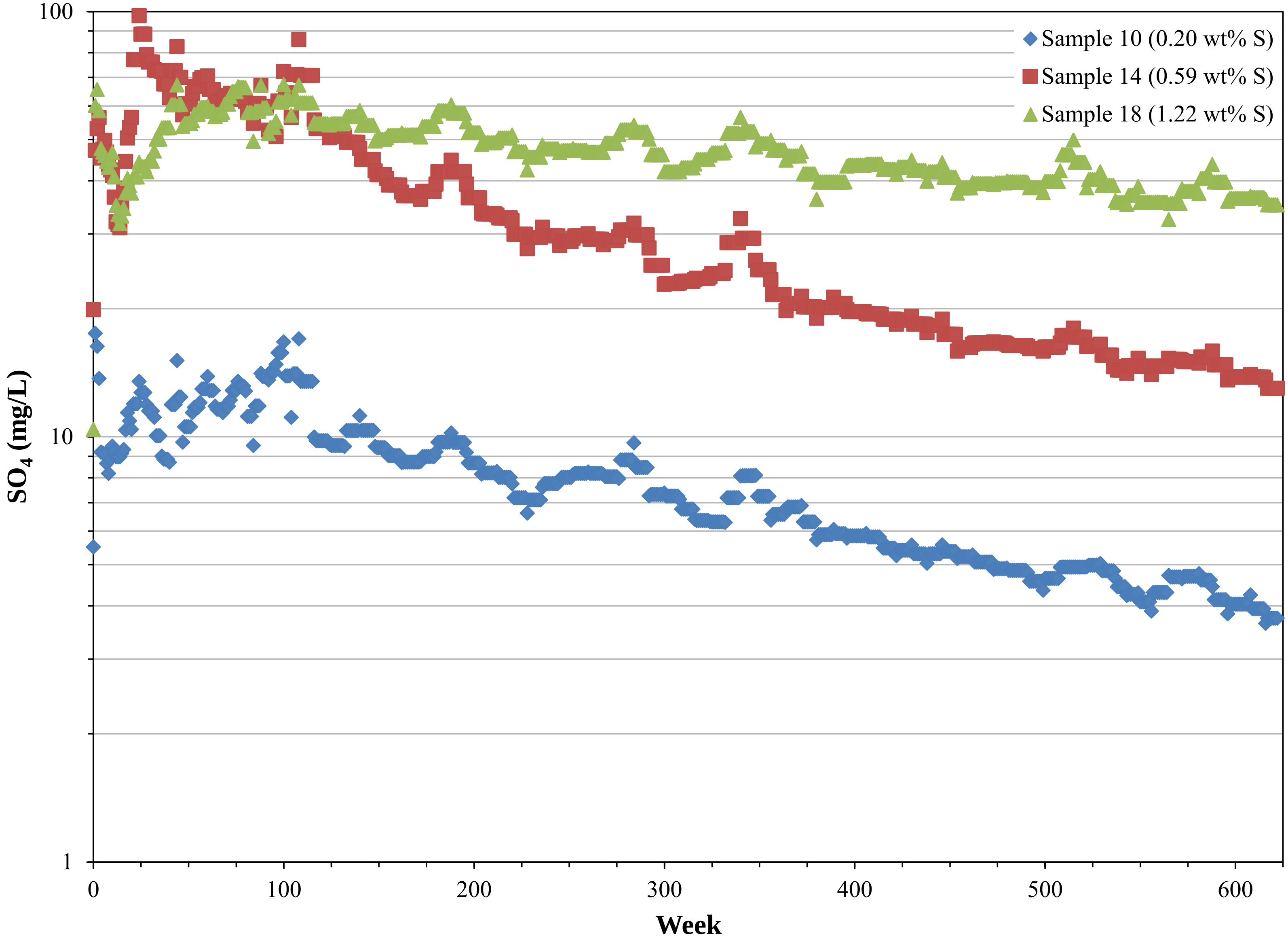

Figure 4.18 Group 3 leachate SO$_4$ concentration time series plot.

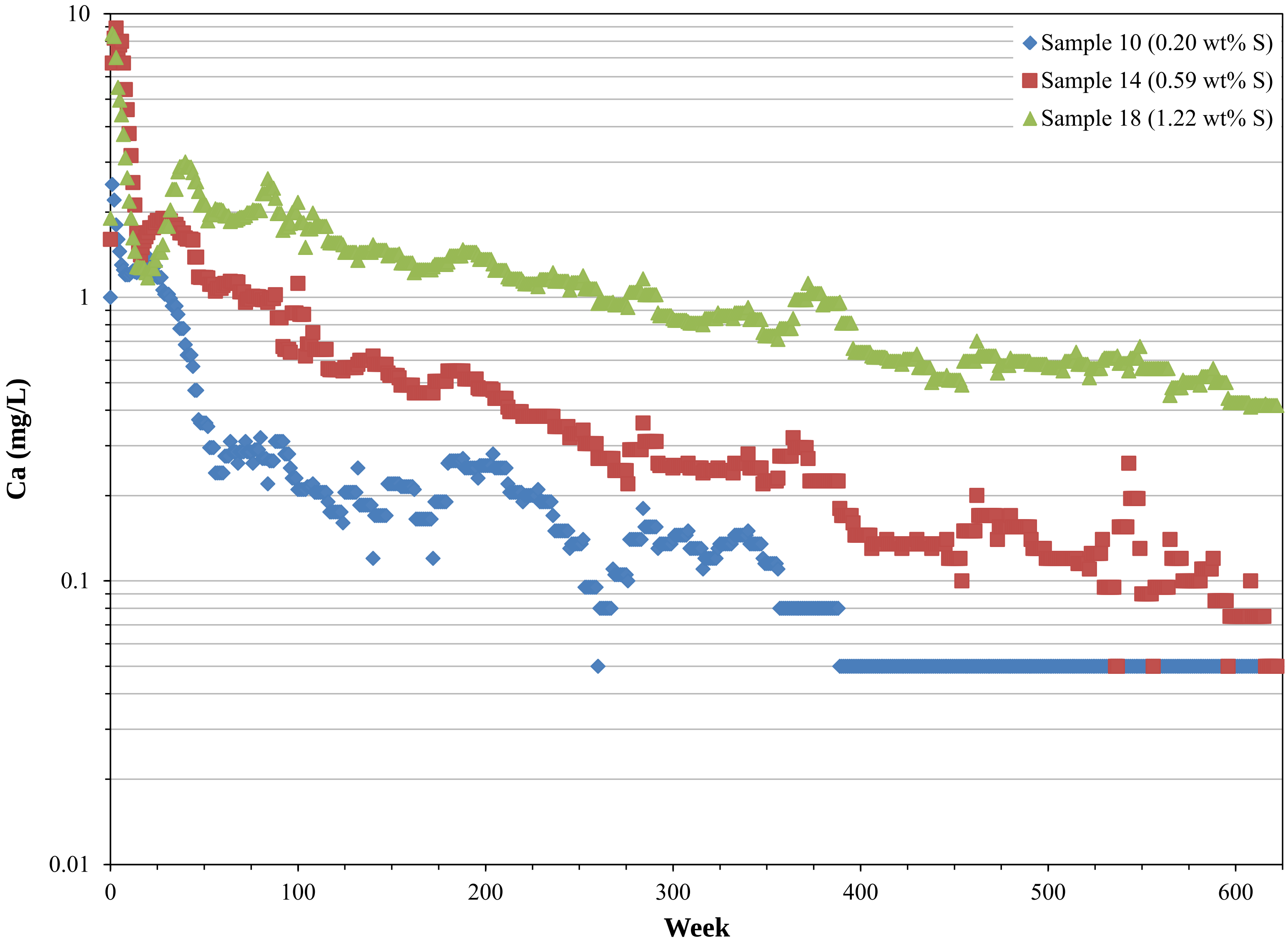

Figure 4.19 Group 3 leachate Ca concentration time series plot. Less than detection limit values (0.1 mg/L) plotted as one half the detection limit (0.05 mg/L).

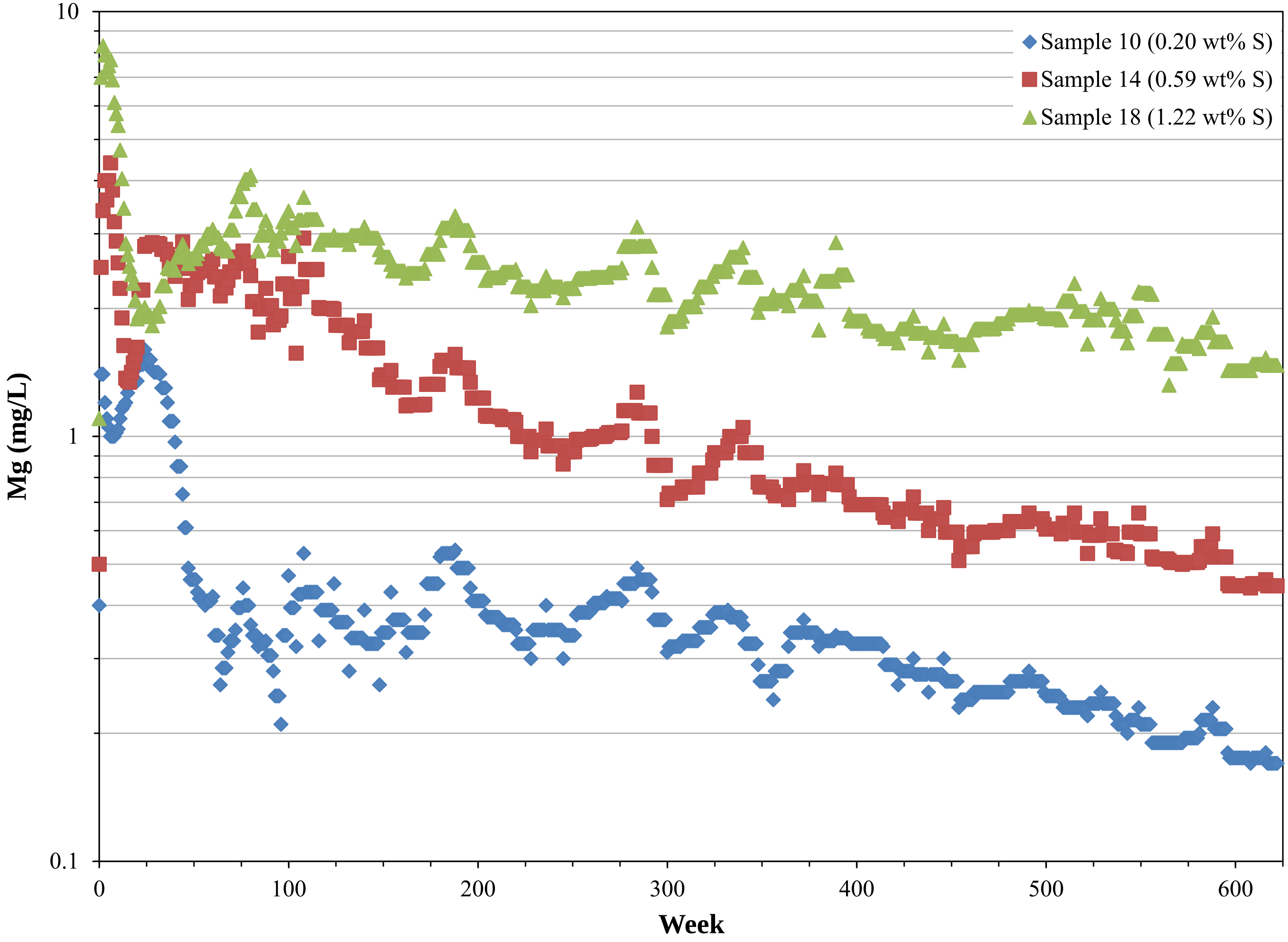

Figure 4.20 Group 3 leachate Mg concentration time series plot.

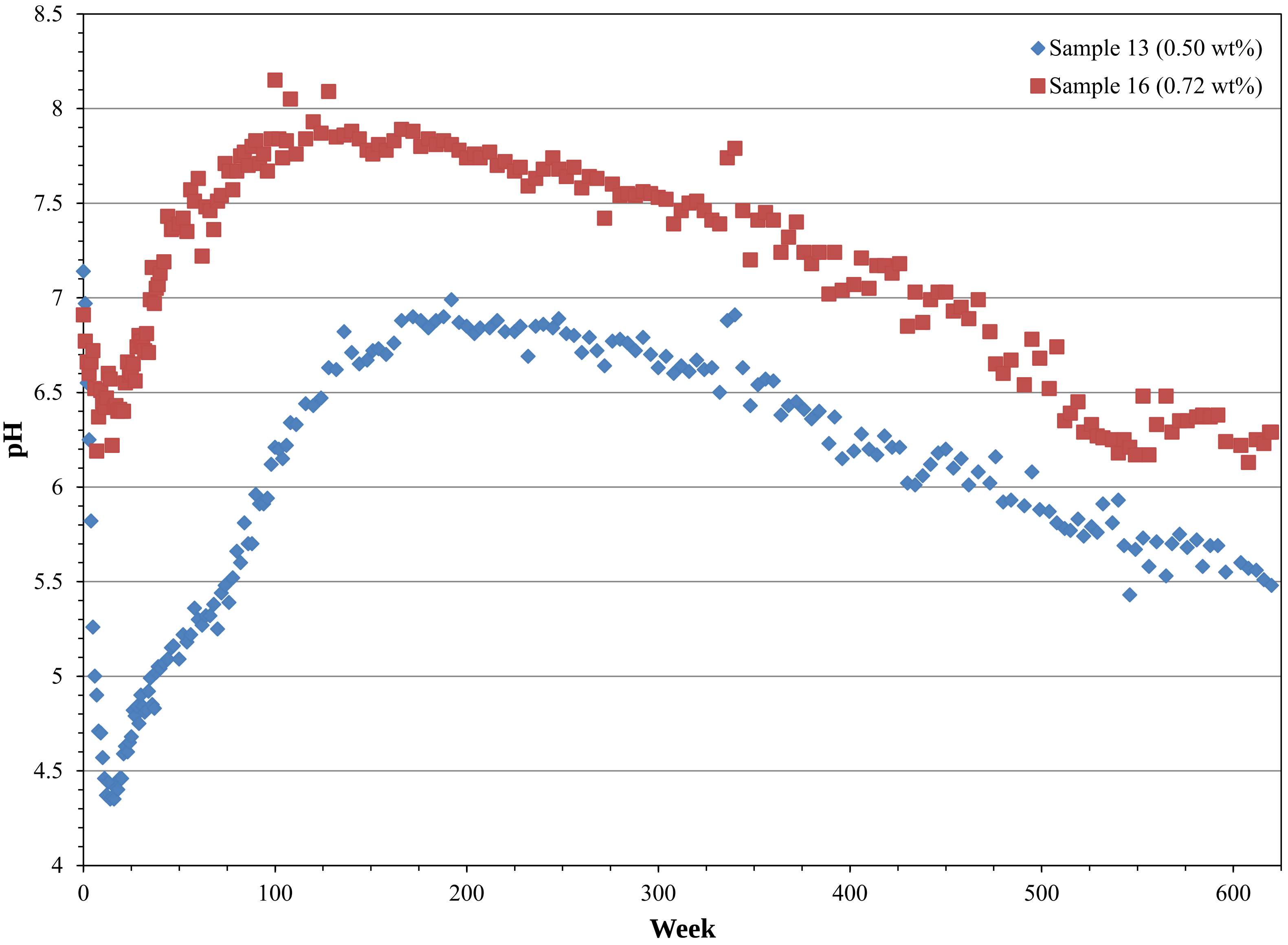

Figure 4.21 Group 4 leachate pH time series plot.

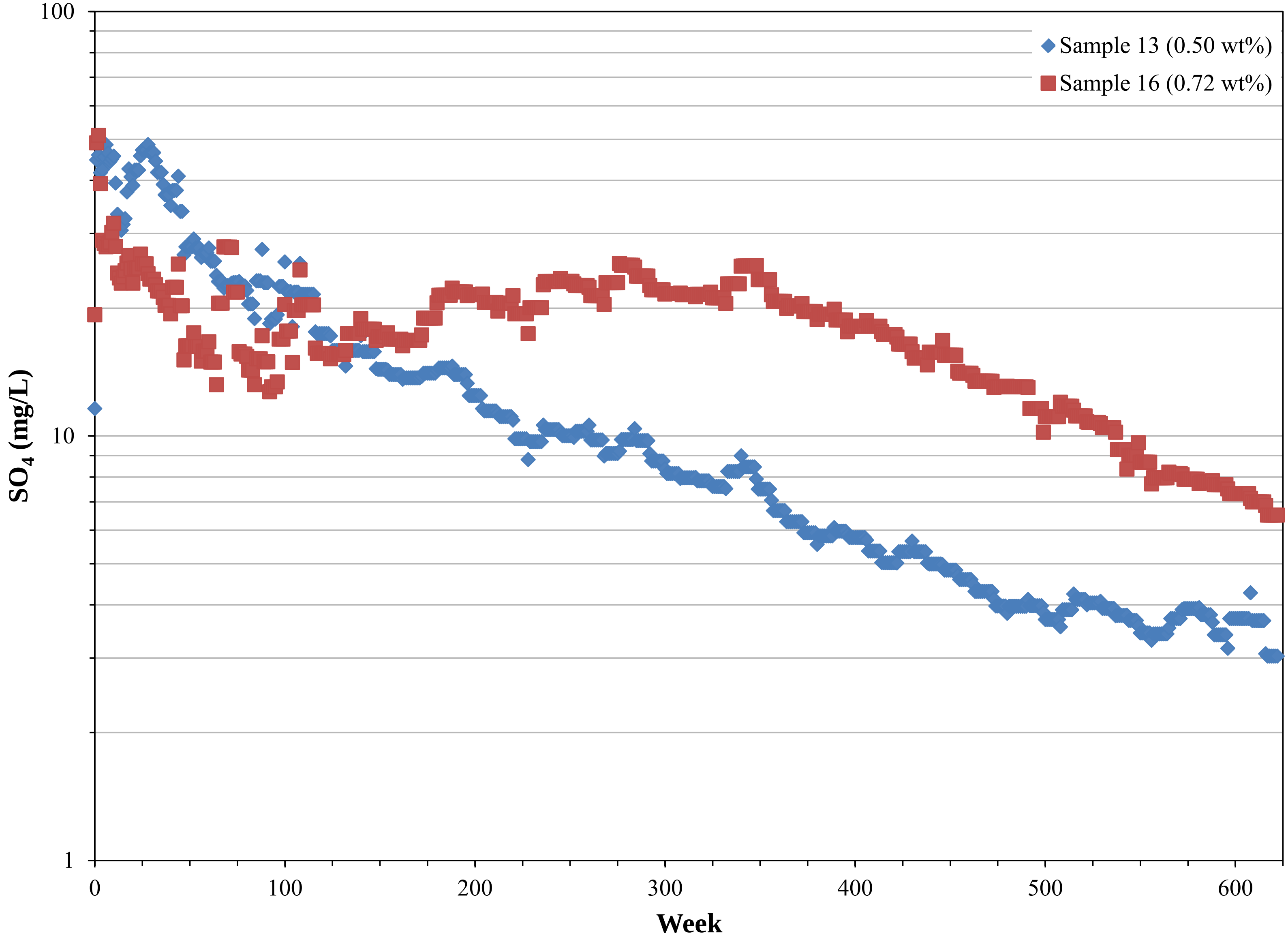

Figure 4.22 Group 4 leachate SO$_4$ concentration time series plot.

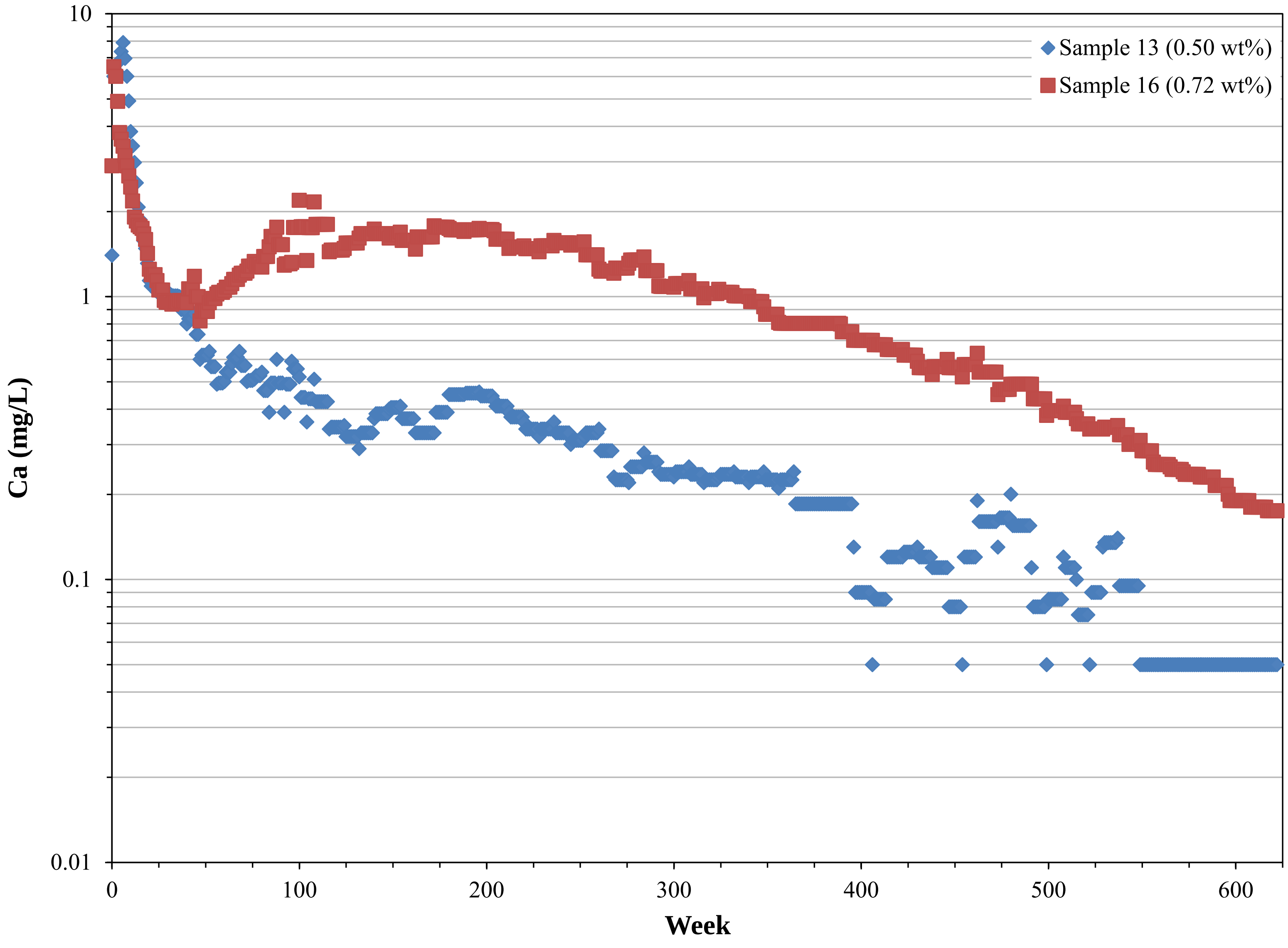

Figure 4.23 Group 4 leachate Ca concentration time series plot. Less than detection limit values (0.1 mg/L) plotted as one half the detection limit (0.05 mg/L).

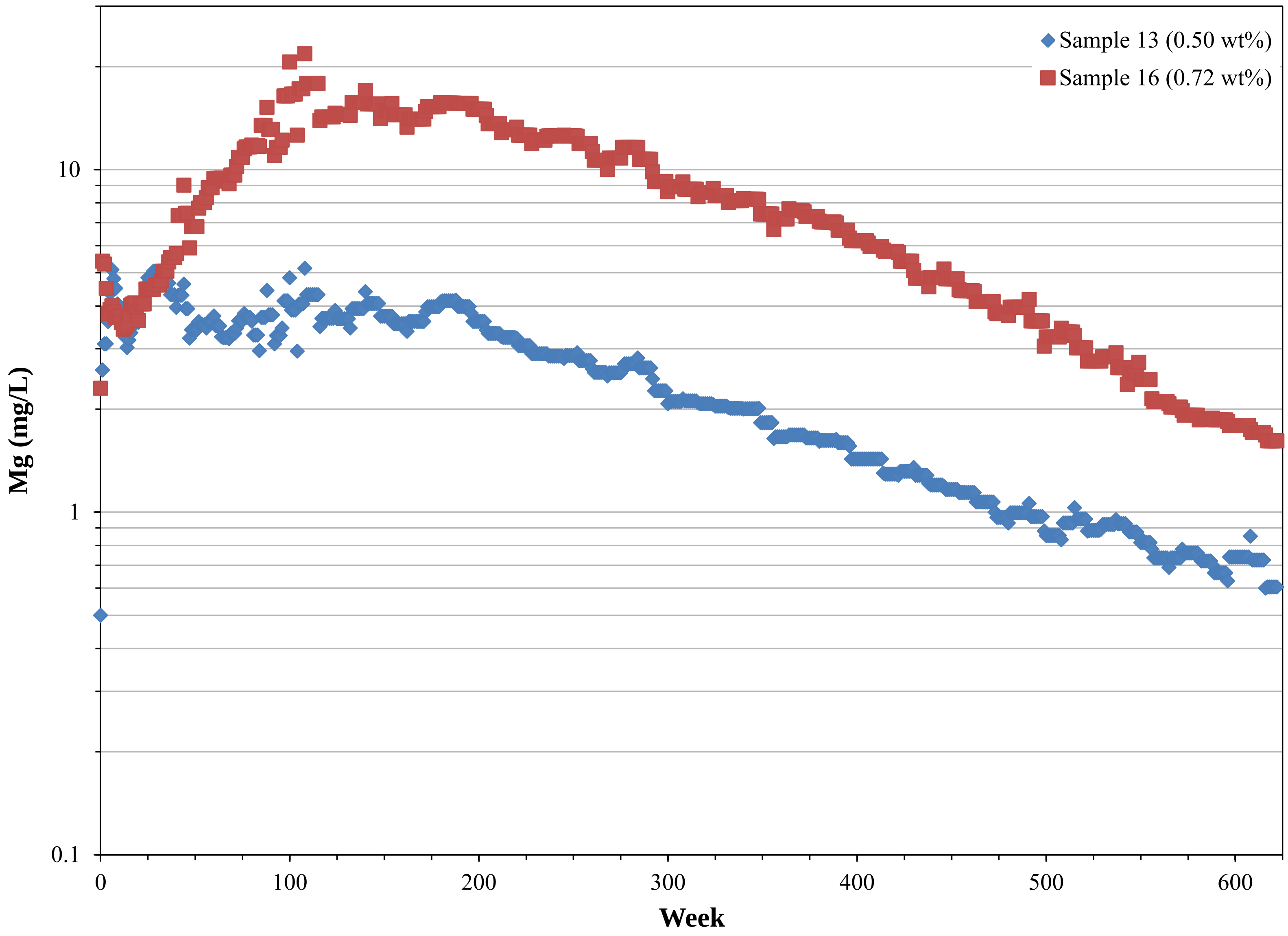

Figure 4.24 Group 4 leachate Mg concentration time series plot.

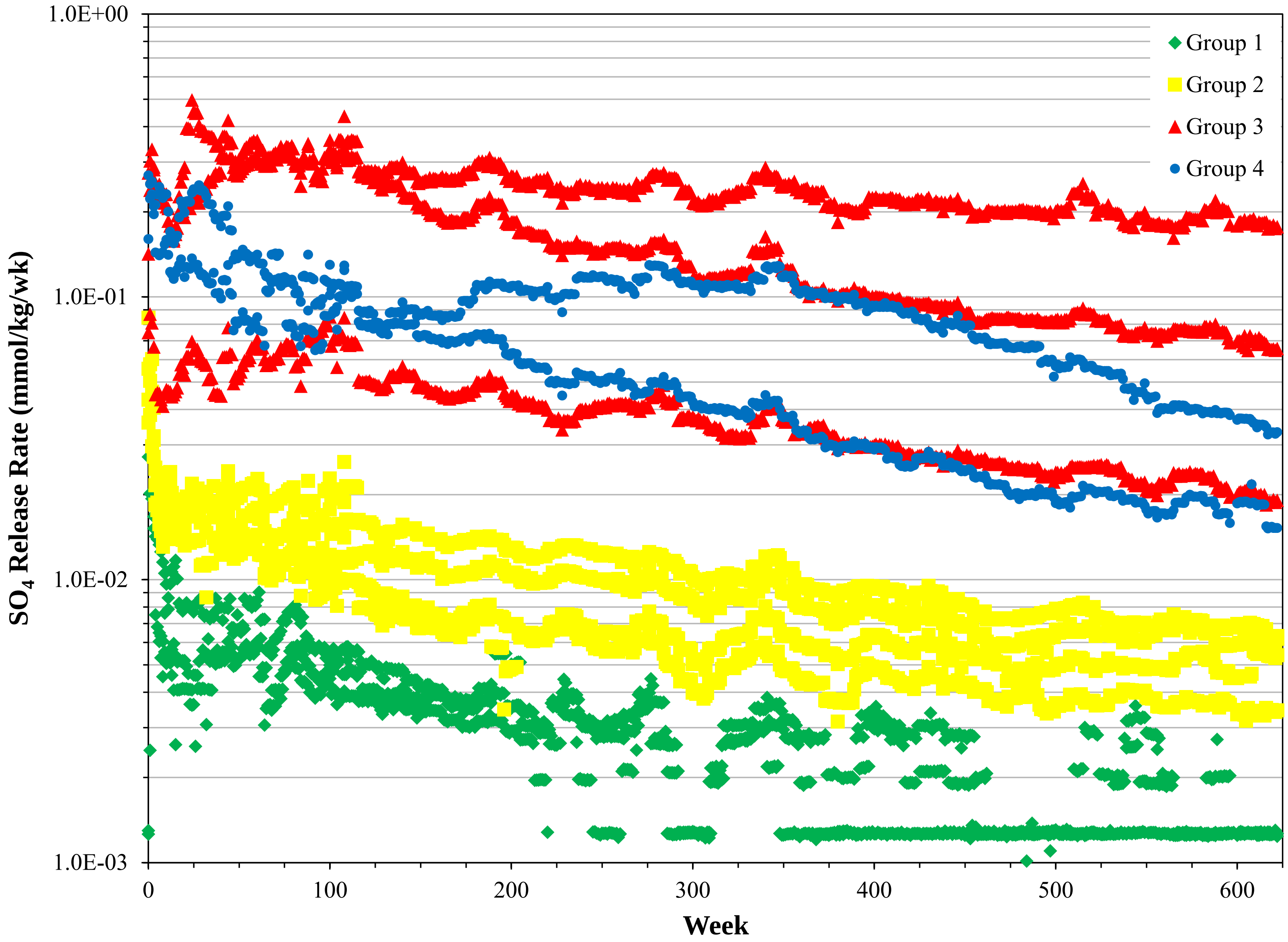

Figure 4.25 All groups leachate SO_4 release rate time series plot.

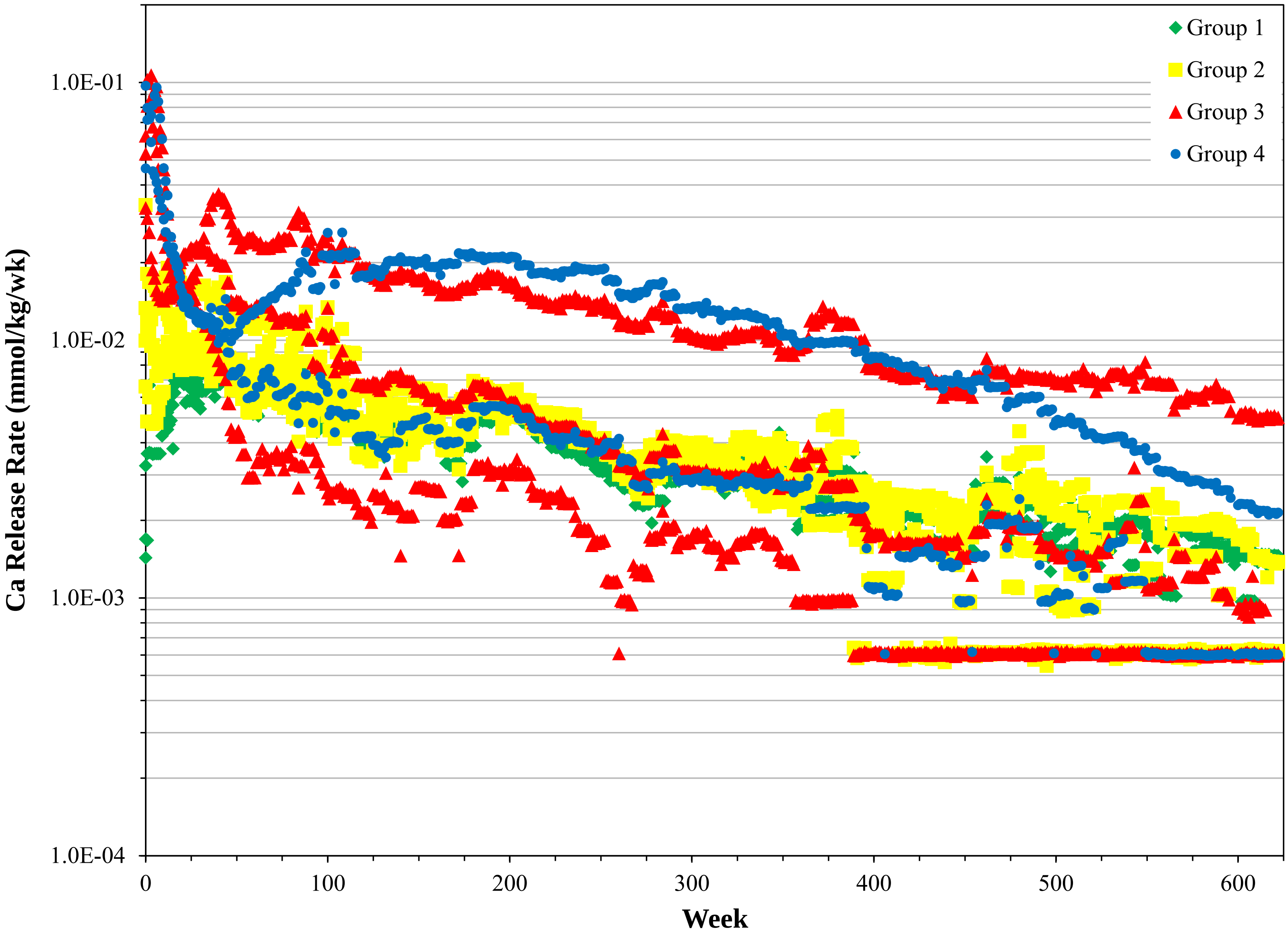

Figure 4.26 All groups Ca release rate time series plot.

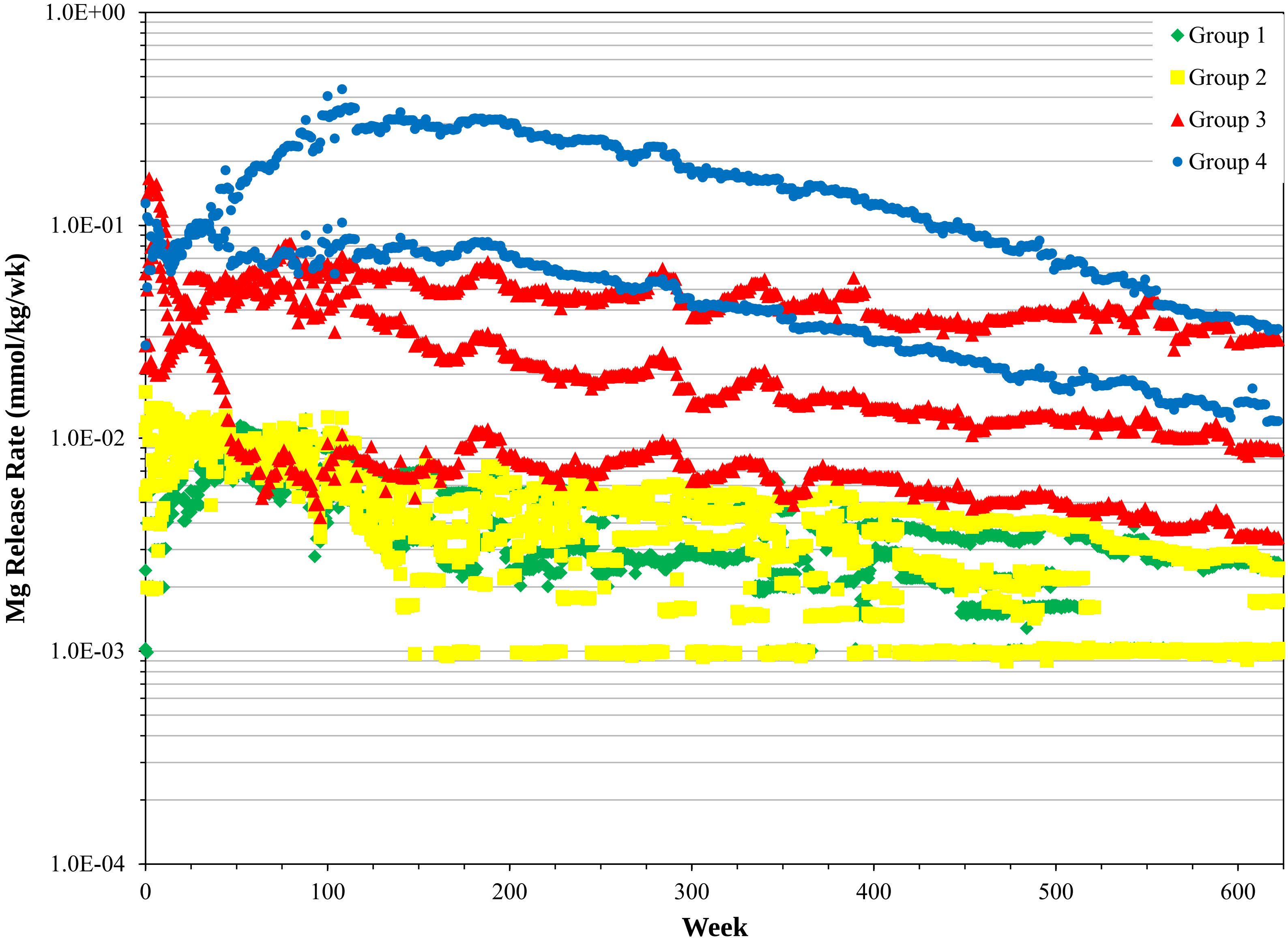

Figure 4.27 All groups Mg release rate time series plot.

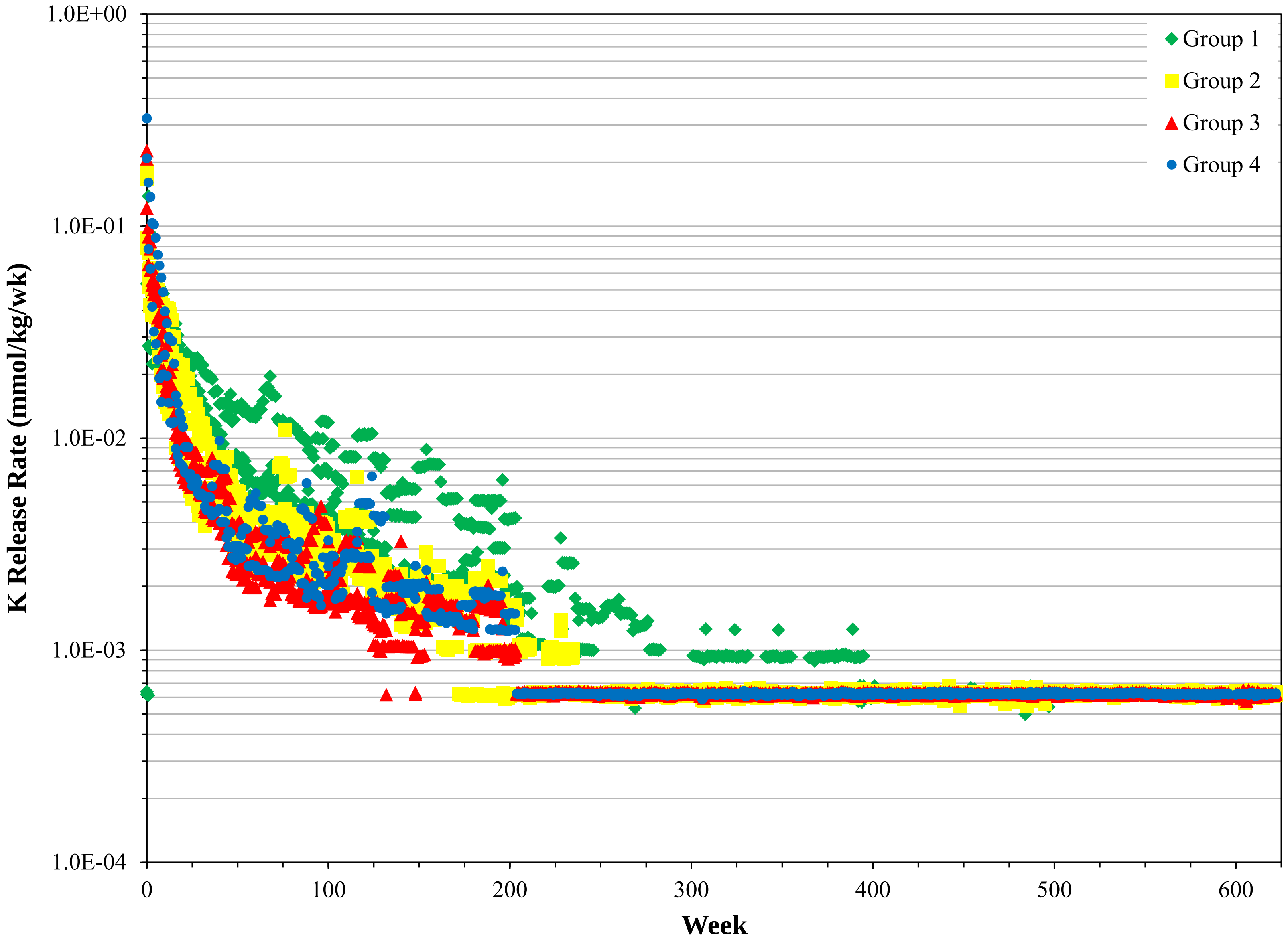

Figure 4.28 All groups K release rate time series plot.

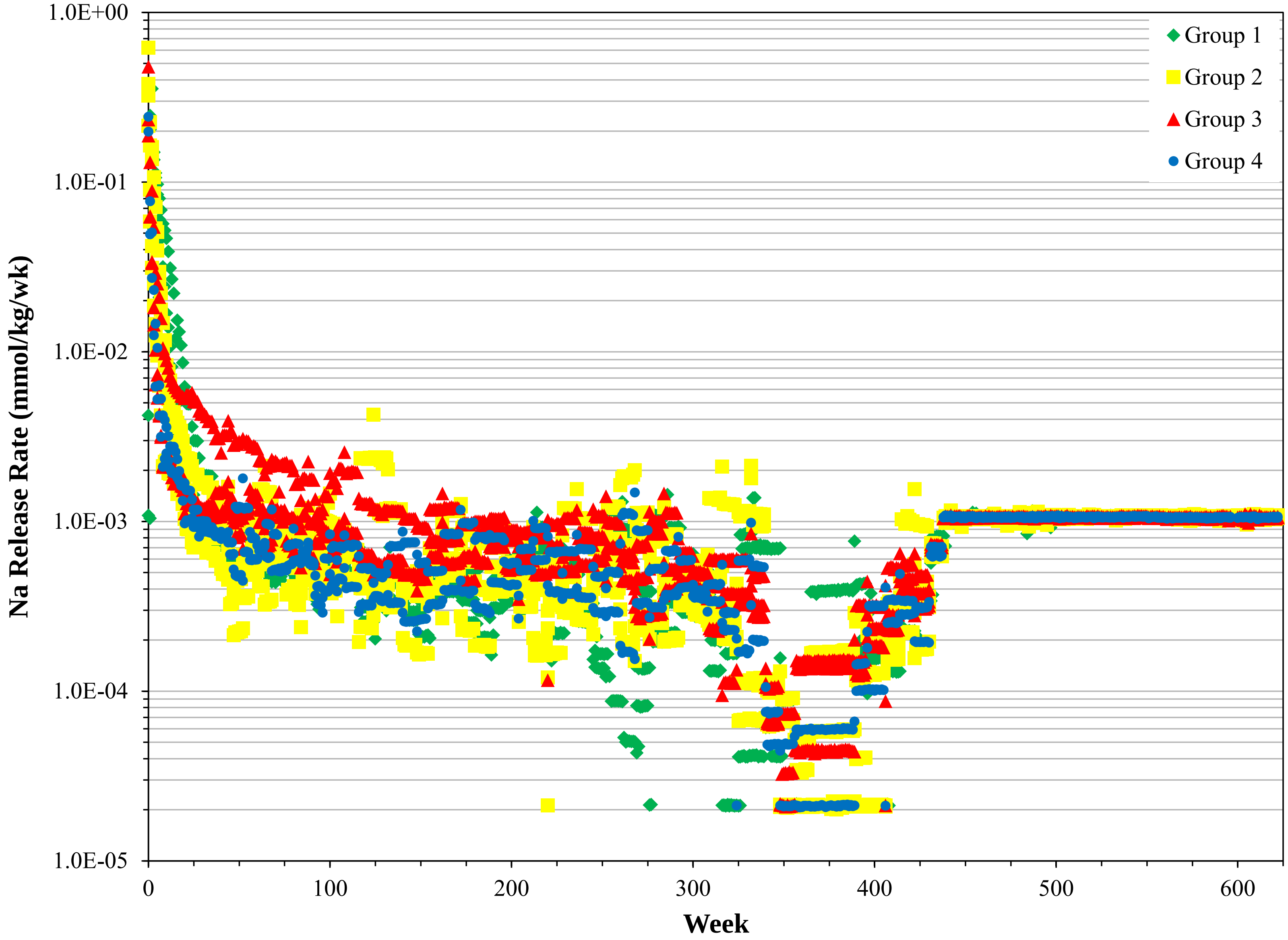

Figure 4.29 All groups Na release rate time series plot.

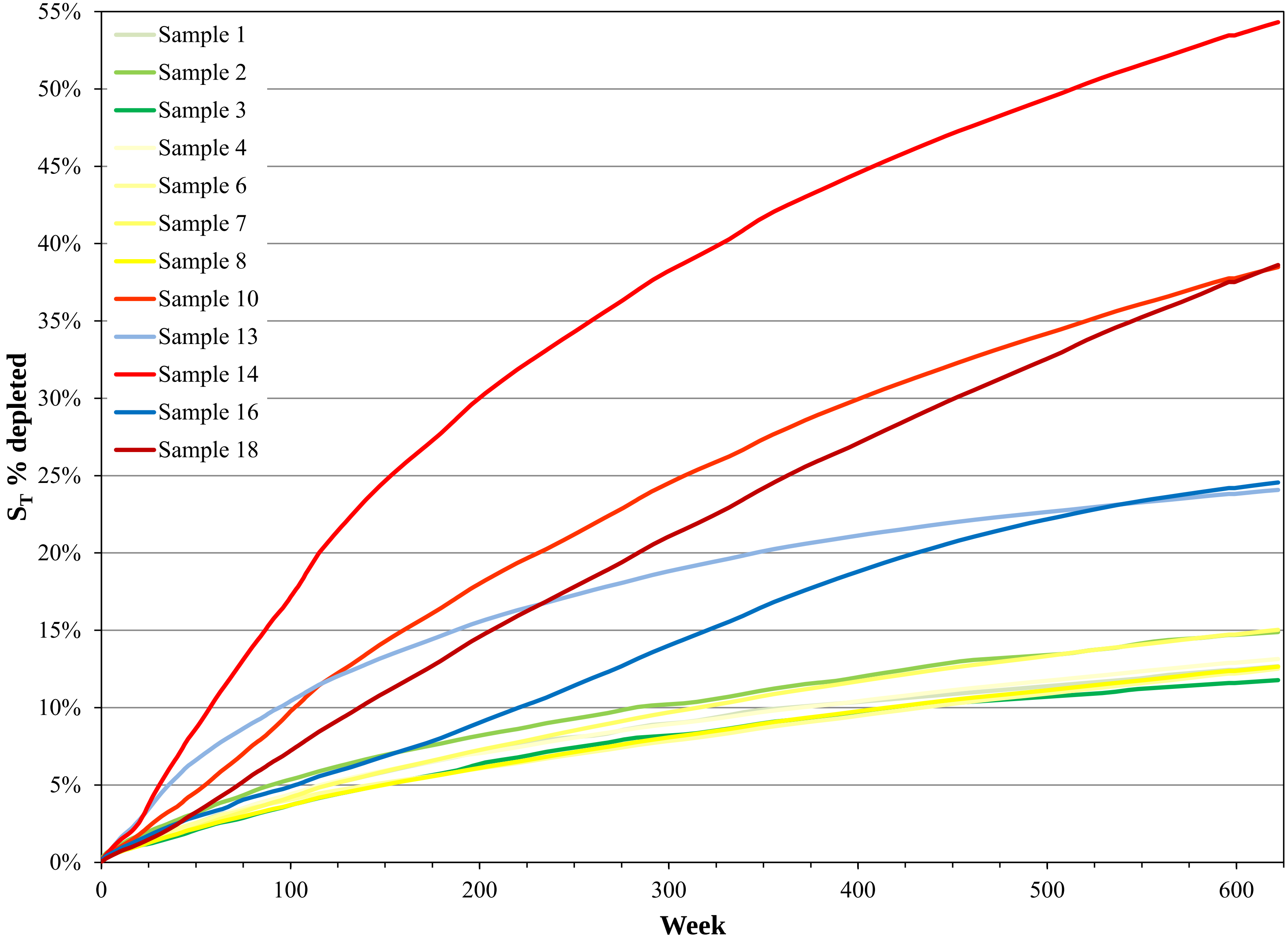

Figure 4.30 Humidity cell samples sulfur depletion time series plot.

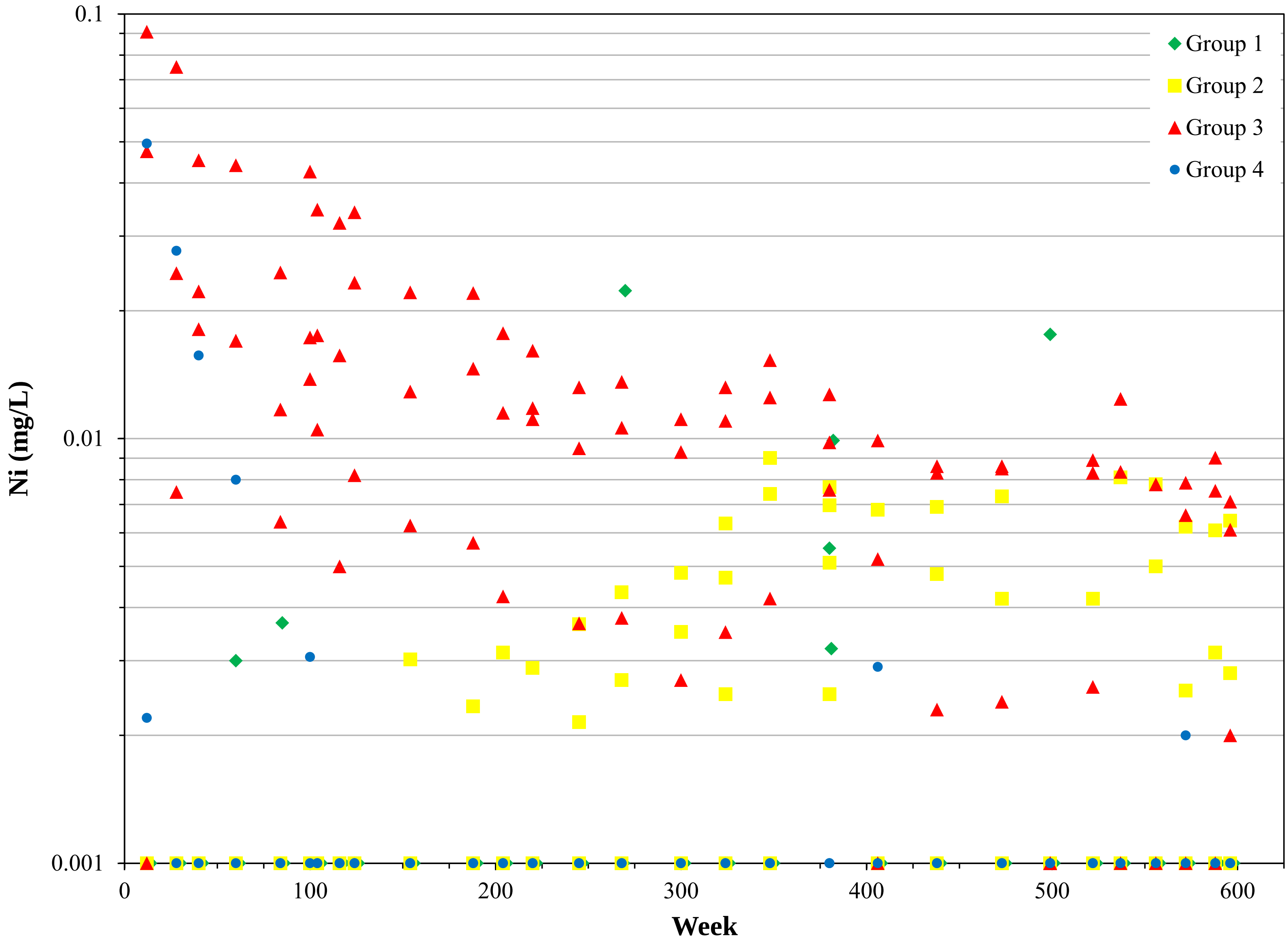

Figure 4.31 All groups leachate Ni concentrations time series plot.

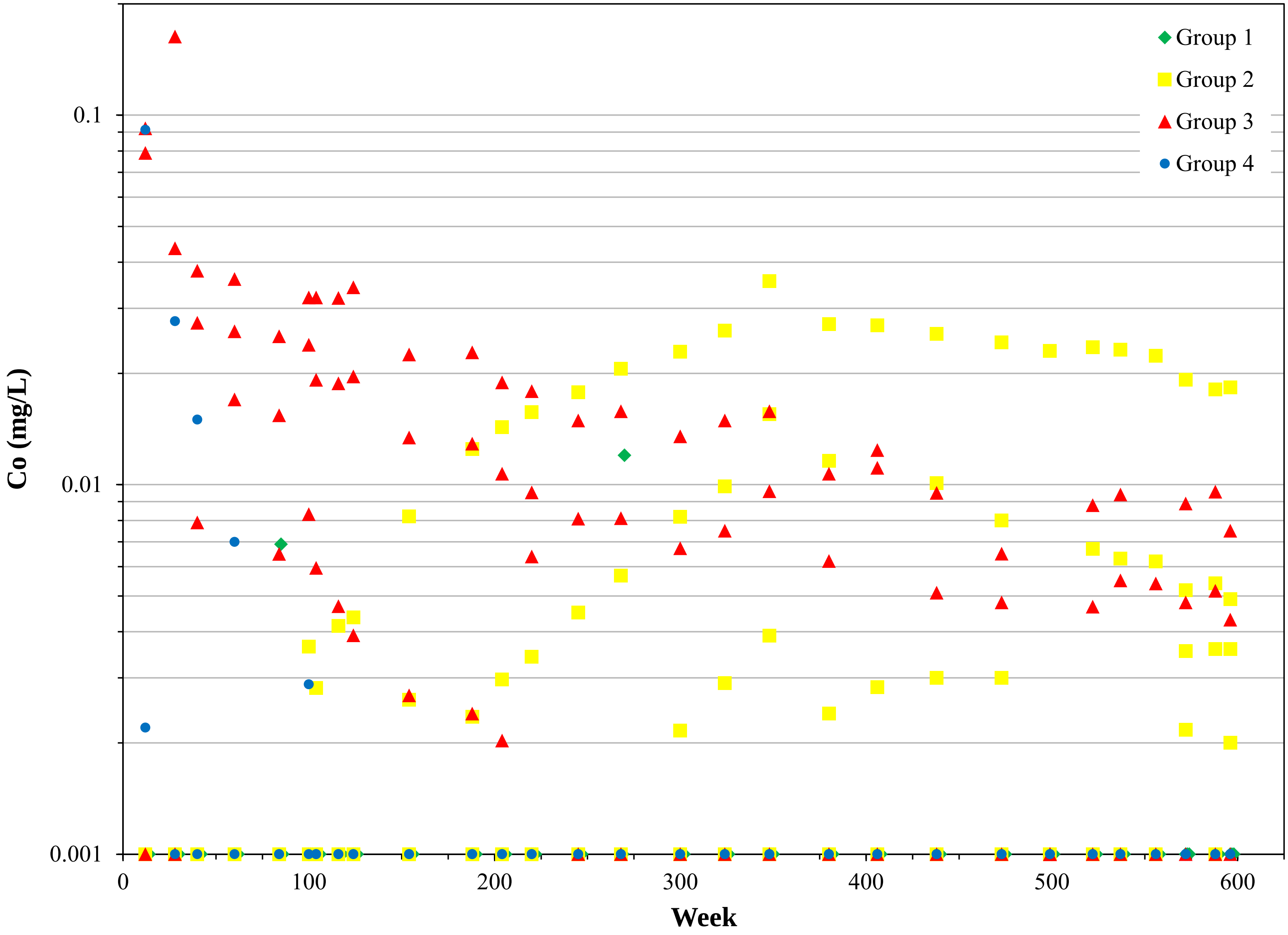

Figure 4.32 All groups leachate Co concentrations time series plot.

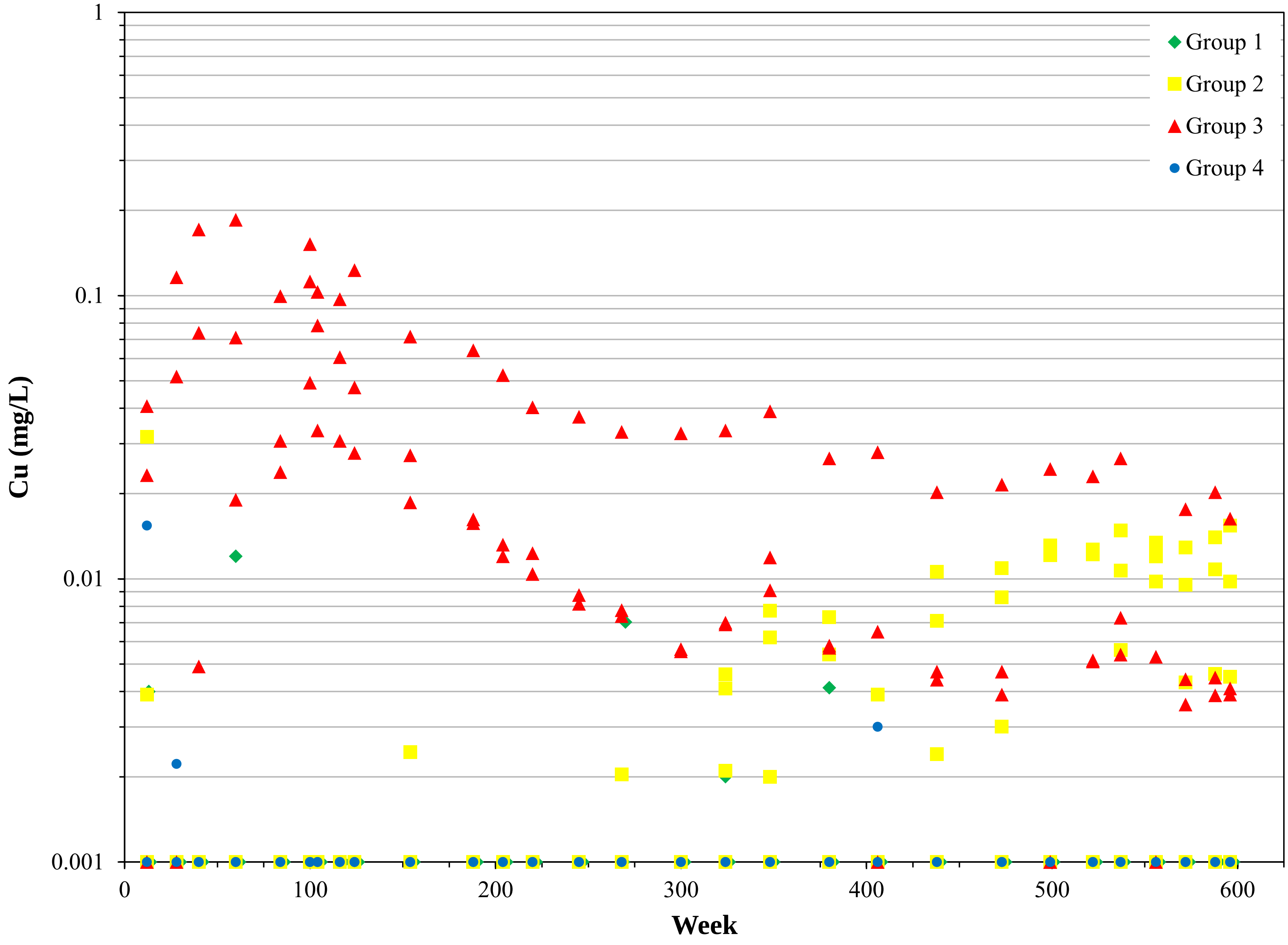

Figure 4.33 All groups leachate Cu concentrations time series plot.

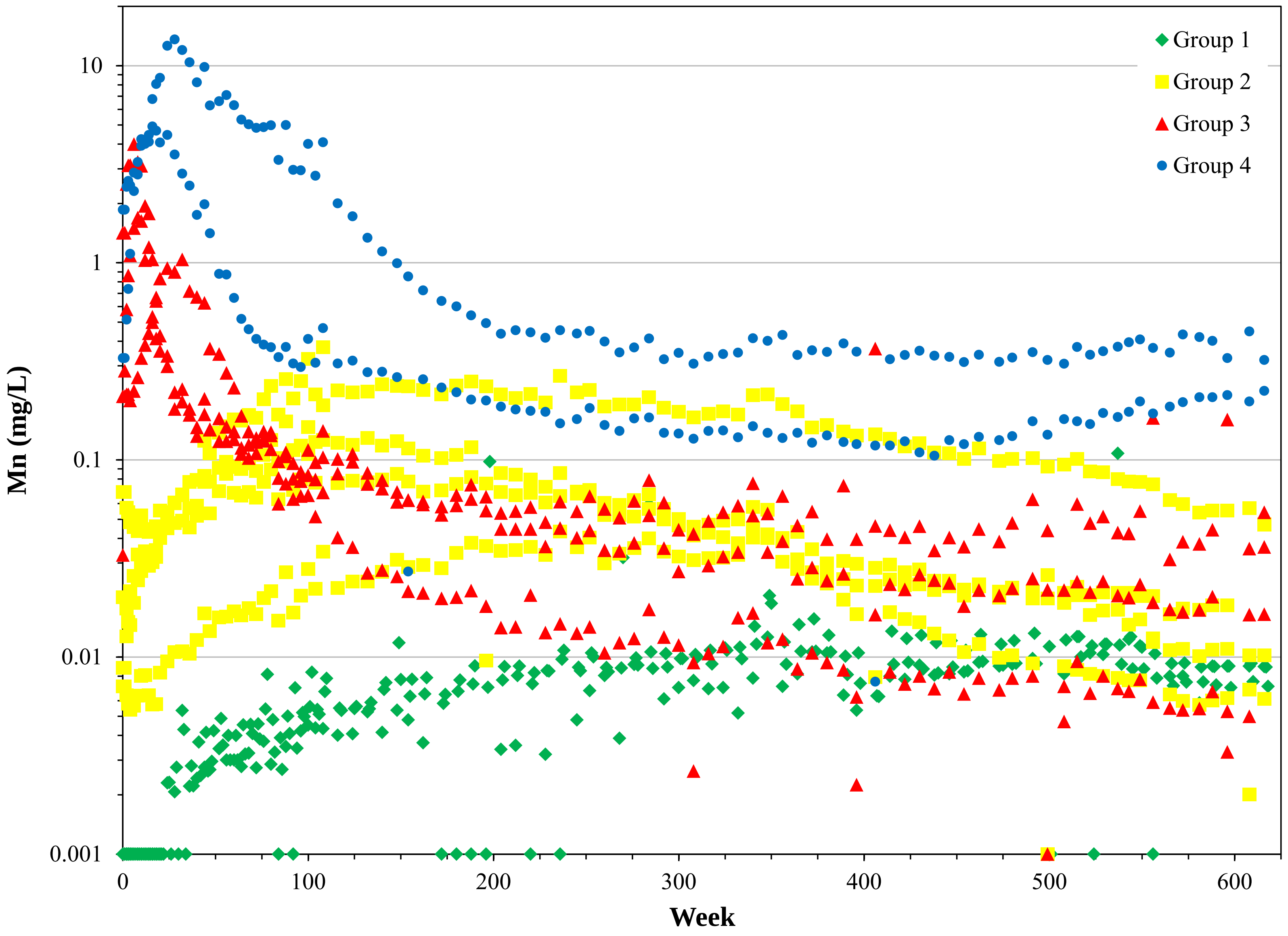

Figure 4.34 All groups leachate Mn concentrations time series plot.

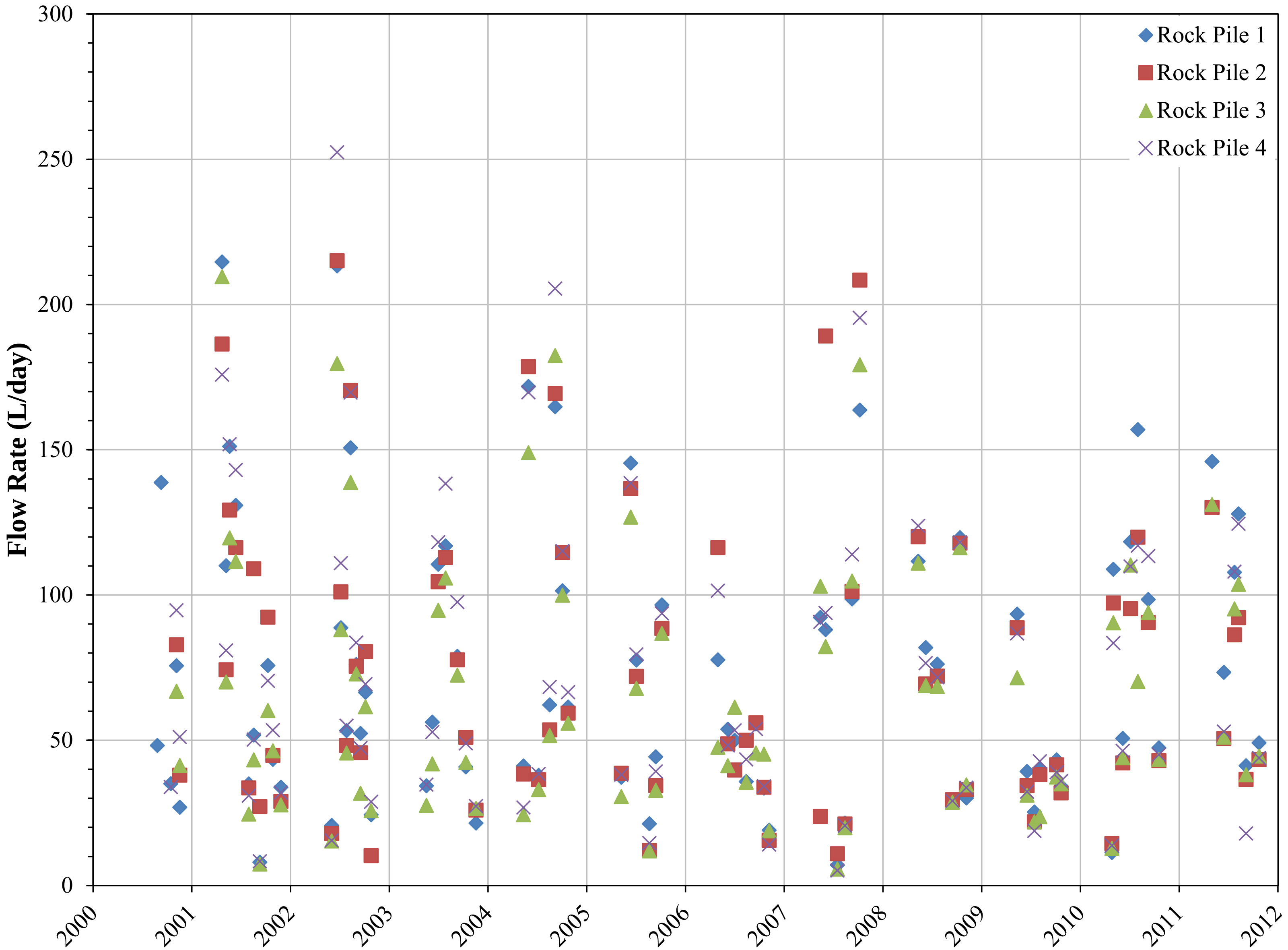

Figure 4.35 Field rock piles individual sampling period leachate flow rates.

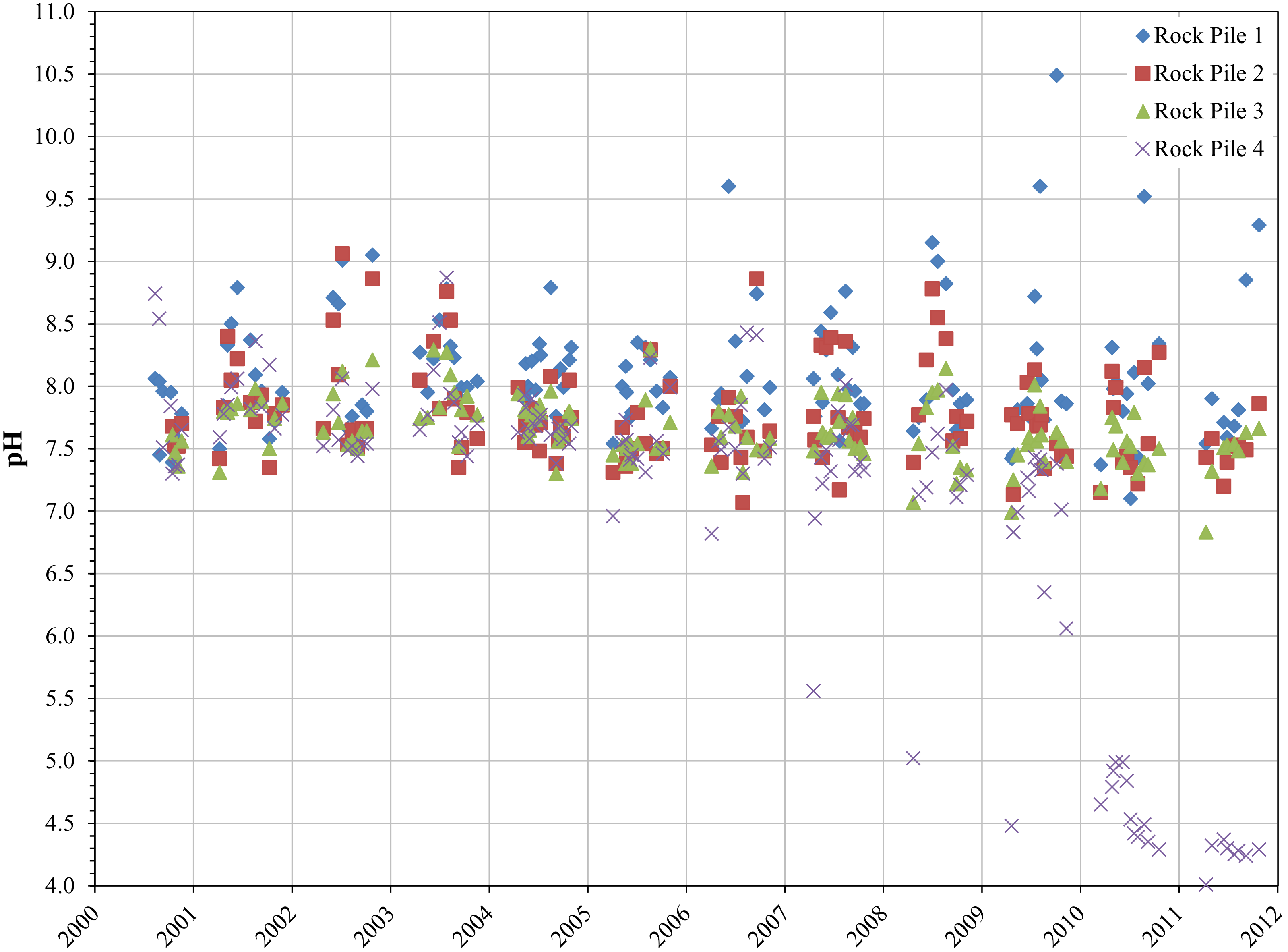

Figure 4.36 Field rock piles individual sampling period leachate pH.

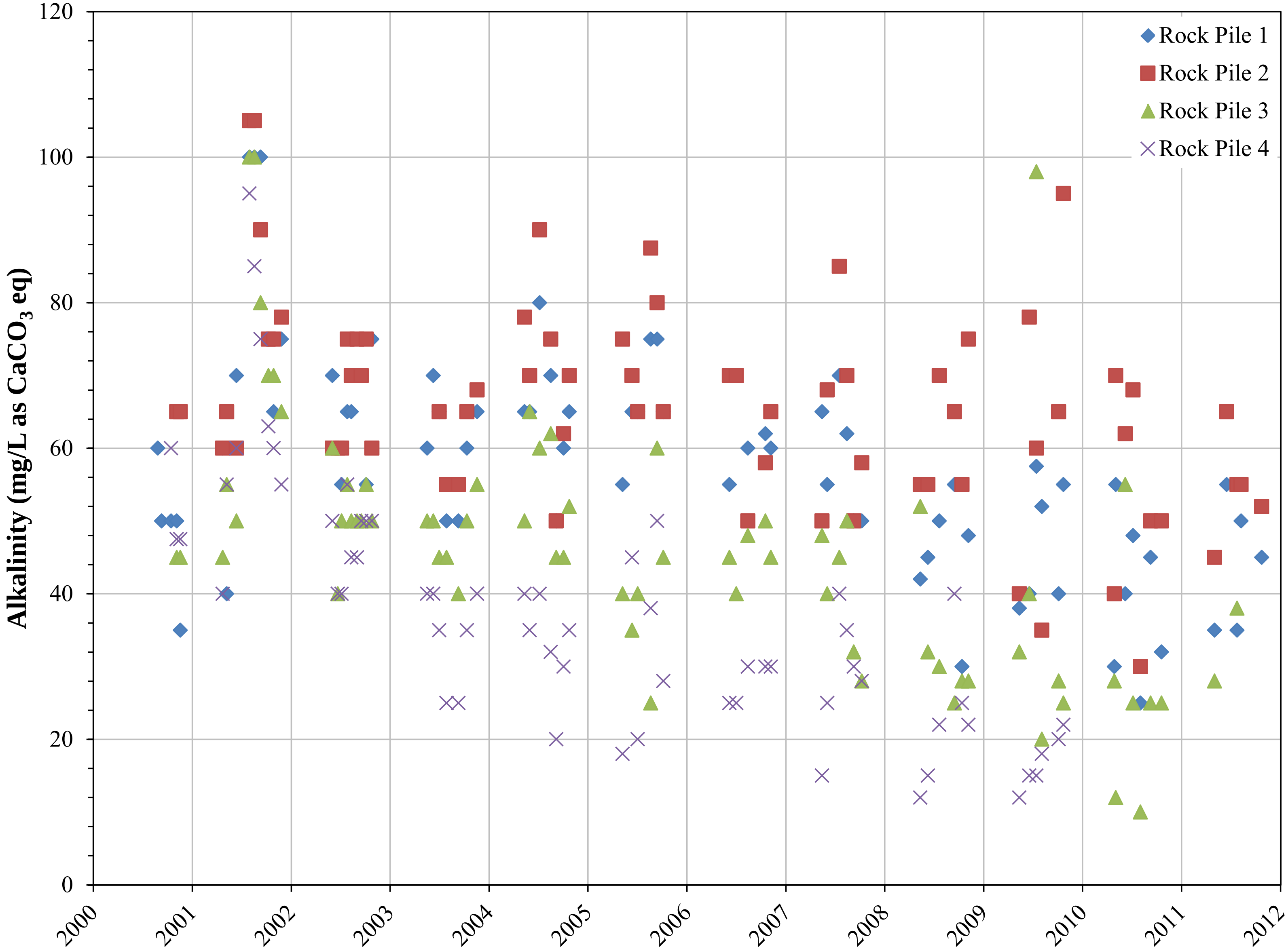

Figure 4.37 Field rock piles individual sampling period leachate alkalinity.

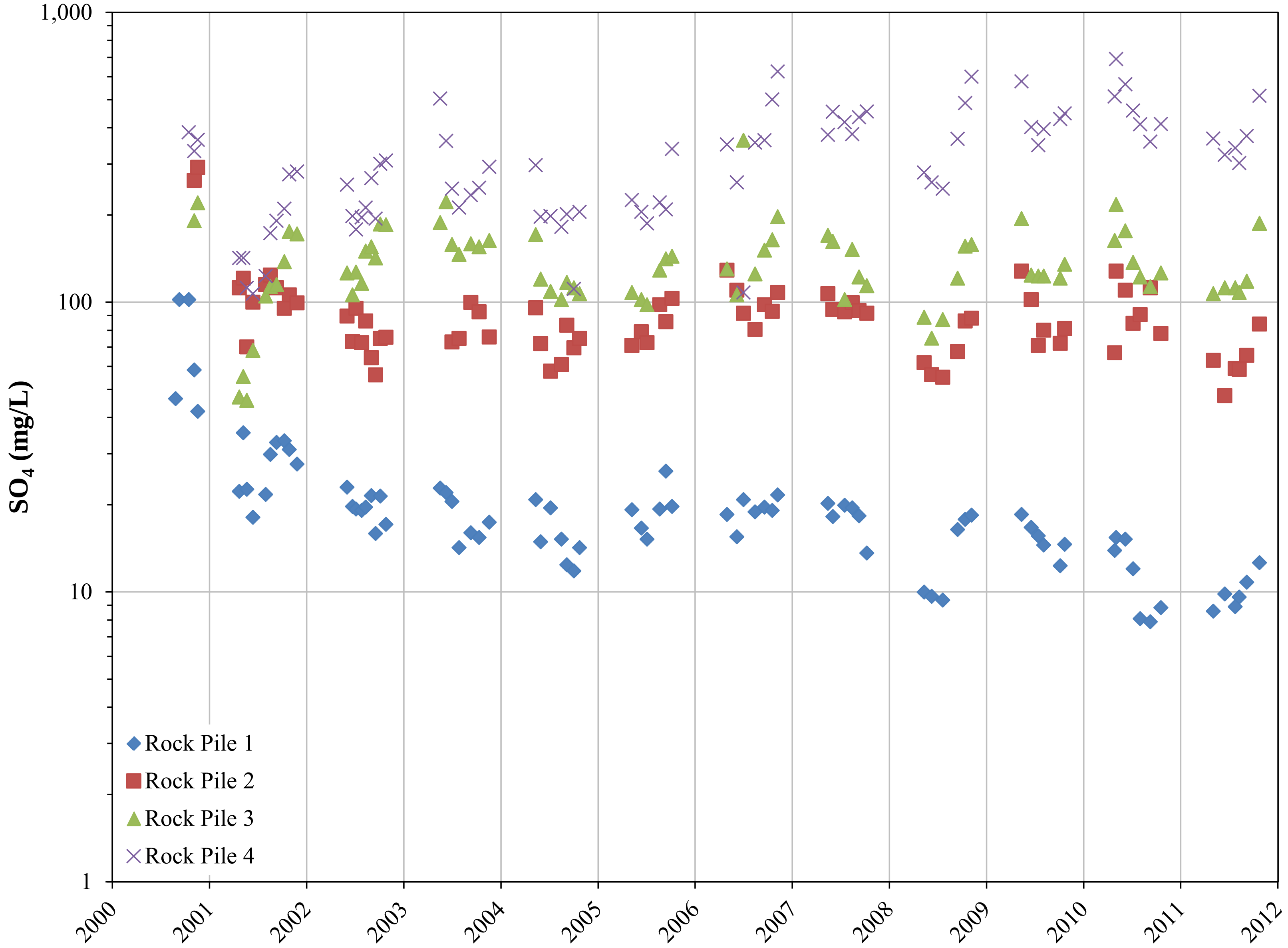

Figure 4.38 Field rock piles SO$_4$ leachate concentrations.

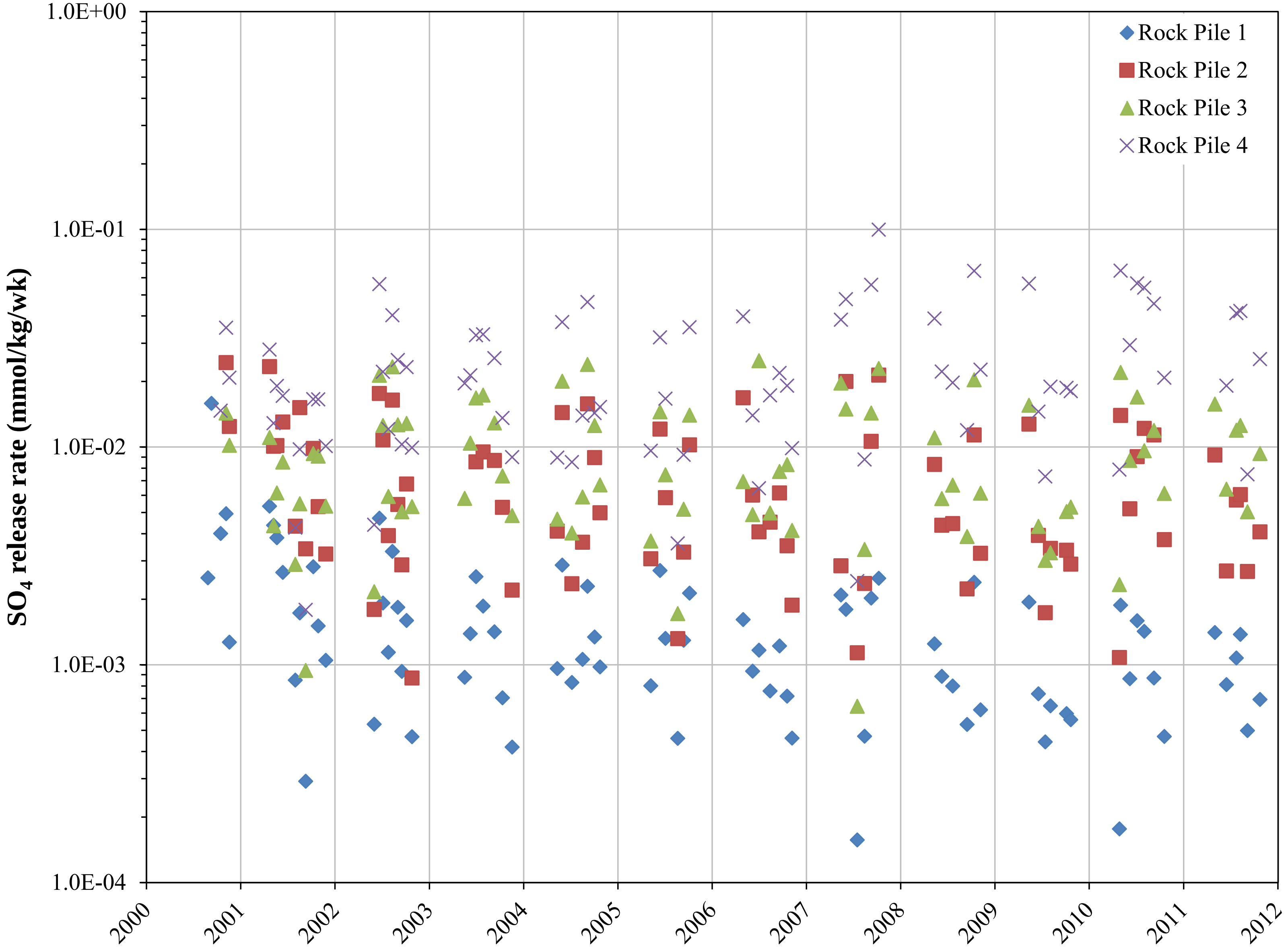

Figure 4.39 Field rock piles individual sampling period leachate SO$_4$ release rates.

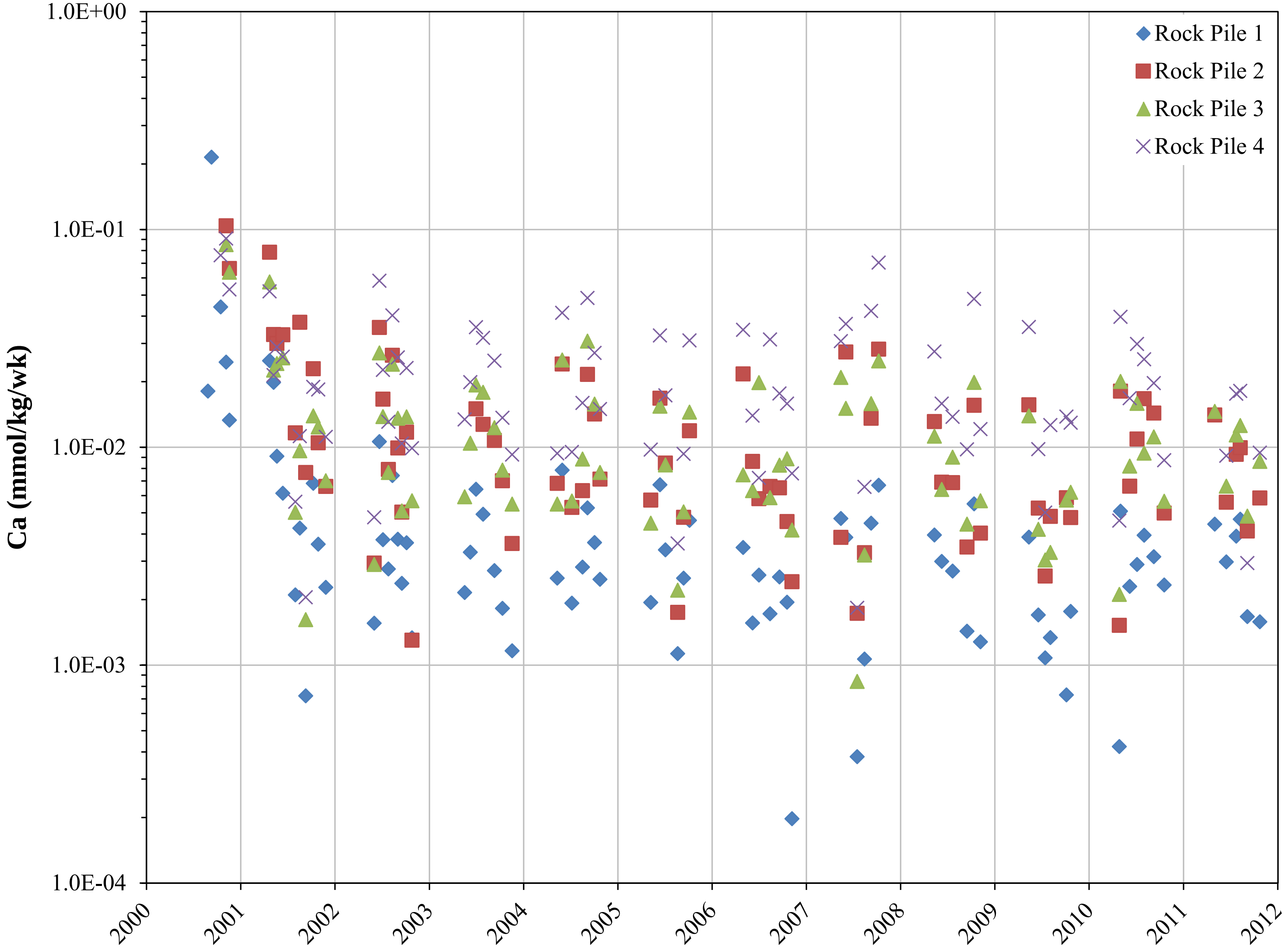

Figure 4.40 Field rock piles individual sampling period leachate Ca release rates.

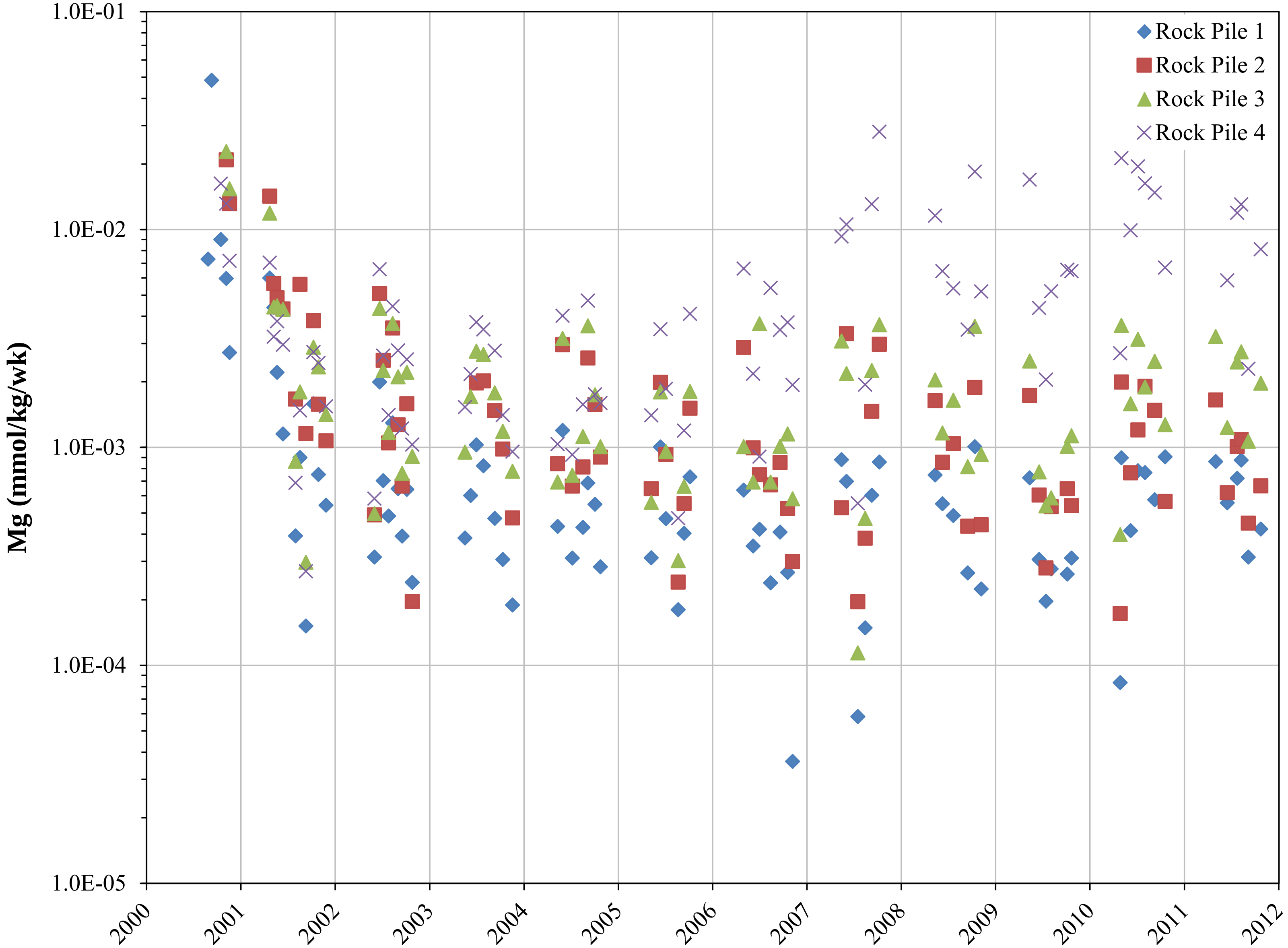

Figure 4.41 Field rock piles individual sampling period leachate Mg release rates.

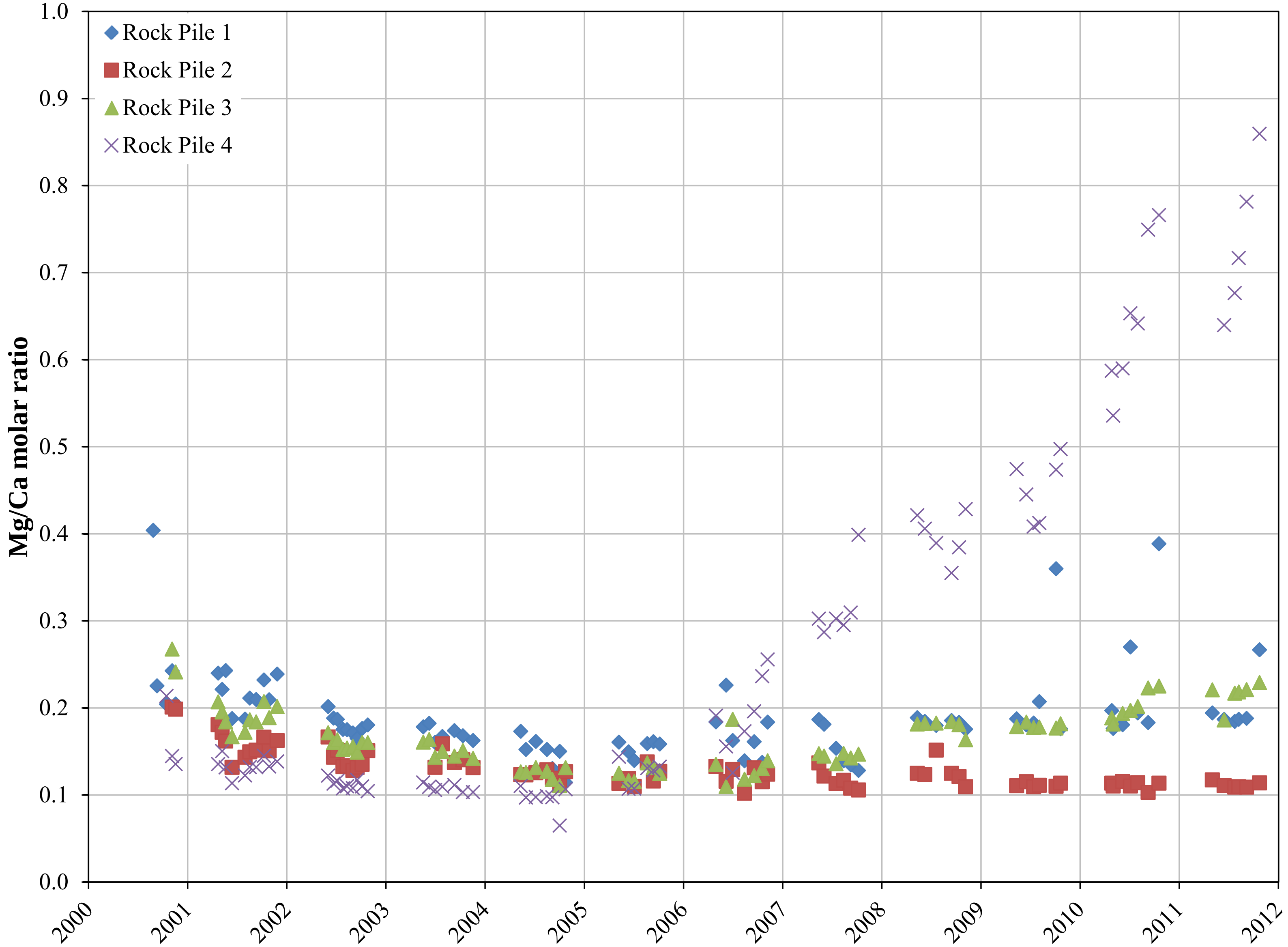

Figure 4.42 Field rock piles individual sampling period leachate Mg/Ca molar ratios.

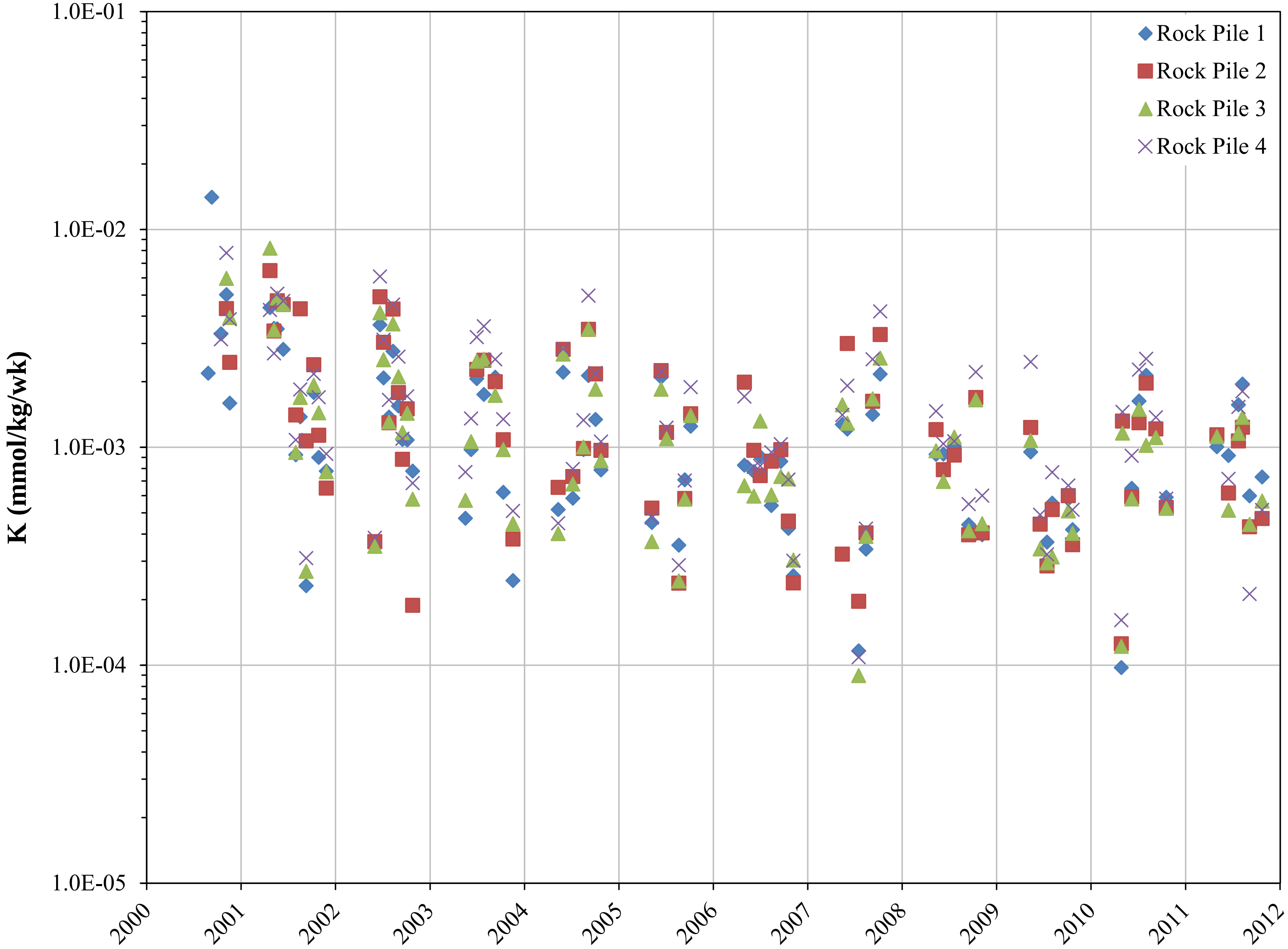

Figure 4.43 Field rock piles individual sampling period leachate K release rates.

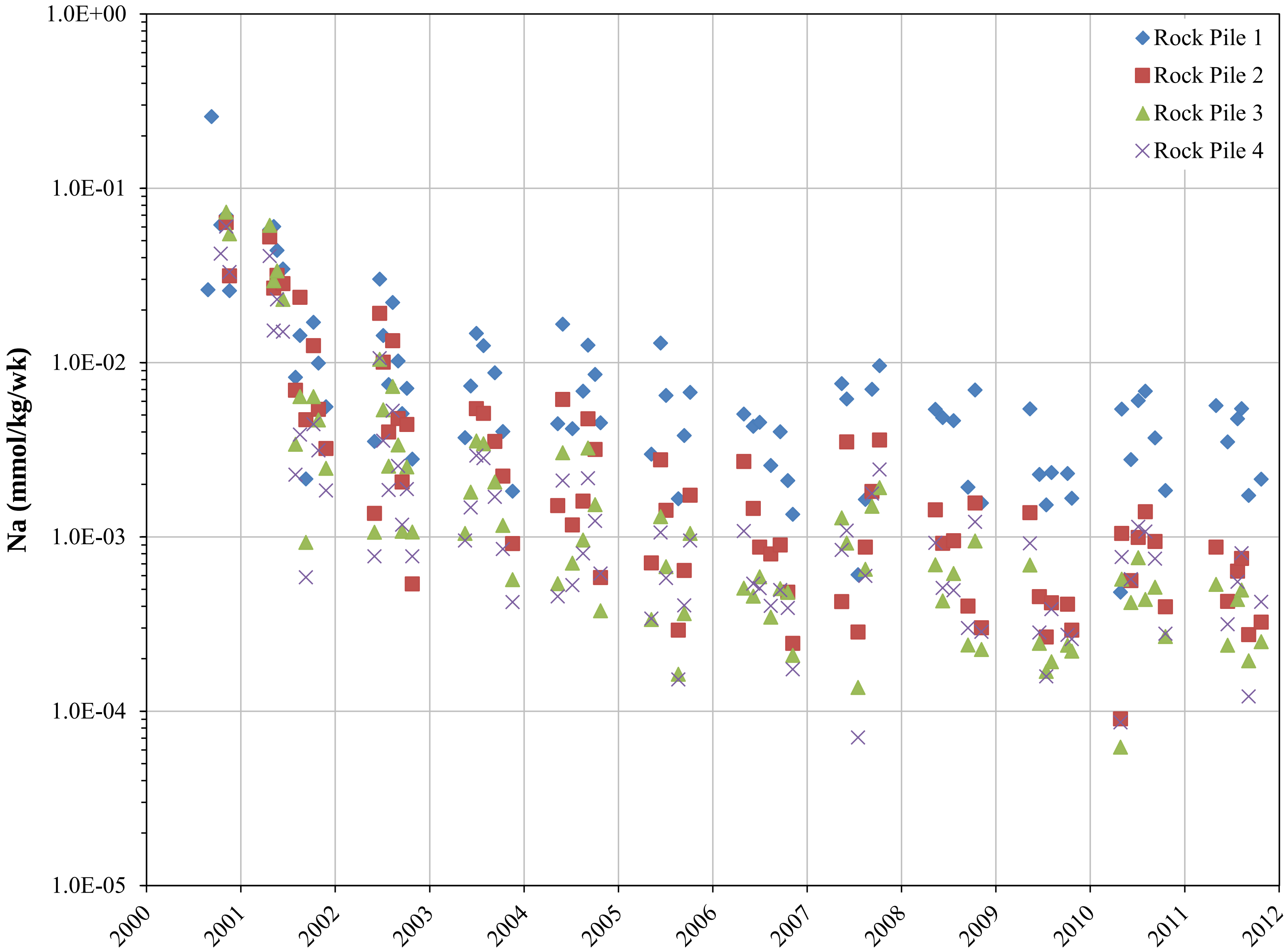

Figure 4.44 Field rock piles individual sampling period leachate Na release rates.

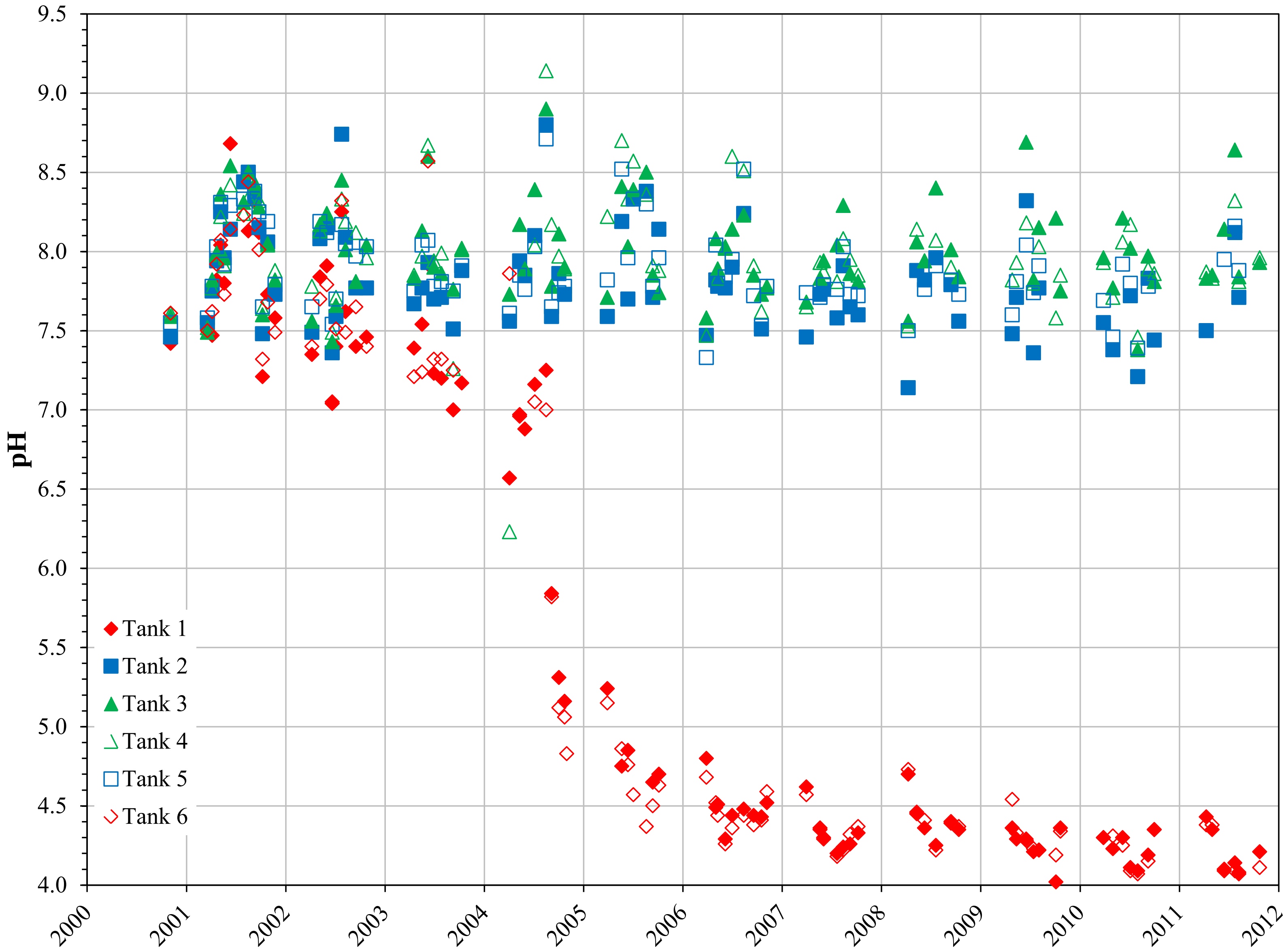

Figure 4.45 Field tanks individual sampling period leachate pH.

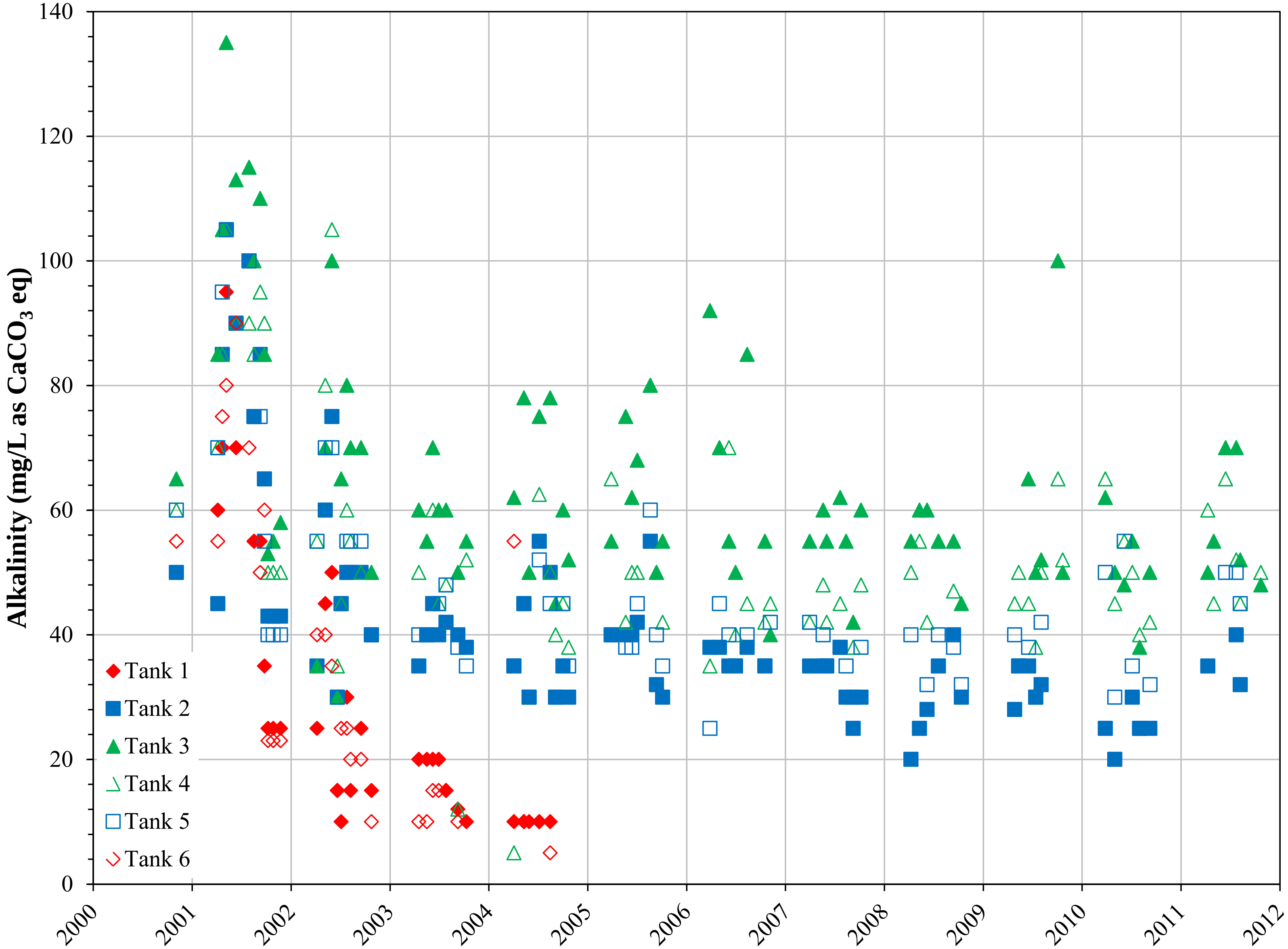

Figure 4.46 Field tanks individual sampling period leachate alkalinity.

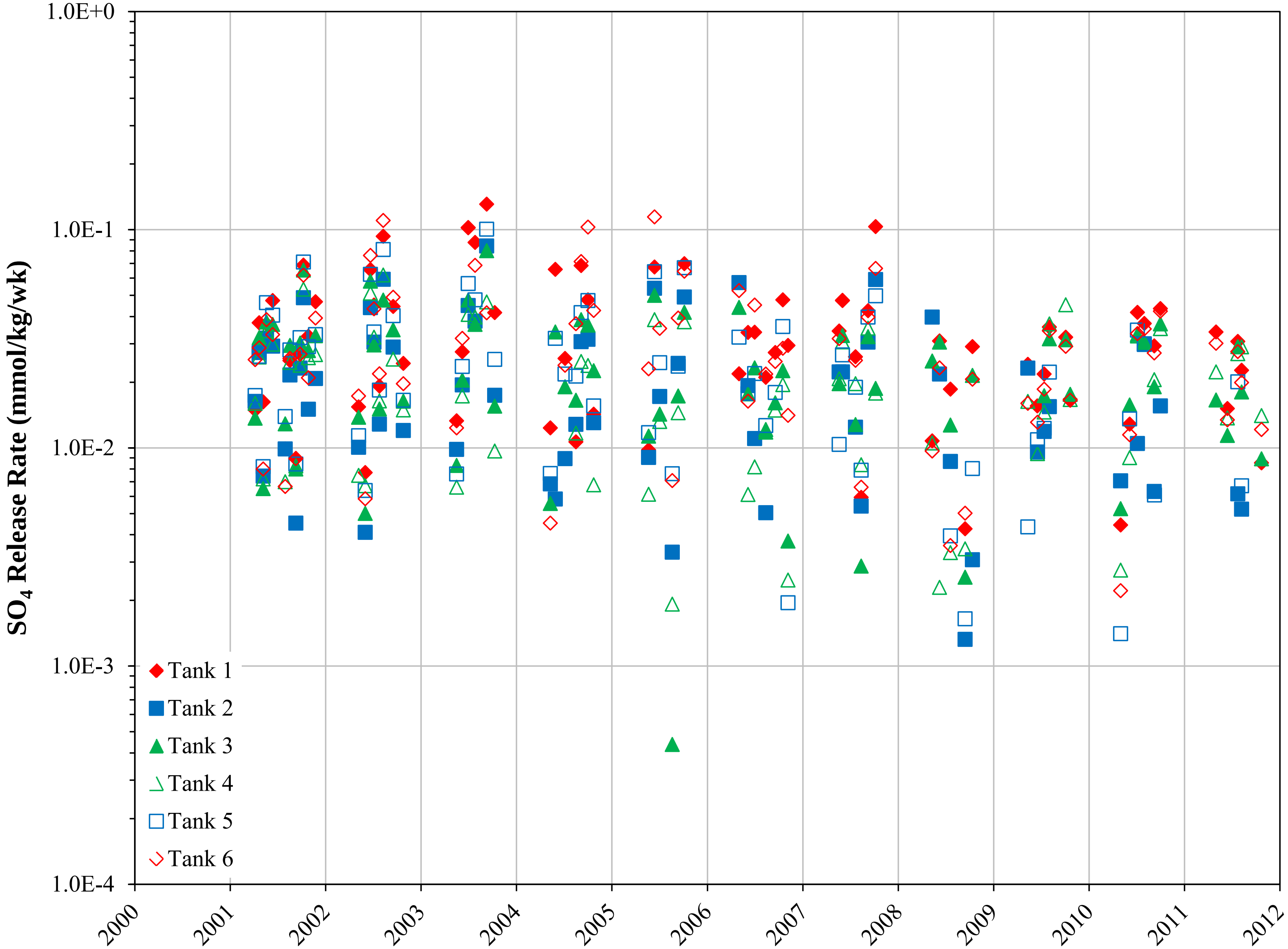

Figure 4.47 Field tanks individual sampling period leachate SO_4 release rates.

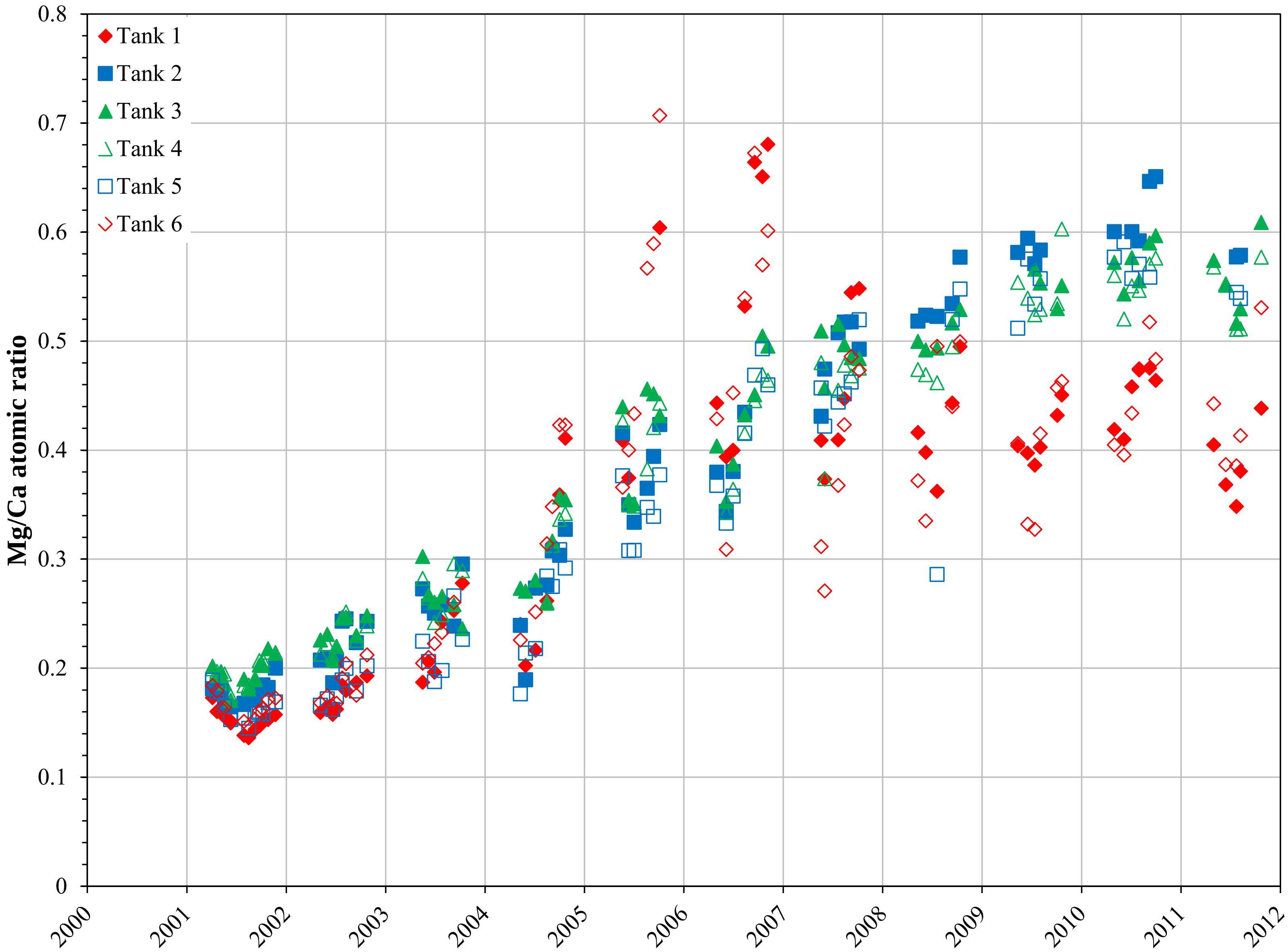

Figure 4.48 Field tanks individual sampling period leachate Mg/Ca molar ratios.

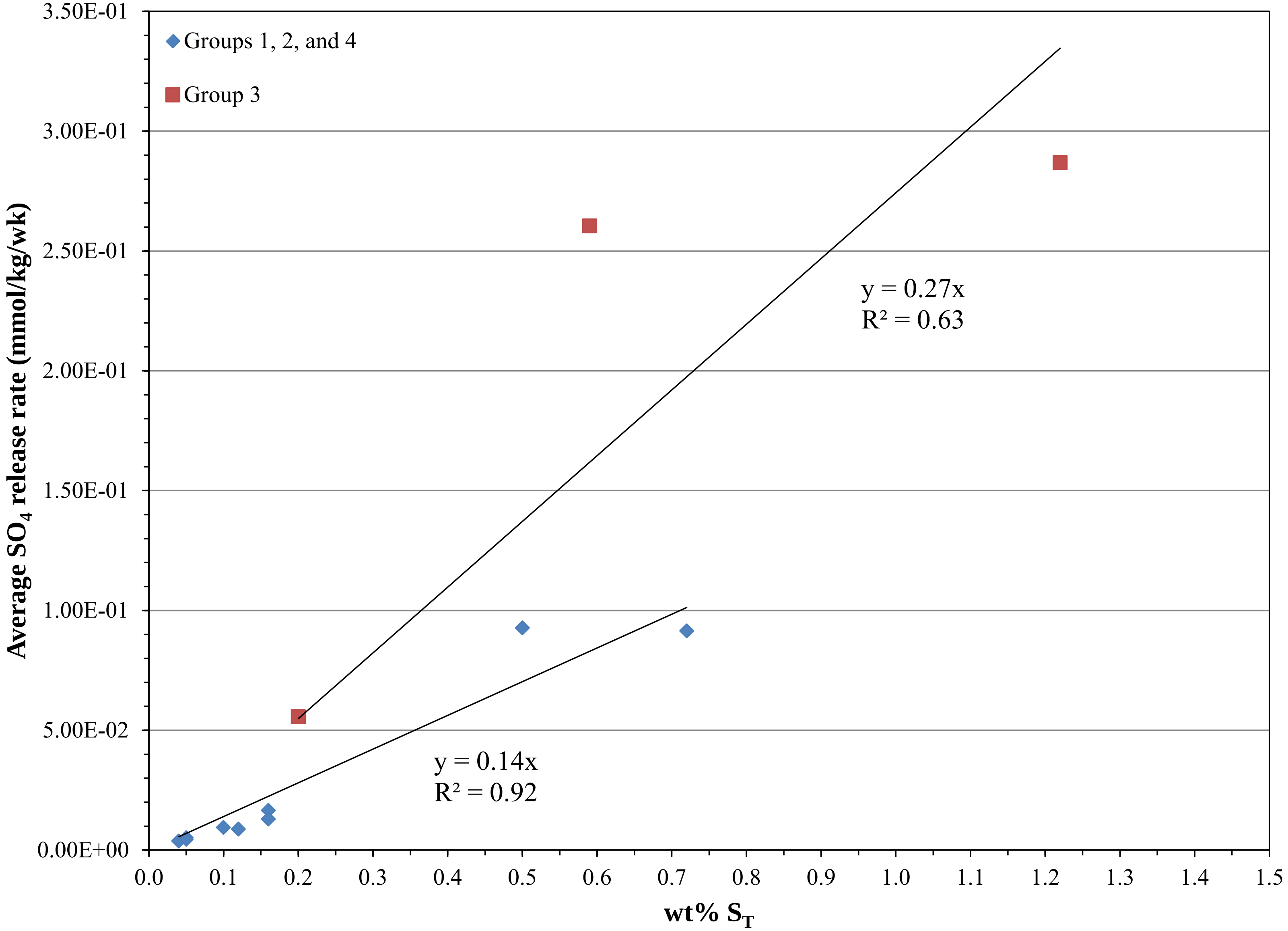

Figure 5.1 Linear regression plot of SO_4 release rates as a function of sulfur concentration for the laboratory samples.

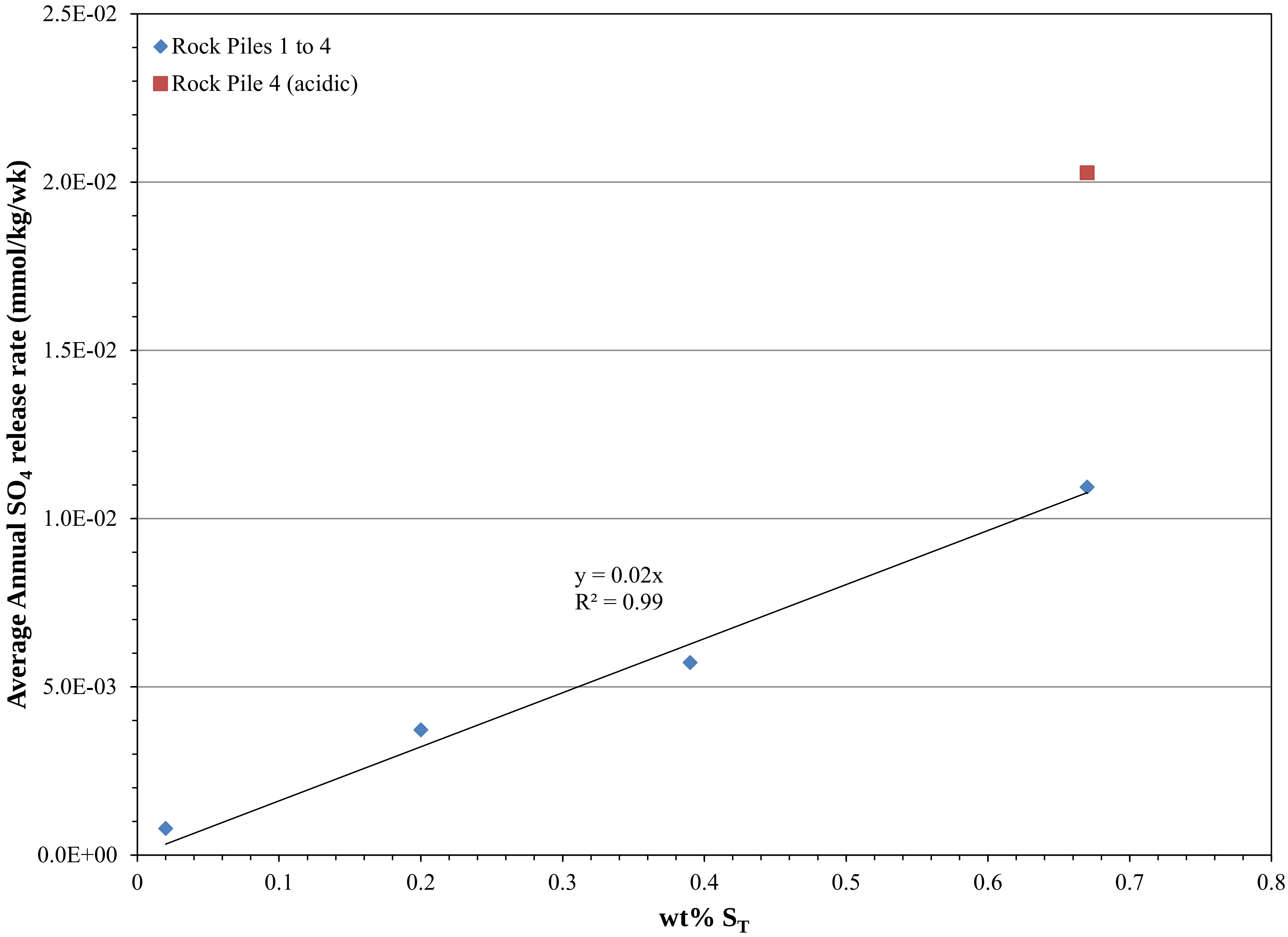

Figure 5.2 Linear regression plot of SO_4 release rates as a function of sulfur concentration for the rock piles.

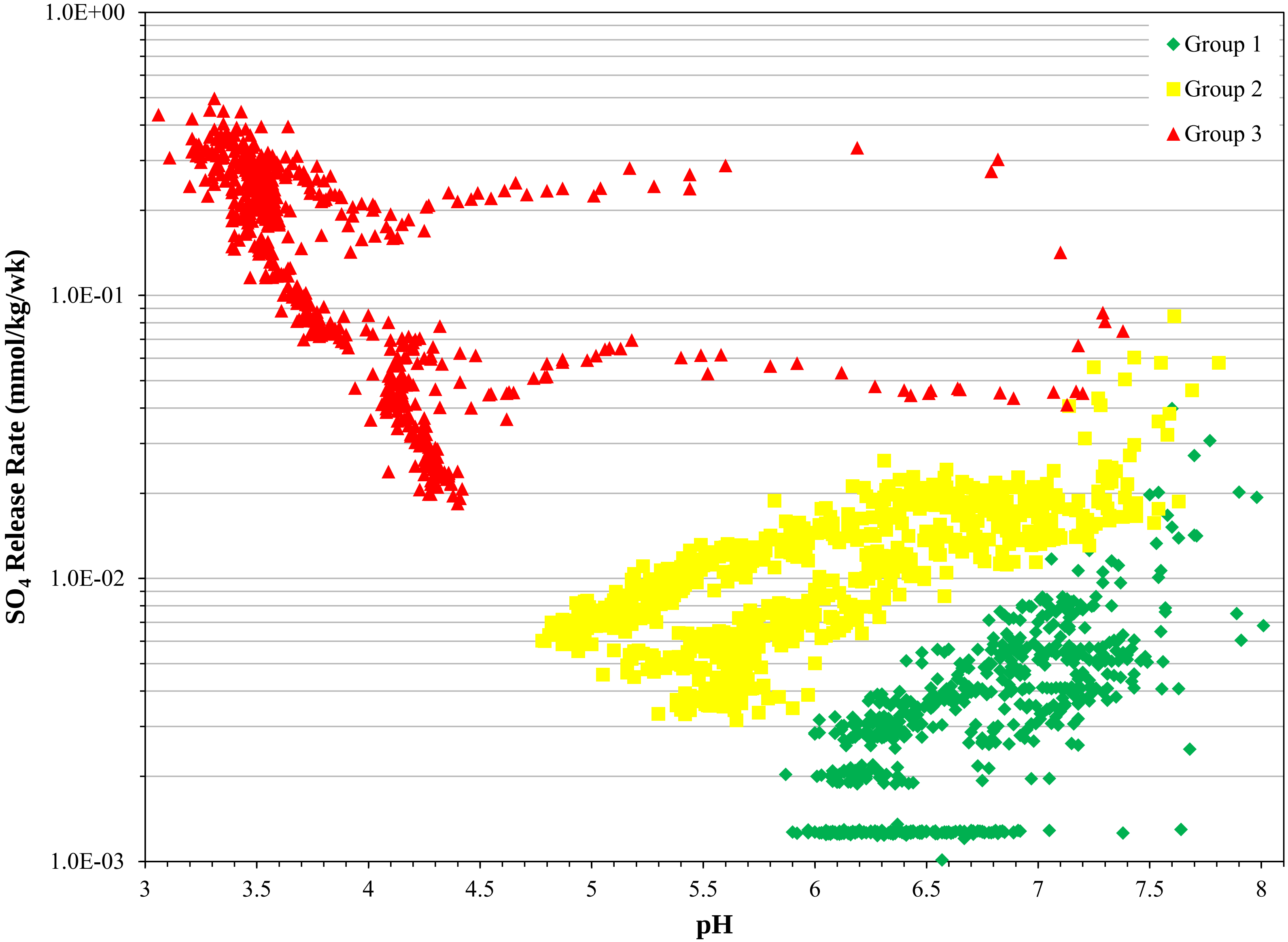

Figure 5.3 Humidity cells SO_4 release rate as a function of leachate pH.

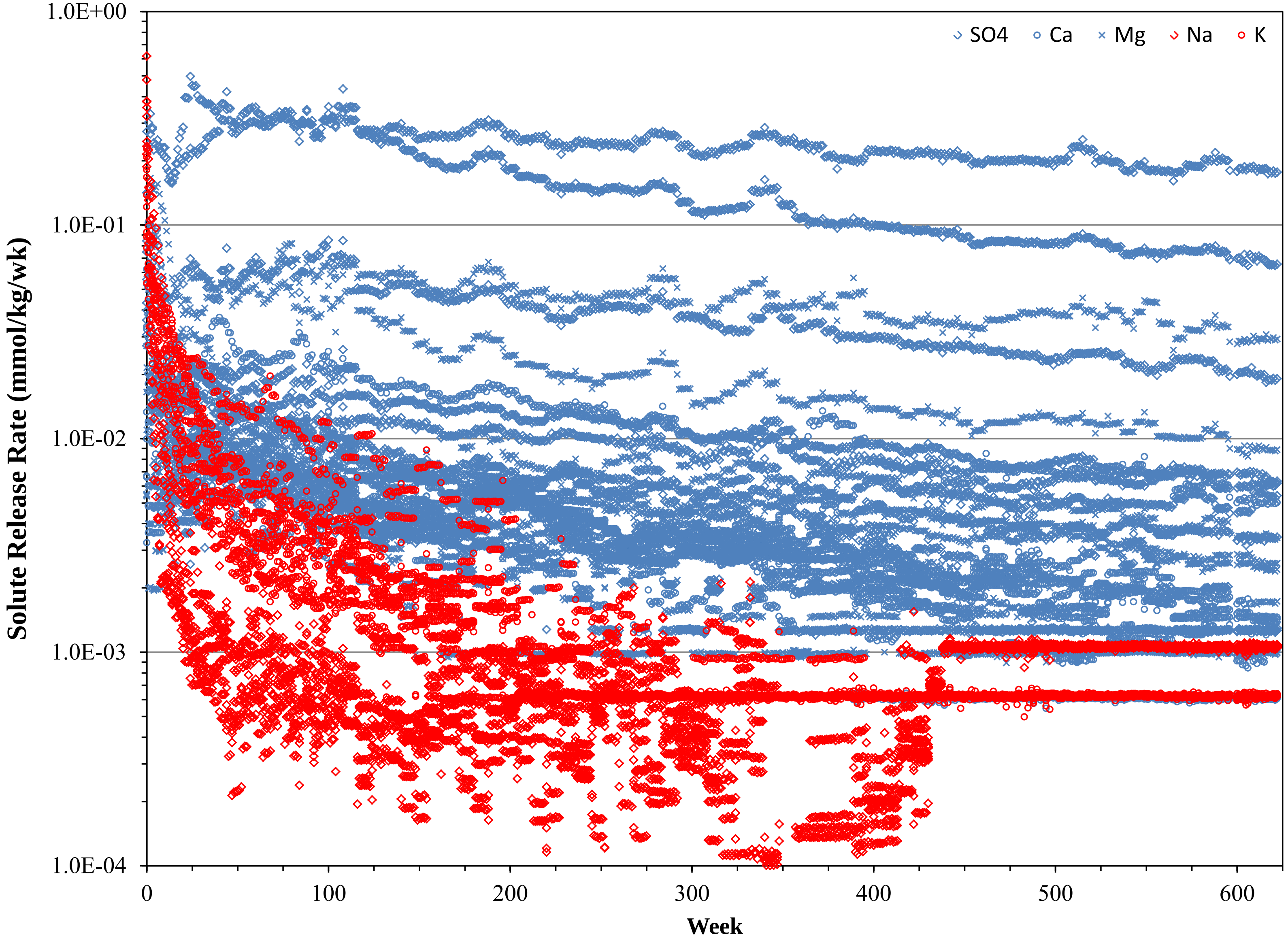

Figure 5.4 Two distinct solute release rate trends.

APPENDIX LIST